Adaptive and optimal variable structure systems: Theory and application in real-time control.

Maslen, Stephen Paul

Award date:
1981

Awarding institution:
University of Bath

ADAPTIVE AND OPTIMAL VARIABLE STRUCTURE SYSTEMS:

THEORY AND APPLICATION IN REAL-TIME CONTROL

submitted by Stephen Paul Maslen
for the degree of Ph.D.
of the University of Bath
1981

COPYRIGHT

S. P. Maslen.

Jan 81

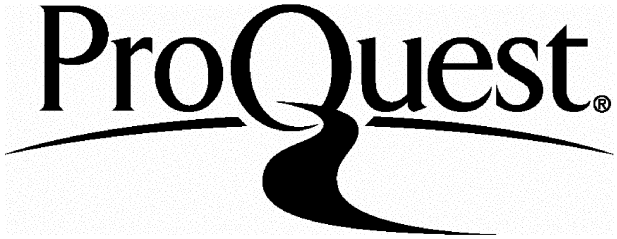

SUMMARY

Variable structure systems are examined from both an adaptive and an optimal control point of view. A theoretical procedure is developed which allows the optimal switching curve for a class of bang-bang variable structure systems to be directly generated. It is shown that the optimal and adaptive control strategies are highly compatible in certain cases and that the advantages of both philosophies may be obtained by the application of a correctly chosen variable structure control law.

The theoretical procedures developed are applied to the practical problem of the speed control of a 5 H.P. D.C. machine. The variable structure controller was realised in the form of a Motorola 6800 Microprocessor based system. The performance of the machine to step speed demands and to step loading was investigated with both a variable structure control law and a conventional linear control law. In both cases, the respective control law is applied after an initial period where the machine is accelerated at the maximum safe value.

It is seen that substantial improvements in the dynamic performance and the consistency of performance over a range of operating conditions are obtained with the variable structure control law, when compared to the performance with the conventional linear control law.

CONTENTS

	page
SUMMARY	i
TABLE OF CONTENTS	ii
LIST OF PRINCIPLE SYMBOLS	viii
1. INTRODUCTION	1
2. VARIABLE STRUCTURE SYSTEMS	4
2.1 Definitions	4
2.2 General Features	5
2.2.1 Continuous control VSS	8
2.2.2 Piece-wise constant control VSS	8
2.2.3 Non-singular control VSS	9
2.2.4 Singular control VSS	9
2.3 Current Design Techniques	10
2.3.1 Continuous control	10
2.3.2 Singular bang-bang control	11
2.3.3 Non-singular bang-bang control	11
3. ADAPTIVE SYSTEMS PHILOSOPHY	13
3.1 General	13
3.2 A Typical Application for Adaptive Control	15
3.3 Review of Adaptive Control Philosophies	17
3.3.1 Gain scheduled systems	19
3.3.2 High gain-limit cycle systems	21
3.3.3 Ad-hoc systems	22
3.3.4 Test signal identification	25
3.3.5 Model reference systems	27

3.4 Selection of the Model Reference Scheme as an Adaptive Control Philosophy 29

4. VARIABLE STRUCTURE SYSTEMS IN MODEL REFERENCE ADAPTIVE CONTROL 32

4.1 General 32

4.2 The Selection of Variable Structure Control as a Design Method for Model Reference Adaptive Systems (MRAS) 32

4.2.1 MRAS designed by local parameter optimisation theory 33

4.2.2 MRAS designed by estimation theory 34

4.2.3 MRAS designed by stability theory 35

4.2.3(a) MRAS design using Liapunov functions 35

4.2.3(b) MRAS design using Hyperstability theory 37

4.2.3(c) MRAS design using variable structure systems 39

4.3 Discussion of Model Reference Design Methods 41

4.4 Design Techniques for Variable Structure Adaptive Systems 43

4.4.1 The equivalent control method 43

4.4.2 The use of filters in the switched gain paths 44

4.4.3 The use of an implied model 45

4.4.4 The interaction of sliding modes 46

5. OPTIMAL CONTROL OF VARIABLE STRUCTURE SYSTEMS 49

5.1 General 49

5.2 The Techniques of Optimal Control 50

5.2.1 Calculus of variations 51

5.2.2 Dynamic programming 52

5.2.3 The maximum principle 54

5.3 The Maximum Principle and the Design of Variable Structure Systems 55

5.3.1 Singular modes 57

5.3.2 Time-optimal variable structure systems 60

5.3.3 Sufficiency conditions 61

5.4 Review of Available Methods for Obtaining Switching Laws for Variable Structure Systems 62

5.5 Towards a More Direct Method of Optimal Switch Curve Generation 63

6. THE DIRECT GENERATION OF THE TIME-OPTIMAL SWITCHING CURVES FOR A CLASS OF VARIABLE STRUCTURE SYSTEM 64

6.1 General 64

6.2 Statement of the Problem 64

6.3 Problem Solution 65

6.3.1 Optimal conditions on the target set 67

6.3.2 Consideration of the reverse-time trajectories from the target set 69

6.3.3 Time domain solution of the state-costate equations 70

6.3.4 Generation of the state-costate transition matrix elements 71

6.3.5 Continuous generation of the optimal switch curve 72

6.3.6 Practical examples of optimal switch curves 73

6.3.7 Discussion of switch curve responses 76

7. CONTINUOUS VARIABLE STRUCTURE SYSTEMS 78

7.1 General 78

7.2 Continuous Control Via the Maximum Principle 79

7.3 Continuous Control Via Stability Considerations 82

7.4 Comments on Continuous Variable Structure Systems 84

8. DISCUSSION OF THEORETICAL STUDIES 85

8.1 General 85

8.2 Salient Points of the Theoretical Studies 86

8.3 The Compatibility of Optimal and Adaptive Control Strategies 88

8.4 Features of a Specific Practical Application 89

9. INTRODUCTION TO PRACTICAL STUDIES 91

10. DESCRIPTION OF THE SYSTEM TO BE CONTROLLED 94

10.1 The D.C. Machines and the Thyristor Bridge 94

10.2 The Thyristor Firing Angle Controller and the Health Monitoring Circuits 96

10.3 The Tachometer Measuring System 100

10.4 The microprocessor System 101

10.4.1 Practical arrangement 102

10.4.2 Software Routines 106

11. DEVELOPMENT OF A MATHEMATICAL MODEL OF THE DIGITALLY CONTROLLED MACHINE 111

11.1 General 111

11.2 The D.C. Machine Equations 111

11.3 The Effect of Discontinuous Armature Current 112

11.3.1 Small perturbation analysis 113

11.4 Consideration of Other Non-Linear Effects 116

11.4.1 Current-limit non-linearity 116

11.4.2 Non-linearity due to unilateral thyristor current flow 116

11.4.3 Non-linear friction characteristic 117

11.5 Representation of the Microprocessor Control Block 119

11.5.1 The estimation of speed error rate 119

11.5.2 Integrating action of the microprocessor controller 120

11.5.3 Controller parameters selectable by the designer 121

11.6 Complete Block Diagram of the Linearised System 121

11.7 Validity of the Linearised Model 122

11.7.1 Comparison of predicted and actual small perturbation responses 123

12. CONTROL LAW SYNTHESIS 125

12.1 General 125

12.2 The System in Phase-Canonical Form 125

12.3 The Choice of Parameters for Linear Control 128

12.4 The Choice of Configuration for Variable Structure Control 129

12.4.1 The choice of a specific sliding plane 132

12.4.2 Specific aspects of the two variable structure control law options 133

12.4.3 Selection of the second arrangement as a practical variable structure control 136

13. DESCRIPTION AND DISCUSSION OF PRACTICAL TESTS 138

13.1 General 138

13.2 Specific Details of Test Conditions 139

13.2.1 Step responses for various conditions 139

13.2.2 Step response with a large amount of added work machine armature resistance 140

13.2.3 Response of machine speed to step torque loads 141

13.2.4 Response to a variety of step speed demands 142

13.2.5 Response to a step speed demand for variable structure control with a variety of sliding planes 142

13.2.6 A digital record of error (x_1) and error rate estimate ($nx_2/100$) 143

13.2.7 Digital records of speed error and error rate estimate displayed as a phase plane response 143

13.3 Discussion of Practical Results 144

14. CONCLUSIONS AND SUGGESTIONS FOR FURTHER WORK 151

14.1 Conclusions 151

14.2 Suggestions for Further Work 155

APPENDIX A 158

APPENDIX B 165

APPENDIX C 167

APPENDIX D 173

APPENDIX E 175

APPENDIX F 178

APPENDIX G 181

APPENDIX H 183

APPENDIX I 185

APPENDIX J 187

APPENDIX K 190

REFERENCES 219

ACKNOWLEDGEMENTS 223

TABLES 224

DIAGRAMS 236

LIST OF PRINCIPAL SYMBOLS

e	error
$\hat{\dot{e}}$	estimated error rate
f	function
H	Hamiltonian function
I	performance index
n	error rate estimation interval
p	costate variable
s	Laplace operator or sliding mode switching function
t	time (secs)
u	control input
V	Liapunov function
x	state variable
z	eigenvector
Φ	transition matrix
λ	eigenvalue or constant
ω	angular frequency (Rads/sec)
ω_a, ω_n	natural frequency
ζ	damping factor
$\cdot$	superscript denoting differentiation w.r.t. time
e_b	machine back emf (Volts)
F	viscous frictional torque (Newton/metres/Rad/sec)
i_a	armature current (Amps)
$\bar{i}_a$	average armature current (Amps)
J	armature moment of inertia (Kg Metres^2)
K_t	torque per unit armature current (Newton/metres/Amp)
K_v	generated emf per unit angular velocity (Volts/Rad/sec) or environmental gain

L	armature inductance (Henrys)
R_a	armature resistance (Ohms)
T	motor torque (Newton metres)
V_i	armature applied voltage (Volts)
V_m	peak supply voltage (Volts)
ω_s	mains supply frequency (Rads/sec)
θ_0	armature position (Radians)
θ_1	angle at start of thyristor conduction (Radians)
θ_2	angle at end of thyristor conduction (Radians)
θ_z	load impedance angle (Radians)

CHAPTER 1

INTRODUCTION

The use of analogue techniques is well established in the field of closed-loop control systems. In the past, the majority of systems have been designed using the classical linear methods such as Bode plots or Root Locus; The resulting designs being realised in terms of linear valve or semiconductor amplifiers and compensating networks.

A particular problem then arises if the "Plant" to be controlled does not have well defined parameters. It is possible to design classical systems to be insensitive to specific plant parameters, but it becomes increasingly difficult to maintain consistent performance if more than one parameter is changing, and large variations are involved.

The branch of control engineering termed "Adaptive Control" has thus been developed, which investigates the synthesis and analysis of control systems which can maintain a certain level of performance in situations where large and unknown changes of the plant parameters occur. Of the design techniques available for the synthesis of adaptive controllers, a relatively recent example is the use of variable structure systems, i.e. systems in which the feedback gains are not fixed, but are functions of some measurable system variables.

As was previously mentioned, analogue techniques have been used extensively in the past. The recent developments in digital technology have, however, seen a rapid increase in the application of minicomputer/microprocessor units to control problems. Previously, digital

computers have been limited by speed and cost considerations to the control of plants that were slow and sufficiently complex to justify the large amounts of capital expenditure and high running cost involved. An example might be blast furnace control, or a manufacturing plant involving chemical processes.

At the present time, microprocessor development has led to the availability of small, cheap computing elements that are sufficiently fast to be considered in control applications where previously purely analogue circuitry was used.

Digital techniques have some inherent advantages over analogue methods. For instance, digital systems are not subject to drift problems as are some linear circuits. The ability of a logic unit to make complex decisions, coupled with the capability to store information, makes possible control strategies that would not be viable with analogue circuits.

Once a microprocessor is included in a system, it can accomplish far more than just the application of control laws. It might be possible, for example, to estimate system states that are not directly measurable, and therefore produce better knowledge of the system. The processor might also take on the role of "Health Monitor", by observing system variables for malfunction conditions.

The present investigation is concerned with the application of variable structure techniques to the adaptive and optimal control of systems, with emphasis placed on the use of microprocessors to implement the control laws.

Variable structure systems often appear in nature, thus it might intuitively be expected that they possess advantages over linear systems. Also, it often happens that variable structure control is required to be one of a number of fixed values of control depending on the result of a comparison between the system states, and of preset functions. This type of operation is ideally suited to microprocessor type logical instructions. Research has previously been reported[1-5] on the adaptive and optimal properties of variable structure systems. This present investigation shows that in some cases the adaptive control laws and the optimal control laws are highly compatible and readily realised by microprocessor type controllers.

As part of the theoretical work, a new technique is developed to allow the optimal control laws of a class of variable structure system to be determined more directly than by existing methods.

As a practical example, adaptive and optimal variable structure control laws are applied to the speed control of a 5 H.P. armature fed D.C. machine, this control being realised in terms of a microprocessor driven thyristor bridge.

Both the transient start up performance and load test performance of this system are then investigated, under normal running conditions and also with large external disturbances to the operating conditions of the machine.

Because of the relevance of some of the theoretical developments to more than one chapter, emphasis is made on the use of appendices to enable such material to be easily referenced.

CHAPTER 2

VARIABLE STRUCTURE SYSTEMS

2.1 Definitions

A general, continuous, finite dimensional process may be described by the following dynamic vector equation

$$\dot{x} = f(x,u,t) \qquad 2.1$$

where, for each t, $x(t) \in R^n$ is the state and $u(t) \in R^p$ is the input (control).

Much theoretical work has been done, in the past, on the simplified form of equation 2.1

i.e. $$\dot{x} = Ax(t) + Bu(t) \qquad 2.2$$

this being the classical linear state-space equation.
Between the relatively straightforward analytical problems of equation 2.2 and the complexities of equation 2.1, lie various intermediate forms. Two of these such forms are the following

$$\dot{x} = f_1(x,t)u + f_2(u,t) \qquad 2.3$$

$$\dot{x} = f_3(u,t)x + f_4(u,t) \qquad 2.4$$

Equation 2.4 is linear in the state, and is often referred to as an equation describing a variable structure system. This is because it may be regarded as a linear system whose parameters are varied according to some control law.

A more particular case of equation 2.4 is

$$\dot{x} = f_5(t)xu + f_6(t)x + f_7(t)u \qquad 2.5$$

In this case, the system is linear with respect to control and linear with respect to state, but not jointly. Systems of this form are known as bilinear systems.

2.2 General Features

It has been seen[1] that many natural control processes may be described by a bilinear equation. For instance, a few examples of bilinear systems occurring within the human body are:

1. Regulation of circulating thyroxin;
2. Regulation of carbon dioxide in the respiratory system;
3. Body temperature regulation system.

Many other natural systems can be shown to exhibit control that can be approximated by a variable structure or bilinear form.

It seems likely therefore that such control will possess advantages over simple linear control policies. Indeed, it has been shown[2] that bilinear systems have, in general, better controllability than linear systems, and also[3] exhibit adaptive qualities.

A simple example will now be considered, to demonstrate the advantages that may be obtained by the use of a variable structure control policy over that of a conventional linear design.

Consider the system diagram of Fig.2.1 which is represented by the state-space equation 2.6.

$$\begin{bmatrix} \dot{x}_1 \\ \dot{x}_2 \end{bmatrix} = \begin{bmatrix} 0 & 1 \\ -K & -A \end{bmatrix} \begin{bmatrix} x_1 \\ x_2 \end{bmatrix} + \begin{bmatrix} 0 \\ Ku_1 \end{bmatrix} \qquad 2.6$$

Assume that the value of K has already been chosen at some fixed level. A linear controller now requires that we fix A at some constant value.

The output of the system will be considered to be the state variable x_1. The ideal response of x_1 to a step input $u_1 = H(t)$ may well be of the form shown in Fig.2.2, i.e. very fast risetime with no overshoot, to the required value of $x_1(t) = 1.0$.

The solution of equation 2.6 is well known in terms of natural frequency and damping factor. The characteristic equation for this system is

$$C.E. = s^2 + As + K \qquad 2.7$$

The standard form for this type of equation is given by

$$s^2 + 2\zeta\omega_n s + \omega_n^2 \qquad 2.8$$

where ζ is the damping factor

and ω_n is the natural frequency

Equating coefficients gives

$$A = 2\zeta\omega_n$$

$$K = \omega_n^2$$

Large values of A will lead to heavily damped responses of the form shown in Fig.2.3. Such conditions lead to excessively slow risetimes and are therefore unacceptable.

Small values of A, however, will lead to responses that, although they may fast enough, are highly oscillatory and have prolonged settling times, as in Fig.2.4.

In practice, a compromise will be made, and a value of A will be selected to give a fairly fast response with a medium amount of damping. A typical response might then be as in Fig.2.5.

Assume now that we have the option of applying a variable structure control, as depicted in Fig.2.6. The state-space equations are now

$$\begin{bmatrix} \dot{x}_1 \\ \dot{x}_2 \end{bmatrix} = \begin{bmatrix} 0 & 1 \\ -K & -u_2 \end{bmatrix} \begin{bmatrix} x_1 \\ x_2 \end{bmatrix} + \begin{bmatrix} 0 \\ Ku_1 \end{bmatrix} \qquad 2.9$$

Intuitively, the control policy for $u_2(t)$ might now be chosen as follows. During the initial period, $u_2(t) = 0$, i.e. zero damping, to provide a fast initial response. As $x_1(t)$ approaches the required value, increase the value of $u_2(t)$ to a level sufficient to prevent overshoot. Thus we get a composite response of the form shown in Fig.2.7.

The variable structure scheme can clearly produce a response that is closer to our chosen "ideal" response than a fixed structure system. This is achieved by removing the need to compromise between the slow, well damped linear system and the fast underdamped linear system.

It is useful to realise that the u_1 additive input determines the steady state condition, whereas the u_2 multiplicative input determines the dynamic response.

The major design problem encountered with the synthesis of variable structure systems is the logical formulation of the multiplicative control laws in order to achieve an improvement (in some sense) over conventional linear design techniques.

As part of the present investigations, a new technique has been developed which greatly aids the formulation of variable structure control laws for a certain class of system. This technique forms the subject matter for chapter 6.

Systems under the general heading of variable structure systems (VSS) may be divided in classes, depending on the form of control in operation. These will be detailed in the following order.

1) Continuous control;
2) Piece-wise constant control;
3) Non singular control;
4) Singular control.

2.2.1 Continuous Control VSS

If the function $f_3(u,t)$ in equation 2.4 is a smooth continuous function of time, the system described by that equation will be known as a VSS with continuous control.

2.2.2 Piece-wise Constant Control VSS

Certain design techniques often require that the components of the variable structure control vector attain either their maximum possible value, or their minimum possible value at any instant of time. Thus the control will undergo a discontinuity every time the control vector components are required to change.

This type of control will be known as piece-wise constant or Bang-Bang VSS.

2.2.3 Non-Singular Control VSS

Consider a Bang-Bang mode VSS. The variable structure control will usually be required to be known as a function of the system states. Thus, there will be regions in state space where the control is required to be the maximum possible value. Likewise, there will be regions where the minimum value of control is required. Separating these regions will be some surface which will be known as the switching surface.

Consider the possible combinations of system trajectories on either side of the switching surface. These are shown in Fig.2.8. In case a of Fig.2.8, the trajectories are shown pointing away from the switching surface on both sides. This case need not be considered, since no control system would be designed to operate such that the switching surface could never be reached, other than by an initial condition position.

Case b shows the trajectories pointing in the same sense across the switch curve. Given that the system is initially moving towards the switch curve, it will eventually cross and then continue moving away from said curve.

A VSS operating with this sort of mode is said to have control, of a non-singular type.

2.2.4 Singular Control VSS

Case c in Fig.2.8 shows both sets of trajectories pointing towards the switch curve. Thus, the system will move from its initial condition, towards the switch curve. Once it has reached the curve, the opposing trajectories will maintain the system on that curve.

A VSS with this property is said to be operating with singular control. In such a mode, the control input will not be well defined, but will be oscillating between two fixed levels.

It may well be that a practical control system will operate with a mixture of singular and non-singular modes.

2.3 Current Design Techniques

The general design techniques that have been applied to VSS will be introduced in the following order:

1) continuous control;
2) singular Bang-Bang control;
3) non-singular Bang-Bang control.

2.3.1 Continuous Control

Synthesis of continuous control VSS makes use of the design methods available for the more general class of problems under the heading of non-linear systems. Assuming that VSS control is being employed to gain better responses than a linear design, then we are likely to be using optimal control methods to improve some index of performance. The optimal non-linear control problem invariably results in a solution that is not analytical. Thus numerical techniques have to be employed, which give very little information on the general form of the required control.

Intuitive design may be used for simple cases, i.e. the second order example of Fig.2.1, but systems with more than one variable structure control input, or having higher orders soon become too complex for intuition.

Methods of designing stable continuous VSS have been reported[4], but stability, although necessary, is not sufficient in itself to guarantee a 'good' response. Some studies have been carried out on continuous VSS in this investigation. These are reported in Chapter 7.

2.3.2 Singular Bang-Bang Control

Singular Bang-Bang control systems may result from design by adaptive synthesis methods or by design based on optimal control theory.

From the adaptive point of view, it has been shown[5] that the behaviour of the plant in a singular mode is independent of plant parameters and disturbance signals, as will be shown in Chapter 4. Appendix A gives the current methods of synthesis for single input VSS of any order, designed from an adaptive point of view, and operating in a singular mode.

Optimal VSS with singular modes are discussed in Chapter 5.

2.3.3 Non-singular Bang-Bang Control

The choice of a non-singular (and sometimes singular) Bang-Bang type of variable structure control often results from the application of the Maximum Principle (Appendix C) of Pontryagin. As was mentioned in 2.2 the general problem in VSS is to calculate the multiplicative control laws. In the particular case of non-singular Bang-Bang control, this problem reduces to the decision as to which fixed structure should be in operation at any particular point in time.

Specific methods of solving this problem are outlined in Chapter 5. These methods rely on variational techniques, or the Maximum Principle. All these available methods are common in the sense that they generate the so-called switching surface, point by point. These techniques therefore require to be applied many times, from various initial conditions, to build up a reasonable picture of the switching surface.

Chapter 6 describes a new technique that allows the switching curve for a class of VSS to be generated more directly.

CHAPTER 3

ADAPTIVE SYSTEMS PHILOSOPHY

3.1 General

In the past, control system design has been dominated by controllers that have a fixed linear structure. i.e. the system states are fed back via linear networks with constant parameters. The choice of these networks is made by the application of one of the standard synthesis techniques such as Bode, Root Locus, state space methods etc. All these methods require that the plant transfer function is known to within certain reasonable limits. In many systems, the plant is fairly constant and well defined. However, there appears to be an increasing number of situations in which control is to be applied, where the plant has unknown widely varying parameters.

To illustrate the problems that arise with variable plants, we shall examine a simple second order system. This system is described by equations 3.1 and is represented in system form in Fig.3.1.

$$\begin{bmatrix} \dot{x}_1 \\ \dot{x}_2 \end{bmatrix} = \begin{bmatrix} 0 & 1 \\ -K_c K_v & -A \end{bmatrix} \begin{bmatrix} x_1 \\ x_2 \end{bmatrix} + \begin{bmatrix} 0 \\ K_c K_v u \end{bmatrix} \qquad 3.1$$

The gain K_c is to be selected by the designer. The gain K_v is part of the plant and subject to variations which are not known functions. The feedback gain A is part of the plant and will be considered for the moment to be fixed.

The form of the root locus for this system has the characteristic shape shown in Fig.3.2.

The characteristic equation for this system is

$$C.E. = s^2 + As + K_c K_v \qquad 3.2$$

Compare this with the standard form.

i.e.

$$s^2 + 2\zeta\omega_n s + \omega_n^2 \qquad 3.3$$

Let $K = K_c K_v$

gives

$$\omega_n = \sqrt{K} \quad \text{and} \quad \zeta = \frac{A}{2\omega_n}$$

$$\therefore \quad \zeta = \frac{A}{2\sqrt{K}} \qquad 3.4$$

It is often the case, that ζ is chosen to have a value of 0.707, as a compromise between speed of response and amount of overshoot of the system, with a step input.

$$\text{i.e.} \quad K = \frac{A^2}{2}$$

If K_v, the environmental gain, changes between twice its nominal value and half its nominal value, the corresponding values of damping factor will vary between the limits $\zeta = 1.0$ and $\zeta = 0.5$. It is quite likely that damping factors of these limits will be unacceptable.

The addition of a compensating zero to the system would enable the modified root locus of Fig.3.3 to be obtained.

It can be seen that the damping factor $\zeta = \cos\phi$ is sensibly constant over the range $K = K_1 \rightarrow K_2$ (assuming second order dominance). There are no such regions in the uncompensated system excluding the case where $\phi \rightarrow 90^\circ$, i.e. $\zeta \rightarrow 0$.

The compensating zero can therefore give a system with a damping factor that is sensibly constant over restricted range of variation of K.

Consider now, the same compensated system which is subject to variations in both K and A. Fig.3.4 shows the movement of the closed loop poles for variations in K and A around a nominal operating point.

It is immediately obvious that the damping factor $\zeta = \cos \phi$ is highly sensitive to the parameter A, and significant changes in this parameter could cause unacceptable responses. Attempts to compensate for A would certainly upset the compensation for K. To try and compensate for unknown changes in A and K simultaneously would be very difficult, even for this uncomplex system.

This example has demonstrated that it is not viable to use simple compensating techniques to produce a system that is insensitive to unknown changes in multiple parameters. It will be appreciated, that plants of higher order and more complex structure would pose a far greater design problem than this simple example.

3.2 A Typical Application for Adaptive Control

One of the earliest problems that required control of a highly variable plant, was that of controlling a high performance aircraft. The plant (aircraft) transfer function is highly dependent on the following factors:

1) Airspeed (Mach Number);

2) Air density i.e. Altitude;

3) Change of mass (due to fuel consumption etc);

4) Change of C of G (due to fuel consumption etc);

and other minor factors too.

The short-period approximation to the general aerodynamic equations of motion using linearised aerodynamics is given by[6]

$$\frac{\dot{\theta}}{\delta} = K\dot{\theta} \frac{T_a s + 1}{\frac{s^2}{\omega_a^2} + \frac{2\zeta_a s}{\omega_a} + 1} \qquad 3.5$$

The quantities $K\dot{\theta}$, T_a, ω_a and ζ_a define the plant characteristics. The way in which these quantities vary with flight conditions is shown in Fig.3.5. The variation is even more clearly seen in Fig.3.6, which is a pole-zero plot of the system over these same flight conditions.

Two major features of these figures are

1) The gain factor $K\dot{\theta}$ varies over a range by a factor of approximately 1000 to 1.
2) The inherent damping in the system is low, and in some cases, negligible.

Thus, at a basic level we require control to introduce some damping into the system. This will produce an acceptable flight response to the pilot and passengers. At the next level of complexity, adaptive control must be applied, to maintain the acceptable response over the complete flight regime.

This represents a typical problem for which a suitable adaptive technique must be found, and it is this type of situation that will be borne in mind when discussing the various philosophies of adaptive control.

3.3 Review of Adaptive Control Philosophies

Before entering the discussion of adaptive control philosophies, it is worth noting that Horowitz[7] has shown that any linear system with time varying coefficients can be made stable, and have a constant overall transfer function that may be selected by the designer. All this, using a classical fixed feedback controller. A simplified version of this argument, due to Diprose[8], is presented in Appendix D.

The fallacy in the argument (as was noted[8]) is that the proof assumes that the plant transfer function is valid up to an indefinitely large frequency. For the argument of Horowitz to work, the plant transfer function must be valid up to, and a little beyond, the gain cross-over frequency. For the feedback loop to be effective in maintaining the desired transfer function, the loop gain must be reasonably large at the highest frequency components of the desired response. Let the desired characteristics be restricted to frequencies below f_o, say. For good gain at f_o, the gain cross-over frequency should be at a minimum of $3f_o$. The gain cross-over frequency will be a function of the environmental gains. Thus if the transfer function gain changes by a factor of 50 to 1, the gain cross-over frequency will change by a similar ratio. That is, we require the highest gain cross-over frequency to be 150 f_o. The plant transfer function will therefore need to be valid up to a frequency of 300 f_o, say, if Horowitz's proof is to work.

For any reasonable plant, this restriction is likely to be too severe by far. Any real system will have a pole-zero representation that increases indefinitely in complexity, as frequency increases.

Fig.3.7 presents the key features of this discussion.

The greater the plant variations, the wider the gain cross-over annulus is required to be. The actual allowable limits of the annulus are of course fixed. At the lower end by the need to maintain good gain over all frequencies to be controlled. At the top end by the limit of transfer function validity. This balance is unlikely to be met in practice. For instance, in the case of an aircraft, the modes to be neglected (at frequencies greater than the limit of transfer function validity) may be only marginally separated from the modes to be controlled. In extreme cases, the annulus gap can disappear and the two regions then overlap.

Thus, the method of Horowitz will not be applicable to many "real" situations. A viable adaptive controller should therefore operate in such a way that the gain cross-over frequency is maintained approximately constant over the variation of environmental parameters.

Current Design Philosophies

Fig. 3.8 shows a completely general representation of an adaptive control scheme. The way in which the function in each box is achieved is dependent on the particular design philosophy proposed. The following section will be a critical review of the prominent methods that have been proposed to achieve the desired adaptive action. Fig.3.9 shows these methods graphically. The discussion will examine these techniques in the following order:

1) Gain Scheduling;
2) High Gain/Limit Cycle Systems;
3) Ad Hoc Systems;
4) Test Signal Identification Systems;
5) Model Reference Systems.

3.3.1 Gain Scheduled Systems

The gain scheduling approach to adaptive control is essentially an open loop one. This type of technique was the first to be used in the adaptive control of aircraft.

The method is, to vary gains in the controller as a function of measurable environmental factors. In the case of an aircraft, gains would be varied as a function of measured air data such as altitude, dynamic pressure, mach no. etc. The problem is then to find the functional relationships between such data and the adjustable gains, so as to nullify the effects of changing environmental gains which are themselves functions of altitude, mach no. etc.

It was discovered early on that there were great problems with this method.

To quote[9] , "During 1955, there was a growing realization that development programs for flight control systems to particular aircraft were becoming exceedingly complex and were requiring a great deal of research time. Air-planes were not being provided with a complete flight control system until two or more years after the aircraft had first flown. Several factors were responsible for this condition. New aircraft were flying at higher altitudes and through greater speed ranges. These greater extremes were causing wider changes in the basic airplane's flight characteristics from one flight condition to another. Also, flight conditions were reached about which insufficient information was available".

"These changes in airplane characteristics require corresponding adjustments of the control system parameters to maintain the response of the aircraft-control system combination relatively constant. If

sufficient information about the aircraft characteristics for all the flight conditions is available when the control system is being designed, the required adjustments could be calculated for the control system".

"It is important to realize that this type of adjustment is an open-loop adjustment. If the adjustment scheduled to take place was not just right, due possibly to poor data, miscalculation, or some unforeseen change in the aircraft configuration, or even ageing of system components, we still get the adjustment even though the response may become worse because of it".

"By the fall of 1955, it was becoming difficult to meet some of the requirements. First, less detailed information was available on the newer vehicles being planned. Second, the vehicles would be operating in environments which would make air data measurements quite unreliable if not altogether impossible. Third, the control system would be needed on first flights, and forth, the possibility of errors due to open-loop adjustment could compromise the mission".

So, gain scheduling is useful for simple systems, where the measurable environmental factors have a well-defined effect on the plant transfer function. For a real system of reasonable complexity, however, some type of closed loop form of adaption will be required.

This is not to say that gain scheduling cannot be used in complex systems. The best solution could be to use open-loop adaption to correct for a large amount of the environmental changes, with a closed-loop adaptive system to compensate for the remaining errors and unexpected conditions.

3.3.2 High Gain-Limit Cycle Systems

The High Gain-Limit Cycle approach follows a similar philosophy to that of Horowitz's argument. The problems that have been pointed out in that type of structure, limit the application of this method in practice.

The general representation of high-gain adaptive systems is shown in Fig.3.10.

The theory of operation is as follows. The plant is included in a stable, unity feedback loop, which has high gains up to and beyond the highest frequencies that are to be controlled. This high-gain loop is then driven by the command inputs, that have been processed by the block labelled "model".

The model is a unit, that in some way embodies the desired "ideal" characteristics of the overall input-output relationships. Thus, when the model is fed with the command inputs, the model output will consist of responses that are considered ideal.

The unity feedback plant loop, will have high gains at all the frequency components contained in the model output (desired response). The actual plant response will therefore be

plant output = desired response x unity (approximately)

i.e. the actual response closely follows that of the ideal response.

The limit-cycle scheme was pioneered by Honeywell[10]. In this type of system, the gain of the unity feedback plant loop is effectively increased to the point of instability by the inclusion of a bang-bang relay element, as shown in Fig.3.11. The filter block F_2 is included to reduce the amount of limit cycle oscillation present at the output

of the plant. The filter F_1 is chosen to produce the required limit cycle frequency.

The amount of limit cycle amplitude present in the output signal is maintained approximately constant, by detecting the limit-cycle amplitude and comparing this with a preset value. The loop gain is then increased or decreased, depending on whether the actual amplitude is lower or higher than the set point.

Good results have been achieved[11,12] using a limit-cycle scheme in the roll-rate control of small aircraft.

This system will only work well in the case where the modes to be neglected are far removed from the modes to be controlled. The limit cycle frequency can then be high enough to provide high gain beyond the maximum frequency to be controlled, and low enough to avoid exciting structural resonances.

3.3.3 Ad-Hoc Systems

Under this heading are some schemes that have been applied in specific applications. The operation of these schemes is seen to rely on chance relationships between the changing environmental factors, and some property of the overall control loop response. It will thus be seen that these ideas are not generally applicable. Two such schemes will be described, i.e.

a) Marx's Frequency Servo;

and b) Osder's Impulse Test System.

a) Marx's Frequency Servo[13]

Consider the system of Fig.3.12. The form of the frequency response of this system is shown in Fig.3.13. There is a resonant frequency ω_r

at which the response is a maximum. This frequency is dependent on the varying environmental gain K_v. The height of this peak is dependent on the system damping factor. The frequency servo system makes use of this dominant frequency in the following manner.

With reference to Fig.3.14, it can be seen that the output signal is passed through both a high pass filter and a low pass filter. The outputs of these filters are rectified, and then compared. This comparison produces a signal which drives a variable gain via an integrating amplifier.

Consider the responses of the system, shown in Fig.3.15a and Fig.3.15b. These show the relationships between the filters and the system frequency responses for two values of loop gain. In the case of Fig.3.15a where the overall loop gain is low, the output of the low pass filter is greater than that of the high pass filter. The integrator thus has a positive input and drives the compensating loop gain in an increasing direction. Thus, the resonant frequency ω_r is increased also. In the case of Fig.3.15b the overall loop gain is high and the high pass filter has the greatest output. The loop gain and corresponding resonant frequency are subsequently reduced.

It is clear that an equilibrium condition exists between these two modes, and that by reaching this equilibrium condition, a constant resonant frequency will be obtained although the environmental gain K_v is not constant.

There are several serious disadvantages with this system, i.e.

i) The validity of the operation is only clear for simple 2nd order transfer functions.

ii) No account is taken of the damping factor of the system.

iii) The operation of the adaptive loop depends on the frequency components of the input commands.

If one imagines a long series of low frequency inputs, the adaptive loop would continuously increase the compensating gain, possibly with the result of instability.

To summarise, the frequency servo should only be considered for simple second-order systems with input commands that contain many harmonics e.g. step functions.

b) Osders Impulse Test System[14]

This scheme requires that the input commands take the form of step functions. To demonstrate the operation of this method, consider the second order control system of Fig.3.16. The step response of this system is shown for three values of environmental gain K_v in Fig.3.17.

We now define upper and lower limits, about the required steady state value. These will be known as the error bounds. If the period before the first entry into the enclosed error bound region is ignored, we can see that

Response a exceeds the bounds n = 6 times

" b " " " n = 3 times

" c " " " n = 0 times

Thus the figure n is a measure of the damping factor of the system. Fig.3.18 shows the implementation of the adaptive impulse test scheme. The principle of operation is as follows. When a step is applied, count the number of times the response exceeds the error bounds in a set time period. Compare this value to the preset "ideal" value.

Make adjustment to the compensating gain accordingly.

Again, there are serious disadvantages with this system. For instance, the gain set computer has to wait for a certain period to elapse before it can calculate n the number of bound excesses. During this period the plant response may be totally unacceptable. The computer, however, cannot make any corrections until the end of the period.

With both the aforementioned schemes, and others of a similar nature, it is very difficult to think of ways of adjusting anything but the main loop gain. This, coupled with the limitations on input signals, severely limits the practical applicability of such schemes.

3.3.4 Test Signal Identification

In this approach to adaptive control, the characteristics of the plant are explicitly identified. Once this has been done, the appropriate adjustment is made to the compensating gains.

The identification is usually made by the use of a special test signal (notably a pseudo-random binary sequence). Such test signals may be used in two ways.

a) Estimation of the system impulse response using cross-correlation techniques.
b) Direct estimation of the system transfer function using spectral density measurements.

It has been shown[15] that the minimum time to measure a transfer function to a specified accuracy in the presence of noise is more or less independent of the measurement method. Also, it has been calculated[8] that:

Time for identification in cycles of the fundamental test frequency is equal to:- the mean noise to test signal power ratio, divided by the fractional variance of the estimate of the transfer function.

Thus, if the test signal is of the same order as the disturbing noise and the transfer function is required to an accuracy of 30%, then about ten cycles of fundamental test signal will be required to make the identification.

The minimum arrangement would be identification at one frequency, i.e. to maintain a constant gain-crossover frequency. For an aircraft with a desired roll-rate response characterised by ω_n = 0.5 Hz and ζ = 0.7 the cross-over frequency would be about 3 radians/second, i.e. 0.477 Hz. The complete identification would thus take approximately 10 x .477, i.e. 5 seconds.

There will be a further delay incurred for the calculation of the adjustment required, before the control action can be applied. This total delay is quite significant when compared to the expected rate of change of environment that an aircraft could experience.

This limitation is fundamental to any adaptive scheme using test signals to explicitly identify plant parameters.

As previously mentioned, the identification using special test signals may be accomplished in one of two ways, i.e.

a) Cross-correlation of the input and output signals of the plant provides an estimate of the plant impulse response. Once this response is obtained, some decision is made as to how the plant should be compensated to allow for the variable environment. In practice, however, it is difficult to know how logical compensation of the plant may be

effected, this being due to the lack of a simple relationship between system parameters, and the form of the impulse response.

b) The transfer function may be estimated by measurement of the spectral densities of input test signal (possibly a Pseudo Random Binary Sequence) and the output signal from the plant. This might be realised using the Discrete Fourier Transform. Once an estimate of gain at various frequencies has been obtained, the appropriate control action can be applied.

With both these techniques, the amount of hardware required to implement the identification would be considerable. In the case of a system designed to a high factor of safety, the possible triplication of such hardware would be prohibitive.

The conclusion is therefore that schemes involving special test signals seem to be good as far as identification is concerned. But, when these schemes form part of an adaptive loop, they appear, in general, to be too costly in terms of both hardware and time to be considered for general use.

A more direct plant measurement-correction technique is required.

3.3.5 Model Reference Systems

The general representation of a model reference adaptive control system is shown[16] in Fig. 3.19. The method of operation is as follows. A model which represents the desired input-output relationships of the plant is formed. The model is then fed with the demand signal (input). Thus, the output from the model is a response which we consider ideal.

The plant is also fed, via some compensating network, with the demand signal. Note, the block labelled "Adjustable System" in Fig.3.19 consists of the plant plus the compensating networks. The difference between the ideal output from the model and the actual output from the plant is then measured, to form an error signal. The adaption mechanism will then operate on this error signal to adjust gains (parameter adaption) and/or add signals (signal synthesis adaption) to the compensation network that drives the plant. The actual way in which these signals and/or gains are adjusted depends on the particular design method used. These will be examined in Chapter 4.

Whatever the method, the aïm of these adjustments is to reduce the model-plant error to zero, i.e. the plant output matches the model output which in turn is equal to the required ideal output.

The case for signal synthesis adaption will not be discussed, since it is really only another form of "high gain" type of adaptive system, whose attendant problems have already been pointed out.

The fundamental advantage of the parameter adaption scheme when compared to high-gain schemes is that the parameter adaptive loop need only be fast enough to cope with environmental changes. The high gain loop on the other hand is required to be fast when compared to the frequency components of the model output. Thus the use of model reference parameter adaption reduces the likelihood of compromising the validity of the plant transfer function, with the assumption that the environmental changes are slow compared to the command frequency components.

3.4 Selection of the Model Reference Scheme as an Adaptive Control Philosophy

In Section 3.3, the various design philosophies have been reviewed. A summary of the relevant features of each method will now be presented.

1) Gain Scheduling

This technique is open-loop, and as such, does not suffer from stability problems. The open-loop nature of this scheme makes it useful only in the case where the environmental changes are

a) Measurable to good accuracy,

and b) Have a well-defined effect on the plant.

These systems get very complex when there are more than one or two environmental factors to compensate for. Also they can take no account of factors like ageing of system components or other unforeseen changes in the plant characteristics. It might therefore be possible to get a worse response with gain scheduling than if there were no adaptive scheme at all.

Gain scheduling may be used in some situations to compensate for perhaps one major well-defined environmental factor, but it would be desirable to also maintain some closed-loop adaption mechanism to provide an automatic, fine adjustment mode.

2) High Gain-Limit Cycle

This is a simple and effective scheme, but should be restricted to situations where

a) changes in plant parameters are small

b) plant transfer functions are valid up to high frequencies

or c) the environmental changes have components of the same order of frequency as the command inputs.

3) Ad-Hoc Ssytems

Those systems studied under this heading have the following major disadvantages:

a) command inputs must be rich in harmonic content

b) the adaptive strategy is only obvious for simple systems

c) the stability of the resulting system is not guaranteed

4) Test Signal Identification

The use of special test signals for the identification part of an adaptive controller introduces much complexity in terms of hardware. Once the identification is complete, i.e. impulse response calculated, it is not always obvious in which way that information could be used to calculate control. Also, it is seen that any technique involving special test signals is quite time consuming, limiting its use to plants with environmental factors that vary relatively slowly.

5) Model Reference

Model reference adaptive control systems have been the subject of much research in recent years. They have been seen to have the following features:

a) Applicability to a very general class of plant, c.f. the limitations of the Ad-Hoc systems.

b) Command signals are not required to be rich in harmonics.

c) The required performance is embodied in a model of the desired plant. This model can be realised easily by operational amplifier circuits, or a mathematical routine if a microprocessor is envisaged in the control system.

Quite often it is easier to specify the desired dynamic properties of a plant in terms of a model, than in terms of a numerical performance index, making design more straightforward.

d) The performance index function is obtained simply by taking the difference of two vectors, i.e.

P.I. = Model states - Plant states

Thus the estimation of system performance is not subject to large delays, c.f. test signal identification.

e) High gain loops around the plant are not necessarily required, c.f. High-gain Limit Cycle systems.

f) One objection that has been raised against model reference schemes is that the environment could change during a long period where command signals are absent. A sudden command would then catch the maladjusted system, and an undesirable response might occur.

This question will be discussed in Chapter 4, with particular regard to a model reference scheme synthesised using variable structure control.

Thus, the Model Reference form of adaptive control has clear advantages over the other proposed methods. It is therefore selected as a general philosophy for adaptive systems. Remembering, of course, that the ideas of gain scheduling and high-gain limit cycling have their limited place in the design of adaptive controllers.

CHAPTER 4

VARIABLE STRUCTURE SYSTEMS IN MODEL REFERENCE ADAPTIVE CONTROL

4.1 General

In chapter 3, the overall philosophies of adaptive control were discussed. It was shown that in general, the model reference type of approach has advantages in terms of performance, realisability and general applicability, when compared to other proposed methods of achieving adaptive behaviour.

This chapter will examine specific methods of synthesising model reference systems and will show that a variable structure type of approach can lead to particularly simple realisations. Also, variable structure strategies allow the transient adaptive response to be partly pre-defined. This ability to specify the form of the adaptive response over a range of operating conditions has not been a feature of previous adaptive schemes.

4.2 The selection of variable structure control as a design method for model reference adaptive systems (M.R.A.S.)

The general representation of a model reference adaptive control system has been shown in Fig. 3.19. Signal synthesis adaptation has already been discounted for general use, for reasons put forward in chapter 3. Thus the problem is now, in what way should parameters of the plant compensator be adjusted to produce a match between the plant output and the model output?

Many specific methods have been proposed, but most of them may be included in one of the more general headings listed below.

Adaptive system designed by:

1) Local parameter optimisation theory;

2) Estimation theory;

3) Stability theory.

These methods will now be considered in turn.

4.2.1 M.R.A.S. designed by local parameter optimisation theory

The general operation of this type of system may be described as follows. A quadratic index of performance (P.I.) is defined, that expresses the distance between the model and the adjustable system in terms of structure and states. Then surfaces of P.I. = Const are defined in the parameter space in the neighbourhood of the nominal point PI = 0. Parameter optimisation theory then gives us methods to change the parameters in order to go from one surface to another surface corresponding to a lower P.I. There are several of these methods available, i.e. the gradient method, the steepest descent method, the Newton-Raphson method.

The M.I.T. scheme[17] was historically the first adaptive scheme to provide a logical way of adjusting any arbitrary number of controller parameters, and this method may be included under the heading of a parameter optimisation technique.

Consider the plant of Fig. 4.1 with an environmental gain K_v. The M.I.T. rule then results[18] in the following equations, to achieve M.R.A.S. operation.

$$b_2\ddot{e} + b_1\dot{e} + e = (K - K_vK_c)u(t)$$

$$\dot{K}_c = B'e\theta_m \qquad 4.1$$

$$b_2\ddot{\theta}_m + b_1\dot{\theta}_m + \theta_m = K\,u(t)$$

as shown in Fig. 4.2. The equation for the error with u(t) = U = Const is thus

$$b_2\dddot{e} + b_1\ddot{e} + \dot{e} + KK_vB'U^2e = 0 \qquad 4.2$$

by application of the Routh-Hurwitz criterion, instability can result if

$$KK_vB'U^2 > \frac{b_1}{b_2} \qquad 4.3$$

i.e. if the adaptive loop gain is too high, or if the input signal U is too large.

It is a general result that M.R.A.S. designed by parameter optimisation are not necessarily guaranteed stable. This fact makes such designs unattractive when compared to M.R.A.S. designed by other methods.

4.2.2 M.R.A.S. designed by estimation theory

These methods[19,20] are basically applicable to systems that adaptively estimate either the states or the parameters of the plant. As such, they are suited to identification of systems rather than control. It is possible of course to adjust some compensating gain as a function of the estimate of a parameter that is varying in some unknown way. This, however, like the test signal identification method discussed in chapter 3 is rather an indirect way to realise adaptive control. This indirectness results in adaptive loops that are relatively slow.

4.2.3 M.R.A.S. designed by stability theory

The major advantage of these methods is that, as the name implies, the control laws are generated in such a way as to guarantee the stability of the resulting adaptive system.

Various methods have been devised to allow the synthesis of stable adaptive systems. However, there are three approaches that have been developed far enough to allow logical design of general adaptive problems. These are:

a) Use of Liapunov functions

b) Use of Hyperstability theory

c) Use of Variable Structure Systems

These will now be discussed.

4.2.3(a) M.R.A.S. design using Liapunov functions

Liapunov's direct method[21] is a well-known method of assessing the stability properties of dynamic systems. Briefly, the method is as follows. A positive definite function of the system states is formed. An example might be

$$V(\underline{x}) = x_1^2 + x_2^2 + x_3^2 \ldots\ldots x_n^2$$

The next stage is to get an expression for the time derivative of $V(\underline{x})$.

$$\text{i.e. } \dot{V}(\underline{x}) = \frac{dV(\underline{x})}{dt}$$

If $\dot{V}(\underline{x})$ is, or can be made negative definite, then asymptotic stability of the system will be assured.

By considering a simple example, the application of this technique to the MRAS problem will be shown. The system in Fig. 4.3 is to be adaptively controlled. The variable gain $B_c(t)$ is made up of a varying environmental gain and the compensating gain. The variable time constant $A_c(t)$ is similarly made up of an environmental part and a compensating part. The equations describing this system are.

$$\begin{aligned} \dot{x} &= A_m x + B_m u \\ \dot{y} &= A_c(t) y + B_c(t) u \\ e &= x - y \end{aligned} \qquad 4.4$$

A_m, $A_c(t)$...-Ve $\quad$ B_m, $B_c(t)$...+Ve

gives

$$\dot{e} = A_m e + [A_m - A_c(t)]y + [B_m - B_c(t)]u \qquad 4.5$$

choose a Liapunov function of

$$V = e^2 + \lambda_1[A_m - A_c(t)]^2 + \lambda_2[B_m - B_c(t)]^2 \qquad 4.6$$

λ_1, λ_2 $+V_e$ constant

Thus $$\dot{V} = -2\lambda_1[A_m - A_c(t)]\dot{A}_c(t) - 2\lambda_2[B_m - B_c(t)]\dot{B}_c(t) + 2e[A_m e + [A_m - A_c(t)]y + [B_m - B_c(t)]u] \qquad 4.7$$

If we choose $\dot{A}_c(t) = \frac{ey}{\lambda_1}$ and $\dot{B}_c(t) = \frac{eu}{\lambda_2}$ $\qquad 4.8$

then $\dot{V} = 2e^2 A_m$

Since A_m is negative, $\dot{V}$ will also be negative. Thus the system is stable and

$V \to 0$ as $t \to \infty$

This implies that the model-plant error and model-plant parameter differences also tend to zero with increasing time. Thus the adaptive

system is now as in Fig.4.4. Consider that, for the moment, $A_c(t)$ is equal to A_m, but that $B_c(t) \neq B_m$. Also, $\theta_m = \theta_p = 0$ and a step input $u(t) = U$ is applied.

From equations 4.8 and 4.5 we get

$$\ddot{e} - A_m\dot{e} + \frac{U^2 e}{\lambda_2} = 0 \qquad 4.9$$

This "adaptive step response" is seen to be highly dependent on the system input U. i.e. for small U the adaptive response is slow, first order. For large U, however, the response will be second order with an oscillatory, low damped solution.

This large variation of the adaptive response is clearly undesirable. In an attempt to overcome this problem a modified scheme has been suggested[22]. This leads to the system as shown in Fig. 4.5. The adaptive step response for this system is governed by

$$\ddot{e} + \dot{e}\,[\,U^2/\lambda_2 - A_m\,] + e\,U^2/\lambda_2 = 0 \qquad 4.10$$

A_m -ve

Thus the adaptive response is now well damped for very small and very large values of input. There will exist, however, some minimum value of damping factor at an input level that is intermediate between the two extremes. The damping factor of this system is thus less sensitive to input level than the original system of Fig.4.4. It does, however, still vary to some extent.

4.2.3(b) M.R.A.S. design using hyperstability theory

The concept of hyperstability was first introduced by Popov[23] in 1963. The resume of the results of Popov given in Appendix G, was presented by Landau[24]. In the same paper, Landau considers a M.R.A.S. described by the following equations:

$$\dot{x} = A_m x + B_m u \qquad 4.11$$

$$\bar{\theta}_m = C x \qquad 4.12$$

$$\dot{y} = A_s(t) y + B_s(t) u \qquad 4.13$$

$$\bar{\theta}_s = C y \qquad 4.14$$

$$\bar{\varepsilon} = \bar{\theta}_m - \bar{\theta}_s \qquad 4.15$$

$$V = D\,\bar{\varepsilon} \qquad 4.16$$

$$\dot{A}_s(t) = \Phi(v(\tau), t) \qquad \tau \leq t \qquad 4.17$$

$$\dot{B}_s(t) = \Psi(v(\tau), t) \qquad \tau \leq t \qquad 4.18$$

where A_m and B_m are respectively n x n and n x m dimensional constant matrices which define the model; $A_s(t)$ and $B_s(t)$ are respectively n x n and n x m dimensional time-variable matrices which define the real system; C is a r x n dimensional constant output matrix; D is a r x r dimensional constant matrix which defines a linear processing block of generalised error; $\bar{\theta}_m$, $\bar{\theta}_s$, $\bar{\varepsilon}$ are vectors which correspond to the model output, the real system output, and the generalised error. Φ and Ψ denote a nonlinear dependence between the elements of matrices $\dot{A}_s(t)$ and $\dot{B}_s(t)$ and the values of V in the interval $\tau \leq t$.

The aforementioned equations are represented in Fig.4.6.

The equations 4.11 - 4.18 may be represented in a form such that the hyperstability results can be applied. This leads to the following conditions for the asymptotic hyperstability of the above model reference scheme.

1) The transfer matrix $Z(s) = DC(SI - A_m)^{-1}$ must be strictly positive real;

2) The vectors $[A_m - A_s(t)]y$; $[B_m - B_s(t)]u$, v must be of the same dimension;

3) The computing blocks of the matrices $\dot{A}_s(t)$, $\dot{B}_s(t)$ must introduce functions with the following form

$$\Phi(t) = [\alpha_{ij}\ v_i\ y_j], \qquad \alpha_{ij} > 0 \qquad 4.19$$

$$\Psi(t) = [\beta_{ij}\ v_i\ u_j], \qquad \beta_{ij} > 0 \qquad 4.20$$

The adaptive control for the system of Fig. 4.3 has been considered[25] for solution by the method of hyperstability. The resulting scheme is shown in Fig. 4.7, and is in essence the same as that of Fig. 4.4, which was achieved by the Liapunov technique.

The hyperstability approach results again in systems whose adaptive step response will vary as a function of the demand input.

It is worth noting that the derivation of the adaptive laws in both the Liapunov and the hyperstability scheme usually assumes that the environment is fixed, constant, while the adjustable parameters are being adapted. In practice, this is unlikely to be the case and so simulation studies should still be performed to check the stability of such systems in the presence of large continuous environmental changes.

4.2.3(c) M.R.A.S. design using variable structure systems

The use of variable structure systems (VSS) in adaptive control is due to the fundamental property of VSS, that, it is possible to define a sliding mode which has parameters that are insensitive to variations in the plant dynamics. This may be seen by reference to Appendix A. The equation of the desired sliding mode (A2) is seen to be dependent only on the constants c_i $i = 1,\ldots,n$ which may be selected by the designer. In the rest of the design procedure the x_i are assumed to be related by

$$\dot{x}_i = x_{i+1} \qquad i = 1,\ldots,n-1$$

Thus, motion on the sliding plane may always be described by a fixed set of equations in state-space, which are not influenced by the variation of internal plant feedback parameters.

Young[26] has suggested a general method for designing variable structure adaptive systems. This method is based on a technique for designing multi-variable v.s.s. known as "The Hierarchy of Controls Method" (Appendix F). The general scheme is shown in Fig. 4.8. It is interesting to compare this to the general plan of hyperstable adaptive systems shown in Fig. 4.6. The variable gains $A_s(t)$ and $B_s(t)$ in the hyperstable system have been replaced by the switched variable structure gains Ψ_p and Ψ_m respectively. Also, an extra switched gain Ψ_e has been introduced. The equations describing the system are thus

$$\dot{e} = A_m e + (A_m - A_p)x_p + B_m u_m - B_p u_p \qquad 4.21$$

with variable structure control given by

$$u_p = \Psi_p x_p + \Psi_e e + \Psi_m u_m \qquad 4.22$$

By considering equ. 4.21 as an error equation $\dot{e} = A_m e$ subject to disturbance by x_p and u_m a sliding mode may be designed in the error state plane, that is insensitive to the aforementioned disturbances. The sliding mode is defined by

$$s = Ge = 0 \qquad 4.23$$

$e \in R^n$, G is an n x n matrix of positive constants.

Thus G can be chosen such that the sliding plane is asymptotically stable, and the plant-model, error vector will tend to zero in a well-defined manner when it is in the sliding mode, i.e. the plant response will approach the model response in a well-defined way.

Two assumptions are made in the design of this type of adaptive system

i) A_m, B_m, A_p, B_p satisfy

$$\text{rank } B_p = \text{rank } (B_p : B_m) = \text{rank } (B_p : A_m - A_p) \qquad 4.24$$

ii) A_p, B_p are unknown and may be time-varying, but the upper and lower bounds of A_p, B_p are known.

In his paper, Young considers the problem of adaptively controlling a subsonic aircraft. Simulated responses show a significant improvement in terms of adaptive error response, when compared to an adaptive controller designed[27] by Landau's hyperstability technique, for the same problem.

4.3 Discussion of model reference design methods

In general, the use of local parameter optimization theory leads to designs that are not necessarily guaranteed to be stable. Even quite simple systems synthesised by this method have been shown to be unstable for certain working conditions.

Adaptive systems designed by estimation theory are applicable mainly to the identification of plant states and plant parameters. Their use as controllers are thus limited to "slow" systems, due to the indirect way in which the plant-model error is evaluated.

The design of MRAC systems by stability theory has the major advantage that the convergence of the system to the required solution is assured. Of the stability methods, the variable structure system approach offers the following advantages over either the Liapunov or the hyperstability technique.

1) The adaptive response may be partly defined, since the final part of the adaptive process is in a sliding mode of operation. Such selection of the adaptive response is not a feature of Liapunov or hyperstability designed systems.

2) The vss scheme allows the plant parameters to vary, whilst the adaptive process is in operation and still guarantees global stability.

3) In the past, model reference schemes have been criticized on the grounds that if there is no input demand signal and the plant parameters change, there can be no adaption, because there is no plant-model error signal. The system would then be caught by a sudden input, in a totally unadapted state. For fast adaptation under these conditions, a Liapunov or hyperstability design would require very high adaptive gains, especially when input signal levels were low. The resulting adaptive responses would then be fast, but probably highly oscillatory. The vss scheme, however, can adapt very quickly due to the use of switched gains, whilst maintaining a well-behaved adaptive response.

4) A vss adaptive controller as shown in Fig. 4.8 has the advantage that the variable gains are only switched between two fixed levels, whereas a Liapunov or hyperstability design requires multipliers that can produce the product of two continuously varying signals. The vss scheme, therefore, offers easier implementation of the multiplication function, whether it be a hardware unit or a software routine.

The conclusion of this comparison of model reference design methods is that a variable structure approach can lead to designs that are simpler in structure and at the same time have a performance that is superior to that of the other techniques considered.

The following section will discuss various aspects of vss adaptive systems design.

4.4 Design techniques for variable structure adaptive systems

4.4.1 The equivalent control method

This method[28] is useful for the design of multi-variable vss. The general philosophy is as follows.

Consider the general vss described by

$$\dot{\underline{x}} = f(\underline{x}, t, \underline{u}) \qquad 4.25$$

$\underline{x} \in R^n$, $u \in R^m$, $f \in R^n$

u is a piecewise constant control vector.

A sliding plane is now defined

$$s = G\,\underline{x} \qquad 4.26$$

G is a constant n x n matrix $s \in R^n$

Now, impose the conditions

$$s = \dot{s} = 0 \qquad 4.27$$

i.e. $$s = G\,\underline{x} = 0 \qquad 4.28$$

and $$\dot{s} = G\,\dot{\underline{x}} = 0 \qquad 4.29$$

that is, if the system is on the sliding plane, it will stay on it, assuming no disturbances in the system. By substituting equations 4.28 and 4.29 into equation 4.25 a continuous control u_{eq} known as the equivalent control may be found in terms of the system states.

i.e. $$u_{eq} = \Omega\,\underline{x} \qquad 4.30$$

Ω is a constant m x n matrix.

To guarantee the existence of a sliding mode in a real system with disturbances, the matrix Ω must be replaced by a matrix Ω^+ which makes $\dot{s}_i > 0$ when s_i is measured as $s_i < 0$ and Ω is replaced by Ω^- giving $\dot{s}_i < 0$ when $s_i > 0$. Thus

$$\dot{s}_i \cdot s_i < 0$$

which is the condition for the existence of the sliding mode[29].

At the same time, Ω^+ and Ω^- must be chosen such that the sliding mode $s = 0$ is reachable from any initial condition in state space.

The design techniques given in Appendix A are a particular form of this philosophy and the Hierarchy of Controls in Appendix F is a more general application of the Equivalent Control method.

4.4.2 The use of filters in the switched gain paths

When a system is operating in a sliding mode, the variable structure gains will be switching continuously to maintain the system states on the sliding plane. These switched signals might excite modes in the plant, that are beyond our transfer function limit of validity c.f. Limit-cycle adaptive scheme. This problem may be solved by reference to the following property of vss.

When operating in a sliding mode, the variable structure control may be considered as consisting of two functions. That is, a high frequency switching component and a mean low frequency component. This mean control is equal to the equivalent control u_{eq}. Since the behaviour of the system is primarily dependent on the u_{eq} control, it seems feasible that the high frequency component could be removed, without affecting the correct operation of the system. Indeed, it has been shown[28] that the

use of first order filters to remove the high frequency components of the variable structure gains does not affect the correct performance of the vss.

Thus, the risk of compromising the plant transfer function may be considerably reduced by the use of such filters.

4.4.3 The use of an implied model

Young's model reference adaptive scheme using vss has been seen to bear resemblance to Liapunov and hyperstability systems. The difference is that the continuous gains are replaced by switched gains (possibly filtered) in the vss scheme. In this sense, it is a logical development in the field of adaptive control. It should not be forgotten though, that a sliding mode can be produced in the state space of the plant, without the use of any explicit model. This sliding mode will still be insensitive to parameter changes and the sliding mode response can be associated with a linear system as described in Appendix B. This "implied" model can be at most of order n-1 if the plant is of order n. However, lower orders of adaptive response are obtainable if the system is designed to have multiple intersecting sliding planes. For example, a third order plant might have two, two dimensional sliding planes that intersect. The system, sliding down this intersection (straight line) will exhibit a first-order response.

A slightly different approach is that the sliding plane is designed in the error-space of the plant. That is, the space whose axes are error, error rate and higher derivatives. The error in this case is between the plant input demand and the plant output. This type of operation has the advantage that at steady-state the error and its derivatives will be zero. The switching of error etc. feedback gains will not, therefore,

produce any jitter at the output of the plant in the steady-state condition.

It will be seen in chapter 6 that the reduction in the order of the plant response that occurs in adaptive vss with implied models may in some cases produce improvement from the point of view of optimal control.

4.4.4 The interaction of sliding modes

Two aspects of sliding mode interaction will be considered, i.e.

a) The elimination of some existing cross-coupling effect in a system.

b) The introduction of cross-coupling between independent systems.

4.4.4(a) The elimination of system cross-coupling

The basic principle of system decoupling will be illustrated by the use of a simple example.

Consider the system represented by Fig. 4.9 and described by equations 4.31

$$\begin{bmatrix} \dot{x}_1 \\ \dot{x}_2 \\ \dot{x}_3 \\ \dot{x}_4 \end{bmatrix} = \begin{bmatrix} -A_1 & A_3 & 1 & 0 \\ A_4 & -A_2 & 0 & 1 \\ -1 & 0 & 0 & 0 \\ 0 & -1 & 0 & 0 \end{bmatrix} \begin{bmatrix} x_1 \\ x_2 \\ x_3 \\ x_4 \end{bmatrix} + \begin{bmatrix} 0 & 0 \\ 0 & 0 \\ u_1 & 0 \\ 0 & u_2 \end{bmatrix} \qquad 4.31$$

We wish to remove the effects of A_3 and A_4 and make system 1 and system 2 independent. We thus define two sliding modes.

$$s_1 = \dot{x}_1 + c_1 x_1 = 0 \qquad 4.32$$

$$s_2 = \dot{x}_2 + c_2 x_2 = 0 \qquad 4.33$$

by setting s_1, s_2, $\dot{s}_1$ and $\dot{s}_2 = 0$ we get the equivalent control.

$$u_{1eq} = - x_1[\, c_1A_1 - c_1^2 - 1] - x_2[- c_2A_3] \qquad 4.34$$

$$u_{2eq} = - x_1[\, - c_1A_4] - x_2[c_2A_2 - c_2^2 - 1] \qquad 4.35$$

Coefficients for variable structure control can now be chosen as greater and less than the feedback coefficients of the equivalent control, to ensure the sliding mode exists and is reachable (c.f. Appendix A).

When the system now operates on the sliding modes, the trajectories of system 1 and system 2 will depend only on equations 4.32 and 4.33. The interaction is seen as a disturbance, and is automatically compensated for by the variable structure control.

In a similar way, more complex systems can be decoupled by the specification of independent sliding modes.

4.4.4(b) The introduction of cross-coupled modes in vss

It may be desirable, in some systems, to introduce cross-coupling between independent subsystems. Consider, for example, the system of Fig. 4.10, described by equations 4.36.

$$\begin{bmatrix} \dot{x}_1 \\ \dot{x}_2 \\ \dot{x}_3 \\ \dot{x}_4 \end{bmatrix} = \begin{bmatrix} -A_1 & 0 & 1 & 0 \\ 0 & -A_2 & 0 & 1 \\ -1 & 0 & 0 & 0 \\ 0 & -1 & 0 & 0 \end{bmatrix} \begin{bmatrix} x_1 \\ x_2 \\ x_3 \\ x_4 \end{bmatrix} + \begin{bmatrix} 0 & 0 \\ 0 & 0 \\ u_1 & 0 \\ 0 & u_2 \end{bmatrix} \qquad 4.36$$

Cross coupling is easily introduced by making the sliding mode of each subsystem dependent on a state in the other.

i.e. $s_1 = \dot{x}_1 + c_1x_1 + A_3x_2 = 0$

$$s_2 = \dot{x}_2 + c_2x_2 + A_4x_1 = 0$$

The equivalent control is easily calculated by substitution of the sliding conditions into the system equations and thus the variable structure gains can be calculated in the usual way.

Thus the design results in two first order systems with cross coupling, when the sliding mode is reached.

CHAPTER 5

OPTIMAL CONTROL OF VARIABLE STRUCTURE SYSTEMS

5.1 General

This aspect of variable structure systems has had a relatively small amount of research effort devoted to it, compared say, to the adaptive properties of VSS. Also, there are only a very few examples of papers that actually show, in a quantitive manner, that a variable structure system designed by optimal control theory can exhibit better performance than a linear scheme. In one of the papers[3] that does show the advantages of VSS, it is seen that a second order system with variable damping has a much smaller mean squared tracking error for a range of sinusoidal inputs, then can be obtained with a linear (fixed damping) design.

This type of improvement is thus the incentive for studying the optimal design for VSS.

In this chapter, the synthesis of optimal VSS with constrained control vectors will be considered. This restriction is considered to be justified by the fact that the controls in any real system will be subject to some limit. Also, it will be seen that the form of optimal control for such systems may often be bang-bang, which is particularly easy to realise in practice. It will then be shown that optimisation via the Maximum Principle of Pontryagin provides a very convenient route for the determination of specific control laws. Even so, the techniques to date for the establishment of the optimal controls will be seen to be very indirect.

A new, much more direct method of obtaining the optimal strategy for a class of VSS will be introduced in preparation for the full development of this technique in Chapter 6.

5.2 The Techniques of Optimal Control

The topic of optimal control is concerned with the determination of the control law that in some sense produces the best performance from a system. A quantitive measure of this performance can be obtained by defining a performance index I.

Given that the system to be controlled can be expressed in state-space form, i.e.

$$\dot{\underline{x}} = f(\underline{x},\underline{u})$$
$$\underline{x}(t_o) = \underline{x}t_o \qquad \underline{x}(t_1) = \underline{x}t_1 \qquad 5.1$$

where $\underline{x}(t_o)$, $\underline{x}(t_1)$ are the states at the beginning of the process and the end of the process respectively. A fairly general performance index may now be defined as

$$I = \int_{t_o}^{t_1} f_o(\underline{x},\underline{u})dt \qquad 5.2$$

The optimal control is now that which either maximises or minimises I, depending on the particular form of the function f_o. The techniques for evaluating the optimal control policy may be divided into three specific areas.

Namely,

1) Calculus of Variation;

2) Dynamic Programming;

3) The Maximum Principle.

These techniques will now be discussed in turn, with regard to the specific problem of optimising variable structure systems with constraints on the control vector.

5.2.1 Calculus of Variations

The application of differential calculus to the problem of maximising or minimising equation 5.2 leads to a special form of calculus called "The Calculus of Variations". By use of this technique we get, for the system of equations 5.1 and 5.2, the so-caller Euler-Lagrange (E-L) equation. This equation provides a relationship between the system structure f, the performance index function f_o and the inputs $\underline{u}$, for the control to be optimal.

One form of the E-L equation is as follows[30]

$$\frac{\partial f_o}{\partial \underline{x}} - \frac{\partial f_o}{\partial \underline{u}} \frac{\partial f/\partial \underline{x}}{\partial f/\partial \underline{u}} - \frac{d}{dt}\left(\frac{\partial f_o/\partial \underline{u}}{\partial f/\partial \underline{u}}\right) = 0 \qquad 5.3$$

The optimal control is thus not available explicitly; instead, the differential equation of 5.3 must be solved. In general, the E-L equations cannot be integrated into any analytical solutions, so numerical methods must be used. By the use of such methods, optimal controls may be found, but any possible relationship that exists between the system and the optimal control will be obscured by the numerical process. Also, a considerable amount of programming could be required to solve equation 5.3.

Another problem that arises with the calculus of variations, is the handling of systems with control vector constraints. One possible way to account for such systems is to introduce a modified performance index, i.e.

$$I' = \int_{t_o}^{t_1} \left[f_o(\underline{x},\underline{u}) + \left(\frac{u}{u_{max}}\right)^{100} \right] dt \qquad 5.4$$

Thus, when $u < u_{max}$, the term $\left(\frac{u}{u_{max}}\right)^{100}$ is very small; when, however, $u > u_{max}$, then $\left(\frac{u}{u_{max}}\right)^{100}$ is very large. The control u is effectively limited to u_{max}, since the $u > u_{max}$ condition is very heavily penalised.

Such complications lead to E-L equations that can never have analytical solutions, leading to the use of numerical methods with even more complexity.

Thus, the calculus of variations is not well suited to the problem of finding the optimal control for VSS with constrained control.

5.2.2 Dynamic Programming

The technique of Dynamic Programming is a numerical method which is best carried out on a digital computer. The control process to be studied must therefore be converted to a discrete form to be compatible with the discrete nature of digital computer data techniques.

Dynamic Programming is basically a searching technique that examines the effect of various possible control values over a small time period, that is, one of N subdivisions of the total time of the process. The search might typically proceed as follows:-

The system states have an initial condition $\underline{x}(t_o) = \underline{x}t_o$, say. The possible values of control are then divided into r discrete levels. The process time $t_1 - t_o$ is divided into N smaller time periods. The effect of each possible control level is then calculated for the first small time period. Thus, we now have r positions of the states and their corresponding performance index costs, at the end of the first

time period. These positions may now act as initial conditions for a similar operation over the second time period. And so this procedure can be repeated until the final time of the process is reached. The cost of travelling each of the many paths from xt_o to xt_1 (final state) may now be calculated, and the best path found, together with its optimal control.

The method of dynamic programming is due to Bellman[31] and is a particularly efficient search method which makes use of the "Principle of Optimality", which can be stated as follows:-

A policy which is optimal over the interval $0 \rightarrow N-1$ is necessarily optimal over any subinterval $V \rightarrow N-1$, where $0 \leq V < N-1$.

This property drastically reduces the amount of computation required to find the optimal control corresponding to the maximum or minimum cost.

Dynamic programming can certainly be applied to VSS with constrained control. In fact, the constrained control makes things easier for dynamic programming. This is because we have less options on the control level, and thus less searching to do.

As with any numerical technique, we will lose insight and miss any possible relationships that might exist between the optimal strategy and structure of the system. It will be seen that there exists a better method of finding the optimal controls for VSS, that does indeed highlight such relationships.

5.2.3 The Maximum Principle

This technique was developed by L.S. Pontryagin[32]. A resume is given in Appendix C.

As distinct from the calculus of variations, the maximum principle is formulated with the control vector $\underline{u}$ to be constrained within a closed bounded region.

The great advantage of the maximum principle is that the control is decided by the maximisation (minimisation) of a function instead of the minimisation (maximisation) of a functional. That is, the Hamiltonian equation C4 is a function of the instantaneous input only, whereas the functional, equation 5.2 depends on the input $\underline{u}(t)$ at all times over the interval $t_o < t < t_1$.

For many systems, the optimal control turns out to be bang-bang. This may be seen by straightforward inspection of the Hamiltonian function. Such features are not simply revealed by the calculus of variations or the dynamic programming method. The remaining problem is then the determination of when to switch the controls. This will be considered shortly. It is thus felt that the maximum principle is, of the optimal techniques considered, the most suited for the analysis and synthesis of VSS with constrained controls, this being because it is naturally formulated with restricted controls, and the form of the optimal control is found very quickly, with little calculation.

The following section will explore more deeply, the design of optimal variable structure systems, from the point of view of the maximum principle.

5.3 The Maximum Principle and the Design of Variable Structure Systems

A summary of the maximum principle is given in Appendix C.

The general procedure for calculating optimal control is then as follows:-

The problem is represented in state-space format and an index of performance is defined. The Hamiltonian function

$$H \triangleq \langle \underline{p}, f \rangle \qquad 5.5$$

is obtained, where $\langle \underline{p}, f \rangle$ is the inner product of $\underline{p}$ and f.

i.e. $H = p_1 f_1 + p_2 f_2 + , \ldots , p_n f_n$

It has been seen[33] that for the VSS described by

$$\dot{\underline{x}} = g(\underline{x},t) + \underline{u}h(\underline{x},t) \qquad 5.6$$

$$I = \int_{t_o}^{t_1} g_o(\underline{x}(t),t)\, dt \qquad 5.7$$

That the Hamiltonian may be written

$$H = \psi(\underline{x},\underline{p},t) + u\phi(\underline{x},\underline{p},t) \qquad 5.8$$

where

$$\psi(\underline{x},\underline{p},t) = \langle \underline{p}, g \rangle - g_o \qquad 5.9$$

$$\phi(\underline{x},\underline{p},t) = \langle \underline{p}, h \rangle \qquad 5.10$$

From 5.8 the optimal control is seen to be

$$u = \begin{cases} A \text{ if } \phi(\underline{x},\underline{p},t) > 0 \\ B \text{ if } \phi(\underline{x},\underline{p},t) < 0 \end{cases} \qquad 5.11$$

assuming I to be minimised
where A is the maximum value of u

and B is the minimum value of u

i.e. bang-bang control.

The costate equations

$$\dot{\underline{p}} = F(\underline{p},\underline{x},\underline{u}) \qquad 5.12$$

may now be obtained from the canonical equations C5 and C6

$$\text{i.e. } \frac{d\underline{p}_i}{dt} = -\frac{\partial H}{\partial \underline{x}_i} \qquad 5.13$$

It has been seen that if the VSS can be represented in the form of equations 5.6, 5.7 that the control will be bang bang. Equation 5.7 includes such performance indexes as minimum time and quadratic types. Given that the control is bang-bang, the next problem is the determination of when the controls switch between their extreme limits. The treatment of this problem is affected by the form of the initial states $x(t_o)$ and the final states $x(t_1)$. If both $x(t_o)$ and $x(t_1)$ are specified, we have to solve a "two-point boundary value problem" (TPBVP). In general, it is not possible to find an analytical solution to a TPBVP, and a numerical technique will have to be used. If, however, we do not specify $x(t_o)$, but we do say that $x(t_1)$ must lie on some smooth surface (target set), it is possible to establish relationships between the state and costate systems, that allow the control switching laws to be found. This is achieved as follows.

The transversality condition (Appendix C) gives the relationship between the state and costate system on the target set at time t_1. A particular point may be chosen on the target set, giving $x(t_1)$ and $p(t_1)$. The state-costate system may now be integrated backwards in time. For the system in question the switching function $\phi(\underline{x},\underline{p},t)$ (equation 5.10) will be known explicitly in terms of $\underline{x}$ and $\underline{p}$. Thus, the control u will be known at all times from equation 5.11. When $\phi(\underline{x},\underline{p},t)$ changes sign, $\underline{u}$ will switch. The system states will be known when the control switches, so a point will be obtained in state-space,

either side of which the control will be different.

By repeating this process many times, i.e. running the system backwards in time from many 'initial' conditions on the target set, the switching points will build up to form a switching surface. This surface thus divides regions of constant control in state-space.

Therefore the optimal switching law may be obtained in terms of a switching surface of known position in state-space, as shown diagrammatically in Fig. 5.1 for a second order system.

5.3.1 Singular Modes

For the adaptive VSS considered in Chapter 4 the adaptive action was due to the system operating in a sliding or singular mode. Such modes can also occur in VSS designed by optimal control. With reference to equation 5.11, it should be noted that u is not defined for $\phi(\underline{x},\underline{p},t) = 0$. The singular condition then arises when $\phi(\underline{x},\underline{p},t) = 0$ for some finite time period. We shall examine this condition further, by considering the following example.

A system is described by the following equations

$$\begin{aligned} \dot{x}_1 &= x_2 \\ \dot{x}_2 &= -x_1 - ux_2 \end{aligned} \qquad 5.14$$

$$I = \int_{t_o}^{t_1} (q_1 x_1^2 + q_2 x_2^2)dt \qquad 5.15$$

q_1, q_2 positive constants and u = some bounded control.

The Hamiltonian is

$$H = p_1 x_2 - p_2 x_1 - p_2 x_2 u - q_1 x_1^2 - q_2 x_2^2 = 0 \qquad 5.16$$

$H = 0$ on the assumption that the final time of the process is free.

The optimal control is thus

$$u = U_{max} \text{ if } p_2 x_2 < 0$$
$$u = U_{min} \text{ if } p_2 x_2 > 0 \qquad 5.17$$

The singular condition occurs if

$$p_2 x_2 = 0 \text{ for some finite time}$$

i.e. either $p_2 = \dot{p}_2 = 0$ or $x_2 = \dot{x}_2 = 0$

The costate equations for this system are

$$\dot{p}_1 = p_2 + 2q_1 x_1$$
$$\dot{p}_2 = -p_1 + 2q_2 x_2 \qquad 5.18$$

If $x_2 = \dot{x}_2 = 0$ then from equation 5.14

$$x_1 = 0$$

Since the origin ($x_1, x_2 = 0$) is not reachable in finite time from a finite initial condition, any singular mode must be due to $p_2 = \dot{p}_2 = 0$.

Whence equation 5.18 gives

$$\dot{p}_1 = 2q_1 x_1$$
$$p_1 = 2q_2 x_2 \qquad 5.19$$

Substituting equation 5.19 and $p_2 = 0$ into the Hamiltonian gives

$$H = q_2 x_2^2 - q_1 x_1^2 = 0 \qquad 5.20$$

i.e. either $\sqrt{q_2}\, x_2 = \sqrt{q_1}\, x_1 \qquad 5.21$

or $\sqrt{q_2}\, x_2 = -\sqrt{q_1}\, x_1 \qquad 5.22$

The former case represents an unstable switching line, and is therefore discarded. The optimal singular condition is thus

$$\sqrt{q_2}\, x_2 = -\sqrt{q_1}\, x_1 \qquad 5.22$$

which implies that

$$u = (\sqrt{q_1}/\sqrt{q_2}) + (\sqrt{q_2}/\sqrt{q_1}) \qquad 5.23$$

in the singular mode.

If u can attain this value, the singular mode will exist. If, however, the condition of equation 5.23 cannot be met, then the singular mode will not appear.

The fundamental cause of the singular mode may be understood by considering the Ideal Model Concept (Appendix E). It can now be seen that the singular trajectory represented by equation 5.22 corresponds to the ideal model for the performance index of equation 5.15. This is hardly surprising since the ideal model principle tells us that if the system is in a state such that equation 5.22 holds, then for a performance index of equation 5.15, the optimum trajectory is that which stays on the line defined by equation 5.22.

The features of this example have also been shown[34] to be true in the more general case of an n dimensional VSS described by

$$\dot{\underline{x}} = A\underline{x} + \underline{u}\underline{x}$$

$$I = \frac{1}{2}\int_0^\infty (\underline{x}(t), Q\,\underline{x}(t))\, dt$$

$\dot{x}$, x are n dimensional vectors;

A is a constant n x n matrix;

u is the n x n control matrix;

( ) denotes the scalar product of the vectors named therein;

Q is a diagonal, positive definite matrix.

We may therefore conclude that

a) Singular modes in VSS are a function of the performance index parameter Q only.

b) The behaviour of the system in the singular mode corresponds to the "Ideal Model" for the particular performance index.

c) The singular mode can only exist if the variable structure controls have a sufficiently large range.

The estimation of the optimal switching curve for systems with singular modes, using the methods of Section 5.3 may therefore be shown diagrammatically as in Fig. 5.2.

5.3.2 Time-Optimal Variable Structure Systems

For the case where the performance index is minimum time, i.e.

$$I = \int_{t_o}^{t_1} 1 \, dt \qquad 5.24$$

it may be seen that no singular trajectories exist. i.e. let a general VSS be represented as follows:

$$\begin{aligned}
\dot{x}_1 &= K_1 x_2 - x_1 [u_1 N_1 + D_1] \\
\dot{x}_2 &= K_2 x_3 - x_2 [u_2 N_2 + D_2] \\
&\vdots \qquad\qquad 5.25 \\
\dot{x}_{n-1} &= K_{n-1} x_n - x_{n-1} [u_{n-1} N_{n-1} + D_{n-1}] \\
\dot{x}_n &= -K_n x_1 - x_n [u_n N_n + D_n]
\end{aligned}$$

K_i, N_i, D_i positive constant $i = 0,1,\ldots,n$

The Hamiltonian as a function of u_i is

$$H(u) = x_1 p_1 N_1 u_1 + x_2 p_2 N_2 u_2 + \ldots + x_n p_n N_n u_n \qquad 5.26$$

The costate equations are

$$\begin{aligned}
\dot{p}_1 &= K_n p_n + [u_1 N_1 + D_1]\, p_1 \\
\dot{p}_2 &= -K_1 p_1 + [u_2 N_2 + D_2]\, p_2 \\
\dot{p}_3 &= -K_2 p_2 + [u_3 N_3 + D_3]\, p_3 \qquad 5.27 \\
&\vdots \\
\dot{p}_n &= -K_{n-1} p_{n-1} + [u_n N_n + D_n]\, p_n
\end{aligned}$$

The singular condition occurs when

$x_i p_i = 0$ for a finite time period.

This implies either

$$\dot{x}_i = x_i = 0 \quad \text{or} \quad \dot{p}_i = p_i = 0 \qquad 5.28$$

over this period.

By examination of equations 5.25 and 5.27 it can be seen that the condition of equation 5.28 will only be met if either

$$x_1 = x_2 = x_3 = \ldots\ldots = x_n = 0$$

or $$p_1 = p_2 = p_3 = \ldots\ldots = p_n = 0$$

Since neither of these conditions can be reached in finite time (assuming non-zero initial conditions), we conclude that no singular trajectories exist.

An intuitive way of looking at this result is as follows. If a singular mode exists, the control must be able to cause the system to cross the singular surface from either side of the said surface. This must require that the control can produce systems with a faster mode and a slower mode than the singular mode. If a faster mode exists, this will be favoured for time-optimal properties when compared to a singular mode.

5.3.3 Sufficiency Conditions

In general, the maximum principle gives only the necessary conditions for controls to be optimal. The sufficiency conditions for bang-bang VSS to be optimal have been found by Boltyanskii[35], and are presented in Appendix H.

Briefly they are

1) The optimal trajectories intersect the switching surface with non-zero angle at a finite number of points.

2) The performance index is a continuous function of $\underline{x}$.

5.4 Review of Available Methods for Obtaining Switching Laws for Variable Structure Systems

Mohler and Rink[2,3] have used a method based on the techniques described in section 5.3 to calculate points on the optimal switching curve for a second order system. The applicability of the technique to higher order systems is noted. As was mentioned previously, the system equations require to be integrated backwards in time repeatedly to produce a reasonable picture of the whole switching curve in state-space.

Mohler and Moon[36] have developed a numerical technique for the determination of switching points, called the Switching Time Variation Method (STVM). This method uses a gradient type of search procedure to calculate the optimum time to switch a variable structure gain when the initial and terminal states of the system are specified. It is assumed that the controls are non-singular. The STVM again, only produces one switch point upon each application.

The paper of Buyakas[34] is concerned mainly with the optimality of VSS with singular solutions and shows that the optimal singular switching plane depends, in the case considered, only on the parameters of the quadratic performance index.

In their book[37], Mohler and Ruberti include a paper by Knudsen which investigates a method for finding the near-optimal controls for a system described by

$$\dot{x} = f(\underline{x},\underline{u}) \qquad |u| \leq 1 \qquad 5.29$$

The method is then based on a numerical technique, performed by a digital computer. By specifying the coarseness of the numerical search, the optimal controls can be found to any specific accuracy. Although the class of systems described by equation 5.29 is quite broad, the author only gives examples of a second and a third order linear time-optimal system with bang-bang control. Even for these simple systems, it is seen that the amount of computation required is quite considerable. It is thus noted that existing methods for the determination of the optimal switching curves of VSS with non-singular controls are very indirect, requiring repeated integration of the system equations for the estimation of successive points on the switch curve. Clearly, it would be highly desirable if, instead, the optimal curve could be produced in a more direct fashion.

5.5 Towards a More Direct Method of Optimal Switch Curve Generation

As part of the present research, a method has been developed which enables the time optimal switching curve of a class of variable structure systems to be generated in a much more efficient way than previous methods. This technique is based upon certain relationships between the state-costate trajectories on the target set, and a method of mechanising the maximum principle equations such that the state costate equations only require to be integrated once to produce a continuous switching curve.

CHAPTER 6

THE DIRECT GENERATION OF THE TIME-OPTIMAL SWITCHING CURVES FOR A CLASS OF VARIABLE STRUCTURE SYSTEM

6.1 General

It has been seen in chapter 5 that the maximum principle provides a particularly convenient way of finding the optimal controls for variable structure systems. The main problem with this method, however, is that the switching curve as a function of the system states can only be obtained point by point, using the methods described to date. In this chapter, a technique is developed that can generate the time optimal switch curves for a class of vss in a continuous manner, whilst requiring that the system equations are only integrated once. This compares with the many integrations necessary with the existing techniques.

The method presented here is basically a mechanisation of the maximum principle equations, which utilise certain relationships between the state system and the costate system on the "target set", i.e. the set of points that consists of all the possible terminal conditions for the optimal trajectory, as described in Appendix C.

6.2 Statement of the Problem

The system to be considered is described by the following equations

$$\begin{aligned} \dot{x}_1 &= K_2 x_2 - u_1 x_1 \\ \dot{x}_2 &= -K_1 x_1 - u_2 x_2 \end{aligned} \qquad 6.1$$

and may be represented as in Fig, 6.1

where K_1, K_2 are positive constant

and $u_{1\,min} < u_1 < u_{1\,max}$

$u_{2\,min} < u_2 < u_{2\,max}$

u_1, u_2 are positive

A target set is defined which has the following form

$$Ax_1^2(t_1) + Bx_2^2(t_1) = R^2 \qquad 6.2$$

where A, B, R are positive constant

t_1 is final time of the process.

The problem is then to choose u_1, u_2 in such a way as to steer the system from any initial condition $x(t_o)$ to the target set, in minimum time.

6.3 Problem Solution

The performance index for the minimum time optimal control problem may be written

$$I = \int_{t_o}^{t_1} 1 \, dt \qquad 6.3$$

where t_o, t_1 are the initial time and final time respectively of the process.

We can now define the auxiliary state (Appendix C) as

$$x_o \triangleq \int_{t_o}^{t_1} 1 \, dt \qquad 6.4$$

The augmented state equations are now

$$\begin{aligned} \dot{x}_o &= 1 \\ \dot{x}_1 &= K_2 x_2 - u_1 x_1 \\ \dot{x}_2 &= -K_1 x_1 - u_2 x_2 \end{aligned} \qquad 6.5$$

The corresponding costate equations are

$$\begin{aligned} \dot{p}_o &= 0 \\ \dot{p}_1 &= K_1 p_2 + u_1 p_1 \\ \dot{p}_2 &= -K_2 p_1 + u_2 p_2 \end{aligned} \qquad 6.6$$

The Hamiltonian for this problem is

$$H = K_2 x_2 p_1 - u_1 x_1 p_1 - K_1 x_1 p_2 - u_2 x_2 p_2 - 1 = 0 \qquad 6.7$$

The optimal controls are thus

$$\begin{aligned} u_1 &= u_{1\,max} \quad \text{if} \quad x_1 p_1 < 0 \\ u_1 &= u_{1\,min} \quad \text{if} \quad x_1 p_1 > 0 \\ & \qquad\qquad\qquad\qquad 6.8 \\ u_2 &= u_{2\,max} \quad \text{if} \quad x_2 p_2 < 0 \\ u_2 &= u_{2\,min} \quad \text{if} \quad x_2 p_2 > 0 \end{aligned}$$

It is immediately obvious that the x_1 axis ($x_2 = 0$) and the x_2 axis ($x_1 = 0$) are switching lines.

The remaining problem is to find the loci of points in the x_1, x_2 plane that correspond to the cases of $p_1 = 0$ or $p_2 = 0$.

Let the state-costate equations be written in matrix form, i.e. equations 6.1 and 6.6 become

$$\dot{\underline{x}} = A_x \underline{x} = \begin{bmatrix} -u_1 & K_2 \\ -K_1 & -u_2 \end{bmatrix} \underline{x} \qquad 6.9$$

$$\dot{\underline{p}} = A_p \underline{p} = \begin{bmatrix} u_1 & K_1 \\ -K_2 & u_2 \end{bmatrix} \underline{p} \qquad 6.10$$

The solution to the problem now requires that the reverse time trajectories of the state-costate system are considered. Thus, equations in the rest of this chapter will refer to the system operating with reverse time flow. The initial condition for the system is thus somewhere on the target set.

In reverse time, equations 6.9 and 6.10 become

$$\dot{\underline{x}} = \begin{bmatrix} u_1 & -K_2 \\ K_1 & u_2 \end{bmatrix} \underline{x} \qquad 6.11$$

$$\dot{\underline{p}} = \begin{bmatrix} -u_1 & -K_1 \\ K_2 & -u_2 \end{bmatrix} \underline{p} \qquad 6.12$$

6.3.1 Optimal Conditions on the Target Set

In Appendix C it has been seen that the following relationships hold on the target set defined by equation 6.2

$$\begin{aligned} p_{10} &= \lambda A x_{10} \\ p_{20} &= \lambda B x_{20} \end{aligned} \qquad 6.13$$

It is implied by the maximum principle[38] that the initial direction of the costate vector points towards the interior of the target set. Thus, it is seen that

$$\lambda < 0 \qquad 6.14$$

Condition 6.14 and equation 6.13 may now be substituted into equation 6.8 to give the initial controls as

$$u_{10} = u_{1\,max}$$
$$u_{20} = u_{2\,max} \qquad 6.15$$

Consider the Hamiltonian for points on the target set. Substituting equation 6.13 into equation 6.7 gives

$$H(o) = K_2 x_{20}\, \lambda A x_{10} - u_{1\,max}\, \lambda A x_{10}^2 - K_1 x_{10}\, \lambda B x_{20}$$
$$- u_{2\,max}\, \lambda B x_{20}^2 - 1 = 0 \qquad 6.16$$

$$\therefore \lambda = \frac{-1}{u_{1\,max} A x_{10}^2 + u_{2\,max} B x_{20}^2 + K_1 x_{10} x_{20} B - K_2 x_{10} x_{20} A} \qquad 6.17$$

For the condition of equation 6.14 to hold, for all x_{10}, x_{20}, K_1 and K_2 in equation 6.17 we must have

$$K_1 x_{10} x_{20} B - K_2 x_{10} x_{20} A = 0$$

i.e. $K_1 B - K_2 A = 0$

Thus given K_1 and K_2 as fixed, A and B can be chosen to satisfy

$$\frac{A}{B} = \frac{K_1}{K_2} \qquad 6.18$$

Whilst the absolute values of A and B may be made as small as required, to approximate the target set to the origin.

The interpretation for the case when equation 6.14 does not hold is that there exist regions on the target set that do not contain any points that form the ends of minimum time trajectories. Such "shaded regions" are illustrated in Fig. 6.2.

6.3.2 Consideration of the Reverse-Time Trajectories from the Target Set

The development of the technique now continues, with the following assumptions:

a) The system has a variable structure control u_1 or u_2, but not both simultaneously. The unused control may, however, take on a fixed value.

b) The final (in forward time) switch of control before the target set is reached, is due to a change in sign of a costate variable. Previous research[3] indicates that this is usually the case.

Consider the equation 6.11. It is clear that the reverse time trajectories can only cross the state axes in certain ways. Fig. 6.3 illustrates this point. Thus, the crossings must be made in an anti-clockwise direction.

Consider now the case where u_1 is fixed and u_2 is the control. The initial state of the system is somewhere on the target set in quadrant 3 or 4 (say). Also we have $u_2 = u_{2\ max}$. The switch curve cannot start in quadrant 3 since there would be trajectories originating from the target set in quadrant 4 that would encounter the positive x_1 axis first, to produce a control switch. This is false by assumption (b). Similarly, the switch curve cannot start in quadrant 1; the x_1 axis again would be encountered first. We therefore conclude that the switch curve must originate from the point where the target set intersects the positive x_1 axis, and then continues in quadrant 4.

Similarly, for initial conditions in the first and second quadrant, the switch curve will start at the intersection between the target set

and the negative x_1 axis.

Switch curves when the control is u_2 must therefore originate as shown in Fig. 6.4.

Similar arguments lead to the equivalent case for the situation where u_1 is the control, as shown in Fig. 6.5.

By assumption (b) we may see that for all points on the target set the reverse time trajectories will encounter first, the switch curve due to the costate variables. This curve is thus a function of the system with $u = u_{max}$ only, since the condition $u = u_{min}$ occurs for the first time only after the switch curve is crossed. It is this important property that allows the switch curve to be directly generated.

6.3.3 Time Domain Solution of the State-Costate Equations

The following results are well known, and are quoted here for easy reference.

Given a system in state-space form

i.e. $\dot{\underline{x}} = A\underline{x}$ 6.19

with initial conditions $\underline{x}(o) = \underline{x}_o$

The time domain solution is then

$\underline{x}(t) = e^{At}\underline{x}_o$ 6.20

We can also define the so-called transition matrix

$\Phi \triangleq e^{At}$ 6.21

The solution to equation 6.19 may also be written

$\underline{x}(t) = \mathcal{L}^{-1}[(sI - A)^{-1}]\underline{x}_o$ 6.22

with $\Phi = \mathcal{L}^{-1}[(sI - A)^{-1}]$ 6.23

where $\mathcal{L}$ is the Laplace operator.

If either a digital or an analogue computer is used to simulate the system by the computation of equation 6.20 (say), then by comparing equations 6.22 and 6.23, we can see that if

$$x_{10} = 1 \qquad x_{20}, x_{30}, \ldots, x_{no} = 0$$

then $x_1(t) = \phi_{11}$, $x_2(t) = \phi_{21}$, ..., $x_n(t) = \phi_{n1}$

where ϕ_{ij} is an element of Φ.

By choosing different initial states to be unity, different columns of the transition matrix may be generated.

6.3.4 Generation of the State-Costate Transition Matrix Elements

It is desired that the transition matrices for equation 6.11 and 6.12 with $u = u_{max}$ are to be generated.

We therefore define the following transition matrices

$$B(t) = \begin{bmatrix} b_1(t) & b_2(t) \\ b_3(t) & b_4(t) \end{bmatrix} \triangleq e^{A_x t} \qquad 6.24$$

and $$C(t) = \begin{bmatrix} c_1(t) & c_2(t) \\ c_3(t) & c_4(t) \end{bmatrix} \triangleq e^{A_p t} \qquad 6.25$$

with $u = u_{max}$ and time in reverse flow.

i.e. $$x_1(t) = b_1(t)x_{10} + b_2(t)x_{20} \qquad 6.26$$
$$x_2(t) = b_3(t)x_{10} + b_4(t)x_{20}$$

and $$p_1(t) = c_1(t)p_{10} + c_2(t)p_{20} \qquad 6.27$$
$$p_2(t) = c_3(t)p_{10} + c_4(t)p_{20}$$

By reference to section 6.33 it may be seen that the elements of B(t) and C(t) may be generated by the arrangements shown in Fig.6.6 and Fig.6.7 respectively.

6.3.5 Continuous Generation of the Optimal Switch Curve

Equations 6.26 and 6.27 may be viewed by considering the transition matrix as a linear transformation through which the initial states $\underline{x}_o$ or $\underline{p}_o$ are transformed into the current states $\underline{x}(t)$ or $\underline{p}(t)$. By considering time at one instant, i.e. $t = t_1$ (say) we get B(t) and C(t) as constant matrices. If we now let $\underline{x}_o$ and $\underline{p}_o$ vary, we get $\underline{x}(t_1)$ and $\underline{p}(t_1)$ for various initial conditions.

It is easy to see that if p_{10}, p_{20} lie on some closed target set that contains the origin, that for any $c_3(t_1)$, $c_4(t_1)$, $c_1(t_1)$ and $c_2(t_1)$ in equation 6.27 we can choose p_{10}, p_{20} such that $p_2(t_1)$ or $p_1(t_1)$ are zero.

The method of continuous switch curve generation thus operates as follows.

As the transition matrix elements vary with time, the initial costate conditions are continuously adjusted to maintain either $p_1(t)$ or $p_2(t)$ at zero. Thus we have the condition for either u_1 or u_2 to switch. Since $\underline{x}_o$ is known as a function of $\underline{p}_o$, we can obtain $\underline{x}(t)$ at all times for these conditions. Fig. 6.8 shows this process in a control system form.

The selected costate variable is amplified. This signal then causes the initial condition of the state to be rotated around the target set. The costate initial condition is thus also rotated. When the initial condition is reached that reduces the selected

costate variable to zero, the rotation ceases. The loop gain K_L is selected to cause this process to be much faster than the dynamics of the transition matrices. Thus the selected costate is approximately zero for all time. The sign of K_L determines which of the two sections of the required switch curve is produced.

6.3.6 Practical Examples of Optimal Switch Curves

The system of Figures 6.6, 6.7 and 6.8 has been realised in terms of a digital computer simulation, using the C.M.S.[39] simulation routine. Details of this program are given in Appendix I.

The first example considered is described by the following equations

Example 1

$$\dot{x}_1 = 0 + 10x_2 \qquad 6.28$$
$$\dot{x}_2 = -10x_1 - u_2x_2$$

with $0 \leq u_2 \leq 40$

also A, B and R in equation 6.2 are all set at unity.

It is clear from Fig. 6.8 that the absolute value of λ will not affect the solution, since we have

$$p_2(t) = c_3(t)\lambda Ax_{10} + c_4(t)\lambda Bx_{20} = 0$$

λ may therefore be conveniently set at -1.

Fig. 6.9 shows the initial section of the switch curve, produced by the simulation. As expected, the curve starts at the target set, x_1 axis intersection and then continues in quadrant 4.

By allowing the simulation to run for a longer time, we can see from Fig. 6.10 that the switch curve tends towards a straight line. This line is in fact the orientation of the eigenvector corresponding to the fast eigenvalue of equation 6.28 with $u_2 = u_{max}$. This property has been previously noted by Mohler.[3]

The eigenvalues of equation 6.28 with $u_2 = 40$ are

-2.68 (slow) and -37.3 (fast)

with corresponding eigenvectors of

$$\frac{x_2}{x_1} = -0.268 \quad \text{and} \quad \frac{x_2}{x_1} = -3.73$$

The variable structure control thus achieves its optimality by allowing the system to move rapidly around state space with zero damping, until the fast eigenvector of the system with maximum damping is encountered. This damping is then applied, and the system approaches the target set (which can be made arbitrarily small to approximate the origin) in the fastest way possible. The effect of the slow eigenvector having been nullified.

Fig. 6.11 is the corresponding curve in the second quadrant, and was obtained by reversing the sign of the loop gain K_L in Fig. 6.8.

Example 2

The system is described by

$$\dot{x}_1 = -u_1 x_1 + 10x_2 \qquad 6.29$$
$$\dot{x}_2 = -10x_1 + 0$$

with $0 \leq u_1 \leq 40$

A, B and R = 1 $\quad \lambda = -1$

Fig. 6.12 shows the initial switch curve, which is in agreement with the configuration predicted in Fig. 6.5. Fig. 6.13 again shows the curve tending to a straight line which corresponds to the fast eigenvector.

i.e. the eigenvalues of the system with $u_1 = 40$ are

-2.68 (slow) and -37.3 (fast)

With corresponding eigenvectors

$$\frac{x_2}{x_1} = 3.73 \quad \text{and} \quad \frac{x_2}{x_1} = 0.268$$

Example 3

The system equations are

$$\dot{x}_1 = -15x_1 + 10x_2 \qquad 6.30$$
$$\dot{x}_2 = -10x_1 - u_2x_2$$

with $0 \leq u_2 \leq 40$

A, B and R = 1 $\quad \lambda = -1$

This case demonstrates a system with some fixed damping and some variable damping.

The eigenvalues with $u_2 = 40$ are

-20 (slow) and -35 (fast)

with corresponding eigenvectors

$$\frac{x_2}{x_1} = -0.5 \quad \text{and} \quad \frac{x_2}{x_1} = -2.0$$

With $u_2 = u_{min} = 0$ the system is underdamped, with a damping factor of $\zeta = 0.75$. The system will, as before, orbit the state space until the fast eigenvector is encountered, as seen in Fig. 6.14.

Example 4

The system equations are

$$\dot{x}_1 = 0 + 10x_2 \qquad 6.31$$
$$\dot{x}_2 = -10x_1 - u_2x_2$$

with $0 \leq u_2 \leq 15$

A, B and R = 1 $\quad \lambda = -1$

This system represents a case where the response is always underdamped. This time, the switch curve is seen in Fig. 6.15, to be looped. This loop represents all the "first time" switch points that can be reached in reverse time from initial conditions on the target set in quadrants 3 and 4. To try and extend this curve would require an initial condition in quadrant 1 or quadrant 2. The system would therefore have had to travel through the $u = u_{min}$ region in quadrant 2. This situation has not been allowed for in the development of this technique, which leads to the limited portion of the curve shown in Fig. 6.15 being obtainable. To compute larger portions, the standard point by point methods must be used.

6.3.7 Discussion of Switch Curve Responses

The optimal switching curves have been seen to approximate to the fast eigenvector in each case examined. This agrees with the curves generated previously by the point by point techniques[3] The optimal response is thus obtained by the nullification of the effect of the slow eigenvector.

It has been seen that only a limited portion of the switch curve is available if the system has complex eigenvectors. This is not considered a serious limitation. For the system of example 3, the maximum damping was $\zeta = 0.75$. With this value, it is seen in Fig. 6.15 that the switch curve extends out in the state space a large distance compared to the target set diameter. If the maximum damping factor were further increased, the switch curve would extend further out in state space. When critical damping is reached, the eigenvectors become real, and the switch curve tends to a straight line extending indefinitely out into state space.

In any real system, it should be possible to introduce sufficient damping, to generate a useful amount of switch curve.

The sufficiency conditions for the control to be optimal in Appendix H have been seen to hold[3] for the switch curves produced by point by point techniques. Since the results generated here are just the same curves produced more efficiently, then we do indeed have optimal switching laws.

CHAPTER 7

CONTINUOUS VARIABLE STRUCTURE SYSTEMS

7.1 General

The studies so far have been mostly concerned with variable structure systems that have bang-bang controls, this bang-bang type of strategy being the natural result of optimisation for minimum time, or quadratic state performance indices. Also, the formulation of adaptive VSS with sliding modes leads to controls that are of a bang-bang type. The great advantage of this form of control is, of course, its simplicity when implemented on a practical system. In an analogue system for instance, the control might be achieved by the switching-in of just one resistor around an operational amplifier, to give two selectable system gains. In a digital system, comprising of a mini-computer or microprocessor, it may well be possible (as will be seen in the practical studies) to achieve the two or more selectable gains by the use of simple, fast binary left or right shift operations.

It has been pointed out in section 4.4.2 that the fast transient signals that arise with bang-bang control may well excite modes in the plant, that are beyond the limit of transfer function validity. The solution to this problem is to use first order filters to remove the unimportant high frequencies whilst passing the lower frequency components of the equivalent control. In an adaptive context, the VSS with these filters become more like the Liapunov or Hyperstability designs, in that the compensating gains are now continuous functions of time rather than switched values.

The need to change gains in a continuous manner introduces the complexity that either an analogue multiplier must be used, in an analogue system, or a multiplication routine be incorporated into a digital system. The most likely situation where these factors could cause problems is that in which a small microprocessor without a single instruction multiply operation, is being used. The time taken to perform a specially written subroutine to calculate a product would then reduce the number of applications, for this form of variable structure strategy.

In the present research, little attention has been directed towards continuous VSS, other than the above stated case. However, for completeness, this chapter presents a few ideas on the way in which such systems could occur, along with some observations on the choice of specific control laws.

7.2 Continuous Control Via the Maximum Principle

It has been seen in chapter 5, that for time-optimal or quadratic state performance indices, the variable structure control is of a bang-bang nature. Let us now investigate a modified type of performance index.

Consider the system of the following equations.

$$\begin{aligned} \dot{x}_1 &= x_2 \\ \dot{x}_2 &= -Kx_1 - ux_2 \end{aligned} \qquad 7.1$$

with an index of performance given by

$$\text{P.I.} = \int_{t_o}^{t_1} (f(x_1,x_2) + k_1 u^2)dt \qquad 7.2$$

k_1 is a positive constant

The auxiliary state is

$$x_o = f(x_1,x_2) + k_1u^2$$

The Hamiltonian is thus

$$H = p_1x_2 - p_2x_1K - ux_2p_2 - f(x_1,x_2) - k_1u^2 \qquad 7.3$$

i.e. $$H(u) = - ux_2p_2 - k_1u^2 \qquad 7.4$$

For equation 7.2 to obtain a minimum, equation 7.3 must be maximised.

$$\frac{dH}{du} = - x_2p_2 - 2k_1u = 0 \quad \text{at a turning point}$$

gives $$u = -\frac{x_2p_2}{2k_1} \qquad 7.5$$

which does in fact maximise equation 7.3.

Thus, the inclusion of the term k_1u^2 in the performance index has resulted in a control which is a continuous function of the state and costate variables.

In conventional fixed structure systems, where the control is additive, such terms as ku^2 represent the amount of effort that is being applied to control the plant. In some cases this effort is directly proportional to the power being used to achieve control, i.e. if the control u is the current in some dissipative circuit, the energy used is u^2R x time Joules, where R is the circuit resistance. It therefore makes sense, in situations where control effort must be restricted i.e. spacecraft with limited fuel or remote battery operated systems, to study performance indices which include control effort.

In variable structure systems, however, there seems to be no obvious reason for applying any restriction directly to the multiplicative

control, since the effort applied to the plant is not a simple function of this control alone.

However, if we consider the effort applied to the "double integrator" plant of equation 7.1, we have

$$\text{effort} = \dot{x}_2 = -Kx_1 - ux_2 \qquad 7.6$$

and modify the performance index to

$$\text{P.I.} = \int_{t_o}^{t_1} (f(x_1,x_2) + k_1\dot{x}_2^2)dt \qquad 7.7$$

We now have a meaningful index in terms of a limited effort situation.

This time we have

$$H(u) = -ux_2p_2 - k_1u^2x_2^2 - 2Kk_1x_1x_2u$$

$$\text{then } \frac{dH(u)}{du} = -x_2p_2 - 2k_1x_2^2u - 2Kk_1x_1x_2 = 0$$

$$\text{gives } u = -\frac{p_2}{2k_1x_2} - \frac{Kx_1}{x_2} \qquad 7.8$$

Again, the control is a continuous function. This time, however, the solution has significance to the practical problem of a system with limited energy resources.

For this type of problem, the value of u as a function of state may be found in the same way as the switching curve is found in the point by point methods, i.e. from a point on the target set the state-costate equations are integrated in reverse time. At any time u will be given by equation 7.8. By starting from a selection of initial conditions, values of u may be mapped onto the state space. Function generators or Read Only Memories could then produce a reasonable approximation of the optimal control, to be used in a practical system.

7.3 Continuous Control via Stability Considerations

By the examination of Liapunov energy functions, it is possible to choose a form of state dependent gain, that will guarantee the asymptotic stability of the resultant system. This technique would seem to have limited application, due to the fact that stability in itself does not imply an acceptable response.

As a simple demonstration of the use of Liapunov function, consider the variable structure system described by the following equations.

$$\dot{x}_1 = x_2$$
$$\dot{x}_2 = -ux_1 \qquad 7.9$$

A suitable Liapunov function could well be given by the positive definite function

$$v = kx_1^2 + x_2^2 \qquad k \text{ is an arbitrary positive constant} \qquad 7.10$$

giving $$\dot{v} = 2kx_1\dot{x}_1 + 2x_2\dot{x}_2 \qquad 7.11$$

Substituting equation 7.9 in equation 7.11 gives

$$\dot{v} = 2kx_1x_2 - 2x_1x_2u \qquad 7.12$$

For the trivial case where u is chosen as a constant, and putting $k = u$ we have

$$\dot{v} = 0$$

i.e. the system is neither stable or unstable, but is quasi-stable.

If, however, we choose

$$u = k + cx_1x_2 \qquad c \text{ is a positive constant} \qquad 7.13$$

then $$\dot{v} = -2cx_1^2x_2^2$$

which is negative definite, indicating an asymptotically stable system.

The variable structure nature of equation 7.13 may be seen upon substitution of this control into equation 7.9

$$\text{i.e.} \quad \begin{aligned} \dot{x}_1 &= x_2 \\ \dot{x}_2 &= -kx_1 - cx_1^2 x_2 \end{aligned} \qquad 7.14$$

Thus, the x_1^2 term appears as a variable amount of damping by affecting the proportion of x_2 fed back. The equilibrium condition of equation 7.14 is $x_1, x_2 = 0$. Thus, if the system initially starts with some finite $x_1 = x_{10}$, say, the system damping will initially be at a maximum and then decay to zero. This is contradictory to the type of action produced by optimal control theory, where the initial damping is low, and then increases when the equilibrium position is being approached. Intuitively, we may now propose a modification to equation 7.14, to obtain some degree of compliance to optimal policies.

$$\text{i.e.} \quad \begin{aligned} \dot{x}_1 &= x_2 \\ \dot{x}_2 &= -kx_1 - cx_2^2 x_2 \end{aligned} \qquad 7.15$$

For some initial $x_1 = x_{10}$, the damping due to x_2^2 will be zero. As x_1 moves towards $x_1 = 0$, x_2 will increase resulting in an increased damping factor.

To obtain the form of equation 7.15, the control u in equation 7.9 must be

$$u = k + \frac{cx_2^3}{x_1}$$

giving $\dot{v} = -2cx_2^4$

indicating a stable system.

Thus, we have seen how continuous variable structure controls may be chosen with the aid of Liapunov functions. There seems to be

no logical way, however, of using these functions to choose a good (in the sense of near optimal) type of control.

In a similar way, Hyperstability theory has been used[4] to find stable, bilinear type, variable structure control laws. But again, no indication of how a 'good' control may be selected is given.

7.4 Comments on Continuous Variable Structure Systems

It has been seen in this chapter that the simplicity of implementing a variable structure strategy is lost when a continuous control is selected rather than a bang-bang control. This complication is, however, unavoidable if the plant to be controlled has undesirable modes that would be excited by a fast switching action. Also, the use of performance indices containing control-effort terms will dictate a continuous control.

Stability techniques are seen to give only a first step towards designing continuous VSS since they give no guide as to how good (relatively) a design is.

CHAPTER 8

DISCUSSION OF THEORETICAL STUDIES

8.1 General

The research contained in Chapters 2-7 has examined the various theoretical sub-divisions of variable structure control. In this Chapter, it is proposed to consider several aspects of this work. Firstly, the salient points of each chapter will be presented, to enable an overall view to be formed. Where relevant, comparisons will be drawn between previous research and the philosophies developed in this work. As a second aspect of the theoretical studies, the concepts of optimal vss and adaptive vss will be examined in relation to each other. It will be seen that systems may be designed with simple, variable structure control laws, that do in fact combine both optimal and adaptive properties.

To summarise the theoretical work, a general procedure, in terms of flow charts, will be given to determine what form of variable structure system is required for a particular type of situation.

This chapter will conclude by considering the features of a practical system for which a variable structure control policy is to be realised. Chapters 9-13 will then consider the details of the practical system, the synthesis of the variable structure control law, and the resulting performance of the system, when compared to conventional control strategies.

8.2 Salient Points of the Theoretical Studies

It was seen in Chapter 2 that variable structure systems often appear in natural processes. The advantages of such systems were then demonstrated by considering a simple system with an intuitively chosen variable structure control law.

Chapter 3 considered the need for adaptive controllers, and the various philosophies available for the design of such systems. The model reference scheme was selected as being the most suitable, due to its direct nature of assessing the adaptive control from the measurement of the plant states. Also, the model reference approach is generally applicable to plants of any order.

The various techniques for realising model reference controls were considered in Chapter 4. The variable structure implementation has the advantages of simplicity, partial definition of the adaptive response and the fact that the control law formulation allows the plant to alter while adaptation is taking place. It was pointed out that the use of an implied model produced a very simple realisation of an adaptive system indeed. It is difficult to think of a more direct adaptive approach than to define the required time domain response (the ultimate objective) in terms of a hyperplane, and then to maintain the system on this hyperplane by the simple selection of fixed gains.

The equivalent control concept is a straightforward means of finding the limiting case of the variable structure control to ensure the existence of a sliding mode. Satisfaction of the reaching condition then completes the variable structure design.

Chapter 5 examined variable structure systems from an optimal control point of view. The maximum principle was seen to be well suited

to the analysis of vss, when compared to variational or numerical techniques. The controls for the minimum time problem or the quadratic state performance index problem are found to be of a bang-bang type. Further, there is the possibility in the quadratic state case of the controls being of a singular or sliding mode type. This sliding mode is a function of the quadratic performance index only and corresponds to the behaviour of the so-called ideal model for that specific performance index.

It was also noted in Chapter 5 that the estimation of the curve in state space, where the variable structure controls switch, has in the past been found very indirectly. That is, that the curve was found point by point by repeated integration of the state - costate equations in reverse time.

A means of finding the time optimal switch curve more directly was the subject matter of Chapter 6. The technique developed is a mechanisation of the maximum principle equations in a way that appears to be new. The method devised was applied to a general second order system. The optimal curve in the case of a system with real eigenvalues in the structure with maximum damping was found to be coincident with the eigenvector corresponding to the fast eigenvalue of that structure. A system with a time optimal control law would thus operate with the low damped structure until the fast eigenvector location was encountered. The control would then switch and the system would approach the origin along the fast eigenvector, thus nullifying the normally dominant effects of the slow eigenvector that appears in fixed structure systems.

Chapter 7 briefly examined variable structure systems with continuous controls. These occur with systems that have undesirable modes that would be excited by switching controls. Also, they occur when

a system is optimised with a control effort term in the performance index.

8.3 The Compatibility of Optimal and Adaptive Control Strategies

Variable structure systems with singular or sliding modes, designed from an adaptive point of view, make use of sliding planes defined either in the plant state space (implied model), or the plant-model error space (actual model).

It has been seen that planes in state space also appear when analysing optimal vss. For systems with real eigenvalues the time optimal switching curve was seen to approach the position of the fast eigenvector (of the structure with large damping) as the target set approximates the origin.

A vss optimised for an nth order quadratic state performance index has a switching curve that is ideally a $n-1^{th}$ order plane dependent only upon the specific performance index. This switching curve, however, is only realised in practice if the variable structure controls have sufficient range.

A general guide to the design of adaptive vss and optimal vss can therefore be represented by the diagrams in Figs. 8.1 and 8.2. For the optimal case with quadratic state performance index it would seem preferable to choose the control such that the sliding mode is not quite attained. This results in almost optimal control, but without the continuous switching associated with the sliding mode.

It now seems a logical progression to try to combine both the adaptive properties and the optimal properties of vss within a single control strategy if possible. This is straightforward in the quadratic state performance index case, i.e. the plane defined by the ideal

model will be of one order less than the order of the performance index. This index in turn will have a maximum order equal to that of the plant state space equations. If the plant is variable and requires adaptive control, we can now use vss with an implied model to design a sliding mode in the plant state space. This sliding mode will again have a maximum order equal to one less than the plant state space equations. Thus the adaptive-optimal system may be achieved by making the implied model equal to the ideal model.

In the case of a time optimal performance index applied to a variable plant, we may choose some nominal condition of the plant, and find the optimal switch curve for that case. Given that the switch curve is in the form of straight switching hyperplane, then the sliding plane in state space may be made coincident to that optimal curve. Thus again the designed system should exhibit adaptive properties, and improvements from an optimal point of view.

To summarise this section and indeed this chapter, a flow chart is shown in Fig. 8.3 that shows which type of variable structure system should be employed for systems operating under various circumstances.

8.4 Features of a Specific Practical Application

The practical application to which the philosophies developed will be applied is the speed control of an armature driven d.c. motor. The motor and controller will be a second order system, due to the introduction of an integrator in the controller to remove steady state speed errors due to loading.

The machine system is required to operate over a wide range of load conditions. This, together with the nonlinear nature of thyristor

bridge that drives the armature, makes the system an ideal candidate for adaptive control.

Optimal control studies will also be applied with a minimum time criterion as the performance index. The overall objective will then be to devise a variable structure control law which produces an optimal response that is insensitive to environmental changes.

CHAPTER 9

INTRODUCTION TO PRACTICAL STUDIES

The study of the practical application of variable structure system theory to a real problem is here concerned with the speed control of a 5 h.p. D.C. machine. The particular machine considered is part of a special test rig that has been developed at the University of Bath, School of Electrical Engineering. This facility will be described in detail in Chapter 10. Briefly, the system is based round an 8-bit microprocessor evaluation module, which, together with some additional dedicated hardware, takes on the dual role of controller and systems "health monitor". From a control point of view, the processor is provided with continuous information about the machine armature current and the machine speed. Controlled excitation of the machine is achieved by feeding the armature from a thyristor bridge that has its firing angle information supplied by the processor. In this way, closed loop control of the machine's speed is possible. The exact nature of the control law can be determined by the choice of the way in which the processor manipulates the measured machine data. This manipulation is defined by the "software" program that is stored in the microprocessor's random access memory. It is a simple matter to modify or rewrite these programs, leading to the capability of implementing various control laws without the necessity of hardware redesign.

The processor, in its other role as health monitor, continuously samples various signals within the system that indicate the correct operation of certain important functions. Should any of these signals indicate a malfunction, then the field and armature supply to the D.C.

machine are immediately removed, as a safety measure.

Connected on the same shaft as the D.C. 'work' machine armature, is another D.C. machine, which has its field fed from a constant D.C. supply. Then, by switching in various resistances across the armature, this 'load' machine will present varying amounts of load torque to the controlled work machine. Thus, the response of the work machine to various load conditions can be found.

In Chapter 11, a mathematical model will be developed which will allow to some extent, the dynamic behaviour of the closed loop system to be predicted. This model which describes a plant with non-linearities and time-varying parameters, will be considered as a linear system with parameters that are a function of some nominal operating point, and certain environmental conditions.

Chapter 12 will consider the synthesis of specific variable structure control laws, which will be based on the previously mentioned mathematical model. Since the control is to produce adaptive properties, it should only be necessary to consider the extremes of the linearised parameters, on the assumption that if the control can produce consistent responses for these extreme cases, then the intermediate conditions pose a less severe problem to the controller.

A linear control law will also be studied i.e. the thyristor firing angle will be a linear function of the system states. This linear control law thus represents a conventional machine drive design philosophy.

The relative performances of the variable structure scheme compared with the linear and other schemes will be discussed with respect

to various test conditions, in Chapter 13. Consideration will also be given to such aspects as the relative complexity and length of the various control routines in terms of the programming required to implement them, on the microprocessor system.

CHAPTER 10

DESCRIPTION OF THE SYSTEM TO BE CONTROLLED

General

The overall structure of the system has briefly been described in Chapter 9. A block diagram representing the complete system is shown in Fig.10.1. This may now be conveniently sub-divided into four smaller sections. These are

1) The D.C. work machine with its associated thyristor bridge, and the D.C. load machine.
2) The thyristor firing angle controller, and the health monitoring circuits.
3) The tachometer measuring system
4) The microprocessor system.

These sub-systems will now be considered in greater detail.

10.1 The D.C. Machines, and the Thyristor Bridge

The work machine which is to be controlled is a 5 hp Mawdsley's D.C. machine with the following general specifications

Maximum rpm = 2000

Maximum armature voltage = 200V

Maximum armature current = 33A

Connected to the same shaft as the work machine is another D.C. machine which operates as adjustable loading for the work machine. The variation of loading is achieved by switching in a variable resistance

across the armature of the load machine, the field being fed by a full-wave rectified 200V A.C. supply.

The armature of the work machine is supplied by a full-wave, controlled thyristor bridge, to be described shortly. The field of this machine is again fed by a full-wave rectified 200V A.C. supply.

Also connected to the shaft of the work machine is a tacho-generator which produces an output of approximately 24V D.C. at a speed of 1000 rpm.

Fig.10.2 shows pictorially the arrangement of the D.C. machines and the tachogenerator.

Fig.10.3 shows the detailed arrangement of the power supply to the field and armature windings of the work machine. Relay 1 and Relay 2 are under the control of the microprocessor, thus providing the ability to apply power to the machine, or switch the power off (possibly in a malfunction condition), under program supervision. Resistors R1 and R2 are of small value. The voltages across them are thus a good representation of the armature and field currents that would flow in the armature and field circuits, without the introduction of these resistors. The measurement of the armature current is used to enable the control to maintain this current at or below a safe level. The field current is continuously monitored to ensure that the field supply has not failed. If the field circuit was interrupted, the machine would not be able to produce any back emf, leading to excessive armature currents being demanded. If this fault condition is detected, the processor will open Relay 1 and Relay 2 to shut the system down.

Protection against induced emf for the diode bridge is provided by the resistor-diode combination of R_3D_1. The thyristor bridge as shown in Fig.10.3 is a simplified representation. In the real system, each arm of the bridge consists of the network shown in Fig.10.4. The series resistor-capacitor section is a conventional "snubber" which absorbs large induced transient voltages. The gate firing pulse is fed via an isolating transformer to a network that ensures that the conditions on the gate never exceed the safe operating regions specified by the thyristor manufacturer. A fuse is also included in series with the thyristor as protection against a high current, fault condition.

10.2 The Thyristor Firing Angle Controller and the Health Monitoring Circuits

The block diagram of the thyristor firing angle controller is shown in Fig.10.5. This system operates as follows.

The zero crossing detector produces a 100 Hz signal from the 50 Hz mains waveform. This 100 Hz signal provides synchronisation for the complete machine-control system. A phase-locked loop with dividers is driven by the 100 Hz signal, to provide a 102.4 KHz frequency that is synchronised to the mains. The phase-locked loop (PLL) then drives a 10 bit binary counter that has its reset driven by the zero crossing detector (ZCD). Thus, at the start of a typical mains half cycle, the 10 bit counter is reset to 0 (decimal). It then increments at a constant rate, until it reaches 1023 (decimal). The next increment represents the end of the half cycle and the ZCD resets the counter. The 10 bit counter can thus be thought of as containing information as to how far through a complete half cycle the mains voltage has progressed.

By specifying a particular number on the 10 bit counter, we can locate any one of 1024 (decimal) subdivisions of a basic mains half cycle.

The microprocessor programmes are synchronised to mains frequency by driving the processor interrupt request from the ZCD. The detailed description of the processor operation will be given later. As a general view, however, on receipt of an interrupt request at the start of a mains half cycle, the processor calculates a ten bit number which represents a firing angle for the thyristors. This number is then loaded into a register which shall be called the Firing Angle Register.

By comparing the firing angle register, which represents the required point in the mains half cycle for the thyristors to be switched on, to the 10 bit counter, i.e. the actual point in the mains half cycle, a signal is obtained that defines when, in time, the processor requires the thyristors to conduct. This signal is then fed to the "fire enable" bistable. This bistable is reset each half cycle by the ZCD. The output from the fire enable bistable is then gated together with the PLL output, and a 50 Hz square wave, to form the input signal for the thyristor drive circuits.

The three signals to the gating block thus have the following functions:

1) Fire Enable - allows the multipulse firing signal to reach the thyristors.
2) Multipulse Signal - provides a multiple driving pulse for the thyristor gates, to ensure that the thyristors turn on. A single pulse might not be sufficient.
3) Inhibit - ensures that only the correct pair of thyristors can conduct at any one time.

A typical 10 mS control period thus proceeds as follows.

The ZCD pulse resets the 10 bit counter and the fire enable bistable, and then causes the processor to calculate the required thyristor firing angle by activating the interrupt request. The firing angle is then loaded into the firing angle register. When the mains half cycle has reached the point such that the 10 bit count equals the required firing angle, the fire enable bistable is set. The gating then applies the multipulse signal to the gates of the pair of thyristors selected by the inhibit circuit. The thyristors selected then conduct.

For the period when the processor is not calculating the firing angle, the programming is arranged such that the processor continuously monitors several important functions within the motor-control system. This aspect of the processor operation will be known as the "Health Monitoring" facility of the system.

The functions monitored are the following

1) The phase-locked loop.
2) The zero crossing detector.
3) The field current.
4) The armature current.

Each of these functions is monitored by a small amount of circuitry. Each circuit produces either a logical 0 or a logical 1. One of these states representing correct (healthy) operation and the other representing a malfunction (unhealthy) condition.

Each of these logical signals then forms 1 bit of a 4 bit "status register", as shown in Fig.10.6. The processor, therefore, continuously reads the status register, and checks that each bit is "healthy".

The above monitored functions are now described in more detail.

1) Failure of the phase-locked loop would result in the loss of synchronisation of the 10 bit counter, with the correspondingly incorrectly timed thyristor fire pulses. The particular phase-locked loop used, has an 'in lock' signal available to indicate when the loop is in fact 'locked'. This signal is then used to provide the logical value to the status resistor.

2) The complete system is dependent on the zero crossing detector for synchronisation. Failure of the zero crossing pulse would, therefore, result in indeterminate operation. It is a simple matter to detect the zero crossing pulses, to provide the logical health monitoring signal.

3) If the machine field current should fail, the system will clearly be unable to function correctly. Field current sensing is achieved by use of a small value resistor in series with the field winding. The voltage developed across this resistor when field current is flowing, is processed to provide the signal for the status register.

4) The status of the armature current is more complex than the three other health signals. This is because there exist situations where large currents may be acceptable for short periods of time. The sensing of an overcurrent situation is achieved as follows.

The armature overcurrent value is represented by an 8 bit binary word. This word is fed to a Digital to Analogue converter (D/A). The actual armature current, which is represented by the voltage across a current sense resistor in series with the armature, is then compared to the output of the D/A. When the actual current exceeds the set current, the armature overcurrent status bit is set to its unhealthy state.

The microprocessor takes the following actions if an unhealthy state occurs.

1. Phase-locked loop unhealthy
2. Zero crossing detector unhealthy
3. Field current unhealthy

} system shut down i.e. machine supply relays opened.

4. Armature overcurrent unhealthy - as mentioned previously, the action in this case is more complex. The system is in fact allowed to operate in an overcurrent state, but only for a limited number of mains half cycles. The number of periods in overcurrent is predetermined and stored in the processor programme. If at the end of a half cycle (10 mS) the system is in overcurrent, the processor will retard the thyristor firing angle by a fixed amount. This amount is set in the programme and will be chosen such that the reduced firing angle should bring the armature current below the overcurrent limit. In normal operation, therefore, the overcurrent condition should not exist over consecutive periods. This method of operation allows the machine to accelerate from rest whilst working in this current limiting mode. The overcurrent limit being set to the maximum, safe, level, thus providing maximum acceleration. It may be that random loading effects might cause the overcurrent situation to occur over more than one period, whilst not endangering the thyristors in the short times involved. The processor programme is therefore arranged such that the system is not shut down unless the overcurrent condition has lasted for more than a preset (safe) number of consecutive periods.

10.3 The Tachometer Measuring System

The tachometer used produces approximately 24V D.C. per 1000 rpm. The tachometer winding has 13 poles, which results in the output signal

having an A.C. ripple superimposed upon it. Conventional filtering of this ripple would introduce considerable phase shift, especially if the filtering was to be effective at low speeds of rotation.

The solution to this filtering problem is achieved by the use of a slotted disk mounted on the rotor of the tachometer. There are 13 slots equispaced around the perimeter of the disk, one for each pole of the tachometer. The slotted disk is arranged such that it spins between the two sections of an opto-coupler, i.e. the light source and the photo sensor. The tachometer circuits are then arranged such that the tachometer output is only read when a slot allows the light from the source to reach the photo sensor. The output value is then stored in a sample and hold unit, until the next slot reaches the opto-coupler. Thus, the speed signal is always measured with the general pole configuration at a fixed angular position, as shown in Fig.10.7. This technique effectively filters the ripple due to the poles whilst not introducing additional phase shift.

The sampled and held signal is then fed to an Analogue to Digital converter (A/D), which may be interrogated by the microprocessor, under programme control.

10.4 The Microprocessor System

The microprocessor section of the system is based on the Motorola M6800B Evaluation Module 11[40], which features the Motorola MC6800 8 bit microprocessing unit. For the purposes of the present discussion, the processor system will be considered initially from the point of view of a workable, practical system. Then, the software programming will be detailed with the aid of flow charts. The complete machine code listing is then given in Appendix K.

10.4.1 The Microprocessor System - Practical Arrangement

The microprocessor evaluation module board may be considered as operating on one of two levels at any particular time. The first is a "monitor" mode. This mode allows a teletype to communicate with the evaluation module under the control of a monitor program which is in a read only memory (ROM) integrated circuit on the evaluation module board. The monitor has among its functions the following

a) Memory loader function - allowing a users program to be loaded from paper tape, into a random access memory (RAM) store, associated with the microprocessor.

b) Print/Punch memory dump function - allowing programmed sections of the RAM to be listed on the teletype and stored on paper tape.

c) Memory examine and change function - allowing individual RAM locations to be examined and modified as required.

d) Run users program function - allowing the evaluation module to leave the monitor mode and execute a users program.

e) Software interrupt function - by inserting a software interrupt command into the users programme, control will be passed back to the monitor when the interrupt command is encountered.

By a combination of the above functions it is therefore possible to write, modify, test and save programmes that are under development.

The second mode of operation is entered by the Run users programme function. In this mode, the processor will execute a users programme, without reference to the monitor, unless a software interrupt command

is encountered. It is in this mode that the evaluation module will be operating when the D.C. machine system is being controlled.

Communication between the evaluation module and the rest of the system is based on the use of dedicated registers. These registers appear to the microprocessor to be like single locations of RAM, with the difference being that some of the registers may only be read, whilst the remainder may only be written to. These registers then interface with the measurement and control functions of the D.C. work machine system. Each register, like a RAM location, will contain an 8 bit binary word (or byte). This word is written or read by the microprocessor via an 8 bit data bus. The particular selection of a register or RAM location for data transfer is achieved by the microprocessor generating a 16 bit addres word (2 bytes) via a 16 bit address bus. Thus any particular address signal will activate only one RAM or register location for the transference of data.

The convention that is used to represent a particular 8 or 16 bit word is the hexadecimal notation, i.e. the word is split up into 4 bit blocks. Each block then has the hexadecimal value for each corresponding binary value as shown below.

binary value	hexadecimal value
0 0 0 0	0
0 0 0 1	1
0 0 1 0	2
0 0 1 1	3
0 1 0 0	4
0 1 0 1	5
0 1 1 0	6
0 1 1 1	7
1 0 0 0	8
1 0 0 1	9
1 0 1 0	A
1 0 1 1	B
1 1 0 0	C
1 1 0 1	D
1 1 1 0	E
1 1 1 1	F

A data word is therefore made up of two hexadecimal (hex) characters, i.e.

Data is 1010 0100 (binary) equals A4 (hex)

Similarly, an address word is made up of four hex characters.

The specific registers that form the processor-machine interface are as follows.

Register Name	Register Address (hex)
a) Firing Angle Registers	D 100 D 101
b) Tachometer Register	D 102
c) Relay Control Register	D 103
d) Status Register	D 105
e) Set Overcurrent Register	D 106

which have the following functions

a) The firing angle registers receive firing angle data from the microprocessor. This data is then used by the thyristor firing angle controller to determine when the thyristors should conduct.

b) The tachometer register holds the data from the tachometer analogue to digital converter. This data is then available to the processor for the calculation of control actions.

c) The relay control register allows the processor to directly control the relays that apply power to the field and armature of the work machine.

d) The status register holds the information about the health of the system, and is continuously read by the processor when the machine is running.

e) The set overcurrent register allows the processor to send a value of overcurrent limit to the digital to analogue converter in the armature overcurrent circuits.

It should also be noted that another important path of communication between the machine system and the processor exists, in the form of the processor interrupt request line, which is driven by the mains zero crossing detector. This connection provides the synchronisation between the control programme and the phase of the thyristor supply voltage.

10.4.2 The microprocessor system - Software Routines

The software must perform the following duties

a) Allow the control of the field and armature supply relays.

b) Monitor the health of the system, and take appropriate action.

c) Compute the speed of the machine.

d) Calculate the thyristor firing angles.

The programming was written in the form of an executive programme which linked together the various subroutines that performed specialised functions. These subroutines are

a) Start up

b) Tachometer read

c) Tachometer average

d) Status register

e) Overcurrent

f) Control

g) Firing angle range and check

h) Shutdown

which have the following actions.

a) The start up subroutine flow chart is shown in Fig.10.8. Its function is to initialise certain stores for programme use, switch on the D.C. work machine supply relays and then monitor the system health (except armature overcurrent) for a fixed period.

b) The tachometer read subroutine flow chart is shown in Fig.10.9. This programme adds together 64 samples of the tachometer A/D output. This enables the tachometer average subroutine to calculate an average value for the machine speed, thus reducing the effects of measurement noise. The health (except armature overcurrent) of the system is then checked. On the assumption that the system is 'healthy', the programme then returns back to the beginning of the tachometer read subroutine and repeats the above process. This loop then continues until an interrupt request is received, after which a branch to the tachometer average subroutine is made.

c) As mentioned above, the tachometer average subroutine calculates the average of 64 tachometer readings. The flow chart is seen in Fig.10.10.

d) The status register subroutine checks the health of the system. If either the field current, the phase-locked loop or the zero-crossing detector fail, then the programme jumps to the shut down routine. If the armature is in overcurrent, the programme will jump to the over-current routine. If the armature is not in overcurrent, then the control routine is reached. The flow chart is shown in Fig.10.11.

e) The overcurrent routine flow chart is seen in Fig.10.12. It first checks that the maximum number of consecutive cycles in over-current has not been exceeded. If this is true, the firing angle is decremented by a fixed amount in an attempt to remove the overcurrent

situation. The programme will then jump to the firing angle and range subroutine. If the maximum number of cycles in overcurrent has been exceeded, the programme jumps to shut down.

f) The precise nature of the control routine will be discussed in Chapter 12. However, from a general point of view the action is as follows. Since the control routine has been entered, the system is not in overcurrent. Therefore the 'number of cycles in overcurrent' register may be reset. The programme then takes in the data generated by the tachometer average routine and calculates (by a means as yet unknown) the thyristor firing angle to be applied. These processes are shown in the flow chart of Fig.10.13.

g) The firing angle and range check subroutine checks that the required firing angle that has been generated by either the control or the overcurrent routine is within the minimum and maximum limits of normal operation of the machine, i.e. 0 decimal (0000 hex) and 1023 decimal (03FF hex) respectively. If the required firing angle is less than 0000 hex, it is set to be equal to 0000 hex. Similarly, the firing angle is set to 03FF hex if the required angle is greater than 03FF hex. The checked firing angle is then outputted to the firing angle registers. The flow chart is seen in Fig.10.14.

h) The shutdown routine is used to remove the power from the D.C. work machine. Initially it stores the status register in a location in RAM, for a post mortem in the case of an unhealthy state causing shut-down. The relays that supply the power to the work machine are then opened. Finally, control of the evaluation module is retuned to the monitor, by the use of a software interrupt operation. The flow chart is given in Fig.10.15.

The flow chart of the executive routine is seen in Fig.10.16. The purpose of this routine is to set up the operating parameters of the system, and then to link the various subroutines. The sequence of events from initial entry to the executive programme is as follows. Note, when the monitor gives programme control to the executive programme, the mask facility on the interrupt request line has previously been set. Thus, at this stage the interrupt request signal from the zero crossing detector will not be actioned.

The executive programme initially sets up the fixed parameters of the system, i.e. required speed, retard value in overcurrent, number of cycles in overcurrent etc. After this there is a branch to startup routine, where the relays are closed and the health of the system is checked before returning to the executive programme. The interrupt mask is then cleared allowing the programme to jump to the tacho average routine upon receipt of the next interrupt pulse. At this point the interrupt mask is set again, and the tacho average (which in this instance is zero) is calculated. Upon returning to the executive programme, a jump to the status register subroutine is made, where the interrupt mask is cleared. If the field, phase-locked loop and zero crossing detector are healthy, the armature current is tested. If there is overcurrent, a jump is made via the overcurrent routine to the firing angle output and range routine, on the assumption that the number of cycles in overcurrent has not been exceeded, a return is then made to the executive programme. If there was no overcurrent, the executive jumps to the control routine before jumping to the firing angle and range routine. On return to the executive from the firing angle and range check the executive resets certain stores before jumping to the

tachometer read subroutine. When a 64 sample sum of tachometer readings has been done, the interrupt mask is set and the sum is transferred to a temporary store. The interrupt mask is then cleared and the status register is checked. If all is healthy, a jump is made back to the beginning of the tachometer read subroutine and the 64 readings are taken again. This process then continuously repeats, until an interrupt occurs. Because the interrupt mask is set when the sum transfer is made, an interrupt will not corrupt this sum. When the interrupt is serviced, a jump is made to the tachometer average subroutine and then continues as previously described.

The full machine code listing of these programmes along with operation mnemonics and notes is given in Appendix K.

CHAPTER 11

DEVELOPMENT OF A MATHEMATICAL MODEL OF THE DIGITALLY CONTROLLED MACHINE

11.1 General

The machine-control system is in effect a sampled data one. The sample period is half of the mains cycle, i.e. 10 mS. In this mathematical development, it will be assumed that this sample rate is sufficiently fast compared to the dynamics of the d.c. machine for the system to be considered as a continuous one.

The validity of the model will be shown by the use of small perturbation tests applied to the machine system around nominal values of speed.

11.2 The D.C. Machine Equations

The equations that describe an armature controlled d.c. machine are as follows

$$e_b = K_v \, d\theta_o/dt \qquad 11.1$$

$$T = K_t i_a \qquad 11.2$$

$$V_i = i_a R_a + e_b + L \, di_a/dt \qquad 11.3$$

where

e_b = motor back emf (Volts)

θ_o = armature position (Radians)

T = motor torque (Newton Metres)

i_a = armature current (Amps)

V_i = armature applied voltage (Volts)

R_a = armature resistance (Ohms)

L = armature inductance (Henrys)

K_v = generated emf per unit angular velocity (Volts/Rad/Sec)

K_t = torque per unit armature current (Newton/Metres/Amp)

Using Newtons second law, we have

$$T - F\frac{d\theta_o}{dt} = J\frac{d^2\theta_o}{dt^2} \qquad 11.4$$

where

F = viscous frictional torque (Newton Metres/Rad/Sec)

J = moment of inertia of the armature (Kg Metres^2)

These equations may be represented by Fig. 11.1.

Note, $\omega = \frac{d\theta_o}{dt}$ 11.5

From the manufacturers data and measurements we find the following values for some of the machine parameters

R_a = 1.0 Ohm

L = 2.5 mH

K_v = 0.668 V/Rad/Sec

K_t = 0.7 Nm/Amp

The parameters F and J will depend on specific loading conditions and will be detailed later.

11.3 The Effect of Discontinuous Armature Current

The equations 11.1 to 11.5 are representative for the case where the armature current is a smooth continuous function of time. For the system under consideration, however, the current fed to the armature

from the thyristor bridge is of a discontinuous nature. An exact analysis of this 'pulsed current' mode would be extremely complex. Therefore, simplifying assumptions will be made which, as will be seen, produce a reasonably valid model whilst maintaining the mathematical analysis at a straightforward level.

The major simplifying assumption is thus

Assumption

The effective D.C. armature current is equal to the average value of the discontinuous current waveform supplied by the thyristor bridge.

The armature conditions over a typical sequence of control periods are shown in Fig.11.2. At θ_1, the selected thyristors conduct, causing a build up of armature current. As the supply voltage falls below the machine back emf, the armature inductance will cause v_i to drop below e_b in an attempt to maintain the current flow. The energy stored in the armature is finally dissipated and current flow ceases at θ_2.

The average armature current is thus

$$\bar{i}_a = \frac{V_m}{\pi R_a} \int_{\theta_1}^{\theta_2} \sin \omega_s t \, dt - \frac{e_b}{\pi R_a} (\theta_2 - \theta_1) \qquad 11.6$$

$$\text{i.e. } \bar{i}_a = \frac{V_m}{\pi R_a} \left[\cos \theta_1 - \cos \theta_2 - \frac{e_b}{V_m} (\theta_2 - \theta_1) \right] \qquad 11.7$$

where ω_s is the supply frequency in Rads/sec

V_m is the peak supply voltage

11.3.1 Small Perturbation Analysis

For the purpose of making a small perturbation model, it is desired to evaluate $\frac{d\bar{i}_a}{d\theta_1}$ and $\frac{d\bar{i}_a}{de_b}$. It can be seen from equation 11.7, however, that $\bar{i}_a$ is also a function of θ_2. The angle θ_2 is in its turn a function

of θ_1 and e_b, and is related by equation[41] 11.8

$$\frac{\frac{e_b}{V_m \cos\theta_z} - \sin(\theta_2 - \theta_z)}{\frac{e_b}{V_m \cos\theta_z} - \sin(\theta_1 - \theta_z)} = e^{-(\theta_2-\theta_1)/\tan\theta_z} \qquad 11.8$$

where θ_z is the load impedance angle given by

$$\theta_z = \tan^{-1} \omega_s L/R_a \qquad 11.9$$

Equation 11.8 has been solved numerically by a digital computer to provide θ_2 for various values of θ_1 and e_b. This was also done with R_a set at 2Ω, to examine the effect of adding extra armature resistance. These results are presented graphically in Fig.11.3. For nominal values of θ_1 and e_b we can now obtain from Fig. 11.3 the angle θ_2 in the following form

$$\theta_2 = k_1 + k_2\theta_1 + k_3 e_b \qquad 11.10$$

k_1 in Rads k_2 in Rads/Rad k_3 in Rads/Volt

Substituting equation 11.10 into equation 11.7 gives

$$\bar{i}_a = \frac{V_m}{\pi R_a}\left[\cos\theta_1 - \cos(k_1 + k_2\theta_1 + k_3 e_b) - \frac{e_b}{V_m}(k_1 + k_2\theta_1 + k_3 e_b - \theta_1)\right] \qquad 11.11$$

differentiating gives

$$\frac{d\bar{i}_a}{d\theta_1} = \frac{V_m}{\pi R_a}\left[k_2 \sin(k_1 + k_2\theta_1 + k_3 e_b) - \sin\theta_1 - \frac{e_b}{V_m}(k_2 - 1)\right] \qquad 11.12$$

and

$$\frac{d\bar{i}_a}{de_b} = \frac{V_m}{\pi R_a}\left[k_3 \sin(k_1 + k_2\theta_1 + k_3 e_b) - \frac{(k_1 + k_2\theta_1 + k_3 e_b - \theta_1) - k_3 e_b}{V_m}\right] \qquad 11.13$$

i.e.

$$\frac{d\bar{i}_a}{d\theta_1} = \frac{V_m}{\pi R_a}\left[k_2 \sin\theta_2 - \sin\theta_1 - \frac{e_b}{V_m}(k_2 - 1)\right] \qquad 11.14$$

and

$$\frac{d\bar{i}_a}{de_b} = \frac{V_m}{\pi R_a}\left[k_3 \sin\theta_2 - \frac{(\theta_2 - \theta_1) - k_3 e_b}{V_m}\right] \qquad 11.15$$

In the practical system, the firing angle θ_f is defined as

$$\theta_f \triangleq \pi - \theta_1$$

i.e. $$\frac{d\bar{i}_a}{d\theta_f} = -\frac{d\bar{i}_a}{d\theta_1} \qquad 11.16$$

We can now consider the current components of equations 11.15 and 11.16 to be due to two voltage components applied to the armature, and define

$$g_1 = \frac{d\bar{i}_a}{d\theta_f} \cdot \frac{\pi R_a}{1024} \quad \text{Volts/Firing angle increment} \qquad 11.17$$

and $$g_2 = -\frac{d\bar{i}_a}{de_b} \cdot R_a \quad \text{Volts/Volt} \qquad 11.18$$

For any nominal values of θ_1 and e_b it is thus possible to calculate g_1 and g_2.

This enables us to represent the developed system equations in the diagrammatical form of Fig. 11.4.

It should be noted that although the armature inductance affects the discontinuous 50 Hz armature current waveform it will not introduce significant phase shift to the expected dynamic control frequencies. The inductance effects on the armature current have been accounted for in the formulation of g_1 and g_2. Thus from all other aspects, the armature inductance will now be ignored.

11.4 Consideration of Other Non-Linear Effects

There are three other major non-linear effects that need to be considered in this system. These are

1) The current-limit mode of operation.
2) Non-symmetrical operation due to the unilateral thyristor current flow.
3) Non-linear friction characteristic.

These aspects are now dealt with in greater detail.

11.4.1 Current-Limit Non-Linearity

There will be a maximum limit to the acceleration of the machine due to the limitation of the armature current to a safe value. Thus, if the responses predicted by the linear model require a greater acceleration than that available in the current-limit mode, then the model is not valid at these times.

11.4.2 Non-Linearity Due to Unilateral Thyristor Current Flow

In contrast to the previous non-linearity, there will be a limit to the rate at which the machine can deccelerate. This limit occurs because the thyristors can act only as a source of current, whereas they should be required to sink current from the motor, in a symmetrical system. Decceleration of the motor with zero armature current is therefore due only to the damping effect of the F/J term in Figs. 11.1 and 11.4.

In practice, for large positive step demands in speed, the system will very quickly enter the current-limit mode, as the machine accelerates from the zero speed initial condition. As the actual speed approaches the desired speed, the system comes out of the current-limit mode.

After this, it has been observed that for all reasonable conditions the armature current does not (a) exceed the current-limit value, or (b) reduce to zero.

Thus, after the initial current-limit operation, the non-linear effects of sections 11.4.1 and 11.4.2 are not encountered and the system responses may be approximated by the linear small perturbation model.

11.4.3 Non-linear Friction Characteristic

The linearised model developed assumes that the viscous friction torque coefficient, F, is constant. Thus, at steady state ($\dot{\omega} = 0$) we have the linear relationship

$$\omega = \frac{i_a K_t}{F} \qquad 11.19$$

between the speed ω and the armature current i_a.

The actual relationships between steady state speed and armature current has been found experimentally for a variety of load conditions, and are shown in Fig.11.5. These curves are clearly non-linear. However, for speeds in the range 200 rpm - 800 rpm, the slopes are sensibly constant.

The resulting friction constant for each case may thus be calculated as

$$F = \frac{\Delta i_a K_t}{\Delta \omega} \qquad 11.20$$

11.5 Representation of the Microprocessor Control Block

For the purposes of calculating control (thyristor firing angle), the microprocessor has available signals which represent the actual speed of the machine and the armature current flowing in the machine. The processor is also programmed with information about the required setspeed, the armature current limit, and the number of consecutive cycles allowable in overcurrent.

Two types of control law are to be investigated, i.e. linear control and variable structure control. Thus at any given moment, the microprocessor output signal (firing angle) will be a linear function of the system states, assuming that a more dominant factor such as current limit is not in operation.

The two system states that will be used for control are speed error and speed error rate. The speed error signal is readily calculated by the processor from the set speed figure and the tachometer signal. The error rate, however, is not directly measurable, and must be estimated using values of error taken over a suitable time period.

Thus, a general representation of the microprocessor as a closed-loop control element is shown in Fig.11.6.

11.5.1 The Estimation of Speed Error Rate

The method used to estimate the speed error rate is to take the current value of speed error e_i and subtract from it the value of speed error e_{i-n}, n samples previous to e_i.

i.e. error rate estimate $\hat{e} = e_i - e_{i-n}$ 11.21

Consecutive error samples have a sample time of 10 ms between them. Thus, $\hat{e}$ has been found using samples separated by 10n ms.

The theoretical definition of the error rate estimate $\hat{e}_T$ is

$$\text{theoretical error rate estimate } \hat{e}_T = \frac{e_i - e_{i-n}}{\text{time taken for n samples}}$$

$$\text{i.e. } \hat{e}_T = \frac{e_i - e_{i-n}}{0.01\ n} \qquad 11.22$$

giving the following scaling for our measure of error rate

$$\hat{e} = \frac{\hat{e}_T\ n}{100} \qquad 11.23$$

11.5.2 Integrating Action in the Microprocessor Controller

It is highly desirable to have some integrating action in the forward path of the control loop to remove the steady state error that would necessarily occur in the case where the error signal was processed by a gain only, with no dynamics.

This integrating action is achieved in the control programme of the microprocessor by taking the value of the combined function of error and error rate. The firing angle is then changed by this value, to get the new firing angle. Thus, if there were a constant error, the firing angle would be altering at a fixed rate, therefore achieving the desired integrating action.

As with the error rate estimate, the 'software integrator' requires a scaling factor to produce a consistent mathematical model. Consider the firing angle is initially set to zero. A constant increment of one unit is then required. After one control period (10 mS) the firing angle will be one unit. After one hundred control intervals (1 second) the firing angle is one hundred units.

Consider now an ideal integrator

i.e. firing angle $= \int_o^t 1 \, dt$

At the end of one second, the ideal integrator has an output of one.

Thus, the software integrator has a gain factor of one hundred when compared to its continuous counterpart.

11.5.3 Controller Parameters Selectable by the Designer

In a conventional analogue controller, the desired system response is achieved by adjusting the relative levels of the error, error rate, integral error etc. to be fed back. In the present system, these adjustments are made by the use of 'software gains', i.e. the binary numbers representing the error and error rate signals have arithmetic left shift or arithmetic right shift operations performed on them. Each left shift represents a gain of 2 and each right shift represents a gain of ÷2. The control programme therefore has provision for multiple shift operations to be applied to the error signal, the error rate signal, and the combined error and error rate control signal. These gains are denoted by K_2, K_3 and K_1 respectively.

11.6 Complete Block Diagram of the Linearised System

The linearised system may now be represented by Fig.11.7.

From measurements, the tachometer scaling factor K_{tacho} is found to be

$K_{tacho} = 1.53$ units/Rad/Sec

The closed loop transfer function (CLTF) of the linearised system is calculated as

$$CLTF = \frac{\frac{K_1 g_1 K_t}{R_a J}\left[100\ K_2 + K_3\ ns\right]}{s^2 + \left[\frac{F}{J} + \frac{K_t g_2 K_v}{R_a J} + \frac{nK_3 K_1 g_1 K_t K_{tacho}}{R_a J}\right]s + \frac{100\ K_2 K_1 g_1 K_t K_{tacho}}{R_a J}} \qquad 11.24$$

This transfer function will form the basis for the synthesis of the controls discussed in the following chapter.

11.7 Validity of the Linearised Model

By considering the characteristic equation of the system, i.e. the denominator of equation 11.24, it is possible to use the standard second order correlation of equation 11.25 to predict the system damping factor and the system natural frequency.

i.e. $$s^2 + 2\zeta\omega_n s + \omega_n^2 = 0 \qquad 11.25$$

The experimental procedure was to run the machine at a variety of fixed speeds with various loading conditions. The parameters K_1 and K_2 were set at nominal values, and K_3 was set equal to zero. Thus only the natural system damping was present. A slight disturbance was then applied to the system, and the resulting speed response was plotted.

At each nominal condition the angle to thyristor conduction θ_1 was noted. This enabled θ_2 in equation 11.8 to be calculated, and k_2 and k_3 in equation 11.10 to be estimated from Fig.11.3. By substituting these values into equations 11.14 and 11.15, g_1 and g_2 could be found. The friction coefficient F for each condition is estimated from Fig.11.5, using equation 11.20. The appropriate manufacturers values of machine

Inertia J now complete the information required to calculate the coefficients of the characteristic equation, i.e. the denominator of equation 11.24.

Before considering the theoretical and practical results of these tests, the test conditions will be presented in greater detail. The range of conditions has been selected to cover a wide variety of operational situations, and is detailed in table 11.1. These same conditions will also be used in the control law synthesis chapter and the practical results chapter. Table 11.2 shows the various values of parameters and variables for each test condition. Table 11.3 shows the characteristic equation for each condition, calculated using the data from table 11.2, substituted into equation 11.24. This is with the adjustable gains set as

$K_1 = \frac{1}{4}$, $K_2 = 1$ and $K_3 = 0$

A sample calculation of the characteristic equation for one condition is given in Appendix J.

11.7.1 Comparison of Predicted and Actual Small Perturbation Responses

Fig. 11.8 shows the actual small perturbation responses for the range of conditions detailed in table 11.1. The responses all feature very low damping. This general feature may be seen to conform to the predicted characteristic equations in table 11.3. Examination of the responses in fig. 11.8 shows that variations in the frequency of oscillation occur within a specific test conditions. The frequency of oscillation for each condition is thus measured as the average frequency over a 10 second period. Since the damping in each case is low, the predicted damped natural frequency will be sensibly the same as the

predicted undamped natural frequency.

i.e. $\omega_d = \omega_n \sqrt{1 - \zeta^2}$

if $\zeta = 0.2$ say

then $\omega_d = .98\ \omega_n$

The predicted natural frequency in radians is then calculated as the square root of the s^o coefficient in table 11.3. The values of the predicted natural frequency (H_z) and the average actual frequency (H_z) are given in table 11.4.

By comparison of the figures in table 11.4 it may be seen that the maximum departure from the predicted response is in condition 13, where the actual frequency is 14.1% low. For all the other test conditions the actual frequency is within 10% of that predicted. It is thus felt that the mathematical model that has been developed is a good engineering estimate of the real system.

CHAPTER 12

CONTROL LAW SYNTHESIS

12.1 General

Two types of control strategy will be implemented on the practical system, i.e. linear control and variable structure control with a sliding mode. The former thus represents a conventional approach, whilst the latter realises the theoretical developments in the first part of this research.

It should be noted that differences between these strategies will only become apparent after the system has come out of the 'current limit' mode, since the response of the machine to maximum safe current will be the same for both control laws.

In the linear case, the specific control law will be determined by examination of the characteristic equation for the system in terms of natural frequency and damping factor. For the variable structure case, the design will consider the relationships between desired switching lines in the state space and the eigenvectors of the comprising structures.

To simplify the synthesis, the system will be represented with the choice of speed error and speed error rate as the state variables. This arrangement allows the eigenvectors to be directly found from the characteristic equation.

12.2 The System in Phase-Canonical Form

When a system is represented by state variables, it can always be transformed into the so-called companion or phase-canonical form. This

transformation results in an A matrix of the general type shown in equation 12.1.

$$\dot{\underline{x}} = A\underline{x}$$

where

$$A = \begin{bmatrix} 0 & 1 & 0 & \cdots & 0 \\ 0 & 0 & 1 & \cdots & 0 \\ \vdots & & & & \\ 0 & 0 & 0 & \cdots & 1 \\ -\alpha_1 & -\alpha_2 & -\alpha_3 & & -\alpha_n \end{bmatrix} \qquad 12.1$$

and for the second order case

$$A = \begin{bmatrix} 0 & 1 \\ -\alpha_1 & -\alpha_2 \end{bmatrix} \qquad 12.2$$

which has eigenvalues λ_i given by

$$|A - \lambda_i I| = 0 \qquad 12.3$$

i.e. $$\lambda_i^2 + \alpha_2\lambda_i + \alpha_1 = 0 \qquad 12.4$$

and eigenvectors z_i given by

$$|A - \lambda_i I|\underline{z} = 0 \qquad 12.5$$

Expanding the first row of equation 12.5 gives

$$-\lambda_i z_1 + z_2 = 0$$

giving the slope of the eigenvectors

$$\frac{z_2}{z_1} = \lambda_i \qquad 12.6$$

It can therefore be seen that the phase-canonical representation leads to the eigenvectors being obtained directly from the eigenvalues, the eigenvalues in their turn being the roots of the characteristic equation.

The natural choice of states to obtain the processor–machine system in phase-canonical form is thus

x_1 = speed error

x_2 = speed error rate

By manipulation of the equations describing Fig.11.7 we get

$$\begin{bmatrix} \dot{x}_1 \\ \dot{x}_2 \end{bmatrix} = \begin{bmatrix} 0 & 1 \\ -\frac{100\ K_2K_1g_1K_tK_{tacho}}{R_aJ} & -\left(\frac{F}{J} + \frac{K_tg_2K_v}{R_aJ} + \frac{nK_3K_1g_1K_tK_{tacho}}{R_aJ}\right) \end{bmatrix} \begin{bmatrix} x_1 \\ x_2 \end{bmatrix} \qquad 12.7$$

which is represented by Fig.12.1.

To simplify the initial synthesis studies, put

$$\alpha_1 = \frac{100\ K_2K_1g_1K_tK_{tacho}}{R_aJ}$$

and $$\alpha_2 = \frac{F}{J} + \frac{K_tg_2K_v}{R_aJ} + \frac{nK_3K_1g_1K_tK_{tacho}}{R_aJ}$$

giving

$$\begin{bmatrix} \dot{x}_1 \\ \dot{x}_2 \end{bmatrix} = \begin{bmatrix} 0 & 1 \\ -\alpha_1 & -\alpha_2 \end{bmatrix} \begin{bmatrix} x_1 \\ x_2 \end{bmatrix} \qquad 12.8$$

and a characteristic equation

$$s^2 + \alpha_2 s + \alpha_1 = 0 \qquad 12.9$$

12.3 The Choice of Parameters for Linear Control

The fixed parameters that are to be chosen are the software gains K_1, K_2 and K_3, and the error rate estimation interval n. The product $K_1.K_2$ effectively sets the natural frequency of the loop. It was seen in chapter 11 that with $K_1.K_2 = \frac{1}{4}$, the loop natural frequency was in the range 3.5 Rads/sec to 6.5 Rads/sec. It was found that attempts to increase $K_1.K_2$ further led to the system responses becoming excessively noisy around the steady state condition. We therefore choose

$$K_1 = \frac{1}{4} \quad \text{and} \quad K_2 = 1$$

To get a reasonable estimate of error rate, n must be chosen to allow $\hat{\dot{e}}$ in equation 11.21 to attain useful values. A typical speed transient in the current limit mode has been seen in practice to have a value of the order of 350 r.p.m./sec, i.e. 56 units/sec from the tachometer A/D. Thus in one sample period (10 ms) there will be an average change of .56 units.

There will be an upper limit on the value of n due to the delay introduced by estimating the current error rate with an error sample n sample periods previous. If this delay becomes excessive, instability will become apparent. Stability problems did in fact appear for n > 10 in the practical system. A choice of n = 7 was thus made as a compromise, giving a typical error rate estimate of 4 units for current limit mode accelerations.

The remaining parameter to be chosen is the error rate gain K_3. With K_3 set at $K_3 = 4$, the characteristic equation for each condition is as shown in Table 12.1. Table 12.2 then shows the corresponding natural frequency and the damping factor for each condition.

The range of damping factors is seen to be centred about the frequently chosen value of $\zeta = 0.7$ and is thus considered a satisfactory design with the parameters chosen as above.

To summarise, we have

$$K_1 = \frac{1}{4}\ ,\quad K_2 = 1\ ,\quad K_3 = 4 \quad \text{and} \quad n = 7$$

in the linear design.

N.B. The value $n = 7$ will also be used in the variable structure design for the same reasons as above.

12.4 The Choice of Configuration for Variable Structure Control

Two possible arrangements for the variable structure control will be considered, the second being chosen for reasons that will be shown. The design methods will be based on the equivalent control concept of section 4.4.1 and the techniques described in Appendix A.

The system is described by equation 12.8, which may be rewritten as

$$\begin{aligned} \dot{x}_1 &= x_2 \\ \dot{x}_2 &= -\alpha_1 x_1 - \alpha_2 x_2 \end{aligned} \qquad 12.10$$

We have control over both α_1 and α_2 by the selection of K_1, K_2 and K_3.

The sliding mode is defined by

$$s = x_2 + c_1 x_1 = 0 \qquad 12.11$$

c_1 is positive constant

The equivalent control method now requires the condition

$$\dot{s} = \dot{x}_2 + c_1 \dot{x}_1 = 0 \qquad 12.12$$

Substituting equations 12.10 and 12.11 into equation 12.12 gives

$$\alpha_2 c_1 - \alpha_1 - c_1^2 = 0 \qquad 12.13$$

Also, we can write

$$\dot{s} = c_1 s - [c_1^2 + \alpha_1] x_1 - \alpha_2 x_2 \qquad 12.14$$

For the first variable structure arrangement, consider control by the variation of α_1 only, i.e. K_1 will be varied. K_3 is therefore set equal to zero giving

$$\alpha_2 = \frac{F}{J} + \frac{K_t g_2 K_v}{R_a J} \qquad 12.15$$

Rearranging equation 12.13 gives the equivalent control, Ω_1, as

$$\alpha_{1eq} = \Omega_1 = \alpha_2 c_1 - c_1^2 \qquad 12.16$$

To satisfy the existence conditions of the sliding mode, we now introduce a variable structure control as

$$\alpha_1 = \Omega_1 + \Delta \operatorname{sgn}(x_1 s) \qquad 12.17$$

Δ is a positive constant

Substituting equations 12.16 and 12.17 into equation 12.14 gives

$$\dot{s} = c_1 s - [c_1^2 + \alpha_2 c_1 - c_1^2 + \Delta \operatorname{sgn}(x_1 s)] x_1 + \alpha_2 c_1 x_1$$

i.e. $$\dot{s} = c_1 s - \Delta |x_1| \operatorname{sgn} s \qquad 12.18$$

from which it can be seen that as

$s \to -0 \qquad \dot{s} > 0$

and as $s \to +0 \qquad \dot{s} < 0$

which are the conditions for the sliding mode existence.

The variable structure control is thus

$$\alpha_1 = \alpha_1^+ > \alpha_2 c_1 - c_1^2 \quad \text{if} \quad x_1 s > 0$$
$$\alpha_1 = \alpha_1^- < \alpha_2 c_1 - c_1^2 \quad \text{if} \quad x_1 s < 0 \qquad 12.19$$

The reaching conditions of Theorem A2 require that the system with $\alpha_1 > \alpha_2 c_1 - c_1^2$ has complex eigenvalues or negative real eigenvalues. By inspection of the characteristic equation 12.9, and by noting that α_2 is positive, it can be seen that the real parts of the eigenvalues will be negative for

$$\alpha_1^+ > 0 \qquad 12.20$$

The second arrangement considers α_1 fixed and α_2 controlled by the variation of K_3. This strategy does not follow the formulation of Appendix A. We can, however, use the equivalent control concept which is a completely general technique.

Equation 12.13 gives the equivalent control Ω_2 as

$$\alpha_{2eq} = \Omega_2 = \frac{\alpha_1}{c_1} + c_1 \qquad 12.21$$

A variable structure control may now be proposed as

$$\alpha_2 = \Omega_2 + \Delta \operatorname{sgn}(x_2 s) \qquad 12.22$$

Substituting equations 12.21 and 12.22 into equation 12.14 gives

$$\dot{s} = c_1 s - [\, c_1^2 + \alpha_1 \,] x_1 + \alpha_1 x_1 + c_1^2 x_1 - x_2 \Delta \operatorname{sgn}(x_2 s) \qquad 12.23$$

i.e. $$\dot{s} = c_1 s - \Delta |x_2| \operatorname{sgn} s \qquad 12.24$$

As before we have the property that

as $s \to -0$ $\quad \dot{s} > 0$

and $s \to +0$ $\quad \dot{s} < 0$

thus the sliding mode exists.

The variable structure control is now

$$\alpha_2 = \alpha_2^+ > \frac{\alpha_1}{c_1} + c_1 \quad \text{if} \quad x_2 s > 0$$

$$\alpha_2 = \alpha_2^- < \frac{\alpha_1}{c_1} + c_1 \quad \text{if} \quad x_2 s < 0 \qquad 12.25$$

The reaching conditions will be considered in the following section 12.4.2, and will be seen to hold by inspection.

12.4.1 The Choice of a Specific Sliding Plane

A typical case of the system operating with linear control is that of condition 4 in table 12.1. The variable structure control is to produce some improvement from a time optimal point of view. We therefore require the system to approach the sliding plane with low damping. The sliding plane itself should then be coincident with the fast eigenvector of the nominal system with damping that is greater than that of the linear case.

The nominal linear system has the characteristic equation

$$s^2 + 6.434s + 20.3 = 0$$

i.e. $\zeta = 0.713$

If $K_3 = 0$ we see from table 11.3 that the characteristic equation is

$$s^2 + 0.7337s + 20.3 = 0$$

i.e. $\zeta = 0.0814$

which is a suitable lightly damped system.

If we choose the higher damped system to be

$$s^2 + 11s + 20.3 = 0 \quad \text{(say)}$$

then $\zeta = 1.22$

and the eigenvalues are -8.65 and -2.346 and the corresponding eigenvectors have slopes -8.65 and -2.346 from equation 12.6.

From the point of view of the practical microprocessor system, we can measure speed error (x_1) and then estimate a representation of the speed error rate which is not x_2 itself, but $\frac{n}{100} x_2$. Then, by applying a scaling factor c_s to x_1 we can define a sliding plane as

$$s = \frac{nx_2}{100} + c_s x_1 = 0 \qquad 12.26$$

i.e. $$s = x_2 + \frac{100\, c_s x_1}{n} = 0$$

and for the case of n = 7

$$s = x_2 + 14.286\, c_s x_1 = 0$$

It is convenient to choose c_s as an integer power of 2, since the scaling of x_1 may then be achieved by simple shift operations. We therefore choose $c_s = \frac{1}{2}$ to give

$$s = x_2 + 7.143\, x_1 = 0 \qquad 12.27$$

making c_1 in equation 12.11

$$c_1 = 7.143$$

Thus the selected sliding mode is the nearest we can get to the fast eigenvector (-8.65) of the higher damped system, with c_s as an integer power of 2.

12.4.2 Specific Aspects of the Two Variable Structure Control Law Options

The two strategies discussed in section 12.4 will now be considered in relation to the chosen sliding plane and typical parameter values.

For the first arrangement we recall the control law of equations 12.19 and 12.20.

i.e. $\alpha_1 = \alpha_1^+ > 0$ if $x_1 s > 0$

$\alpha_1 = \alpha_1^- < \alpha_2 c_1 - c_1^2$ if $x_1 s < 0$

It seems reasonable to choose K_1K_2 (thus setting α_1^+) as $K_1K_2 = \frac{1}{4}$ for $x_1 s > 0$. This choice results in the characteristic equations of table 11.3. Thus, for the region of state space where the system is approaching the sliding mode, the response will be of second order, lightly damped and with the same natural frequency as the linear design of section 12.3. The form of the system trajectories in this mode is shown in Fig.12.2.

The limiting case for α_1^- is $\alpha_1^- = \alpha_2 c_1 - c_1^2$. The values of α_2 are simply the coefficients of s in table 11.3, and c_1 has already been chosen as $c_1 = 7.143$. It is thus easy to calculate the limiting values for α_1^- as those shown in table 12.3(a). To satisfy the condition $\alpha_1^- < \alpha_2 c_1 - c_1^2$, the value of K_1K_2 is chosen as $K_1K_2 = -1$. The values of α_1^- with $K_1K_2 = -1$ are shown in table 12.3(b). The characteristic equations in this mode are given in table 12.4. Inspection of these characteristic equations shows that they have one stable real eigenvector and one unstable real eigenvector resulting in the typical system trajectories shown in Fig.12.3.

The composite variable structure trajectories will thus be as shown in Fig.12.4.

To summarise, we have for this arrangement

$K_3 = 0$ $K_2 = 1.0$ $n = 7$

$$K_1 = \frac{1}{4} \quad \text{if } x_1 s > 0$$

$$K_1 = -1 \quad \text{if } x_1 s < 0$$

For the second arrangement the control law was seen to be

$$\alpha_2 = \alpha_2^+ > \frac{\alpha_1}{c_1} + c_1 \quad \text{if } x_2 s > 0$$

$$\alpha_2 = \alpha_2^- < \frac{\alpha_1}{c_1} + c_1 \quad \text{if } x_2 s < 0$$

Again, we set $K_1 K_2 = \frac{1}{4}$ to result once more in the same natural frequency as for the linear case. By setting $K_3 = 0$ for $x_2 s < 0$ the characteristic equations are as in table 11.3, and the condition $\alpha_2^- < \frac{\alpha_1}{c_1} + c_1$ is immediately seen to be satisfied. Thus, the region in state space where the system is approaching the sliding mode has exactly the same control law as the corresponding region discussed in the first arrangement, and has typical trajectories shown in Fig. 12.5.

The limiting values of $\alpha_2^+ = \frac{\alpha_1}{c_1} + c_1$ are shown in table 12.5(a). To satisfy the condition $\alpha_2^+ > \frac{\alpha_1}{c_1} + c_1$, the value of K_3 is chosen as $K_3 = 16$. The values of α_2^+ with $K_3 = 16$ are shown in table 12.5(b). The characteristic equations in this mode are given in table 12.6. This time, the characteristic equations are seen to have two stable eigenvectors resulting in typical system trajectories as shown in Fig. 12.6.

The composite variable structure trajectories will now be as seen in Fig.12.7. By inspection of Fig.12.7, it is obvious that the sliding mode will be reached from any initial condition.

In summary, we have for this arrangement

$$K_1 = \frac{1}{4} \qquad K_2 = 1.0 \qquad n = 7$$

$$K_3 = 16 \quad \text{if } x_2 s > 0$$

$$K_3 = 0 \quad \text{if } x_2 s < 0$$

12.4.3 Selection of the Second Arrangement as a Practical Variable Structure Control

With reference to Fig.12.7 it can be seen by inspection that, for an initial condition between the fast eigenvector and the x_2 axis, the response approaches the origin in the way required by the optimal studies of chapter 6, i.e. the first and third quadrants are heavily damped. In Fig.12.4, however, it is seen that the first and third quadrants are lightly damped. The second arrangement is therefore chosen for the practical system, due to its closer conformation to the time optimal control strategies of chapter 6.

A variable structure control policy has thus been determined, that should result in a real system that will show an improvement in two ways when compared to the system with a conventional linear control law; namely better performance from a time optimal point of view, and consistent responses in the presence of a variable environment.

The microprocessor control subroutine will thus perform the following operational functions.

1) calculate the speed error (x_1).
2) calculate the speed error rate ($\frac{nx_2}{100}$) using error values separated by n = 7 samples.
3) calculate $s = x_2 + \frac{100\, c_s x_1}{n}$
4) calculate $K_1 \left[K_2 x_1 + \frac{K_3 n x_2}{100} \right]$

where $K_1 = \frac{1}{4}$, $K_2 = 1$, $n = 7$

and $K_3 = 16$ if $x_2 s > 0$

or $K_3 = 0$ if $x_2 s < 0$

5) add the number generated by step (4) to the present firing angle.

6) return from subroutine.

This procedure is illustrated in flow chart form in Fig.12.8. The actual machine code program has certain extra features which apply only in limited circumstances, i.e. the firing angle change is not permitted to exceed ±10 (hex). This prevents the control program generating very large firing angles when the speed errors are large. Such large demands would cause excessive armature currents, which the overcurrent routine could not clear quickly enough to prevent damage or a blown fuse.

The second feature refers to step (4) above. If the term $K_2x_1 + \frac{K_3nx_2}{100}$ is small, the division by 4 that is then applied will result in the binary representation that has been shifted right twice having all bits equal to zero . There would thus be a range of $K_2x_1 + \frac{K_3nx_2}{100} = \pm 3$ (decimal) where no control action would be taken. In steady state, $x_2 = 0$ giving a dead band of speed error $x_1 = \pm 3$. To overcome this, we store $K_2x_1 + \frac{K_3nx_2}{100}$, if the division by 4 then results in zero, the sign of the stored undivided number is checked. If that sign is positive, the firing angle change is set to +1. In the case of a negative sign, the firing angle change is -1.

It should be noted that before step (3) above is made the values of x_1 and $\frac{nx_2}{100}$ are checked. If both are equal to zero, the firing angle change is zero and the return from subroutine is made immediately.

The machine code program is given in Appendix K.

CHAPTER 13

DESCRIPTION AND DISCUSSION OF PRACTICAL TESTS

13.1 General

This chapter will consider the actual performance of the processor-machine system, with both linear and variable structure control laws. As was noted in Chapter 12, the difference in effect of the various control strategies will only become apparent when the system comes out of the current-limit region.

The types of test applied to the system can be divided into two general categories. The first of these is the response of the machine to a step demand of speed, with the initial condition of machine speed (ω) at zero and the derivative of speed ($\dot{\omega}$) also at zero. The second type of test is to run the machine up to a certain demanded speed, and then to apply step load torques by means of switching the resistance value in the armature circuit of the load machine.

Records of the system performance are taken in two ways. Firstly, by the direct connection of an x-y recorder with integral timebase, to the tachometer attached to the shaft of the work machine. This arrangement allows the step-demand speed response and the variation of speed due to loading, to be permanently plotted as a function of time. The second method used to obtain system responses involves a small amount of additional machine code programme, which arranges for the system variables used for the calculation of control, i.e. speed error and estimate of error rate, to be stored in a block of random access memory at regular intervals.

At the end of a test, this stored data may then be recalled and displayed (via digital to analogue converters) on either an oscilloscope or the x-y recorder. By plotting the stored values of speed error on one axis, against estimated error rate on the other axis, we can then obtain the system response as a phase-plane trajectory. The expected sliding modes should then be seen as trajectories that approximate to straight lines on the phase-plane.

13.2 Specific Details of Test Conditions

By reference to Tables 11.1 and 12.2 it may be seen for the system with the "compromise" linear control law, that the major variations in the transfer function characteristics are due to the various loading configurations, and the addition of armature resistance. The effect of running the system at a variety of nominal speeds, however, results in only minor changes when compared to the two aforementioned factors. To keep the number of results down to a reasonable level, it was thus decided to make the majority of the tests with the speed demand set at a nominal value of 500 rpm.

13.2.1 Step Responses for Various Conditions

The responses shown in Figs. 13.1 - 13.5 correspond to conditions detailed in Table 11.1. Thus we have

Figure Number	Condition Number (Table 11.1)
13.1	2
13.2	5
13.3	8
13.4	11
13.5	14

Each figure then contains three responses to a step speed demand of 50 (HEX) ≃ 500 rpm. Each of the three plots per figure is the response of the system with a certain control law, i.e.

a) The control law is the linear law determined as the best compromise in section 12.3.

b) The control law is the variable structure law detailed in section 12.4.3, with a sliding plane defined by

$$s = x_2 + 7.143\ x_1 = 0$$

c) The control law is linear with the parameters and characteristics detailed in table 12.6, i.e. heavily damped.

It will be seen in the load tests that this control law produces comparable load performance to that with variable structure control. It was thus felt that step performance with this control should also be investigated.

All these step responses were taken by the x-y plotter connected such that the tachometer output went to the y channel and the x channel was fed from the internal timebase.

13.2.2 Step Response with a Large Amount of Added Work Machine Armature Resistance

The responses shown in Fig. 13.6 are taken for the arrangement of condition 14 in table 11.1 except that the amount of added armature resistance is 3Ω. The system characteristic for this condition has not been found theoretically. However, it is still valid to draw conclusions

from a comparison between the compromise linear control (Fig. 13.6(a)) and the variable structure control (Fig. 13.6(b)), with the effective armature resistance at four times the natural resistance of the unmodified armature circuit.

13.2.3 Response of Machine Speed to Step Torque Loads

The responses shown in Fig. 13.7 and Fig. 13.8 are the speed responses of the system when step torque loads are applied. The test is carried out by initially running the machine up to 500 rpm. The sequence of events is then:

1) Switch in some load machine armature resistance to produce a load torque.

2) Switch out the load machine armature resistance to remove the load torque.

3) Continuously switch the load machine armature resistance to excite the system at its resonant frequency. This representing a worst case fluctuating load situation.

The responses in Fig. 13.7 are with no added work machine armature resistance whereas the responses in Fig. 13.8 are with 1Ω added armature resistance.

Again we have the three control strategies given in section 13.2.1, i.e.

a) The compromise linear control law.

b) The variable structure control law.

c) The heavily damped linear control law.

Each of these divisions is then sub-divided into

i) Medium torque loads

and ii) Large torque loads

where the following definitions apply.

Definitions

For the machine operating at 500 rpm with the load machine connected, but with no load machine armature resistance, the average work machine armature current is ≈ 1.8 A. We then define a medium load such that the amount of load machine armature resistance inserted results in a work machine average armature current of 4A, to produce sufficient torque to maintain the speed at 500 rpm. A large load is then defined in a similar way except that the load is such that the average work machine armature current is 6 A.

13.2.4 Response to a Variety of Step Speed Demands

Fig. 13.9 illustrates the response of the system to a range of speed demands. The load machine is connected and the loading is that of condition 2. Again we have

a) The compromise linear control law

and b) The variable structure control law

13.2.5 Response to a Step Speed Demand for Variable Structure Control with a Variety of Sliding Planes

Fig. 13.10 shows the responses of the system to a step speed demand of 500 rpm. The loading arrangements are as for condition 2. Each response in the figure is taken with a different desired sliding mode, as follows

Response	c_s (in equation 12.26)	Sliding Mode
(a)	1/16	$s = x_2 + 0.89\ x_1 = 0$
(b)	1/8	$s = x_2 + 1.786\ x_1 = 0$
(c)	1/4	$s = x_2 + 3.57\ x_1 = 0$
(d)	1/2	$s = x_2 + 7.143\ x_1 = 0$
(e)	1	$s = x_2 + 14.286\ x_1 = 0$

13.2.6 A Digital Record of Error (x_1) and Error Rate Estimate ($\frac{nx_2}{100}$)

Fig. 13.11 shows the time responses for a step speed demand of (a) the speed error and (b) the estimated speed error rate. Both responses consist of 256 samples, with a sample being stored at every control interval, i.e. store data every 10 ms. Thus the total record covers a duration of 2.56 seconds. The load condition for this test is as given for condition 2 in table 11.1.

13.2.7 Digital Records of Speed Error and Error Rate Estimate, Displayed as a Phase Plane Response

Fig. 13.12 shows the phase plane response (error against error rate estimate) for a variety of desired sliding modes as follows

Response	c_s (in equation 12.26)	Sliding Mode
(a)	1/16	$s = x_2 + 0.89\ x_1 = 0$
(b)	1/8	$s = x_2 + 1.786\ x_1 = 0$
(c)	1/4	$s = x_2 + 3.57\ x_1 = 0$
(d)	1/2	$s = x_2 + 7.143\ x_1 = 0$
(e)	1	$s = x_2 + 14.286\ x_1 = 0$

The load configuration for these tests is that of condition 14 in table 11.1.

13.3 Discussion of Practical Results

By inspection of the "compromise" linear responses shown in Fig. 13.1-13.5, it may be seen that there is a significant variation in the form of these responses over the range of operating conditions. For condition 8 for instance, it can be seen that there is virtually no overshoot whereas condition 14 provides a response with approximately 7% overshoot. Examination of the variable structure responses, however, shows a far greater degree of consistency. The responses for the variable structure control for conditions 2, 5 and 11 are sensibly the same after the initial current limit mode has ended. The variable structure response for condition 8 is 'good' but appears to be faster at the final portion of the trajectory than for the three previous mentioned conditions. The probable reasons for this will be discussed later. The variable structure response for condition 14 has a final portion that is slightly faster and has a very small overshoot when compared to the variable structure responses for conditions 2, 5 and 11. Again, the reasons for this will be covered later.

It was explained in section 13.2.1 that a well-damped linear control law was considered because (as it will be seen) good performance in loading tests may be obtained. It is immediately obvious, however, that the step speed demand responses shown in Figs. 13.1(c) to 13.5(c) are very sluggish for the well-damped control, when compared to either the compromise linear law or the variable structure law.

It has thus been seen from Figs. 13.1 to 13.5 that the variable structure control law produces the most consistent, desirable responses.

It is appreciated that, although the range of conditions over which these tests were taken, is large and varied, the responses with the compromise linear control do not vary dramatically. The compromise linear responses shown so far whilst being inferior to the variable structure responses, would in most circumstances still be acceptable.

The responses shown in Fig. 13.6 were taken with the load machine connected but with no load machine armature resistance inserted. The armature of the work machine has had 3Ω extra armature resistance added. In a practical engineering situation such added resistance might appear unavoidably due to several possible causes, i.e.

a) As protection for armature drive circuits.

b) By substitution of a new machine of different manufacture.

or c) Operation of the machine at a distance from the controller, with the attendant resistance of the armature supply cables.

The response with the compromise linear control exhibits a 35% overshoot and a long settling time. The variable structure response, however, has only a 7% overshoot, and can be seen to settle much sooner than the aforementioned response.

In this situation the variable structure law has a clear and worthwhile advantage over the compromise linear law.

Fig. 13.7 shows the response of the machine speed to the step torque load tests described in section 13.2.3.

The deviations from the nominal speed for the compromise linear control can be seen to be between 2 and 3 times as great as for those deviations recorded with the variable structure control.

The responses with the well-damped linear control are comparable to the variable structure case, but as we have seen, the step speed demand responses for the well-damped control are very slow when compared to the responses obtained with either the compromise linear control or the variable structure control.

Fig. 13.8 shows the responses to similar load tests except for the addition of 1Ω extra resistance in the work machine armature circuit. Again, the variable structure responses are superior to those obtained with the compromise linear law. The variable structure responses may also be seen to have better properties than the well damped responses, i.e. when the load is switched on, the deviations in Fig. 13.8(c) can be seen to be of a similar magnitude to the deviations in Fig. 13.8(b). However, because of the slow mode inherent in a well-damped second order system, the return of the machine to its nominal speed in Fig. 13.8(c) is considerably slower than the return to nominal speed in Fig. 13.8(b).

The tests considered so far have shown the the variable structure control law results in a system that has good consistent step speed demand responses over a wide range of operating conditions. For the same range of conditions, the compromise linear law resulted in a variety of responses of which some would in all probability be unacceptable, in a real application. The variable structure scheme also results in a system that is at least twice as insensitive to torque loads, when compared to the compromise linear law.

Fig. 13.9 shows that the variable structure scheme operates over a wide range of operating speeds.

Fig. 13.10 illustrates how the response of the system may be selected by the simple choice of the sliding mode parameter c_s in equation 12.26. At Fig. 13.10(e) it can be seen that overshoot occurs. This will be discussed later.

Fig. 13.11 illustrates the type of plot that is obtainable by storing the values of speed error and speed error rate estimate, used by the microprocessor to calculate the control action. For this figure only the error rate estimation interval n was increased to 10 periods. This allowed a larger, more detailed picture of the error rate estimate to be obtained.

Fig. 13.12 shows the digital records plotted as phase plane responses, for various desired sliding modes. The error rate estimation interval has now been returned to n = 7. It is immediately obvious that the error rate estimate signal is very noisy. Also, the estimate signal is highly quantised, being typically between +1 and -5 bits over the total trajectory.

At Fig. 13.12(a) it can be seen that the sliding mode is reached almost immediately from the initial condition e = 80 bits and $\hat{e}$ = 0 bits. The trajectory then approaches the origin by a path that, on average, tends to the desired sliding mode. In Figs. 13.12(b) and 13.12(c) the desired sliding modes are selected for a faster response. In both cases, the system is seen to enter the current limit mode (approximately constant acceleration) and then, as before, it approaches the origin via the desired sliding mode. In Fig. 13.12(d)

the desired sliding mode is again approximately realised, but a small amount of overshoot has resulted. This corresponds to the time domain response shown at Fig. 13.5(b). In 13.12(e) the desired sliding mode is again made to give a faster response, and the overshoot in this case is now even more pronounced.

Having presented the various results and discussed the main features of those results, we are now in a position to examine some of the effects that were not predicted by the theoretical studies. Specifically, these effects are the overshoots noted at Figs.13.5(b), 13.10(e), 13.12(d) and 13.12(e). Also, the faster than expected response at Fig. 13.3(b).

The mathematical model developed in chapter 11 is of course only an approximation to the real behaviour of the system. It is part of the attraction of adaptive control systems that highly accurate models need not be formulated to achieve good, consistent performance.

Equation 12.25 shows that if certain conditions are fulfilled the sliding mode will exist. The most likely part of equation 12.25 to be violated is that

$$\alpha_2^+ \not> \frac{\alpha_1}{c_1} + c_1$$

i.e. the heavily damped structure cannot provide a mode faster than the desired sliding mode. Table 12.5, however, shows a reasonable safety margin exists to guarantee the existence of the sliding mode. The linear model parameters would thus have to be in error by a fairly large amount for the inequality of equation 12.25 to fail.

In the formulation of the mathematical model it was assumed that the system was continuous. In reality, however, the system is a sampled one, i.e. for any 10 ms mains half cycle the control is fixed. New control can only be applied in the next half cycle. Thus there will be delays between the time when the control is to be applied, and the actual time when the control is applied.

For a typical step response, i.e. Fig. 13.4(b), the speed increases at a rate of approximately 50 bits/sec. When the desired sliding mode is reached, there may well be a delay of 10 ms before the control can act. In that 10 ms therefore the system trajectory will pass across the sliding plane. However, the speed will only have changed by 50 x 0.01, i.e. $\frac{1}{2}$ bit on average, in this time. The 10 ms delay would thus not appear to be a direct major contributory factor to the sliding mode being overshot.

The factor that does appear to cause the system trajectory to deviate from that expected is apparent in the responses shown in Fig. 13.12, i.e. the highly quantised, noisy error rate signal. The way in which the error rate estimate is found is effectively differentiation of the speed error signal. Thus any noise on that speed error signal will be magnified by the differentiation process. The solution to the noise and quantisation problem could be accomplished by the introduction of an improved tachometer system. This will be briefly considered in the next chapter.

It is thus considered that the deviations from the theoretical responses are due to the poorly estimated acceleration signal. These deviations can be seen on all the phase plane plots, but the effect

on the time domain response is only appreciable for the faster sliding planes. These deviations do not alter the fact that the responses with variable structure control are still superior to the responses with fixed linear control.

To complete the results section, some figures for the speed of execution of the microprocessor programme will now be given.

Time between the start of a 10 ms control period to the output of the firing angle is less than 800 μS.

Time to read the tachometer once is approximately 50 μS.

CHAPTER 14

CONCLUSIONS AND SUGGESTIONS FOR FURTHER WORK

14.1 Conclusions

Variable structure systems have been seen theoretically to be capable of producing superior performance when compared to systems designed with fixed structure control laws. These improvements fall into two categories, i.e. optimal performance and adaptive performance. Variable structure systems designed with sliding modes are seen to provide a generally applicable philosophy for the synthesis of model reference adaptive controllers (MRAC). The variable structure approach comparing well with the other, presently more popular, methods of designing MRAC, i.e. by Liapunov stability theory or by the hyper-stability approach. The advantages gained by using the variable structure technique are primarily those of partial adaptive response definition and the simplicity achieved by switching between fixed gain values rather than requiring continuously variable gain functions. Particularly simple schemes have been seen to result if the reference model which specifies the "ideal" desired performance of the system is formulated implicitly by defining a hyperplane in the state space of the system to be controlled. The parameters of the hyperplane being decided by consideration of the linear system that motion on the hyperplane represents.

The ability of variable structure systems to logically select at any instant of time from a variety of feedback control laws allows the best features of each control law to be exploited. In the same way, it

is possible in some cases to avoid the undesirable features present in the comprising feedback control laws. The problem of deciding exactly when to select a particular structure to obtain the aforementioned benefits was seen to be well suited to the Maximum Principle method of determining optimal controls. To this end, a new technique has been developed which will directly generate the line (switching curve) that separates the regions of fixed control, for a class of second order variable structure system with minimum time as a performance index. Previous methods allowed the switching curve to be generated only in a point by point fashion.

The choice of the switching curve for the case of a quadratic state performance index has also been considered and the appearance of singular modes in variable structure systems with such indices has been clarified by the use of the ideal model concept.

The final chapter in the theoretical studies considered the compatibility of optimally and adaptively designed variable structure systems. It was shown that by correctly choosing a sliding mode, a variable structure system could provide both the adaptive and the optimal properties previously discussed. To summarise the design of optimal/adaptive variable structure systems, a series of flow charts have been constructed. This presentation of the unified optimal/adaptive system design appears to be new.

The practical application of an optimal/adaptive variable structure control law to the real system of a microprocessor controlled d.c. machine has demonstrated the viability of such controls in real engineering situations. The ability of the microprocessor to make fast decisions on the result of a logical comparison operation means that

the position in state space relative to the switching surface and the corresponding selection of structure can be performed very efficiently by the processor programme. This is demonstrated by the fact that only 22 extra machine code lines of programme are required in the control subroutine to extend the control from fixed linear to variable structure. This represents an increase of about 12% in length of the control routine, and an increase of about 3% in the total programme length.

Although in this study a microprocessor based system was used to control the thyristor bridge that supplied the machine armature, the application of variable structure control is just as feasible for systems that operate with analogue devices. The position in state space might be determined by a simple arrangement of operational amplifier summers fed from transducer signals. The signals from these, passing through appropriate logic circuits, could then alter feedback gains by switching a variety of resistances that set the gains of the signal feedback amplifiers.

The actual performance of the machine-processor system with variable structure control is seen to be superior to the system with linear control. The optimal improvements predicted by the theoretical studies are demonstrated by a reduction (between 2 and 3 times) in the sensitivity of the system with variable structure control, to load torque disturbances when compared to a fixed linear control.

The adaptive properties of the variable structure system were demonstrated by step speed demand tests for a variety of operating conditions. The responses with the variable structure control law were seen to be far more consistent than with the linear control law. Under certain conditions the responses for linear control had large overshoots

and long settling times. For the same conditions the responses with the variable structure control featured little overshoot and fast settling times.

For the step speed demand tests, the variable structure control had little chance to demonstrate any improvement from an optimal point of view. This is due to the machine operating in a current limit condition for the majority of the rise in speed to the required value.

Small discrepancies between the expected variable structure responses and the actual responses in some cases, i.e. slight amounts of overshoot, were almost certainly due to the poor quality of the estimated speed rate signal used in the control.

The results obtained with the variable structure control also compare favourably with a previous study[42] which used a technique called the matrix method, to control the same machine. In this method, the state space was divided up into 9 regions. Various fixed firing angle changes then applied, in each of these regions. Although the details of the tests carried out with the matrix control differ to those in this study, the responses can be seen in general to have significant overshoot and limit cycling present where again generally the variable structure responses in this work have very little. The matrix control was never intended to be adaptive and as such the operating conditions of the machine were not subject to great variation.

In their paper[43] Courtiol and Landau consider the adaptive control of an armature driven d.c. machine. Their system was designed by a hyperstability approach and may be seen to have quite a complex system

block diagram when compared to the variable structure controller developed in this work. The hyperstability scheme requiring an explicit model, several filters and several analogue multipliers. It is felt that a variable structure scheme implemented with operational amplifiers and a small amount of logic circuitry would result in a far simpler system which would also have the optimal benefits associated with the first order implied model that has been used in the present practical system.

The general conclusion of this research is that variable structure control can provide a considerable increase of optimal/adaptive performance in many control applications where previously a fixed linear control would have been used. The increase in complexity of a variable structure controller compared to a linear controller is not great, especially in the case where control is performed by a software routine in a mini or micro-computer. When purely adaptive controllers are considered, the variable structure scheme has had relatively little reported research of practical applications when compared to other schemes, i.e. Liapunov or hyperstability techniques. It is hoped that this research has shown that variable structure systems are a good alternative to the other presently more popular adaptive design methods.

14.2 Suggestions for Further Work

From a theoretical aspect there are several paths of investigation that the author would have liked to follow up, but did not for lack of time. Two of these are now briefly described.

The direct generation of the time-optimal switch curve has been achieved only for a general second order system. The extension of the method to higher order systems is now a natural path of research to take.

For higher order systems with purely real eigenvectors it seems likely that the fastest of these will define a switching line. To 'hit' that line in a three dimensional (say) space would probably require the definition of two intersecting sliding planes to produce the sliding line. Such a variable structure system would then be realised by the use of the hierarchy of controls technique.

The second extension to the generation of optimal control laws for variable structure systems is to broaden the type of performance index. If a performance index which includes a control effort term is considered it has been seen that the variable structure control is now a continuous function of the state and costate variables. It might now be possible to generate a series of lines (in a second order system) representing constant control values, over the state space. By obtaining sufficient lines a good approximation to the continuous optimal control would be produced. The practical implementation of such a control would then be well suited to a microprocessor system, which could store the 'map' of the control values on the state space and look up the required control at each point in the system trajectory.

From a practical point of view, the processor-machine system would undoubtedly benefit from an improved tachometer system. A digital tachometer would certainly result in better speed and error rate estimate signals. With those signals, the small discrepancies of the present system responses with the theoretical responses should be for the most part removed.

The application of the variable structure control law to a machine system that had active deceleration, i.e. back to back thyristor bridges, would lead to much faster systems. In cases like this, the assumption

that the system was continuous could fail. There has been very little research in the area of discrete variable structure systems. This then is another very obvious area for further research.

APPENDIX A

A.1 The Design of Single Input Variable Structure Systems with Sliding Modes

The plant to be controlled is described by the following equations.

$$\dot{x}_i = x_{i+1} \qquad i = 1,\ldots,n-1$$

$$\dot{x}_n = -\sum_{i=1}^{n} a_i x_i + u \qquad \text{A1}$$

a_i are constants or time-varying parameters and may be unknown.
u is the control.

The general design procedure is as follows

1) Choose the coefficients c_i in equation A2 that correspond to the "ideal" desired linear system, i.e.

$$s = \sum_{i=1}^{n} c_i x_i = 0 \qquad \text{A2}$$

2) Find a control that guarantees the existence of sliding modes at every point of the desired sliding plane s = 0.

3) Make sure that the selected control will steer the representative point of the system towards the sliding plane, for any initial position in state space.

The method of achieving the design has been well developed, and is detailed below.

The object is to design a variable structure controller to zero the output x_1 of the system.

The sliding plane is described by

$$s = \sum_{i=1}^{n} c_i x_i = 0, \quad c_i = \text{positive constant}, \; c_n = 1$$

and is chosen by defining some "ideal" linear system, as discussed in Appendix B.

For the sliding mode to exist, it is sufficient that the inequalities

$$\lim_{s \to -0} \dot{s} > 0 \quad \text{and} \quad \lim_{s \to +0} \dot{s} < 0 \qquad \text{A3}$$

hold[29]

Let the plant parameters a_i be constant initially. The control u is chosen as a piece-wise linear function of $\underline{x}$, with discontinuous coefficients i.e.

$$u = -\sum_{i=1}^{k} \psi_i x_i - \delta_o \; \text{Sgn } s \qquad 1 \leq k \leq n-1$$

$$\psi_i = \begin{cases} \alpha_i & \text{if } x_i s > 0 \\ \beta_i & \text{if } x_i s < 0 \end{cases} \qquad \text{A4}$$

$$\text{Sgns} = \begin{cases} +1 & \text{if } s > 0 \\ -1 & \text{if } s < 0 \end{cases}$$

$\alpha_i, \beta_i, \delta_o$ = constant

δ_o is a small positive scalar.

A.1.1 Existence of the Sliding Mode

It has been shown[44,45,46] that equation A3 is satisfied if

$$\alpha_i \geq c_{i-1} - a_i - c_i c_{n-1} + c_i a_n = \Omega_1$$
$$\beta_i \leq c_{i-1} - a_i - c_i c_{n-1} + c_i a_n = \Omega_2 \qquad \text{A5}$$

$$i = 1,\ldots,k \qquad c_o = 0$$

$$\frac{c_{i-1} - a_i}{c_i} = c_{n-1} - a_n \qquad i = k+1,\ldots,n-1$$

These equations represent (n - k - 1) constraints for (n - 1) coefficients c_i. These constraints only vanish for k = n - 1. Thus the choice of sliding mode is only completely free when k = n - 1.

It is instructive to derive the above conditions for a more specific case. Therefore a general third order example will be considered.

Consider the system of Fig.A1.

Let the representative point (r.p.) be somewhere on the sliding plane.

i.e. $s = x_3 + c_2x_2 + c_1x_1 = 0$ A6

We also require the r.p. to stay on the sliding plane.

$$\dot{s} = \dot{x}_3 + c_2\dot{x}_2 + c_1\dot{x}_1 = 0 \qquad \text{A7}$$

We are now in a position to determine u to satisfy equations A6 and equation A7.

The equation describing Fig.A1 is

$$\dot{x}_3 = u - x_3a_3 - x_2a_2 - x_1a_1 \qquad \text{A8}$$

Rearranging equation A6 gives

$$x_3 = -c_2x_2 - c_1x_1 \qquad \text{A6(a)}$$

Rearranging equation A7 gives

$$\dot{x}_3 = -c_2\dot{x}_2 - c_1\dot{x}_1 \qquad \text{A7(a)}$$

Substituting A6(a) and A7(a) into A8 gives

$$u = - x_1 [- a_1 - c_1c_2 + c_1a_3] - x_2[- a_2 - c_2c_2 + c_2a_3 + c_1] \qquad A9$$

This, thus represents the limiting condition of equation A5 with $\alpha_i = \beta_i$.

i.e.
$$\alpha_1 = \beta_1 = - a_1 - c_1c_2 + c_1a_3$$
$$\alpha_2 = \beta_2 = - a_2 - c_2c_2 + c_2a_3 + c_1 \qquad A10$$

In the more general condition, let $\alpha_i = \Omega_i + \Delta_i$ and $\beta_i = \Omega_i - \Delta_i$ Δ_i positive

Substituting equation A6 and equation A8 into equation A7 gives

$$\dot{s} = s[c_2 - a_3] - \Delta_1|x_1| \text{ Sgn } s - \Delta_2|x_2|\text{Sgn } s - \delta_o \text{ Sgn } s \qquad A11$$

It is thus clear that the following is true

$\dot{s} > 0$ and $\dot{s} < 0$

$s \to -0$ and $s \to +0$

as required.

The term $- \delta_o$ Sgn s is for the case when $\Delta_i = 0$. In any real system with finite Δ_i, however, the practical control will not include this term.

For the case of equation A5 with $k < n - 1$, the following theorem applies[46,47,48].

Theorem A1

Let $\lambda_1,\ldots,\lambda_n$ be eigen values of the system of equations A1 with

$$u = -\sum_{i=1}^{k} \Omega_i x_i \qquad A12$$

$$\Omega_i = c_{i-1} - a_i - c_i c_{n-1} + c_i a_n$$

The sliding mode in the sliding plane is asymptotically stable in systems of equations A1, A4 if and only if $R_e \lambda_i < 0$, $i = 1,\ldots,n-1$; one of the eigen values λ_n is equal to $c_{n-1} - c_n$ and may be arbitrary.

A.1.2 Reaching Conditions

The final part of the synthesis is to guarantee that the sliding plane is reached from any initial condition in the state space.

Theorem A2[45,49,50]

The necessary and sufficient condition for the state to reach $s = 0$ defined by equation A2 is that, given the sliding plane exists and is asymptotically stable, that all the real eigen values of the systems of equations A1 and A4 with $\psi_i = \alpha_i$ $(i = 1,\ldots,k)$ be negative.
N.B. Unstable complex eigenvalues with positive real parts are permitted.

A.1.3 Design Example[5]

Consider the following third order system

$$\dot{x}_1 = x_2 \qquad \dot{x}_2 = x_3 \qquad \dot{x}_3 = u$$

Apply theorem A1

Try $u = - \Omega_1 x_1$

If $\Omega_1 < 0$ two of the three eigen values have negative real parts. Thus variable structure control with $u = - \psi_1 x_1$ can be found that will assure the existence of an asymptotically stable sliding plane. In fact the condition of equation A5 and the stability of equation A1 are met if

$$s = x_3 + x_2 c_2 + x_1 c_1 , \qquad c_1 = c_2^2$$

$$\alpha_1 > - c_1 c_2 \qquad \beta < - c_1 c_2$$

$$c_1 > 0, \; c_2 > 0$$

The reaching condition of theorem A2 is met if $\alpha_1 > 0$.

A.1.4 Comments

1) It is possible to produce a stable variable structure system, even though none of the comprising structures are stable

i.e. A second order example

$$\ddot{x} - \rho\dot{x} + \psi x = 0$$

ρ is positive constant

$$\psi = \begin{cases} \alpha \text{ if } xs > 0 \\ -\alpha \text{ if } xs < 0 \end{cases} \qquad \alpha \text{ positive constant}$$

$$s = cx + \dot{x}$$

Fig.A2 shows phase plane responses of the two comprising structures.

By choosing s appropriately we get the resulting composite VSS phase portrait shown in Fig.A3.

2) Design example 1 showed a third order system stabilised by variable structure feedback of x_1 only. It is important to note that the states x_2 and x_3 are still required to be measured, since they comprise the function s which must be known at all times.

A.1.5 Time-Varying Plants

Assume now that the plant parameters are allowed to vary with time, and are not measurable. However, they are known to lie within certain limits

i.e. $a_i \min \leq a_i(t) \leq a_i \max$

$$i = 1,\ldots,n$$

The equality constraints for c_i in equation A5 cannot be met if a_i are unknown. However, these constraints disappear if $k = n - 1$.

The inequality constraints of equation A5 can always be met if for any c_i

$$\alpha_i \geq \max_t \left[c_{i-1} - a_i(t) - c_i c_{n-1} + c_i a_{n-1}(t) \right]$$

$$\beta_i \leq \min_t \left[c_{i-1} - a_i(t) - c_i c_{n-1} + c_i a_{n-1}(t) \right] \qquad \text{A13}$$

$$i = 1,\ldots,n-1$$

A.1.6 Existence Conditions for Time-Varying Plants

Theorem A3[51]

It has been shown that the conditions A13 are necessary and sufficient for a sliding plane to exist.

A.1.7 Reaching Conditions for Time-Varying Plants

Theorem A4[52]

Sufficient reaching conditions are

$$c_i > 0 \qquad \alpha_i \geq - a_i(t) \qquad \beta_i \leq - a_i(t) \qquad a_n(t) \geq 0$$

APPENDIX B

B.1 Representation of Linear Systems as Hyperplanes in State Space

Any linear system of order n can be represented by an n^{th} order hyperplane (straight surface) in n+1 space. This can be seen as follows.

The equation for a certain n^{th} order hyperplane passing through the origin is

$$s = \sum_{i=1}^{n} c_i x_i = 0 \qquad c_i \text{ positive constant}, \quad c_n = 1 \qquad \text{B1}$$

Consider now, a system whose representative point is constrained to lie on this hyperplane.

Assuming this system has the following structure.

$$\dot{x}_i = x_{i+1} \qquad i = 1,\ldots,n-1 \qquad \text{B2}$$

Substituting B2 into B1 gives

$$\dot{x}_i = x_{i+1} \qquad i = 1,\ldots,n-1$$

$$\dot{x}_{n-1} = -\sum_{i=1}^{n-1} c_i x_i \qquad \text{B3}$$

i.e. The companion form of an $(n-1)^{th}$ order linear system with feedback gains equal to c_i.

A simple example will now be considered to demonstrate this representation.

Consider a straight line (1st order hyperplane) in two dimensional state space. As shown in Fig. B1. The equation of this line is

$$s = c_1 x_1 + x_2 = 0 \qquad c_1 \text{ positive constant}$$

Now, given that $\dot{x}_1 = x_2$

we have $c_1 x_1 + \dot{x}_1 = 0$

i.e. $\dot{x}_1 = - c_1 x_1$

The describing equation for a simple first order system.

APPENDIX C

THE MAXIMUM PRINCIPLE

C.1 Consider systems of the form

$$\dot{\underline{x}} = f(\underline{x},\underline{u}) \qquad C1$$

u is constrained so as to lie within some closed bounded region at all times.

Also we have a measure of performance

$$I = \int_{t_o}^{t_1} f_o(\underline{x},\underline{u})\, dt \qquad C2$$

The object is to achieve transition from the initial state xt_o to the terminal state xt_1 whilst giving either the maximum or the minimum value of I, depending on the context of the problem.

An auxiliary state is defined

$$\dot{x}_o = f_o(\underline{x},\underline{u}) \qquad x_o(t_o) = 0 \qquad C3$$

We now introduce the costate system which has costate variables $p_0, p_1, \ldots, p_n$.

The Hamiltonian function is now defined as

$$H \triangleq \sum_{i=0}^{n} p_i f_i(\underline{x},\underline{u}) \qquad C4$$

The following equations are then known as the canonical equations.

$$\frac{dp_i}{dt} = -\frac{\partial H}{\partial x_i} \qquad (i = 0,1,\ldots,n) \qquad C5$$

$$\frac{dx_i}{dt} = \frac{\partial H}{\partial p_i} \qquad (i = 0,1,\ldots,n) \qquad C6$$

Also we have

$$\frac{dp_i}{dt} = -\sum_{j=0}^{n} p_j \frac{\partial f_j}{\partial x_i} \qquad (i = 0,1,\ldots,n) \qquad C7$$

and for a linear system

$$\dot{\underline{x}} = A_x \underline{x} \qquad C8 \qquad \text{and} \qquad \dot{\underline{p}} = -A_x^T \underline{p} \qquad C9$$

The maximum principle[32] now states that for I to be minimised (maximised), $\underline{u}$ must be chosen such that H is maximised (minimised) at every instant of time. In many cases, this means that components of $\underline{u}$ should assume their maximum possible value or their minimum possible value.

N.B. In the case of the final time not specified, it can be shown[38] that H = constant = 0, throughout the entire process.

In all cases, the value of $p_o(t)$ is

$$p_o(t) = \text{constant} = -1 \qquad C10$$

C.1.1 Initial Condition Relationships

At the right-hand end of the state-costate trajectories, we can invoke the Transversality Condition.

In general, this can be written as

$$\left[dx_o - Hdt + \sum_{i=0}^{n} p_i dx_i \right]_1 = 0 \qquad C11$$

p_o is always equal to - 1

therefore we have

$$\left[- Hdt + \sum_{i=1}^{n} p_i dx_i \right]_1 = 0 \qquad C12$$

It can also be shown[38] that when the final time t_1 is completely free, that

$$\left[Hdt \right]_1 = 0 \quad \text{and}$$

$$\left[\sum_{i=1}^{n} p_i dx_i \right]_1 = 0 \quad \text{independently.}$$

Thus, if we run the system from the right hand endpoint in reverse time, we have a relationship for the initial conditions of p_i and x_i.

$$\text{i.e.} \quad \sum_{i=1}^{n} p_i dx_i = 0 \qquad C13$$

in the second order case

$$p_{10} dx_{10} + p_{20} dx_{20} = 0 \qquad C14$$

where p_{io} and x_{io} are the costate and state variables at the right hand end of the trajectories, considered as initial conditions in reverse time.

The dx_i in equation C14 are not independent, but indicate infinitesimal variations in the coordinates of the endpoints such that the point remains on the prescribed smooth surface.

Equation C13 can be interpreted geometrically to mean that $\underline{p}_o$ must be in such a position on the specified surface, such that $\underline{p}_o$ is orthogonal to the surface at point $\underline{x}_o$.

C.1.1.1 A simple Illustrative Example

Let the $\underline{x}_o$ vector be related as follows

$$x_{10}^2 + x_{20}^2 = R^2 \qquad C15$$

R positive constant, as shown in Fig.C1.

The set of points x_{10}, x_{20} on the locus are known as the target set. In forward time, the system starts at some initial condition and is then steered to some point on the target set, whilst minimising (maximising) some performance index. In reverse time, the target set is the set of initial conditions.

Fig.C2 shows the relationship of the $\underline{x}_o$ and $\underline{p}_o$ vector for this particular target set.

It can easily be seen that the vector $\underline{p}_o$ will have the same orientation as the $\underline{x}_o$ vector, for any point on the target set.

i.e. $p_{10} = \lambda x_{10}$

$p_{20} = \lambda x_{20}$

where λ will be determined by other conditions of the Maximum Principle.

C.1.1.2 A More General Initial Condition Relationship

We have already considered the relationships for a target set of the form

$$x_{10}^2 + x_{20}^2 = R^2$$

Let us now consider a target set of the form

$$A\, x_{10}^2 + B\, x_{20}^2 = R^2 \qquad C16$$

A, B, R positive constant

as shown in Fig.C3.

The transversality condition gives

$$p_{10}dx_{10} + p_{20}dx_{20} = 0$$

$$\therefore \quad \frac{dx_{20}}{dx_{10}} = -\frac{p_{10}}{p_{20}}$$

also we have $A\,x_{10}^2 + B\,x_{20}^2 = R^2$ C16

differentiate equation C16 w.r.t. x_{10}

gives $2A\,x_{10} + 2B\,x_{20}\frac{dx_{20}}{dx_{10}} = 0$

$$\therefore \quad \frac{dx_{20}}{dx_{10}} = -\frac{2A\,x_{10}}{2B\,x_{20}} = -\frac{A\,x_{10}}{B\,x_{20}}$$

$$\therefore \quad -\frac{A\,x_{10}}{B\,x_{20}} = -\frac{p_{10}}{p_{20}} \qquad \text{C17}$$

i.e. $p_{10} = \lambda A\,x_{10}$ and $p_{20} = \lambda B\,x_{20}$ C18

Again, λ is determined by other conditions.

C.1.2 Calculation of λ

For a process where the final time is not specified, we have

$H = 0$ for all time

also $H = \sum_{i=0}^{n} p_i f_i(\underline{x},\underline{u})$

for any process $p_o(t) = -1$

For a second order system with a target set given by

$$A\,x_{10}^2 + B\,x_{20}^2 = R^2$$

We have seen that $p_{10} = \lambda A x_{10}$ and $p_{20} = \lambda B x_{20}$

The initial condition of the Hamiltonian is then given by

$$H_o = - f_{oo}(\underline{x}_o, \underline{u}_o) + p_{10} f_{10}(\underline{x}_o, \underline{u}_o) + p_{20} f_{20}(\underline{x}_o, \underline{u}_o) = 0$$

i.e. $$H_o = \lambda A x_{10} f_{10}(\underline{x}_o, \underline{u}_o) + \lambda B x_{20} f_{20}(\underline{x}_o, \underline{u}_o) - f_{oo}(\underline{x}_o, \underline{u}_o) = 0$$

$\underline{u}_o$ will take some fixed value dependent on the maxmimisation (minimisation) of H_o.

λ can therefore be found purely in terms of $\underline{x}_o$. i.e. for any position on the target set, λ can be calculated.

APPENDIX D

D.1 Proof that Adaptive Control is Unnecessary[8]

Suppose we have a plant with a transfer function P/Q where P and Q are polynomials in the complex frequency s, of degree p and q respectively. Any or all of the coefficients of P and Q vary over a large but finite range. The coefficients of the higher powers of s remain of one sign (which we may take as positive without loss of generality), and P has never any roots with positive real parts. These are reasonable assumptions to make about many physical plants.

Suppose we wish the combination of plant and its controller to have a response given by the transfer function M/N, over all frequencies from zero to ω_o, M and N being fixed polynomials of degree m and n. Again, quite reasonable assumptions.

The designer meets this specification by using a controller with a forward gain G/H (another fixed polynomial fraction) and a feedback gain of N/M. Then, by ordinary feedback theory, the overall transfer function is given by

$$\frac{M}{N}\left[\frac{1}{1+\frac{MHQ}{NGP}}\right]$$

This tends to the desired function M/N as (MHQ/NGP) tends to zero, provided the system is stable.

To see how to meet these two conditions, consider the behaviour of the transfer functions for large values of $|s|$. There will be some value of $|s|$, greater than ω_1, say, for which P/Q tends to as^{p-q} for

all the expected sets of values of the coefficients, i.e. environmental conditions. a will be a positive coefficient which varies with these conditions. Similarly the transfer functions G/H and M/N will tend to $bs^{(g-h)}$ and $cs^{(m-n)}$ except that in these cases b and c will be constants. The feedback loop gain will then be given by

$$\left(\frac{ab}{c}\right) s^{(p+g+n-q-h-m)}$$

for all $|s| > \omega_1$. The exponents g and h are at the designers disposal, and he chooses them so that

$$(g - h) = m + q - n - p - 1$$

thus making the loop gain equal to

$$\frac{ab}{cs} \quad \text{for} \quad |s| > \omega_1$$

for real frequencies ω, this becomes

$$\frac{ab}{cj\omega} \quad \text{for} \quad \omega > \omega_1$$

The phase shift is thus 90° lagging in this frequency range (since all elements in the loop can be 'minimum phase shift' systems), and the loop will be stable if the gain crossover frequency occurs above ω_1. This will be the case if $|ab/c\omega_1| > 1$ for the relevant values of a.

The designer can ensure this by choosing a large enough value for b, the forward gain of the controller. Raising this gain also helps to achieve the condition

$$|MHQ/NGP| << 1$$

so that it is always possible to meet the design specification and achieve stability using a fixed gain controller with feedback.

APPENDIX E

E.1 The Ideal Model Concept

When optimising a control system with respect to a quadratic performance index, it is interesting to note that it is possible to identify certain trajectories that exhibit "strong optimality". This may be seen by considering the following simple example.

A general plant is represented in companion form, i.e.:

$$\dot{x}_{i-1} = x_i \qquad i = 1,\ldots,n-1 \qquad \text{E1}$$

The performance index is as follows

$$I = \frac{1}{2}\int_o^T (q_1 x_1^2 + q_2 x_2^2)dt \qquad \text{E2}$$

q_1, q_2 positive constant

The required steady state condition is the origin i.e.

$$x_1(T) = x_2(T) = \ldots\ldots = x_n(T) = 0 \qquad \text{E3}$$

It will now be shown that the performance index may be written as follows

$$I = \frac{1}{2}\int_o^T (\sqrt{q_1}x_1 + \sqrt{q_2}x_2)^2 dt + \frac{1}{2}\sqrt{q_1 q_2}\, x_1^2(0) \qquad \text{E4}$$

The proof follows thus

$$\text{define } I_1 \triangleq \frac{1}{2}\int_o^T (\sqrt{q_1}x_1 + \sqrt{q_2}x_2)^2 dt \qquad \text{E5}$$

expanding equation E5 gives

$$I_1 = \frac{1}{2}\int_o^T (q_1x_1^2 + q_2x_2^2 + 2\sqrt{q_1q_2}\, x_1x_2)dt \qquad E6$$

but $x_2 = \dot{x}_1$

$$\therefore \quad I_1 = \frac{1}{2}\int_o^T (q_1x_1^2 + q_2x_2^2)dt + \int_o^T \sqrt{q_1q_2}\, x_1\, dx$$

$$I_1 = \frac{1}{2}\int_o^T (q_1x_1^2 + q_2x_2^2)dt - \frac{\sqrt{q_1q_2}\, x_1^2(0)}{2} \qquad E7$$

Substituting for I_1 in equation E4 results in the original performance index form of equation E2, as was to be shown.

Consider the implications of equation E4. For any initial condition, the performance index I will have an absolute minimum if the system behaves such that

$$\sqrt{q_1}\, x_1 + \sqrt{q_2}\, x_2 = 0$$

i.e. $\sqrt{q_1}\, x_1 = -\sqrt{q_2}\, x_2$

but, $x_2 = \dot{x}_1$

i.e. $$\dot{x}_1 = -\frac{\sqrt{q_1}}{\sqrt{q_2}}\, x_1 \qquad E8$$

is the condition for minimum I.

Equation E8 corresponds to a linear first order system with parameters that are dependent only upon the performance index of equation E2. It should be noted that the general plant structure of equation E1 is not restricted in dimension. There thus exists a n-1 dimensional hyperplane in the n dimensional state space of the plant that describes the optimal behaviour of the plant, for the given performance index.

To summarise, for the example shown, it has been seen that for a given quadratic performance index, there exists a trajectory in state space that results in a minimum value for that index. This trajectory is associated with a certain linear system of order one less than the performance index. This linear system is known as the 'Ideal Model' corresponding to the given index and is independent of the plant structure beyond the basic assumption of equation E1.

As a second example, consider the following

$$I = \frac{1}{2}\int_o^T (x_1^2 + 2x_2^2 + x_3^2)dt \qquad E9$$

$$\dot{x}_{i-1} = x_i \qquad i = 1,.....,n-1 \qquad E10$$

$$x_1(T) = x_2(T) = ... = x_n(T) = 0 \qquad E11$$

It may be shown that

$$I = \int_o^T (x_1 + 2x_2 + x_3)^2 dt + x_{1(0)}^2 + x_{1(0)}x_{2(0)} + x_2^2(0) \qquad E12$$

The ideal model is now a second order system with dynamics described by

$$\ddot{x}_1 + 2\dot{x}_1 + x_1 = 0 \qquad E13$$

Thus, by using similar methods, the ideal model for any quadratic performance index may be obtained.

Further references to the ideal model concept are found in the works of Feldbaum[53] and Rekasius[54].

APPENDIX F

F.1 Hierarchy of Controls Method[26]

Consider a variable structure system given by

$$\dot{x} = Ax + Bu + Ew \qquad F1$$

where $x \in R^n$, $w \in R^r$ is a measurable vector signal and $u \in R^m$ is a variable structure control of the form

$$u_i = \begin{cases} u_i^+(x,w) & \text{for } s_i(x) > 0 \\ u_i^-(x,w) & \text{for } s_i(x) < 0 \end{cases} \qquad F2$$

where u_i is the ith component of u and $s_i(x)$ is the ith component of the switching hyperplane

$$s(x) = Gx = 0 \qquad F3$$

To introduce the hierarchy of controls method, we use the following definitions.

Definition 1: The system (F1) is in sliding mode on the hyperplane $s_i(x) = 0$ if the condition

$$\lim_{s_i \to +0} \dot{s}_i < 0, \qquad \lim_{s_i \to -0} \dot{s}_i > 0 \qquad F4$$

is satisfied.

Definition 2: If sliding mode occurs first on $s_p(x) = 0$ and then on $s_p(x) = 0$ and $s_q(x) = 0$, then the hierarchy of switching hyperplanes is denoted by $s_p \to s_q$. The hierarchy of control method consists of the following steps.

Step 1: Suppose a hierarchy of switching planes is specified by $s_1 \to s_2 \to \ldots \to s_m$.

Step 2: We begin with the bottom switching plane $s_m = 0$ in the hierarchy by letting $i = m$.

Step 3: Suppose sliding mode occurs on the first $i - 1$ switching planes, that is, $s_j = 0$, $j = 1,\ldots,i-1$. Solve for the equivalent control u_{eq}^{i-1} of the variable structure control $(u^{i-1})^T = (u_1,\ldots,u_{i-1})$ as a function of u_i and $u^{i+1} \equiv (u_{i+1},\ldots,u_m)^T$ from the algebraic equations $s_j = 0$, $j = 1,\ldots,i-1$.

Since system (F1) is linear, u_{eq}^{i-1} is linear in x, u_i, u^{i+1} and w, that is

$$u_{eq}^{i+1} = P_{i-1}x + Q_{i-1}u^{i+1} + T_{i-1}w + \alpha_i u_i \qquad \text{F5}$$

where matrices P_{i-1}, Q_{i-1} and T_{i-1} and scalar α_i depend on the first i-1 rows of matrices GA, GB, and GE. We note that u^{i+1} is known since u_k^+, u_k^-, $k = i+1,\ldots,m$ have been determined previcusly.

Step 4: For the ith switching plane $s_i = 0$, find $u_i^+(x,w)$ and $u_i^-(x,w)$ such that

$$\dot{s}_i s_i < 0 \qquad \text{F6}$$

(F6) assures the trajectories of (F1) move towards $s_i = 0$ and sliding mode occurs when $s_i = 0$ is reached. Condition (F6) is satisfied if

$$\alpha_i^* u_i^+(x,w) < -\min_{u^{i+1}} [\, p_i^T x + t_i^T w + q_i^T u^{i+1} \,] \qquad \text{F7}$$

$$\alpha_i^* u_i^-(x,w) > -\max_{u^{i+1}} [p_i^T x + t_i^T w + q_i^T u^{i+1}] \qquad F8$$

where $\alpha_i^* \neq 0$, the vectors p_i, q_i and t_i depend on the matrices P_{i-1}, Q_{i-1}, T_{i-1}, respectively, and all of them depend on α_i and the ith rows of the matrices GA, GB, and GE. If $u_i^+(x,w)$ and $u_i^-(x,w)$ is linear in x and w, for example,

$$u_i^+(x,w) = [(k_i^+)^T|x| + (r_i^+)^T|w|] \qquad F9$$

$$u_i^-(x,w) = [(k_i^-)^T|x| + (r_i^-)^T|w|] \qquad F10$$

then the minimizations in (F7) can be performed component wise, that is

$$\alpha_i^* k_{ij}^+ < \min_{k_{i+1,j}^+,\ldots,k_{m,j}^+} [(p_{ij} + \sum_{k=i+1}^{m} q_{ik} k_{kj}^+)\operatorname{sgn} x_j], \quad j=1,\ldots,n \qquad F11$$

$$\alpha_i^* r_{ij}^+ < \min_{r_{i+1,j}^+,\ldots,r_{m,j}^+} [(t_{ij} + \sum_{k=i+1}^{m} q_{ik} r_{ij}^+)\operatorname{sgn} w_j], \quad j = 1,\ldots,r \qquad F12$$

where p_{ij}, t_{ij}, q_{ij}, r_{ij}^+ and k_{ij}^+ are the jth component of p_i, t_i, q_i, r_i^+, and k_i^+,,respectively. The maximizations in (F8) can be done in similar fashions.

Step 5: Let i = i-1. If i > 0, to Step 3, else stop.

Remark: In the case when there are parameter variations in the system matrices A, B, and E, the maxima of the arguments on the right-hand sides of (F11), (F12) with respect to the uncertain parameter is minimized (maximized in (F8)).

APPENDIX G

G.1 Hyperstable Systems[24]

Consider the multivariable standard system represented in Fig.G1 and described by state equations of the form

$$\dot{x} = Mx + Nu_1 \qquad G1$$

$$v = Px \qquad G2$$

$$u_1 = -u \qquad G3$$

$$u(t) = F(v(\tau),t), \qquad \tau \leq t \qquad G4$$

where M, N and P are matrices, x, u, u_1 and v are vectors. It is assumed that the pair P,M is completely observable, and the pair M,N is completely controllable. It is also assumed that the vectors u and v have the same dimension, and that F denotes a nonlinear dependence (functional dependence) between u and the values of v in the interval $\tau \leq t$. Consider also the subset of u, which satisfies the following inequality for all t

$$\int_o^t u'(\tau).v(\tau)\, d\tau \geq \gamma_o^2 \qquad G5$$

where γ_o^2 depends on the initial state of the system and eventually of $\sup\ 0 < \tau < t\ ||x(\tau)||$, but does not depend on time t.

Definition

The system G1-G4 is termed asymptotically hyperstable if for any u(t) belonging to the subset defined by G5, the null solution of the system is asymptotically stable in the large. At the same time the following inequality holds

$$||x(t)|| \leq k(||x(o)|| + \delta), \quad \forall t \geq 0,$$

$$k, \delta > 0$$

The Popov theorem for asymptotic hyperstability of system G1-G4 is the following.

Theorem

Necessary and sufficient conditions, in order that the system described by G1-G4 and the inequality G5, be an asymptotically hyperstable system, are that

1) the transfer matrix from u_1 to v: $Z(s) = P(sI - M)^{-1}N$ be strictly positive real (in the sense that Z(s) is positive real for all s);
2) all the poles of Z(s) lie in the half plane $R_e s < 0$;
3) $Z(j\omega) + Z'^{*}(j\omega)$ should be positive definite Hermitian for all real ω.

APPENDIX H

H.1 Sufficiency Conditions for the Maximum Principle to Produce Optimal Controls[35]

The process dynamics are described by

$$\dot{x} = f(\underline{x},\underline{u}) \qquad \underline{x} \in E^n \qquad \text{H1}$$

where $u(t)$ is any piece-wise continuous vector function constrained to some subset Ω of Euclidean m-space E^m; f and $\partial f/\partial x$ are continuous on $\Omega \times E^n$.

The performance index for a control that transfers the state from some initial $x(t_o)$ to some terminal state $x(t_1)$ is

$$J(u) = \int_{t_o}^{t_1} f_o(\underline{x},\underline{u})dt \qquad \text{H2}$$

$x(t_1)$ will be some point on the smooth terminal hypersurface S known as the target set.

$f_o(\underline{x},\underline{u})$ is positive for all $u \in \Omega$ and all states $\underline{x}$ which are either on S or exterior to S. Also, $\partial f_o/\partial \underline{x}$ is continuous on $\Omega \times E^n$.

Theorem

If the exterior of S is partitioned into a finite number of connected cells by hypersurface elements whose union is designated V, with $\partial u(x)/\partial x$ continuous on the interior of each cell, then an extremal control $u(x)$ is optimal if

1) The extremal trajectory $\phi(\tau)$, traversing from $x(t_o)$ to S with control $u[\phi(\tau)]$, intersects V with nonzero angle at a finite number of points and intersects S after an elapsed time $t(x)$.

2) The cost to reach S from $x(t_o)$

$$J(x) = \int_o^{t(x)} f_o \{\phi(\tau), u[\phi(\tau)]\} \, d\tau \qquad H3$$

is a continuous function of x on all of E^n.

APPENDIX I

COMPUTER PROGRAM TO GENERATE TIME-OPTIMAL SWITCH CURVES

This program was used to generate the optimal switch curves in the examples of chapter 6. The program is specific case of the general simulation package C.M.S.[39] (Conversational Mode on-line Simulation Program).

To run C.M.S., the process to be simulated must be represented by a series of statements in a file called EQNS.FOR. These statements are for the most part made up of standard Fortran mathematical operations. Added to these are variables that represent the time derivatives of other variables. The statements in EQNS.FOR in this case relate closely to the system diagrams in Figs. 6.6, 6.7 and 6.8.

The program is thus;

```
SUBROUTINE EQNS (NO, DX, X, Y, C, L, T, IST, ICLOCK, IN)
DIMENSION DX (1), x(1), Y(1), C(1), L(1)
NO = 9
DX(1) =   C(4)*X(1) - C(2)*X(2)
DX(2) =   C(1)*X(1) + C(3)*X(2)
DX(3) =   C(4)*X(3) - C(2)*X(4)
DX(4) =   C(1)*X(3) + C(3)*X(4)
DX(5) = - C(4)*X(5) - C(1)*X(6)
DX(6) =   C(2)*X(5) - C(3)*X(6)
DX(7) = - C(4)*X(7) - C(1)*X(8)
DX(8) =   C(2)*X(7) - C(3)*X(8)
 Y(5) =   C(5)*COS(X(9))/C(6)**0.5
 Y(6) =   C(5)*SIN(X(9))/C(7)**0.5
 Y(7) =   C(6)*C(8)*Y(5)
 Y(8) =   C(7)*C(8)*Y(6)
 Y(1) =   Y(7)*X(5) + Y(8)*X(7)
 Y(2) =   Y(7)*X(6) + Y(8)*X(8)
 Y(3) =   Y(5)*X(1) + Y(6)*X(3)
 Y(4) =   Y(5)*X(2) + Y(6)*X(4)
DX(9) =   C(9)*(Y(2)*C(10) + Y(1)*C(11))
RETURN
END
```

Where the following relationships apply

C.M.S. variable	Corresponding variable in Fig. 6.6, 6.7 or 6.8
X(1)	$b_1(t)$
X(2)	$b_3(t)$
X(3)	$b_2(t)$
X(4)	$b_4(t)$
X(5)	$c_1(t)$
X(6)	$c_3(t)$
X(7)	$c_2(t)$
X(8)	$c_4(t)$
X(9)	θ
DX(1)	$\dot{b}_1(t)$
DX(2)	$\dot{b}_3(t)$
DX(3)	$\dot{b}_2(t)$
DX(4)	$\dot{b}_4(t)$
DX(5)	$\dot{c}_1(t)$
DX(6)	$\dot{c}_3(t)$
DX(7)	$\dot{c}_2(t)$
DX(8)	$\dot{c}_4(t)$
DX(9)	$\dot{\theta}$
Y(1)	$p_1(t)$
Y(2)	$p_2(t)$
Y(3)	$x_1(t)$
Y(4)	$x_2(t)$
Y(5)	x_{10}
Y(6)	x_{20}
Y(7)	p_{10}
Y(8)	p_{20}
C(1)	K_1
C(2)	K_2
C(3)	$u_{2\ max}$
C(4)	$u_{1\ max}$
C(5)	R
C(6)	A
C(7)	B
C(8)	λ
C(9)	K_L

C(10) = 0 for $p_1(t) = 0$ curve or 1 for $p_2(t) = 0$ curve

C(11) = 1 for $p_1(t) = 0$ curve or 0 for $p_2(t) = 0$ curve

APPENDIX J

SAMPLE CALCULATION OF THE CHARACTERISTIC EQUATION FOR ONE CONDITION OF TABLE 11.1

This appendix shows the way in which one of the characteristic equations in table 11.3 was obtained. By a similar procedure, the characteristic equations for other conditions may also be found.

Condition 5

We have from measurements and data (Chapter 11)

$\frac{1}{J} = 7.09 \quad K_t = 0.7 \quad K_v = 0.668 \quad R_a = 1.0$

$K_{tacho} = 1.53 \quad e_b = 35$

and we set $K_1 = \frac{1}{4}$, $K_2 = 1$ and $K_3 = 0$.

To evaluate the characteristic equation 11.24 we need to find

F, g_1 and g_2

these will be considered in turn.

1) Calculation of F

For condition 5 the armature current is $\bar{i}_a = 4A$ at a machine speed of 500 r.p.m. With reference to Fig.11.5, the curve for this condition may be seen. Equation 11.20 gives

$$F = \frac{\Delta \bar{i}_a K_t}{\Delta \omega}$$

$$\frac{\Delta \bar{i}_a}{\Delta \omega} = \frac{1}{300} \times \frac{60}{2\pi} = 0.0318 \quad \text{(from Fig.11.5)}$$

giving $F = 0.0318 \times 0.7 = 0.0223$.

2) Calculation of g_1

Manipulation of equations 11.17, 11.16 and 11.14 gives

$$g_1 = -\frac{V_m}{1024}\left[k_2 \sin \theta_2 - \sin \theta_1 - \frac{e_b}{V_m}(k_2 - 1) \right]$$

V_m is the peak supply voltage = 300 V.

From table 11.2, θ_1 was measured as

$$\theta_1 = 139.5^\circ$$

The appropriate curve ($e_b = 35$, $R_a = 1$) on Fig.11.3 then gives

$$\theta_2 = 195.25^\circ$$

k_2 is found by evaluating $\frac{\Delta\theta_2}{\Delta\theta_1}$ at the point $\theta_1 = 139.5^\circ$ on the curve in Fig.11.3, and is found to be $k_2 = -0.392$.

This gives

$$g_1 = -\frac{300}{1024}\left[-0.392 \sin 195.25 - \sin 139.5 - \frac{35}{300}(-0.392 - 1) \right]$$

i.e. $g_1 = 0.1125$

3) Calculation of g_2

Manipulation of equations 11.18 and 11.15 gives

$$g_2 = -\frac{V_m}{\pi}\left[k_3 \sin \theta_2 - \frac{(\theta_2 - \theta_1) - k_3 e_b}{V_m} \right]$$

k_3 is found by evaluating $\frac{\Delta\theta_2(\text{rads})}{\Delta e_b(\text{volts})}$

at the point $\theta_1 = 139.5^\circ$ on the $R_a = 1\ \Omega$ curves of Fig.11.3, and is found to be

$$k_3 = -0.005$$

This gives

$$g_2 = -\frac{300}{\pi}\left[-0.005 \sin 195.25 - \frac{(195.25 - 139.5)2\pi}{300 \times 360} - \frac{-0.005 \times 35}{300}\right]$$

i.e. $g_2 = 0.129$

For condition 5 we thus have

$F = 0.0223$ Nm/Rad/Sec

$g_1 = 0.1125$ Volts/firing angle increment

$g_2 = 0.129$ Volts/Volt

These values complete the information required to calculate the characteristic equation which is the denominator of equation 11.24

$$\text{i.e. C.E.} = s^2 + \left[\frac{f}{J} + \frac{K_t g_2 K_v}{R_a J} + \frac{nK_3 K_1 g_1 K_t K_{tacho}}{R_a J}\right]s + \frac{100 K_2 K_1 g_1 K_t K_{tacho}}{R_a J}$$

The coefficients of s are thus

s^2) 1

s) $0.0223 \times 7.09 + 0.7 \times 0.129 \times 0.668 \times 7.09 = 0.5857$

s^0) $100 \times 0.25 \times 0.1125 \times 0.7 \times 1.53 \times 7.09 = 21.36$

giving

$$\text{C.E.} = s^2 + 0.5857s + 21.36$$

as shown in table 11.3.

APPENDIX K

MACHINE CODE LISTING FOR THE MICROPROCESSOR CONTROLLER

The following is a complete listing of the microprocessor machine code programme. The routines are listed in the following order

1) Start up subroutine
2) Tachometer read subroutine
3) Tachometer average subroutine
4) Status register subroutine
5) Overcurrent subroutine
6) Firing angle output and range check subroutine
7) Shutdown subroutine
8) Executive programme
9) Control law subroutine

To aid the understanding of these programmes, a description of the stores used for fixed parameters and variable information is now given.

Microprocessor - Motor interface

Store Address	Function
D100, D101	Firing angle registers
D102	Tachometer register
D103	Relay register
D105	Status register
D106	Overcurrent register

Fixed parameters set by operator

Store Address	Function
30CC	Cycles allowed in overcurrent
30C7	Overcurrent limit
30DB	Set speed
30D6	Firing angle retardation in overcurrent
317D 317E 317F 3180	Sliding mode scaling factor c_s
318D 318E 318F 3190	Shift operations to set K_3 when $sx_2 < 0$
3193 3194 3195 3196	Shift operations to set K_3 when $sx_2 > 0$
319D 319E	Shift operations to set K_1
321E	Error rate estimation interval minus one

Additional fixed parameters used by programme during on-line control

Store Address	Function
0007	Loop count used in start up and tachometer read subroutines
000C	Set speed
008D	Firing angle retardation in overcurrent
008E	Cycles allowed in overcurrent
A000 A001	Interrupt Address

Variable Information

Store Address	Function
0001 0002	Running tachometer stores
0003 0004	Tachometer total stores
0005	Tachometer loop count
0006	Tachometer average
0008	Start up loop count
000B	Firing angle change
000D	Speed error
0020 ↓ 002A	Stores containing past values of speed error
002F	Value of $K_2 e + K_3 \hat{\dot{e}}$
005D	System status saved on shutdown
008F	Actual cycles in overcurrent
00E0 00E1	Firing angle

315F 3167	Contains the address of the old speed error, to calculate error rate
313C	Temporary error rate store
321F	Actual loop count for achieving the required error rate estimation interval

Address	Machine Code	Mnemonic	Comments
3000	7F	CLR	Set stores for programme use
3001	00		
3002	00		
3003	7F	CLR	
3004	00		
3005	01		
3006	7F	CLR	
3007	00		
3008	02		
3009	7F	CLR	
300A	00		
300B	03		
300C	7F	CLR	
300D	00		
300E	04		
300F	7F	CLR	
3010	00		
3011	06		
3012	86	LDA A	
3013	3E		
3014	B7	STA A	
3015	00		
3016	07		
3017	7F	CLR	
3018	00		
3019	08		
301A	86	LDA A	Switch on relays
301B	AB		
301C	B7	STA A	
301D	D1		
301E	03		
301F	86	LDA A	Set interrupt vector

CODE FOR START UP SUBROUTINE (sheet 1 of 3)

Address	Machine Code	Mnemonic	Comments
3020	30		
3021	B7	STA A	
3022	A0		
3023	00		
3024	86	LDA A	
3025	50		
3026	B7	STA A	
3027	A0		
3028	01		
3029	0E	CLI	Clear interrupt
302A	3E	WAI	Wait for interrupt
302B	B6	LDA A	Check status register
302C	D1		
302D	05		
302E	06	TAP	
302F	2B	BMI	
3030	06		
3031	7F	CLR	
3032	00		
3033	08		
3034	7E	JMP	
3035	30		
3036	1A		
3037	26	BNE	
3038	03		
3039	7E	JMP	
303A	30		
303B	1F		
303C	24	BCC	
303D	03		
303E	7E	JMP	
303F	30		

Address	Machine Code	Mnemonic	Comments
3040	1F		
3041	7C	INC	Increment loop count
3042	00		
3043	08		
3044	B6	LDA A	
3045	00		
3046	07		
3047	B0	SUB A	
3048	00		
3049	08		
304A	27	BEQ	Check if loop count done
304B	03		
304C	7E	JMP	
304D	30		
304E	1F		
304F	39	RTS	
3050	3B	RTI	

Address	Machine Code	Mnemonic	Comments
3060	B6	LDA A	Read tachometer and add to
3061	00		running store
3062	01		
3063	F6	LDA B	
3064	00		
3065	02		
3066	FB	ADD B	
3067	D1		
3068	02		
3069	B9	ADC A	
306A	00		
306B	00		
306C	B7	STA A	
306D	00		
306E	01		
306F	F7	STA B	
3070	00		
3071	02		
3072	B6	LDA A	Check if loop count done
3073	00		
3074	07		
3075	B0	SUB A	
3076	00		
3077	05		
3078	25	BCS	
3079	06		
307A	7C	INC	
307B	00		
307C	05		
307D	7E	JMP	
307E	30		
307F	60		

CODE FOR TACHOMETER READ SUBROUTINE
(sheet 1 of 3)

Address	Machine Code	Mnemonic	Comments
3080	0F	SEI	
3081	B6	LDA A	Transfer tachometer total
3082	00		to tachometer total stores
3083	01		
3084	B7	STA A	
3085	00		
3086	03		
3087	B6	LDA A	
3088	00		
3089	02		
308A	B7	STA A	
308B	00		
308C	04		
308D	0E	CLI	
308E	7F	CLR	Clear running tachometer stores and loop counter
308F	00		
3090	01		
3091	7F	CLR	
3092	00		
3093	02		
3094	7F	CLR	
3095	00		
3096	05		
3097	B6	LDA A	Read status register
3098	D1		
3099	05		
309A	06	TAP	
309B	0E	CLI	
309C	2B	BMI	
309D	03		
309E	7E	JMP	
309F	00		

Address	Machine Code	Mnemonic	Comments
30A0	50		
30A1	26	BNE	
30A2	03		
30A3	7E	JMP	
30A4	00		
30A5	50		
30A6	24	BCC	
30A7	03		
30A8	7E	JMP	
30A9	00		
30AA	50		
30AB	7E	JMP	
30AC	30		
30AD	60		

Address	Machine Code	Mnemonic	Comments
3220	F6	LDA B	Load tachometer lower bits in Accumulator B
3221	00		
3222	04		
3223	86	LDA A	
3224	06		
3225	B7	STA A	Shift 6 places
3226	00		
3227	0A		
3228	54	LSR B	
3229	7A	DEC	
322A	00		
322B	0A		
322C	27	BEQ	
322D	03		
322E	7E	JMP	
322F	32		
3230	28		
3231	86	LDA A	
3232	02		
3233	B7	STA A	
3234	00		
3235	0A		
3236	B6	LDA A	Load tachometer upper bits and shift 2 places
3237	00		
3238	03		
3239	0C	CLC	
323A	49	ROL A	
323B	7A	DEC	
323C	00		
323D	0A		
323E	27	BEQ	
323F	03		

CODE FOR TACHOMETER AVERAGE SUBROUTINE
(sheet 1 of 2)

Address	Machine Code	Mnemonic	Comments
3240	7E	JMP	
3241	32		
3242	39		
3243	1B	ABA	Add the accumulators and store the result
3244	B7	STA A	
3245	00		
3246	06		
3247	39	RTS	

Address	Machine Code	Mnemonic	Comments
0090	B6	LDA A	Load the status register into accumulator A
0091	D1		
0092	05		
0093	06	TAP	Load the condition code register with the status
0094	0E	CLI	
0095	2B	BMI	Check field current
0096	03		
0097	7E	JMP	
0098	00		
0099	50		
009A	26	BNE	Check P.L.L
009B	03		
009C	7E	JMP	
009D	00		
009E	50		
009F	24	BCC	Check zero-crossing
00A0	03		
00A1	7E	JMP	
00A2	00		
00A3	50		
00A4	29	BVS	Check overcurrent
00A5	04		
00A6	7F	CLR	
00A7	00		
00A8	8F		
00A9	39	RTS	
00AA	BD	JSR	
00AB	00		
00AC	60		
00AD	39	RTS	

CODE FOR STATUS REGISTER SUBROUTINE

(sheet 1 of 1)

Address	Machine Code	Mnemonic	Comments
0060	7C	INC	Increment overcurrent count
0061	00		
0062	8F		
0063	B6	LDA A	
0064	00		
0065	8F		
0066	F6	LDA B	
0067	00		
0068	8E		
0069	10	SBA	
006A	26	BNE	Check if too long in overcurrent
006B	03		
006C	7E	JMP	
006D	00		
006E	50		
006F	0C	CLC	
0070	B6	LDA A	Retard the firing angle
0071	00		
0072	E0		
0073	F6	LDA B	
0074	00		
0075	E1		
0076	BB	ADD A	
0077	00		
0078	8D		
0079	C9	ADC A	
007A	00		
007B	B7	STA A	
007C	00		
007D	E0		
007E	F7	STA B	
007F	00		

CODE FOR OVERCURRENT SUBROUTINE(sheet 1 of 2)

Address	Machine Code	Mnemonic	Comments
0080	E1		
0081	BD	JSR	
0082	00		
0083	B0		
0084	39	RTS	

Address	Machine Code	Mnemonic	Comments
00B0	F6	LDA B	Check if firing angle is less than zero
00B1	00		
00B2	E1		
00B3	CB	ADD B	
00B4	00		
00B5	2A	BPL	
00B6	03		
00B7	7E	JMP	
00B8	00		
00B9	D1		
00BA	F6	LDA B	Check if firing angle is greater than 03FF
00BB	00		
00BC	E1		
00BD	C0	SUB B	
00BE	04		
00BF	25	BCS	
00C0	03		
00C1	7E	JMP	
00C2	00		
00C3	D8		
00C4	F6	LDA B	Output the firing angle
00C5	00		
00C6	E1		
00C7	B6	LDA A	
00C8	00		
00C9	E0		
00CA	B7	STA A	
00CB	D1		
00CC	00		
00CD	F7	STA B	
00CE	D1		
00CF	01		

CODE FOR FIRING ANGLE OUTPUT AND RANGE CHECK SUBROUTINE (sheet 1 of 2)

Address	Machine Code	Mnemonic	Comments
00D0	39	RTS	
00D1	C6	LDA B	Set firing angle equal to 0000
00D2	00		
00D3	86	LDA A	
00D4	00		
00D5	7E	JMP	
00D6	00		
00D7	CA		
00D8	C6	LDA B	Set firing angle equal to 03FF
00D9	03		
00DA	86	LDA A	
00DB	FF		
00DC	7E	JMP	
00DD	00		
00DE	CA		

Address	Machine Code	Mnemonic	Comments
0050	B6	LDA A	Load the status register
0051	D1		
0052	05		
0053	B7	STA A	Store the status register
0054	00		
0055	5D		
0056	86	LDA A	Switch off the machine supply relays
0057	A8		
0058	B7	STA A	
0059	D1		
005A	03		
005B	01		
005C	3F	SWI	Return control to the microprocessor monitor

CODE FOR SHUTDOWN SUBROUTINE (sheet 1 of 1)

Address	Machine Code	Mnemonic	Comments
30B0	86	LDA A	Set stores and variable parameters
30B1	FD		
30B2	B7	STA A	
30B3	D1		
30B4	00		
30B5	B7	STA A	
30B6	00		
30B7	E0		
30B8	86	LDA A	
30B9	03		
30BA	B7	STA A	
30BB	D1		
30BC	01		
30BD	B7	STA A	
30BE	00		
30BF	E1		
30C0	7F	CLR	
30C1	31		
30C2	3F		
30C3	7F	CLR	
30C4	31		
30C5	1C		
30C6	86	LDA A	
30C7	50		
30C8	B7	STA A	
30C9	D1		
30CA	06		
30CB	86	LDA A	
30CC	07		
30CD	B7	STA A	
30CE	00		
30CF	8E		

CODE FOR EXECUTIVE PROGRAMME (sheet 1 of 4)

Address	Machine Code	Mnemonic	Comments
30D0	86	LDA A	
30D1	00		
30D2	B7	STA A	
30D3	00		
30D4	8F		
30D5	86	LDA A	
30D6	10		
30D7	B7	STA A	
30D8	00		
30D9	8D		
30DA	86	LDA A	
30DB	50		
30DC	B7	STA A	
30DD	00		
30DE	0C		
30DF	86	LDA A	
30E0	10		
30E1	B7	STA A	
30E2	00		
30E3	0B		
30E4	86	LDA A	
30E5	50		
30E6	B7	STA A	
30E7	00		
30E8	0D		
30E9	BD	JSR	Branch to startup subroutine
30EA	30		
30EB	00		
30EC	86	LDA A	Set interrupt vector
30ED	F6		
30EE	B7	STA A	
30EF	A0		

Address	Machine Code	Mnemonic	Comments
30F0	01		
30F1	B7	STA A	
30F2	00		
30F3	0F		
30F4	0E	CLI	
30F5	3E	WAI	Wait for interrupt to commence on-line control
30F6	BD	JSR	Branch to tachometer average subroutine
30F7	32		
30F8	20		
30F9	BD	JSR	Branch to status register subroutine
30FA	00		
30FB	90		
30FC	B6	LDA A	Check if in overcurrent
30FD	00		
30FE	8F		
30FF	26	BNE	
3100	03		
3101	BD	JSR	Branch to control subroutine
3102	31		
3103	40		
3104	BD	JSR	Branch to firing angle output and range subroutine
3105	00		
3106	B0		
3107	8E	LDS	Reset stack pointer
3108	A0		
3109	78		
310A	86	LDA A	
310B	10		
310C	B7	STA A	
310D	00		
310E	0B		
310F	86	LDA A	Reload interrupt vectors

Address	Machine Code	Mnemonic	Comments
3110	30		
3111	B7	STA A	
3112	A0		
3113	00		
3114	86	LDA A	
3115	F6		
3116	B7	STA A	
3117	A0		
3118	01		
3119	7E	JMP	Jump to tachometer read subroutine
311A	30		
311B	8E		

Address	Machine Code	Mnemonic	Comments
3140	7F	CLR	Clear overcurrent counter
3141	00		
3142	8F		
3143	B6	LDA A	Load required speed
3144	30		
3145	DB		
3146	F6	LDA A	Load actual speed
3147	00		
3148	06		
3149	10	SBA	Find speed error
314A	7C	INC	Update error rate estimation interval count
314B	32		
314C	1F		
314D	B7	STA A	Store speed error
314E	00		
314F	0D		
3150	86	LDA A	Load address of first store which will contain old speed error values
3151	20		
3152	BB	ADD A	Gives address of old error value to calculate error rate
3153	32		
3154	1F		
3155	B7	STA A	Store that address at locations marked **
3156	31		
3157	5F		
3158	B7	STA A	
3159	31		
315A	67		
315B	B6	LDA A	Load error
315C	00		
315D	0D		
315E	90	SUB A	Find an estimate of error rate by subtracting error n samples previous
315F	**		

CODE FOR CONTROL LAW SUBROUTINE
(sheet 1 of 7)

Address	Machine Code	Mnemonic	Comments
3160	B7	STA A	Store error rate estimate
3161	31		
3162	3C		
3163	B6	LDA A	Load error
3164	00		
3165	0D		
3166	97	STA A	Store error for future calculation of error rate
3167	**		
3168	F6	LDA B	Load required error rate estimation interval minus one
3169	32		
316A	1E		
316B	F0	SUB B	Load actual interval count
316C	32		
316D	1F		
316E	2A	BPL	Count complete ?
316F	03		
3170	7F	CLR	Count completed so clear loop count
3171	32		
3172	1F		
3173	F6	LDA B	Load error rate
3174	31		
3175	3C		
3176	4D	TST A	Test if error equals zero
3177	26	BNE	
3178	04		
3179	5D	TST B	Test if error rate equals zero
317A	26	BNE	
317B	01		
317C	39	RTS	Return if e and $\dot{e}$ are zero
317D			
317E			Space available for shift operations on e, to calculate $s = \frac{n\,x_2}{100} + c_s\,x_1$
317F			

Address	Machine Code	Mnemonic	Comments
3180			
3181	1B	ABA	Calculate s
3182	5D	TST B	Test the sign of error rate
3183	2A	BPL	
3184	05		
3185	4D	TST A	Test the sign of s
3186	2A	BPL	
3187	05		
3188	20	BRA	
3189	09		
318A	4D	TST A	Test the sign of s
318B	2A	BPL	
318C	06		
318D			Space available for shift operations to set K_3 for x_2s -ve
318E			
318F			
3190			
3191	20	BRA	
3192	04		
3193			Space available for shift operations to set K_3 for x_2s +ve
3194			
3195			
3196			
3197	B6	LDA A	Load error
3198	00		
3199	0D		
319A	1B	ABA	Calculate $x_1 + \frac{K_3 n\, x_2}{100}$
319B	97	STA A	Store result
319C	2F		
319D	47	ASR A	Calculate $K_1 \left[K_2 x_1 + \frac{K_3 n x_2}{100} \right]$
319E	47	ASR A	(note $K_2 = 1$)
319F	26	BNE	Branch if the result is not zero

Address	Machine Code	Mnemonic	Comments
31A0	15		
31A1	96	LDA A	Recall $x_1 + \frac{K_3 n\, x_2}{100}$
31A2	2F		
31A3	2B	BMI	Branch if -ve
31A4	08		
31A5	86	LDA A	Apply minimum +ve firing angle change
31A6	01		
31A7	B7	STA A	
31A8	00		
31A9	0B		
31AA	7E	JMP	
31AB	31		
31AC	E1		
31AD	86	LDA A	Apply minimum -ve firing
31AE	01		angle change
31AF	B7	STA A	
31B0	00		
31B1	0B		
31B2	7E	JMP	
31B3	31		
31B4	F4		
31B5	01		
31B6	81	CMP A	Check for firing angle change greater than 10(HEX)
31B7	10		
31B8	2E	BGT	
31B9	07		
31BA	81	CMP A	Check for firing angle change more -ve than -10(HEX)
31BB	F6		
31BC	2D	BLT	
31BD	0B		
31BE	7E	JMP	
31BF	31		

Address	Machine Code	Mnemonic	Comments
31C0	D1		
31C1	C6	LDA B	Limit firing angle change to 10(HEX)
31C2	10		
31C3	F7	STA B	
31C4	00		
31C5	0B		
31C6	7E	JMP	
31C7	31		
31C8	E1		
31C9	C6	LDA B	Limit firing angle change to -10(HEX)
31CA	10		
31CB	F7	STA B	
31CC	00		
31CD	0B		
31CE	7E	JMP	
31CF	31		
31D0	F4		
31D1	4D	TST A	Test the sign of a firing angle change between the limits ±10(HEX)
31D2	2B	BMI	
31D3	06		
31D4	B7	STA A	Store firing angle change
31D5	00		
31D6	0B		
31D7	7E	JMP	
31D8	31		
31D9	E1		
31DA	40	NEG A	Negate and store the firing angle change
31DB	B7	STA A	
31DC	00		
31DD	0B		
31DE	7E	JMP	
31DF	31		

Address	Machine Code	Mnemonic	Comments
31E0	F4		
31E1	B6	LDA A	Increment the firing angle
31E2	00		
31E3	E1		
31E4	F6	LDA B	
31E5	00		
31E6	E0		
31E7	F0	SUB B	
31E8	00		
31E9	0B		
31EA	B2	SBC A	
31EB	00		
31EC	00		
31ED	F7	STA B	
31EE	00		
31EF	E0		
31F0	B7	STA A	
31F1	00		
31F2	E1		
31F3	39	RTS	Return
31F4	B6	LDA A	Decrement the firing angle
31F5	00		
31F6	E1		
31F7	F6	LDA B	
31F8	00		
31F9	E0		
31FA	FB	ADD B	
31FB	00		
31FC	0B		
31FD	B9	ADC A	
31FE	00		
31FF	00		

Address	Machine Code	Mnemonic	Comments
3200	F7	STA B	
3201	00		
3202	E0		
3203	B7	STA A	
3204	00		
3205	E1		
3206	39	RTS	Return

REFERENCES

1. Mohler, R.R.: "Natural bilinear control processes", IEEE Trans. Sys. Sci. and Cybernetics, Vol.ssc-6, No.3, July 1970, pp.192-197.

2. Rink, R.E. and Mohler, R.R.: "Completely controllable bilinear systems", SIAM J. Control, Vol.6, 1968, pp.477-486.

3. Mohler, R.R. and Rink, R.E.: "Control with a multiplicative mode", A.S.M.E. Trans. J. Basic Engineering, June 1969, pp.201-206.

4. Ionescu, T. and Monopoli, R.V.: "On the stabilization of bilinear system via hyperstability", IEEE Trans. A.C., April 1975, pp.280-284.

5. Utkin, V.I.: "Variable structure systems with sliding modes", IEEE Trans. A.C., Vol.AC-22, No.2, April 1977, pp.212-222.

6. Ostgaard, M.A., Stear, E.B. and Gregory, P.C.: "The case for adaptive controls", AGARD Report No. 406, July 1962.

7. Horowitz, I.M.: "Plant adaptive systems versus ordinary feedback systems", IRE Trans. A.C., January 1962, pp.48-56.

8. Diprose, K.V.: "Self adaptive control systems". The Aeronautical Journal, Vol.72, No.688, April 1968, pp.367-372.

9. Rath, R.R.: "Summary and status of adaptive control system programs", WADC TN 58-330, AST IA Document No. AD205548, Sept. 1958.

10. Minneapolis-Honeywell Aero-Document R-ED5100, June 1960.

11. McClean and Schmidt: "On the design of a high-gain saturating control system for use as an adaptive autopilot", N.A.S.A. Tech. Note D-305, Feb. 1960.

12. McNeill, McClean, Hegarty and Heinle: "Design and flight tests of an adaptive control system employing normal acceleration command", N.A.S.A. Tech. Note D868, April 1961.

13. Marx: "Recent adaptive control work at G.E.", A.R.C. Reprint 21, 961, G.C.S. 212.

14. Osder: "Adaptive flight control system", A.R.C. Reprint 21,962, G.C.S. 213.

15. Lindenlaub, J.C. and Cooper, G.R.: "Noise limitations of system identification techniques", IEEE Trans. A.C., January 1963, pp.43-48.

16. Landau, I.D.: "Model reference adaptive systems - a survey (MRAS) - what is possible and why?", A.S.M.E. Journal of Dynamic Systems, Measurement and Control, June 1972, pp.119-132.

17. Osburn, P.V., Whitaker, H.P. and Kezer, A.: "New developments in the design of adaptive control systems", Inst. of Aeronautical Sciences, Paper 61-39.

18. Parks, P.C.: "Liapunov redesign of model reference adaptive control systems", IEEE Trans. A.C., Vol.AC-11, No.3, July 1966.

19. Oza, K.G. and Jury, E.I.: "Adaptive algorithms for identification systems", Proc. 4th IFAC Congress, Warszawa, Pologne, Tech. Sess. 26, pp.72-103, 1969.

20. Young, P.C.: "Applying parameter estimation to dynamic systems", Control Engineering 16, 1969, pp.119-125.

21. La Salle, J. and Lefschetz, S.: "Stability by Liapunov's Direct Method", Academic Press Inc., New York, 1961.

22. Phillipson, P.H.: "Concerning 'Liapunov redesign of model reference adaptive control systems'", IEEE Trans. A.C., Vol.AC-12, 1967, p.625.

23. Popov, V.M.: "The solution of a new stability problem for controlled systems", Automation and Remote Control, Vol.24, January 1963, pp.1-23.

24. Landau, I.D.: "A hyperstability criterion for model reference adaptive control systems", IEEE Trans. AC, Vol.AC-14, Oct. 1969, pp.552-555.

25. - : "Analyse et synthèse des commandes adaptatives a l'aide d'un modèle par des méthodes d'hyperstabilité", Automatisme, Vol.14, No.7-8, July-Aug. 1969, pp.301-309.

26. Young, K.K.D.: "Design of variable structure model following control systems", IEEE Trans. AC, Vol.AC-23, No.6, Dec. 1978, pp.1079-1085.

27. Landau, I.D. and Courtiol, B.: "Design of multivariable adaptive model following systems", Automatica, Vol.10, 1974, pp.483-494.

28. Utkin, V.I.: "Equations of sliding mode in discontinuous systems, Vols.1,11", Automation and Remote Control, 1972, No.12, pp.1897-1907, No.2, pp.211-219.

29. Barbashin, E.A.: "Introduction to the Theory of Stability", Wolters-Noordhaff Publishing, Groningen, The Netherlands, 1970.

30. Elgerd, O.I.: "Control Systems Theory", McGraw-Hill Publishing, 1967.

31. Bellman, R.: "Adaptive Control Processes - A Guided Tour", Princeton University Press, Princeton, N.J., 1961.

32. Pontryagin, L.S., Boltyanskii, V.G., Gamkrelidze, R.V. and Mischchenko, E.F.: "The Mathematical Theory of Optimal Processes", Interscience (Wiley), 1962.

33. Johnson, C.D.: "Singular Solutions in Problems of Optimal Control", Advances in Control Systems, Vol.2, Academic Press, N.Y., 1965, pp.209-269.

34. Buyakas, V.I.: "Optimal control of systems with variable structure", Automation and remote control, No.4, 1966, pp.579-589.

35. Boltyanskii, V.G.: "Sufficiency conditions for optimality and the justification of the dynamic programming method", SIAM Journal on Control, Vol.4, No.2, 1966.

36. Mohler, R.R. and Moon, S.F.: "Computation of optimal trajectories for a class of nonlinear control processes", Proc. IFAC Symp., Systems Engineering Approach to Computer Control, Kyoto, Japan, Aug. 1970.

37. Mohler, R.R. and Ruberti, A.: "Theory and Applications of Variable Structure Systems", Academic Press, New York and London, 1972.

38. McCausland, I.: "Introduction of Optimal Control", Wiley Publishing 1969.

39. Munro, N. and Brown, L.S.: "Users Guide to C.M.S. A Conversational Mode On-line Simulation Program", Control Systems Centre, University of Manchester Institute of Science and Technology.

40. "Evaluation Module 11 User's Guide", Motorola Inc., 1976.

41. Dewan, S.B. and Straughen, A.: "Power Semiconductor Circuits", Wiley-Interscience Publications.

42. Lipczynski, R.T.: "Direct Digital Control of Thyristor Controls", Ph.D. Thesis, University of Bath, 1977.

43. Courtiol, B. and Landau, I.D.: "High speed adaptation system for controlled electrical drives", Automatica, Vol.11, 1975, pp.119-127.

44. Barbashin, E.A. and Tabueva, V.A.: "A method of stabilizing third-order control systems with large gains", Automation and Remote Control, Vol.1, No.10, pp.1215-1222, Vol.11, No.5, pp.562-567, 1963.

45. Emelyanov, S.V. et al: "On design of variable structure control systems for control of linear plants", Eng. Cybern., No.2, 1963, pp.69-78.

46. - : "Theory of variable structure systems", (in Russian), Moscow Nauka, 1970.

47. Bakakin, A.A. and Utkin, V.I.: "Conditions of stability of sliding mode in variable structure systems" in Analysis and Design of Control Systems (in Russian) Moscow, Nauka, 1968.

48. Gerashchenko, E.I.: "On stability in a sliding plane of a class of variable structure systems", Eng. Cybern., No.4, 1963, pp.92-98.

49. Bezvodinskaya, T.A. and Sabaev, E.F.: "Study of state space features in variable-structure control systems", Automation and remote control, No.7, 1973, pp.1105-1108.

50. - : "Stability conditions in large for variable structure systems", Automation and Remote Control, No.10, 1974, pp.1596-1599.

51. Emelyanov, S.V. and Utkin, V.I.: "Variable structure systems for control of plants with large parameter variations" (in Russian) Doklady ANSSSR, Vol.152, No.2, 1963, pp.299-301.

52. Bermant, M.A. and Utkin, V.I.: "On stability of time-varying variable structure control systems", in Variable Structure Systems and their Application to Flight Automation (in Russian) Moscow, Nauka, 1968, pp.72-74.

53. Feldbaum, A.A.: "Electrical Automatic Control Systems", 2nd Edition, Chap.9, Oborongiz, Moscow 1957.

54. Rekasius, Z.V.: "A general performance index for analytical design of control systems", IRE Trans. PGAC, AC-6, 1961, pp.217-222.

Note: Certain of the references (notably the Russian texts) are the original source for various variable structure results and as such have not been seen. These results have been seen however in the survey paper of reference 5.

ACKNOWLEDGEMENTS

The author would like to thank Dr. Brian White under whose supervision this work was carried out, for his interest and guidance given throughout the course of these studies.

The author gratefully acknowledges the financial support of the Science Research Council, without which this work would not have been possible.

Finally, thanks are extended to Mrs. Agnes Balchin, for her careful and efficient typing of this thesis.

Condition	Speed	Mechanical arrangement	Loading	Other factors
1	300 r.p.m.	Load machine connected	No load machine armature current	
2	500 r.p.m.	as above	as above	
3	700 r.p.m.	as above	as above	
4	300 r.p.m.	as above	Adjusted for 4 Amps work machine armature current	
5	500 r.p.m.	as above	as above	
6	700 r.p.m.	as above	as above	
7	300 r.p.m.	Load machine disconnected		
8	500 r.p.m.	as above		
9	700 r.p.m.	as above		
10	300 r.p.m.	Load machine connected	Adjusted for 4 Amps work machine armature current	1.0Ω armature resistance added
11	500 r.p.m.	as above	as above	as above
12	700 r.p.m.	as above	as above	as above

TABLE 11.1

Condition	Speed	Mechanical arrangement	Loading	Other factors
13	300 r.p.m.	Load machine connected	No load machine armature current	1.0Ω armature resistance added
14	500 r.p.m.	as above	as above	as above
15	700 r.p.m.	as above	as above	as above

TABLE 11.1 (cont.)

Condition	1/Ra	1/J	F/J	$\overline{i_a}$	eb	θ_1°	θ_2°	k_2	k_3	g_1	g_2
1	1.0	7.09	0.016	1.65	21	151.2	193.75	-0.492	-0.005	0.0763	0.089
2	1.0	7.09	0.016	1.8	35	145.8	192.5	-0.486	-0.005	0.0831	0.1
3	1.0	7.09	0.016	2.0	49	142.2	190.0	-0.467	-0.005	0.086	0.1045
4	1.0	7.09	0.316	4.0	21	143.1	197.5	-0.444	-0.005	0.107	0.126
5	1.0	7.09	0.158	4.0	35	139.5	195.25	-0.392	-0.005	0.1125	0.129
6	1.0	7.09	0.118	4.0	49	133.2	193.75	-0.375	-0.005	0.122	0.151
7	1.0	22.0	negligible	1.0	21	154.8	191.75	-0.571	-0.005	0.0585	0.076
8	1.0	22.0	negligible	1.1	35	150.3	190.2	-0.533	-0.005	0.0651	0.0826
9	1.0	22.0	negligible	1.2	49	146.7	187.7	-0.509	-0.005	0.0686	0.086
10	0.5	7.09	0.316	4.0	21	127.8	194.6	-0.1	-0.00405	0.2	0.248
11	0.5	7.09	0.158	4.0	35	124.2	191.75	-0.117	-0.00405	0.197	0.2517
12	0.5	7.09	0.118	4.0	49	119.7	189.2	-0.089	-0.00405	0.198	0.26

TABLE 11.2

Condition	1/Ra	1/J	F/J	$\overline{i_a}$	e_b	θ_1°	θ_2°	k_2	k_3	g_1	g_2
13	0.5	7.09	0.016	1.65	21	142.2	192.25	-0.2174	-0.00405	0.141	0.196
14	0.5	7.09	0.016	1.8	35	137.7	189.8	-0.178	-0.00405	0.148	0.1785
15	0.5	7.09	0.016	2.0	49	132.3	187.6	-0.17	-0.00405	0.154	0.193

TABLE 11.2(cont.)

Condition	Characteristic Equation (with $K_1=\frac{1}{4}$, $K_2=1$ and $K_3=0$)
1	$s^2 + 0.311\ s + 14.48 = 0$
2	$s^2 + 0.3475\ s + 15.775 = 0$
3	$s^2 + 0.3624\ s + 16.326 = 0$
4	$s^2 + 0.7337\ s + 20.3 = 0$
5	$s^2 + 0.5857\ s + 21.36 = 0$
6	$s^2 + 0.619\ s + 23.16 = 0$
7	$s^2 + 0.7818\ s + 34.45 = 0$
8	$s^2 + 0.8497\ s + 38.35 = 0$
9	$s^2 + 0.8847\ s + 40.4 = 0$
10	$s^2 + 0.727\ s + 18.98 = 0$
11	$s^2 + 0.575\ s + 18.7 = 0$
12	$s^2 + 0.549\ s + 18.8 = 0$
13	$s^2 + 0.3409\ s + 13.38 = 0$
14	$s^2 + 0.3119\ s + 14.05 = 0$
15	$s^2 + 0.336\ s + 14.62 = 0$

TABLE 11.3

Condition	Theoretical natural frequency(Hz)	Average actual frequency(Hz)
1	0.606	0.58
2	0.632	0.62
3	0.643	0.58
4	0.718	0.78
5	0.735	0.7
6	0.764	0.74
7	0.934	0.92
8	0.985	0.98
9	1.01	1.0
10	0.694	0.7
11	0.687	0.68
12	0.69	0.65
13	0.582	0.5
14	0.597	0.54
15	0.609	0.6

TABLE 11.4

Condition	Characteristic Equation(with $K_1=\frac{1}{4}, K_2=1, K_3=4$ and $n=7$)
1	$s^2 + 4.371\ s + 14.48 = 0$
2	$s^2 + 4.768\ s + 15.775 = 0$
3	$s^2 + 4.932\ s + 16.326 = 0$
4	$s^2 + 6.434\ s + 20.3 = 0$
5	$s^2 + 6.566\ s + 21.36 = 0$
6	$s^2 + 7.099\ s + 23.16 = 0$
7	$s^2 + 10.432\ s + 34.45 = 0$
8	$s^2 + 11.55\ s + 38.35 = 0$
9	$s^2 + 12.185\ s + 40.4 = 0$
10	$s^2 + 6.027\ s + 18.98 = 0$
11	$s^2 + 5.805\ s + 18.7 = 0$
12	$s^2 + 5.809\ s + 18.8 = 0$
13	$s^2 + 4.088\ s + 13.38 = 0$
14	$s^2 + 4.245\ s + 14.05 = 0$
15	$s^2 + 4.429\ s + 14.62 = 0$

TABLE 12.1

Condition	Natural Frequency(Rads/Sec)	Damping Factor
1	3.805	0.574
2	3.97	0.6
3	4.04	0.61
4	4.51	0.713
5	4.62	0.71
6	4.8	0.739
7	5.87	0.888
8	6.192	0.933
9	6.356	0.958
10	4.36	0.691
11	4.32	0.672
12	4.34	0.669
13	3.658	0.559
14	3.748	0.566
15	3.824	0.579

TABLE 12.2

Condition	Limiting value of $\alpha_1^- = \alpha_2 c_1 - c_1^2$	Value of α_1^- with $K_1K_2 = -1$
1	-48.8	-57.92
2	-48.5	-63.1
3	-48.4	-65.3
4	-45.78	-81.2
5	-46.84	-85.44
6	-46.6	-92.64
7	-45.44	-137.8
8	-44.95	-153.4
9	-44.7	-161.6
10	-45.83	-75.92
11	-46.9	-74.8
12	-47.1	-75.2
13	-48.59	-53.52
14	-48.79	-56.2
15	-48.62	-58.48
	a)	b)

TABLE 12.3

Condition	Characteristic Equation (with $K_1=-1, K_2=1$ and $K_3=0$)
1	$s^2 + 0.311\ s - 57.92 = 0$
2	$s^2 + 0.3475\ s - 63.1 = 0$
3	$s^2 + 0.3624\ s - 65.3 = 0$
4	$s^2 + 0.7337\ s - 81.2 = 0$
5	$s^2 + 0.5857\ s - 85.44 = 0$
6	$s^2 + 0.619\ s - 92.64 = 0$
7	$s^2 + 0.7818\ s - 137.8 = 0$
8	$s^2 + 0.8497\ s - 153.4 = 0$
9	$s^2 + 0.8847\ s - 161.6 = 0$
10	$s^2 + 0.727\ s - 75.92 = 0$
11	$s^2 + 0.575\ s - 74.8 = 0$
12	$s^2 + 0.549\ s - 75.2 = 0$
13	$s^2 + 0.3409\ s - 53.52 = 0$
14	$s^2 + 0.3119\ s - 56.2 = 0$
15	$s^2 + 0.336\ s - 58.48 = 0$

TABLE 12.4

Condition	Limiting value of $\alpha_2^+ = \frac{\alpha_1}{c_1} + c_1$	Value of α_2^+ with K_3=16
1	9.17	16.551
2	9.35	18.03
3	9.429	18.64
4	9.98	23.53
5	10.13	24.51
6	10.385	26.54
7	11.966	39.38
8	12.51	43.65
9	12.8	46.1
10	9.8	21.93
11	9.761	21.48
12	9.77	21.59
13	9.02	15.33
14	9.11	16.04
15	9.19	16.71
	a)	b)

TABLE 12.5

Condition	Characteristic Equation (with $K_1=\frac{1}{4}, K_2=1, K_3=16$ and $n=7$)
1	$s^2 + 16.551\,s + 14.48 = 0$
2	$s^2 + 18.03\,s + 15.775 = 0$
3	$s^2 + 18.64\,s + 16.326 = 0$
4	$s^2 + 23.53\,s + 20.3 = 0$
5	$s^2 + 24.51\,s + 21.36 = 0$
6	$s^2 + 26.54\,s + 23.16 = 0$
7	$s^2 + 39.38\,s + 34.45 = 0$
8	$s^2 + 43.65\,s + 38.35 = 0$
9	$s^2 + 46.1\,s + 40.4 = 0$
10	$s^2 + 21.93\,s + 18.98 = 0$
11	$s^2 + 21.48\,s + 18.7 = 0$
12	$s^2 + 21.59\,s + 18.8 = 0$
13	$s^2 + 15.33\,s + 13.38 = 0$
14	$s^2 + 16.04\,s + 14.05 = 0$
15	$s^2 + 16.71\,s + 14.62 = 0$

TABLE 12.6

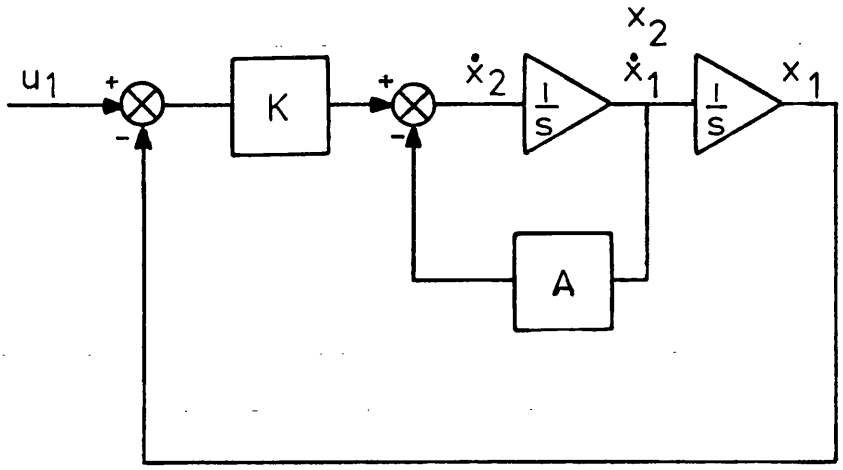

FIG. 2.1 SIMPLE FIXED-STRUCTURE SYSTEM

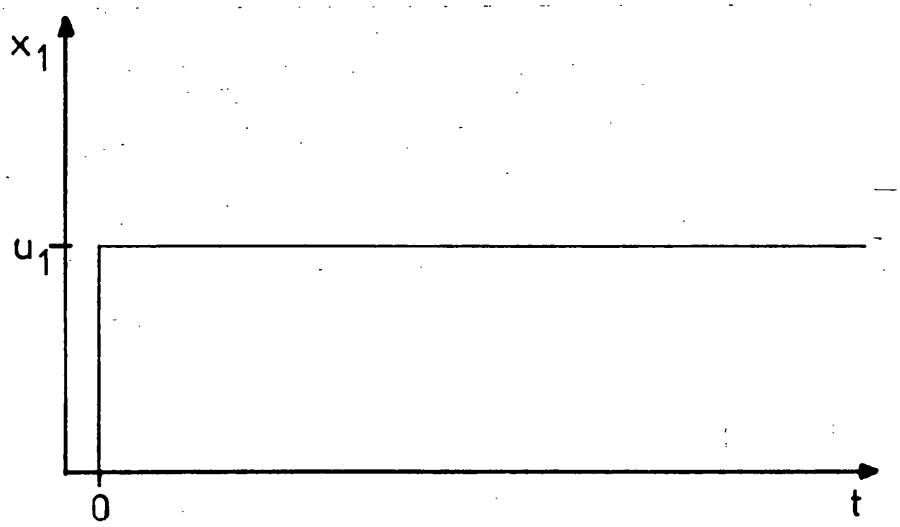

FIG. 2.2 "IDEAL" TIME RESPONSE FOR x_1

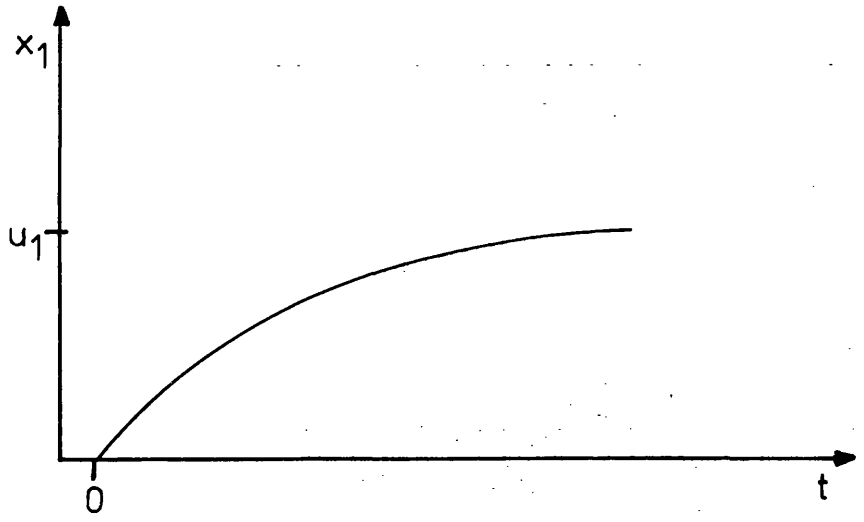

FIG. 2.3 RESPONSE WITH "A" LARGE

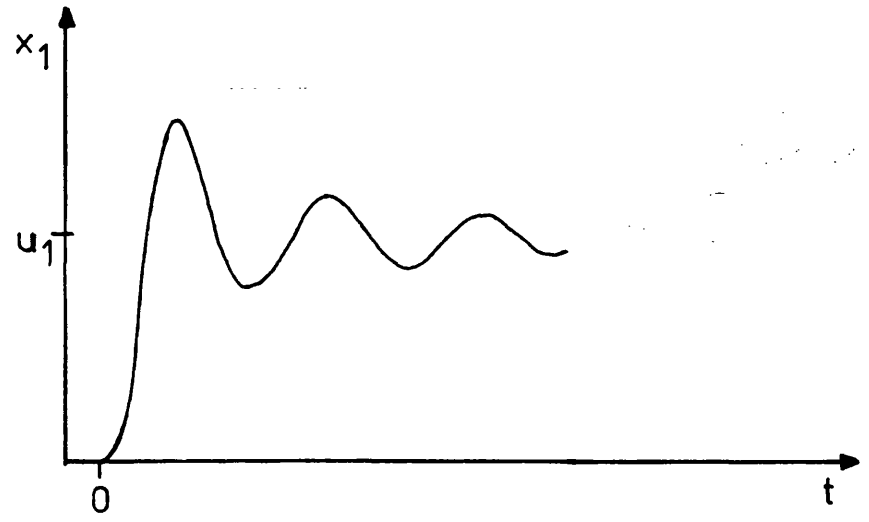

FIG. 2.4 RESPONSE WITH "A" SMALL

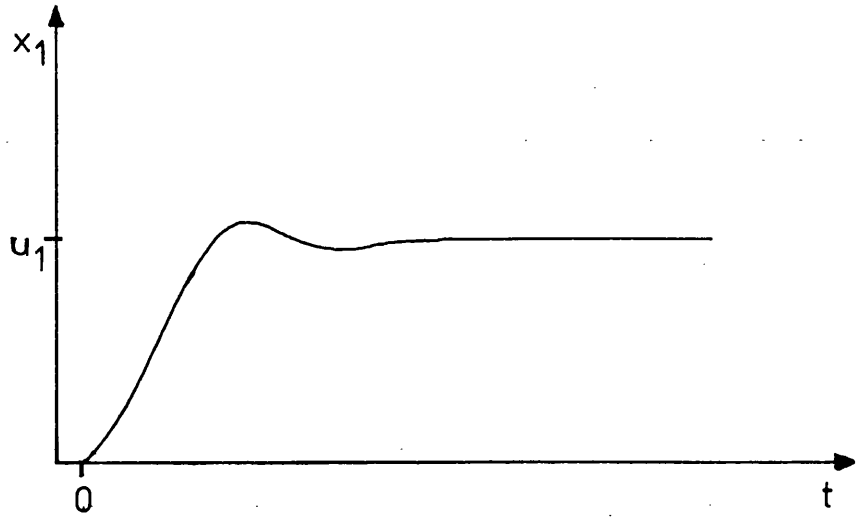

FIG. 2.5 RESPONSE WITH "A" AT A COMPROMISE VALUE

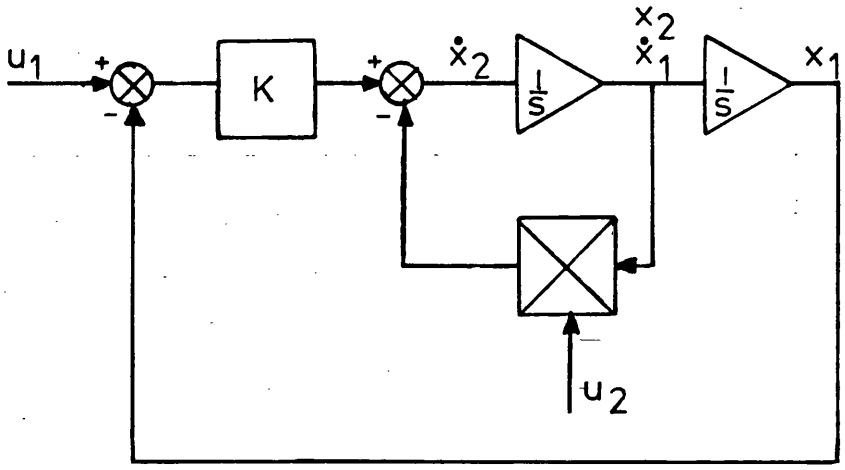

N.B. The symbol ⊠ represents a time domain multiplication operator.

FIG. 2.6 VARIABLE STRUCTURE CONTROL

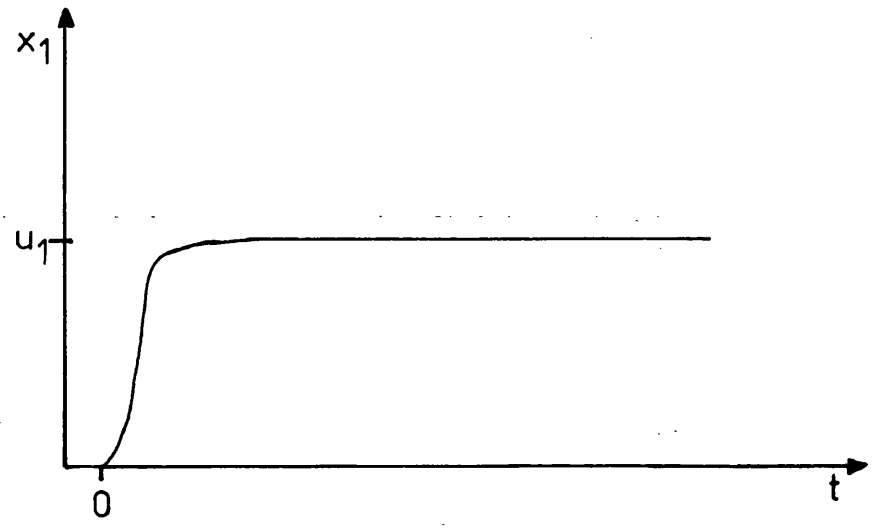

FIG. 2.7 RESPONSE WITH VARIABLE STRUCTURE CONTROL

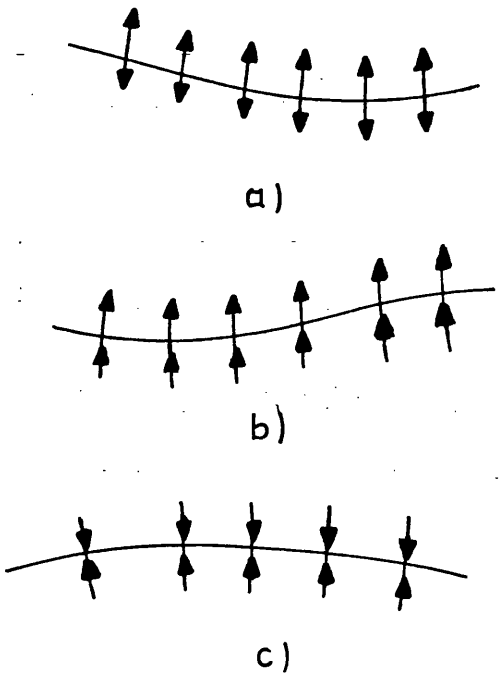

FIG. 2.8 SWITCHING SURFACE TRAJECTORIES

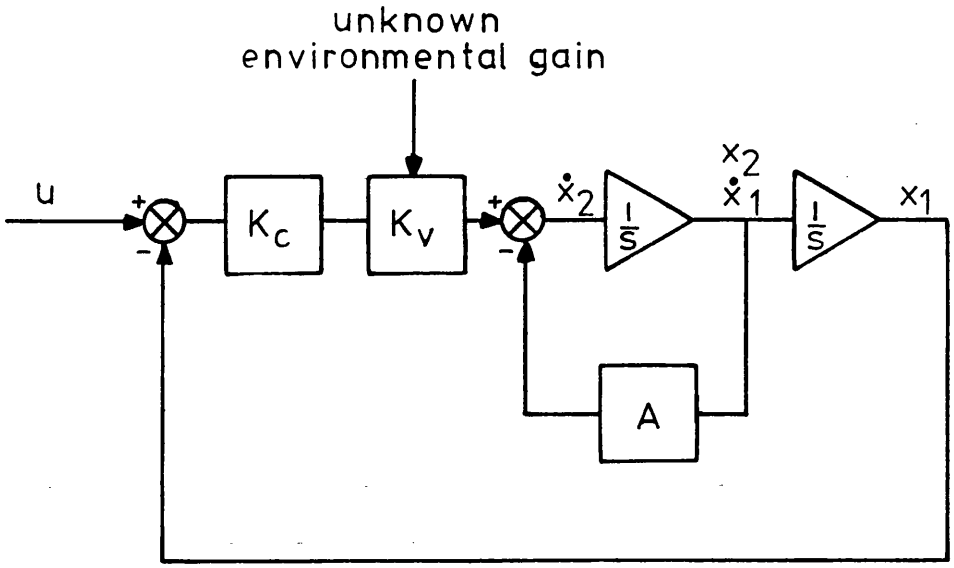

FIG. 3.1 VARIABLE PLANT WITH FIXED CONTROL

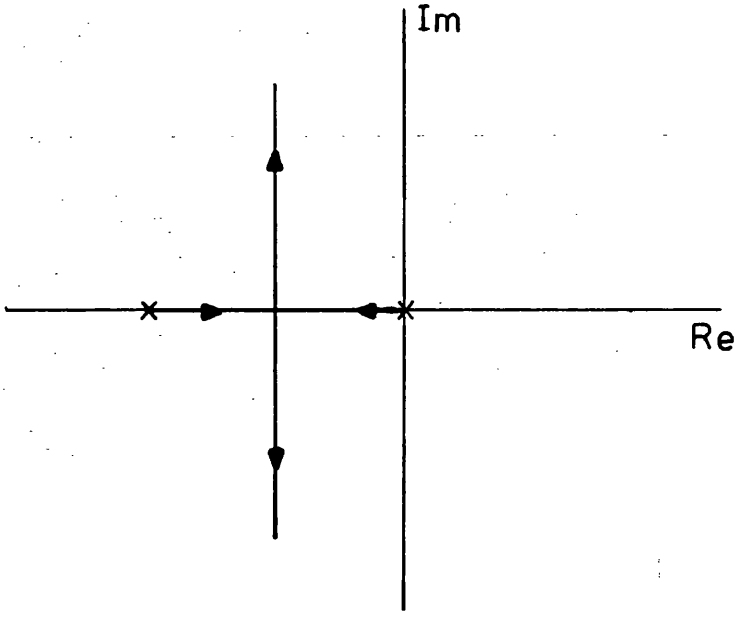

FIG. 3.2 ROOT LOCUS FOR $K_c K_v$ VARYING

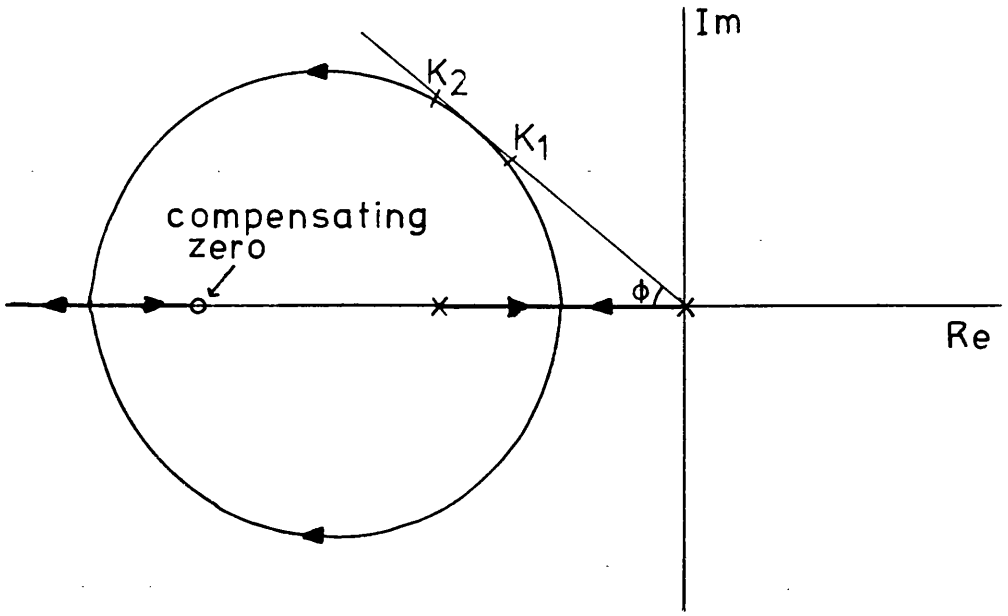

FIG. 3.3 ROOT LOCUS WITH COMPENSATION

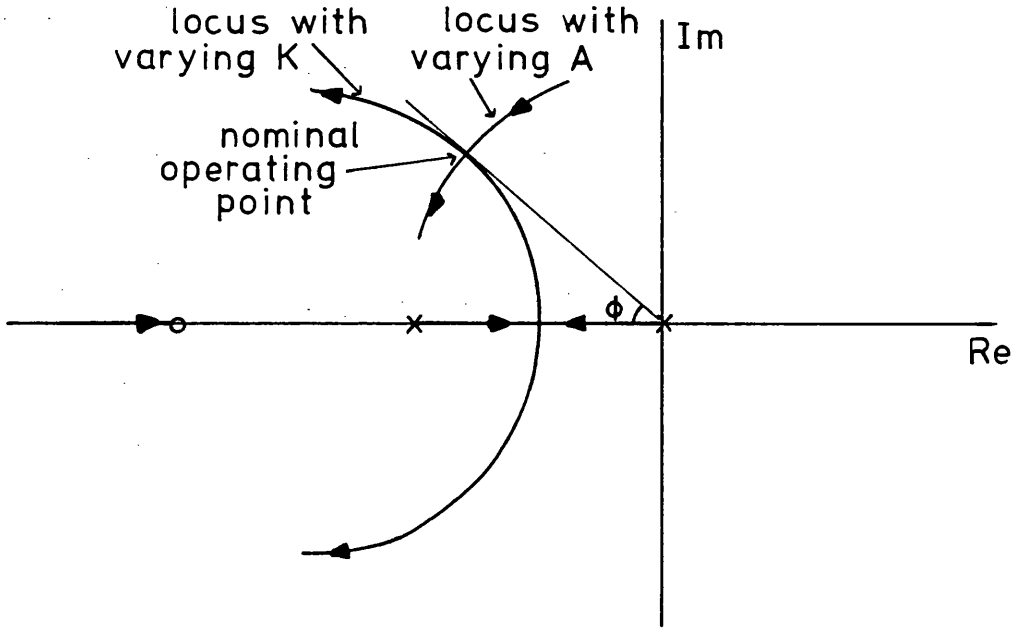

FIG. 3.4 LOCI VARIATION ABOUT A NOMINAL POINT FOR CHANGES IN K AND A

Condition	Altitude	Mach N°	$-\frac{1}{T_a}$	$K\dot{\theta}$	$\zeta_a \omega_a$	ω_a
1	35,000	0.3	-0.123	0.1066	0.2604	1.988
4	40,000	1.0	-0.282	0.312	0.445	2.972
5	40,000	1.0	-0.206	0.262	0.375	2.769
9	70,000	2.0	-0.088	0.0583	0.1052	2.631
13	100,000	4.0	-0.0366	0.0223	0.0396	1.919
16	140,000	6.0	-0.00794	0.00865	0.00823	0.8067
17	120,000	6.0	-0.0184	0.0198	0.019	1.203
18	120,000	6.0	-0.02585	0.0199	0.0276	1.859
21	60,000	5.0	-0.325	0.362	0.326	4.327
28	10,000	1.2	-2.07	1.950	2.49	7.492
29	10,000	1.0	-1.975	3.42	2.31	4.915
30	10,000	0.6	-0.955	2.03	0.943	2.5708
31	5,000	0.6	-1.163	2.92	1.113	2.550
32	0	0.2	-0.0356	0.00343	0.151	1.511
33	160,000	6.0	-0.00368	0.00394	0.0038	0.555

FIG. 3.5 VARIATION OF AIRCRAFT CHARACTERISTICS OVER A RANGE OF FLIGHT CONDITIONS

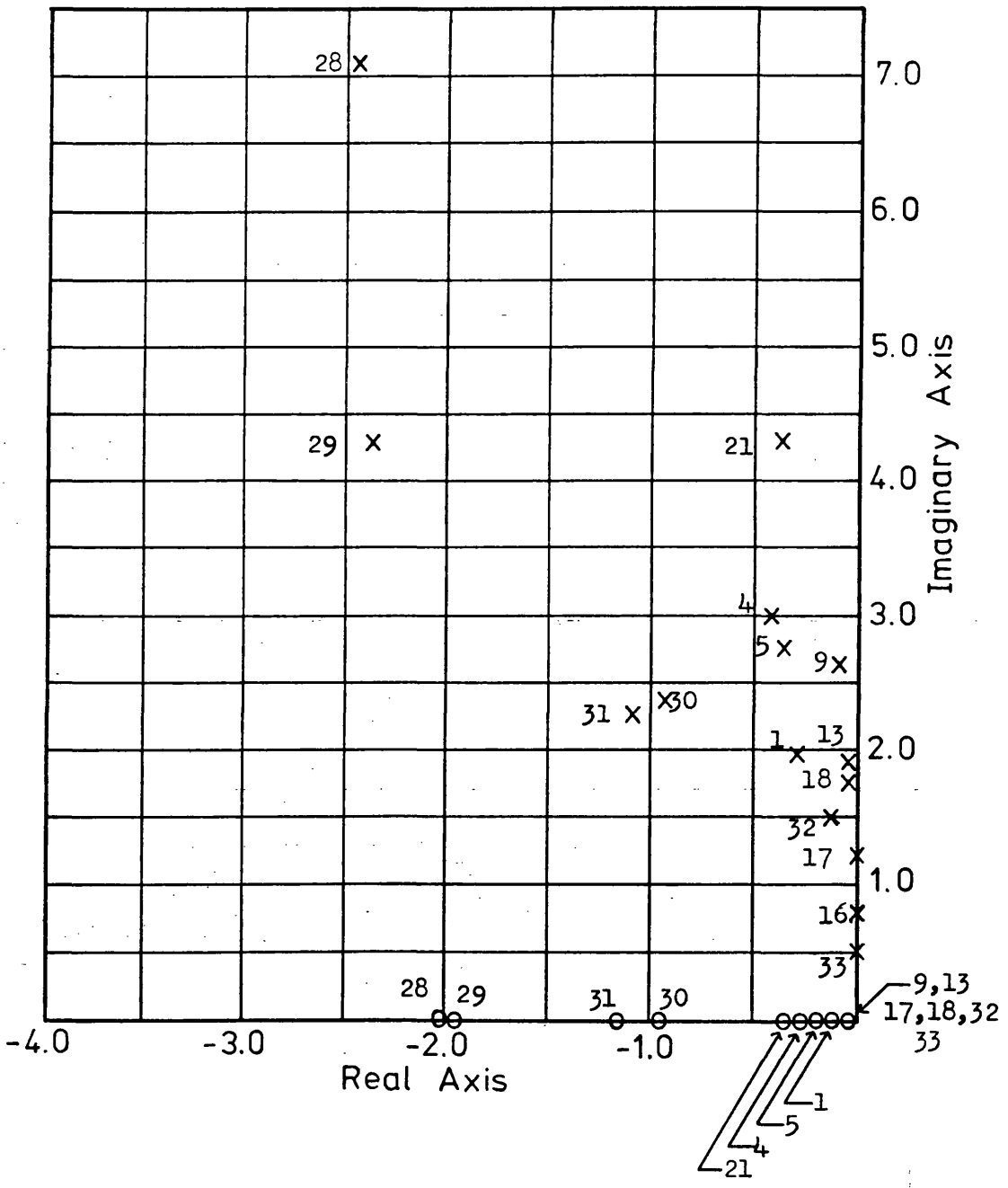

FIG. 3.6 VARIATION OF POLE-ZERO LOCATION OVER A RANGE OF FLIGHT CONDITIONS

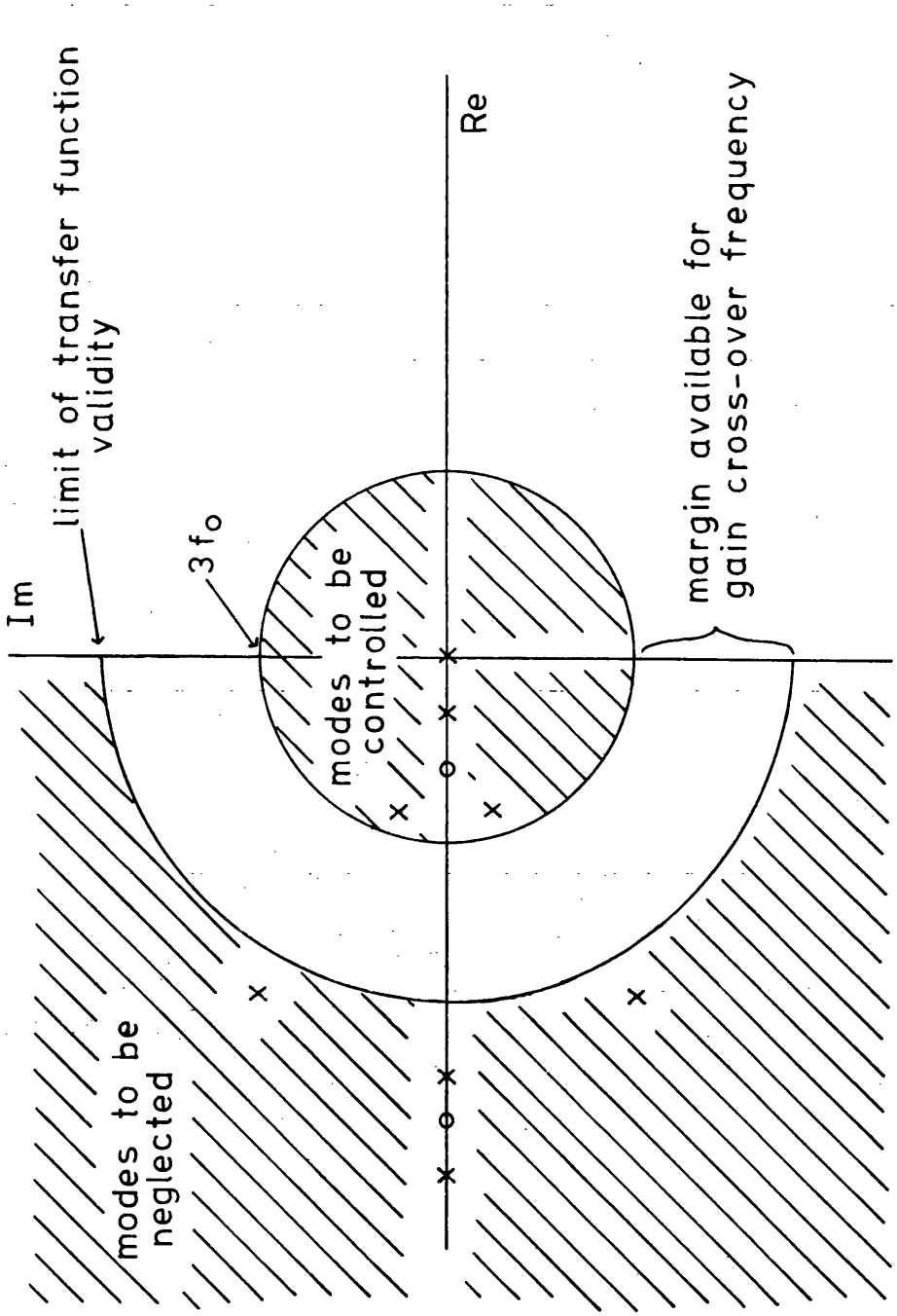

FIG. 3.7 CONSTRAINTS DUE TO THE POLES AND ZEROS OF A REAL SYSTEM

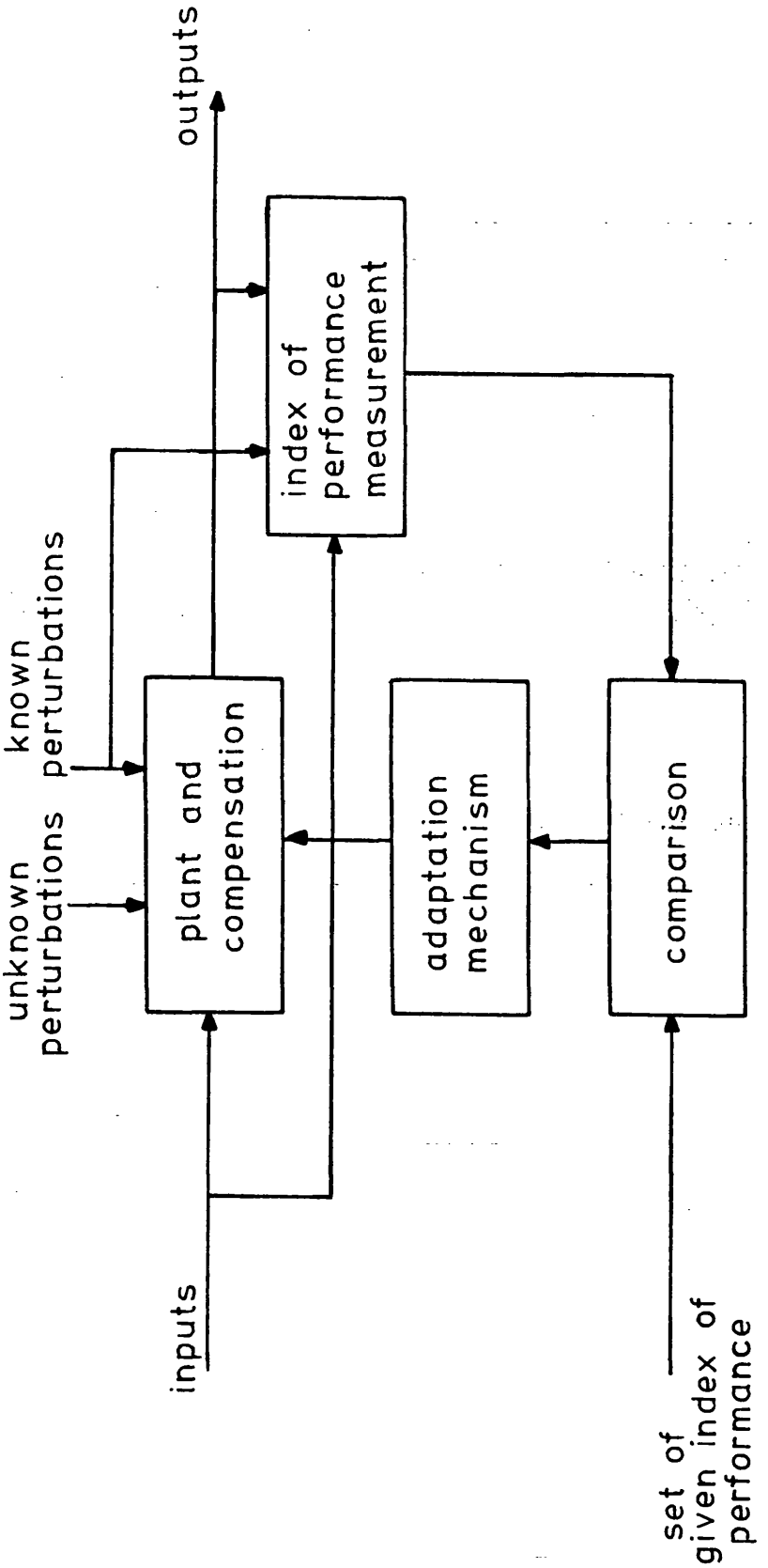

FIG. 3.8 BASIC CONFIGURATION OF AN ADAPTIVE SYSTEM

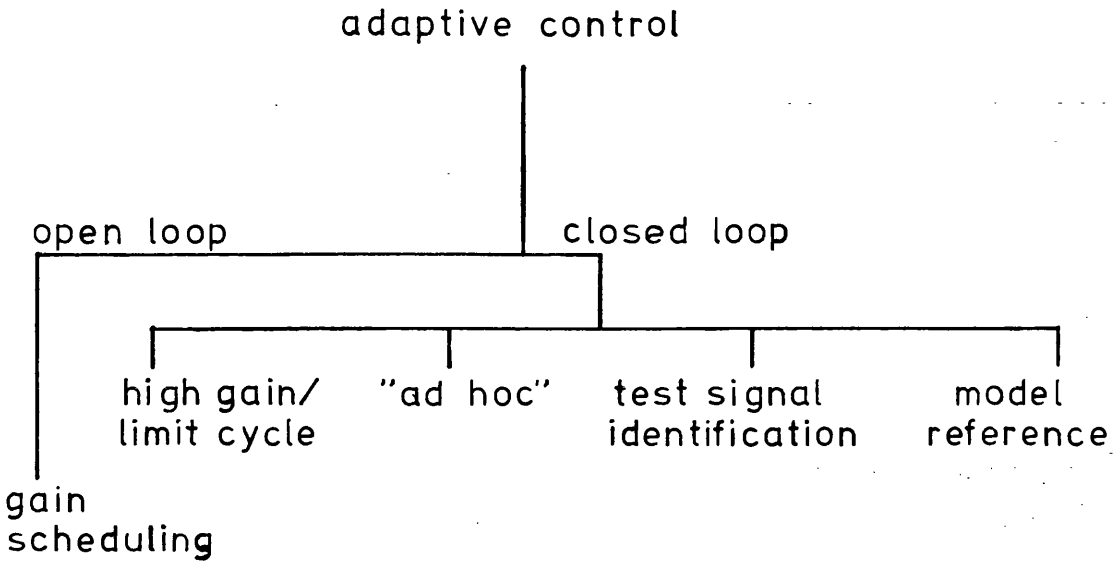

FIG. 3.9 ADAPTIVE CONTROL DESIGN PHILOSOPHIES

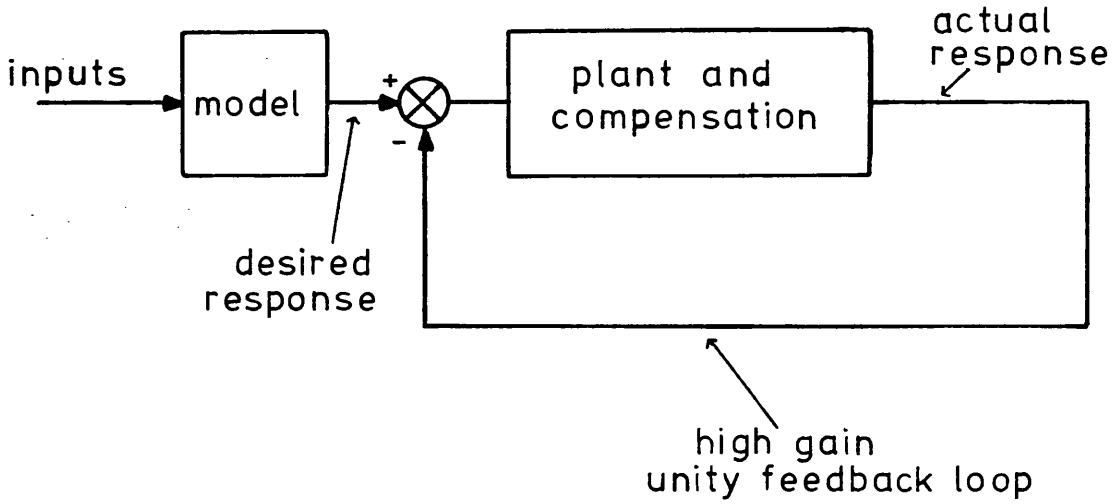

FIG. 3.10 REPRESENTATION OF THE HIGH GAIN LOOP PRINCIPLE

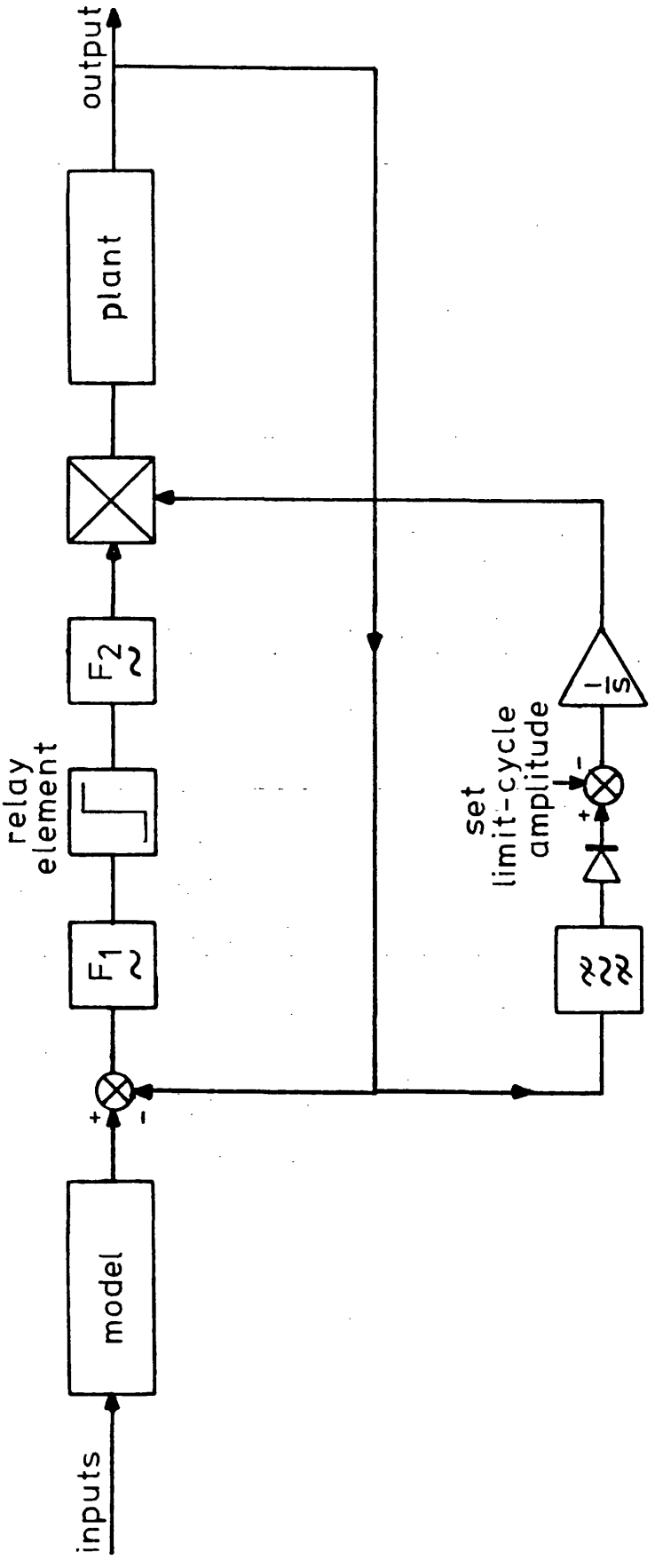

FIG. 3.11 LIMIT-CYCLE SYSTEM

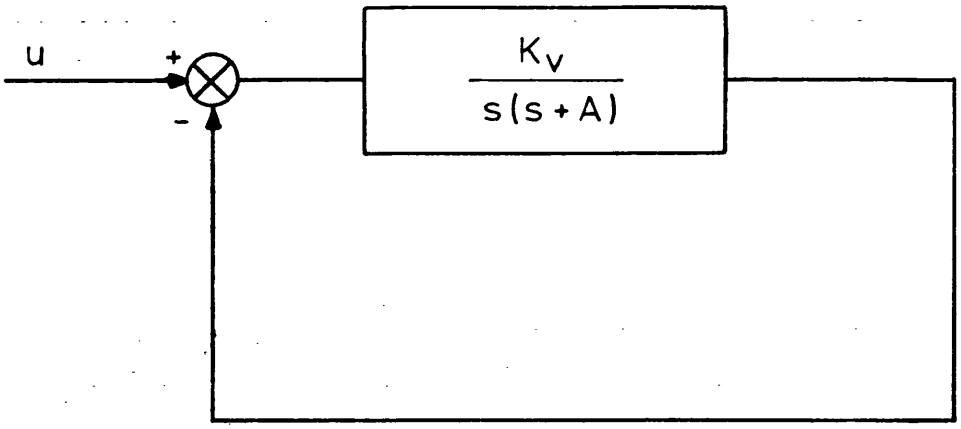

FIG. 3.12 SECOND ORDER SYSTEM WITH VARIABLE GAIN K_V

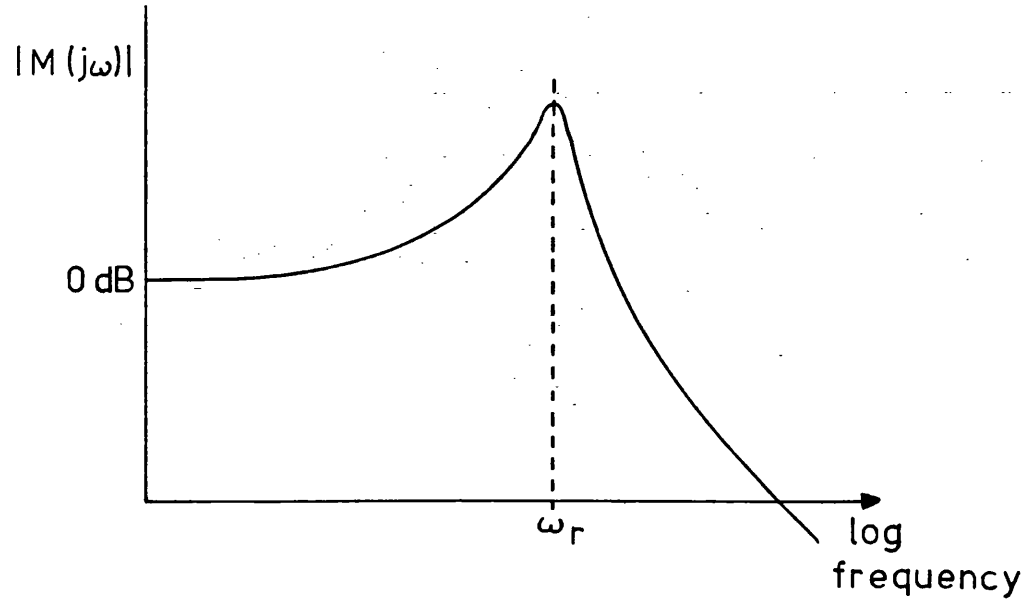

FIG. 3.13 FREQUENCY RESPONSE OF AN UNDERDAMPED SECOND ORDER SYSTEM

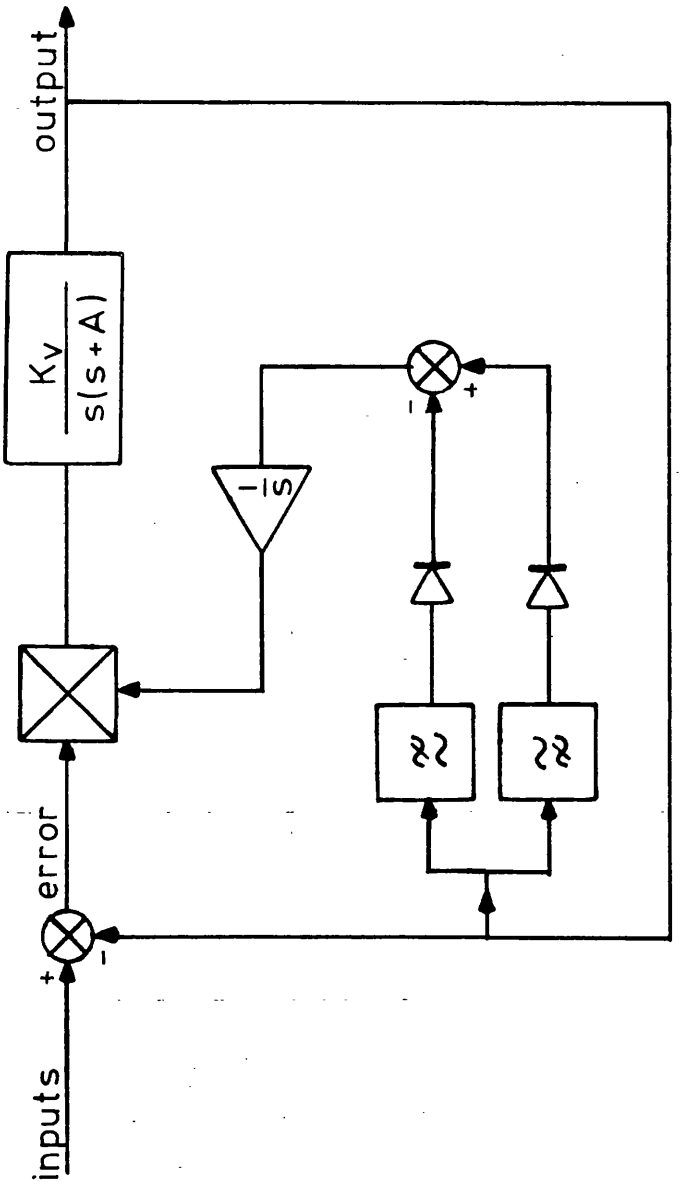

FIG. 3.14 MARX'S FREQUENCY SERVO

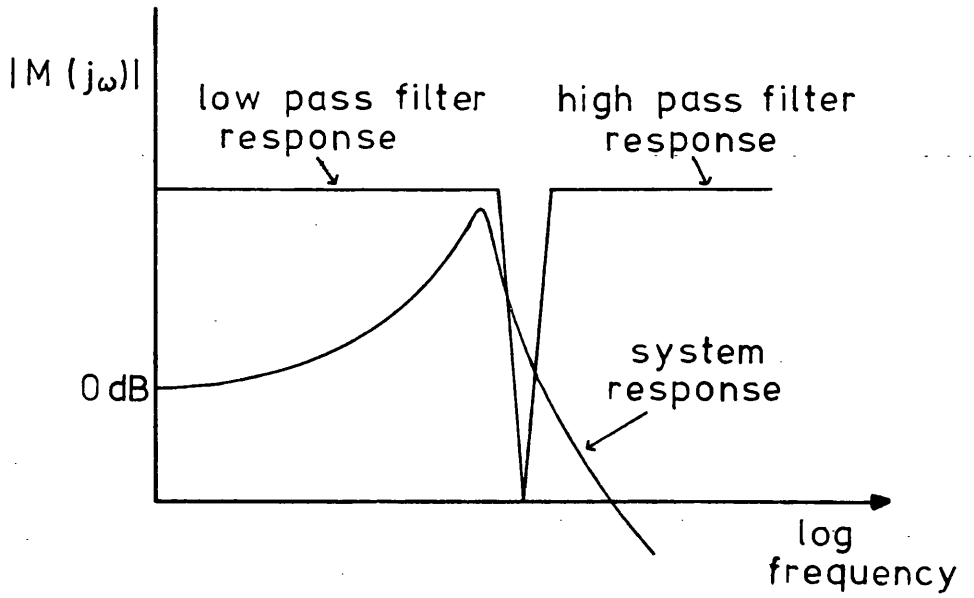

a) loop gain low

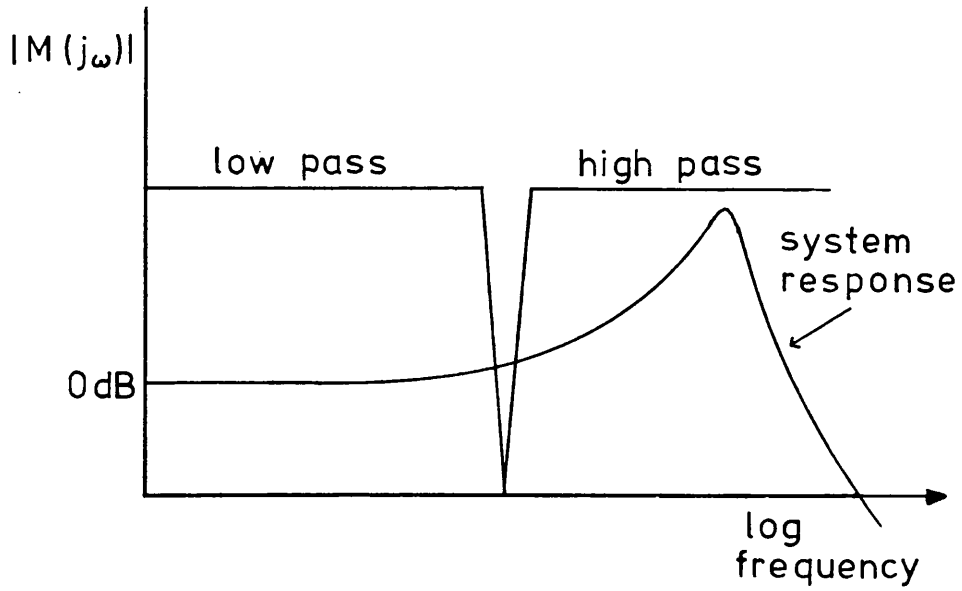

b) loop gain high

FIG. 3.15 RELATIONSHIPS BETWEEN SYSTEM AND FILTER RESPONSES

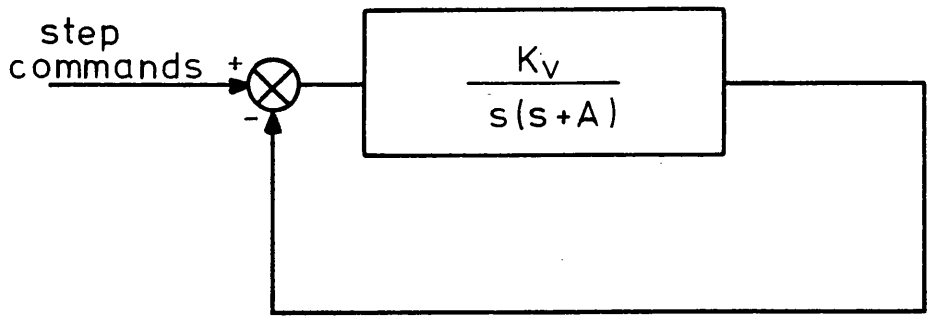

FIG. 3.16 VARIABLE SECOND ORDER SYSTEM WITH STEP INPUTS

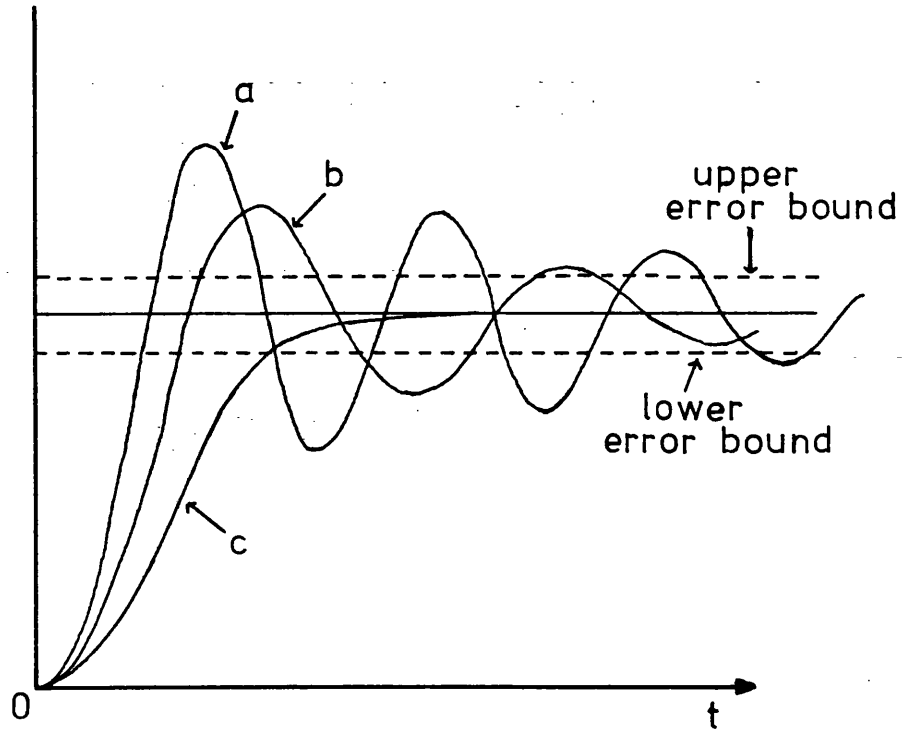

FIG. 3.17 STEP RESPONSES OF A SECOND ORDER SYSTEM UNDER VARIOUS ENVIRONMENTAL CONDITIONS

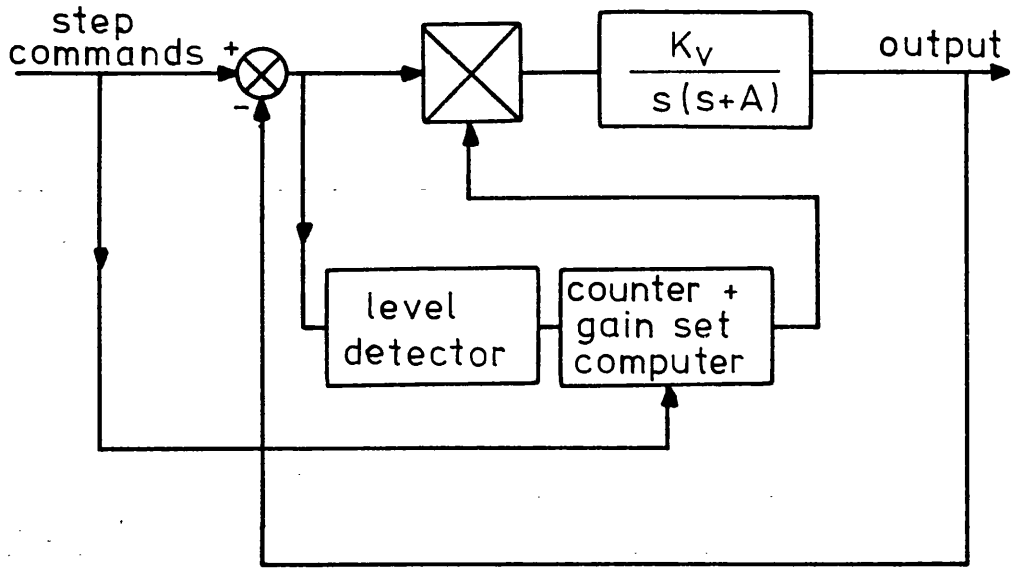

FIG. 3.18 OSDER'S IMPULSE TEST SYSTEM

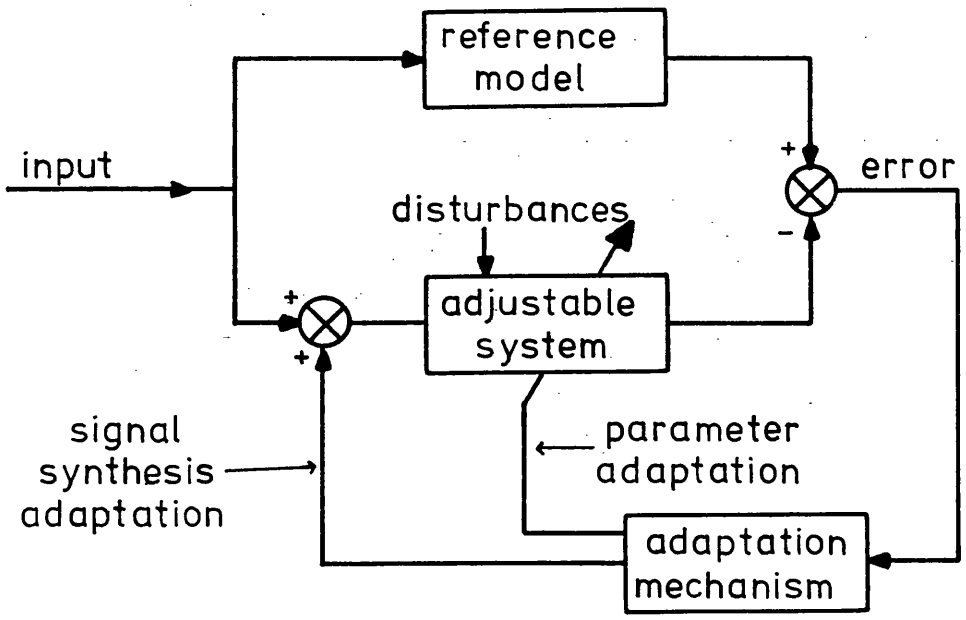

FIG. 3.19 GENERAL REPRESENTATION OF THE MODEL REFERENCE SCHEME

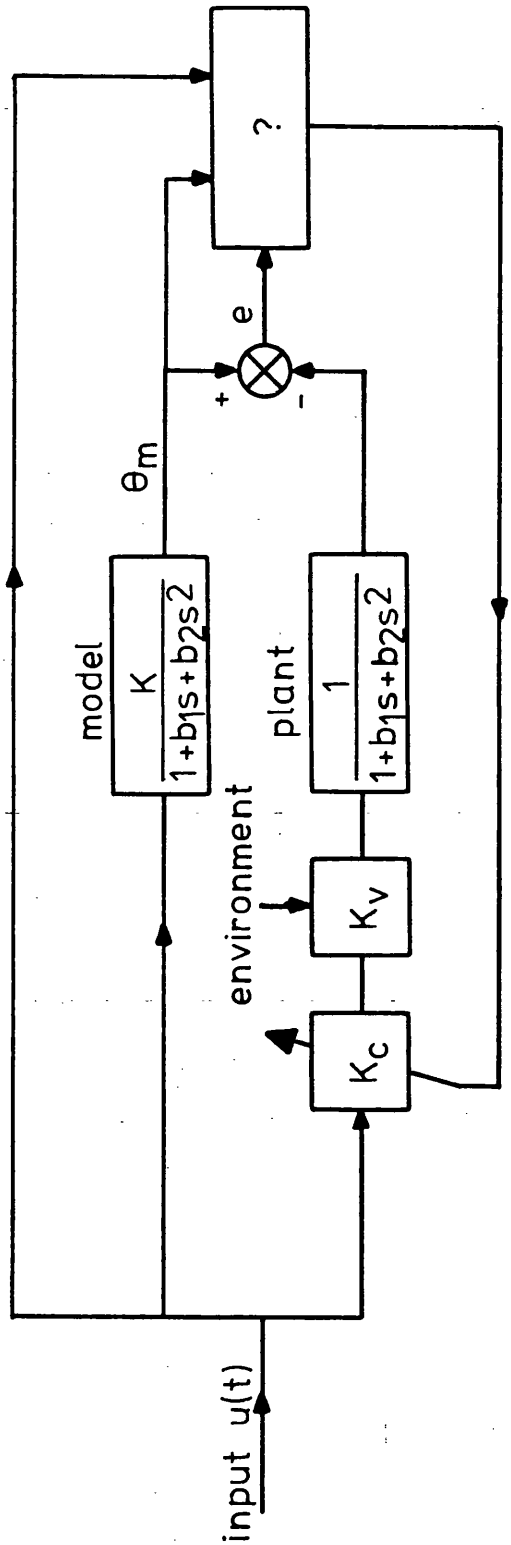

FIG. 4.1 GAIN ADAPTATION PROBLEM

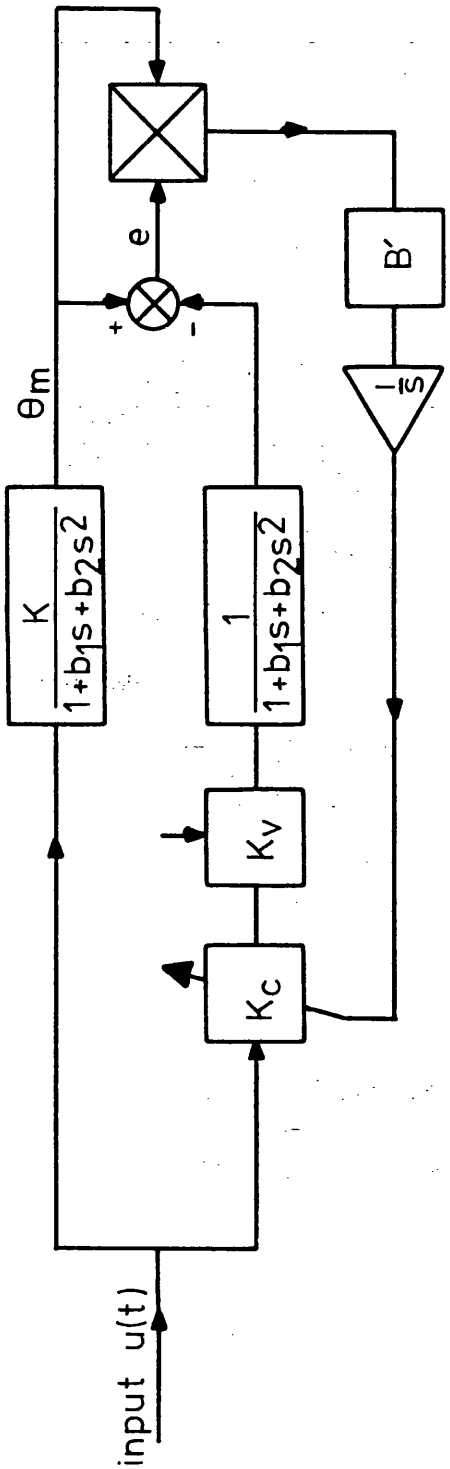

FIG. 4.2 M.I.T. ADAPTIVE CONTROL STRATEGY

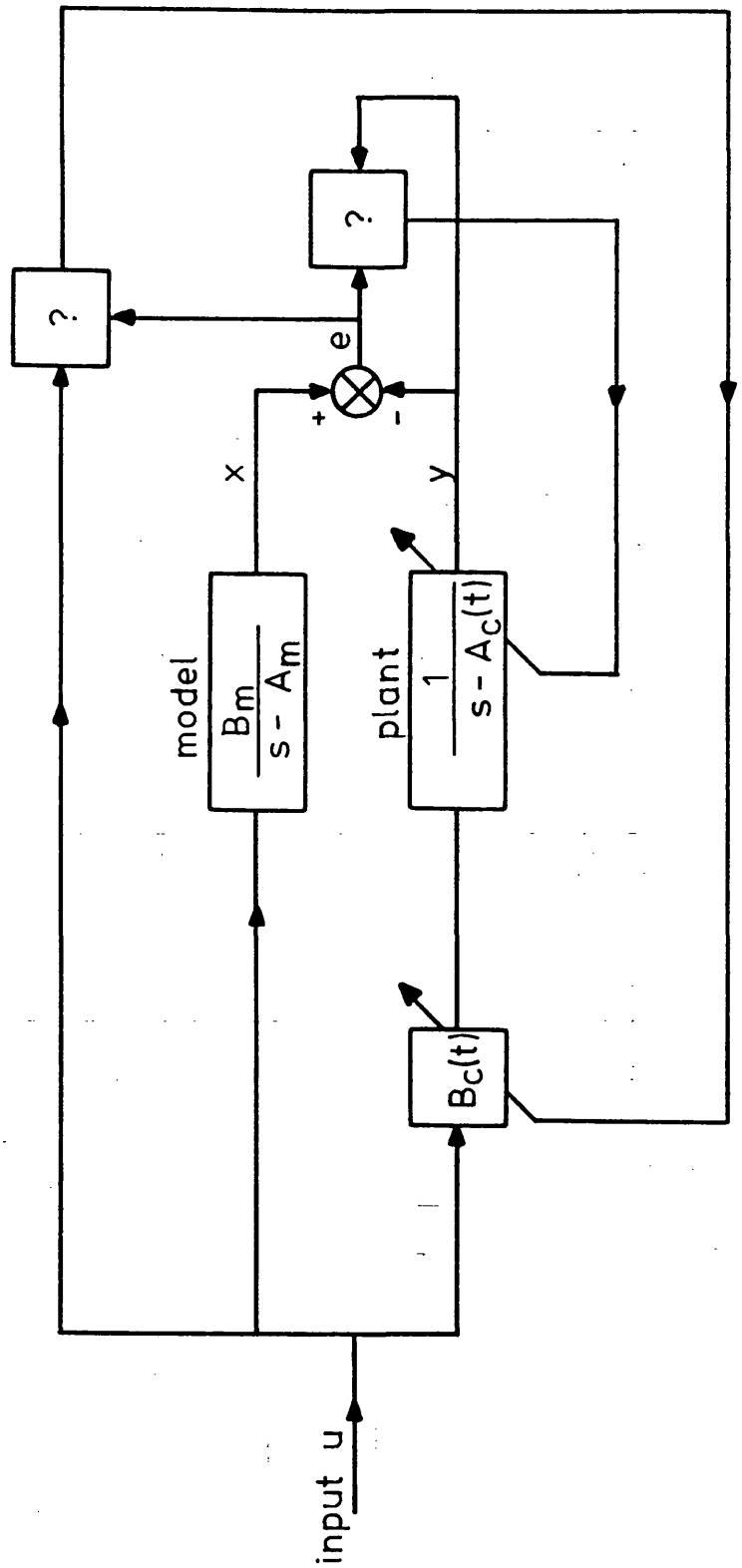

FIG. 4.3 TWO PARAMETER GAIN ADAPTATION PROBLEM

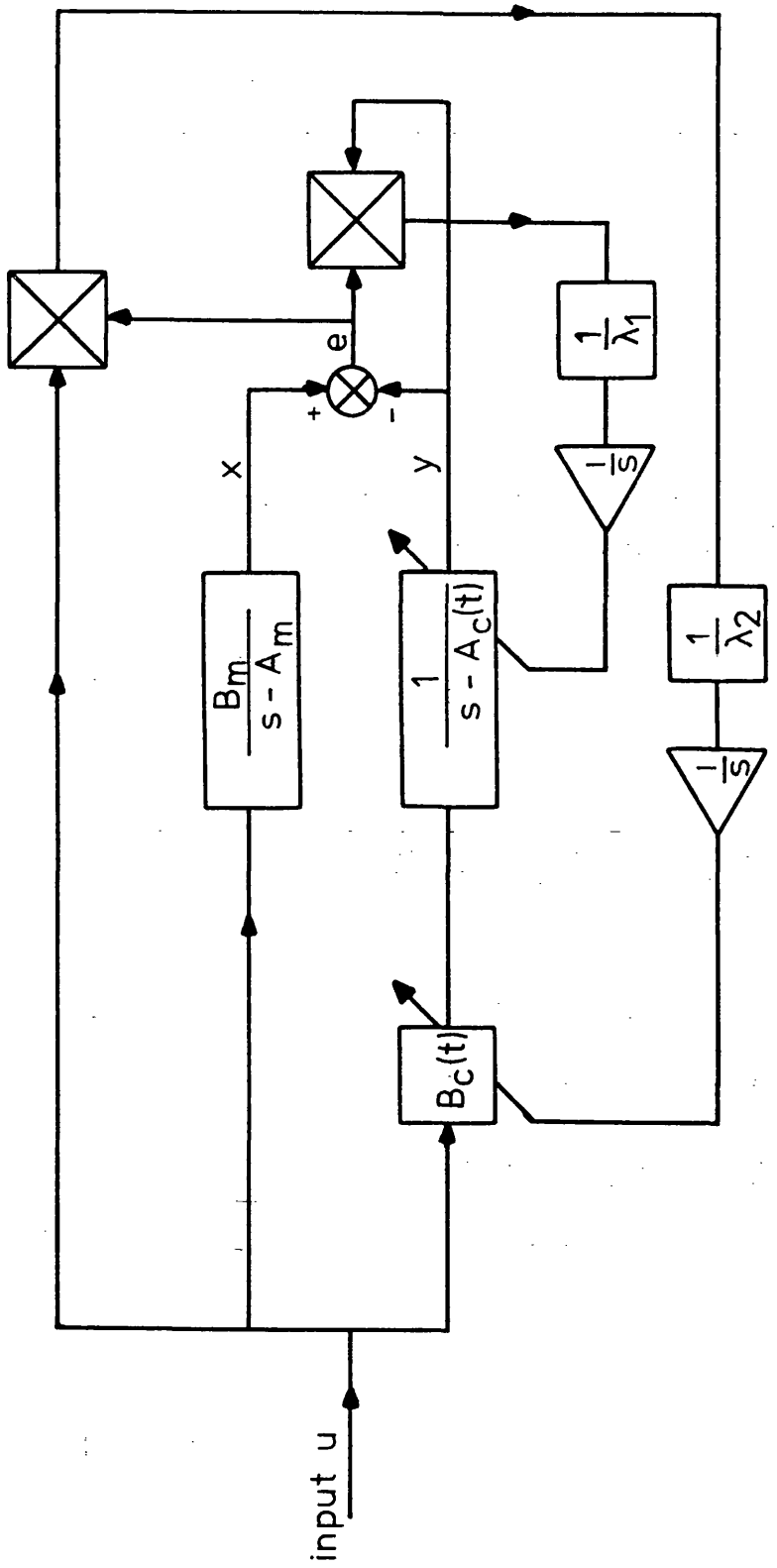

FIG. 4.4 LIAPUNOV ADAPTIVE CONTROL STRATEGY

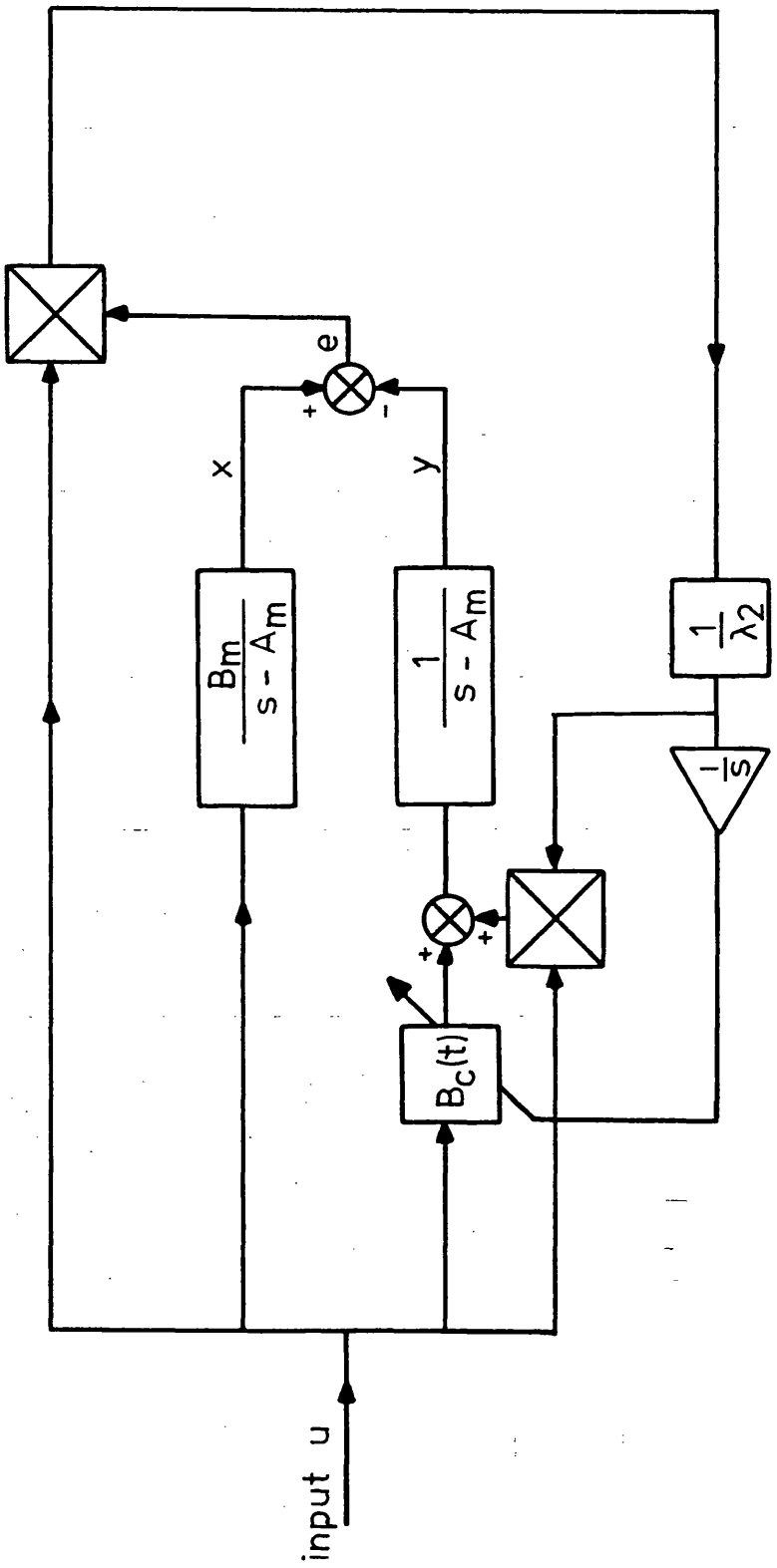

FIG. 4.5 SCHEME TO REDUCE ADAPTIVE LOOP SENSITIVITY

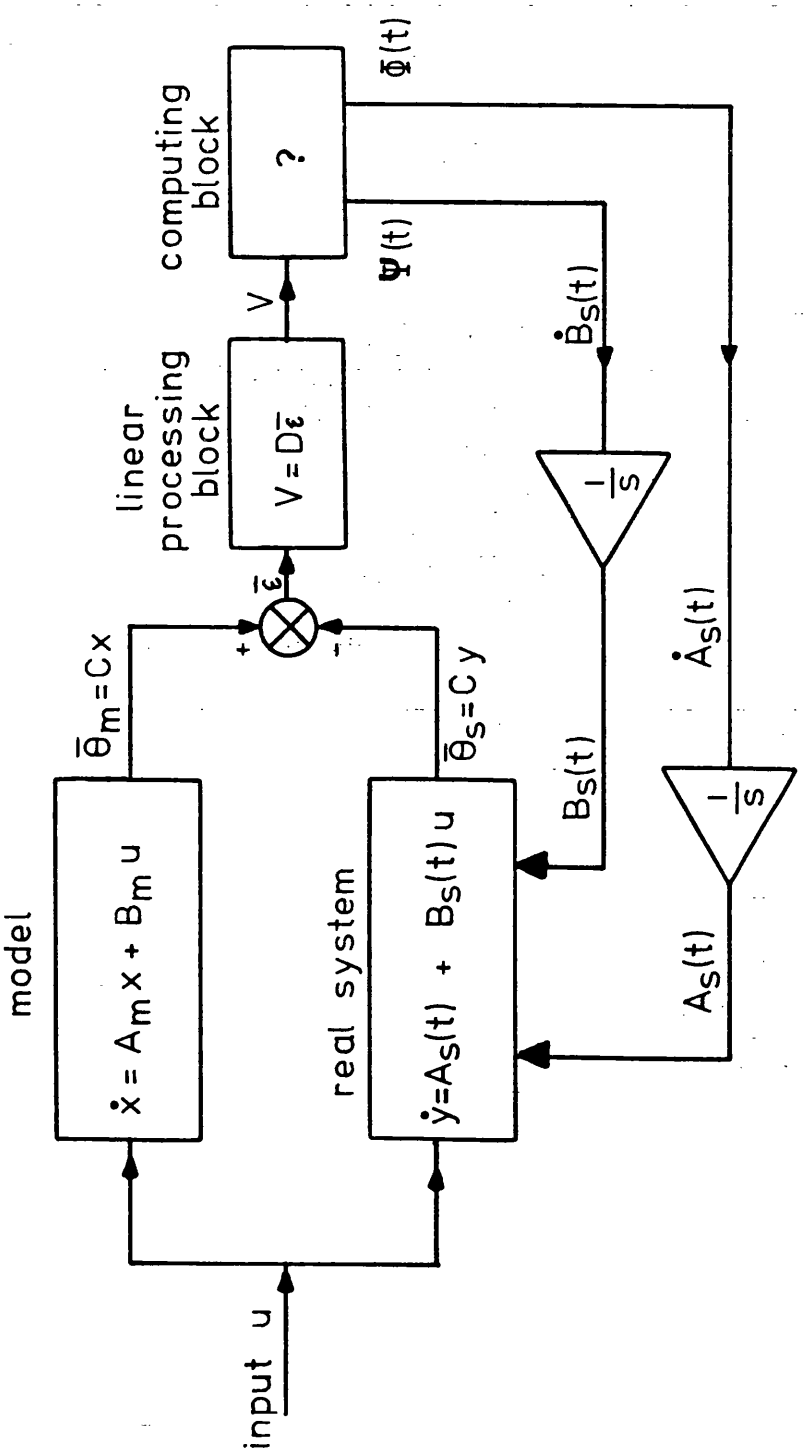

FIG. 4.6 MULTIVARIABLE MODEL REFERENCE ADAPTIVE SYSTEM

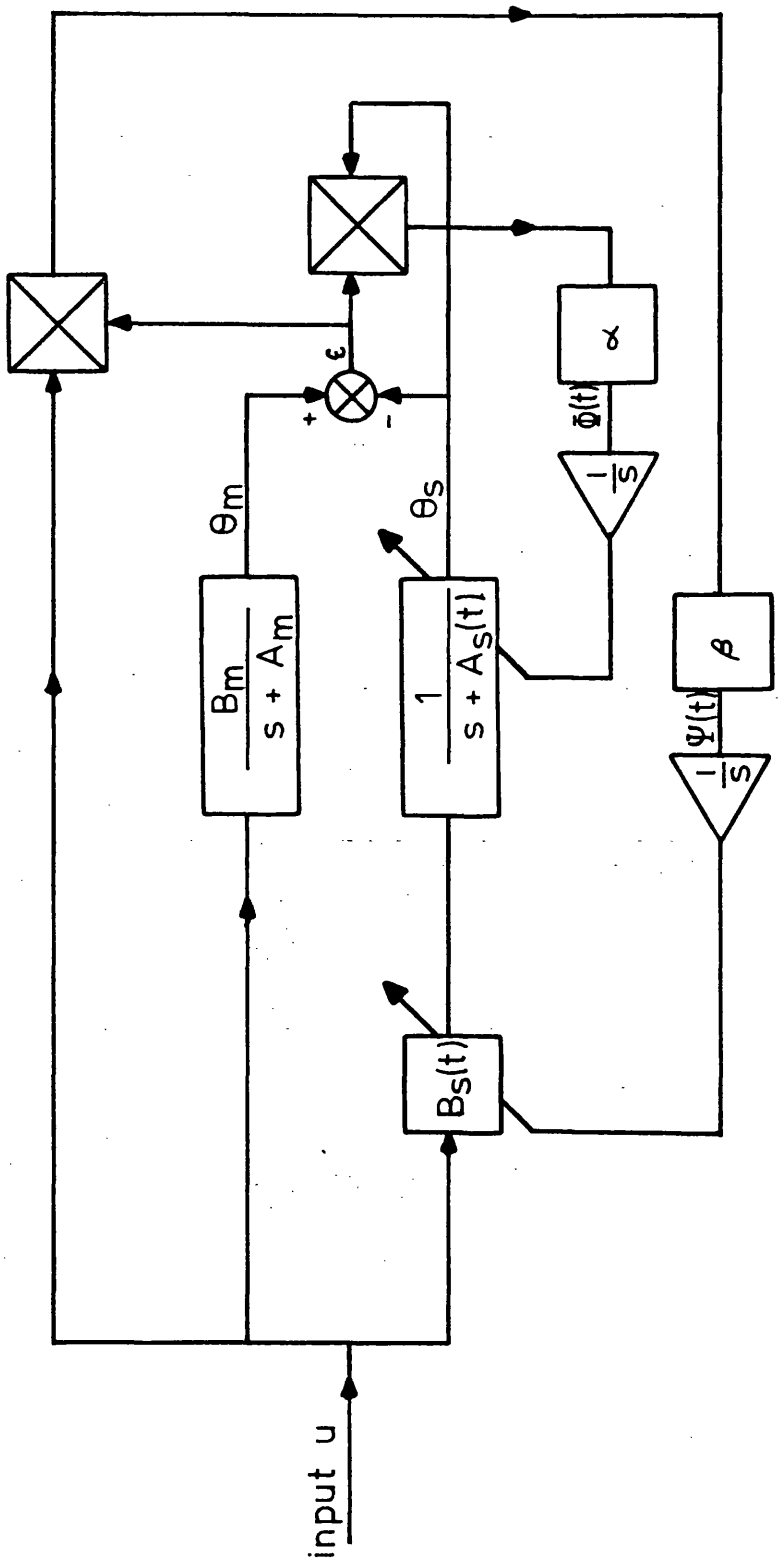

FIG. 4.7 HYPERSTABLE ADAPTIVE CONTROL STRATEGY

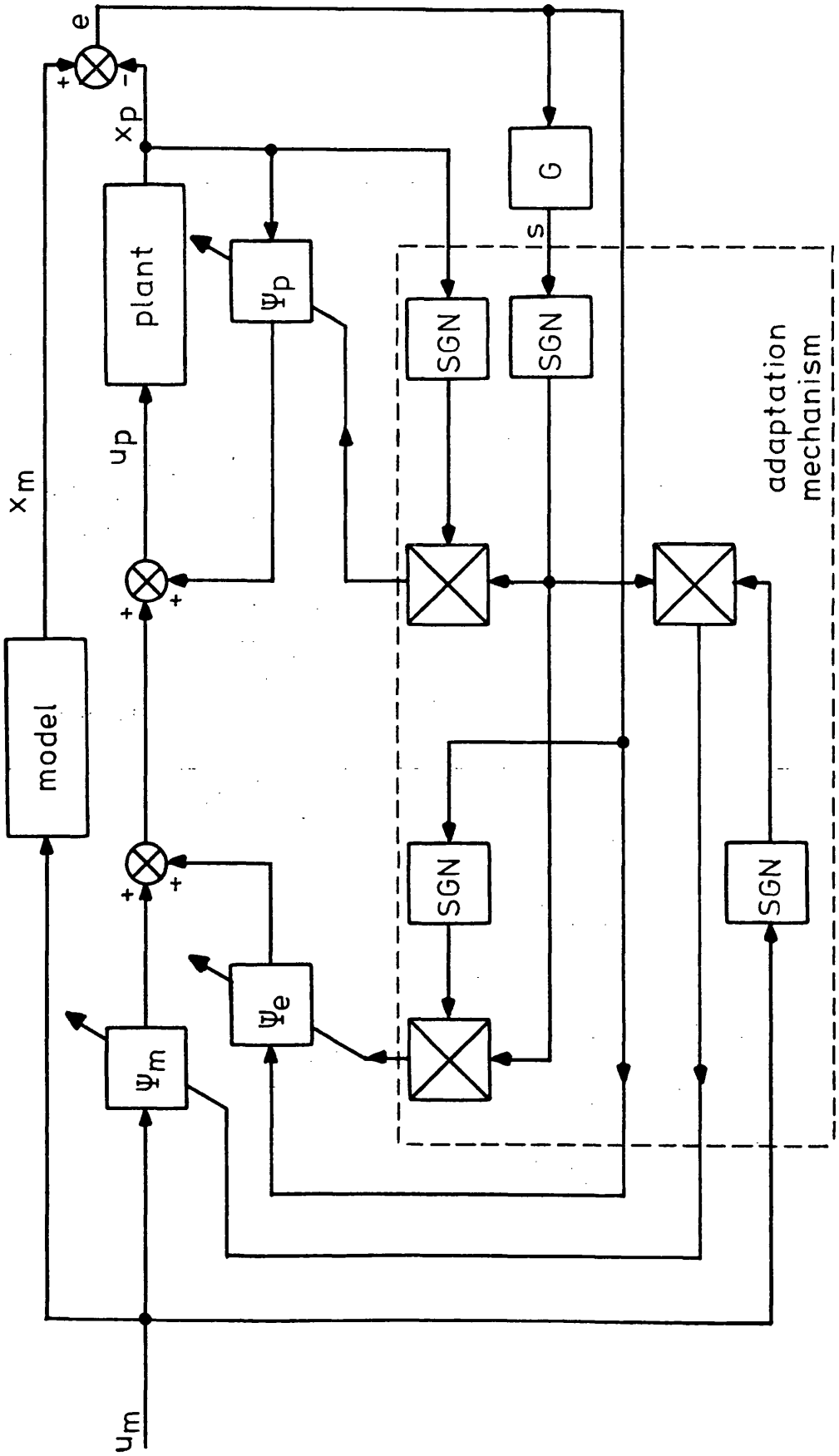

FIG. 4.8 VARIABLE STRUCTURE MODEL REFERENCE ADAPTIVE SYSTEM

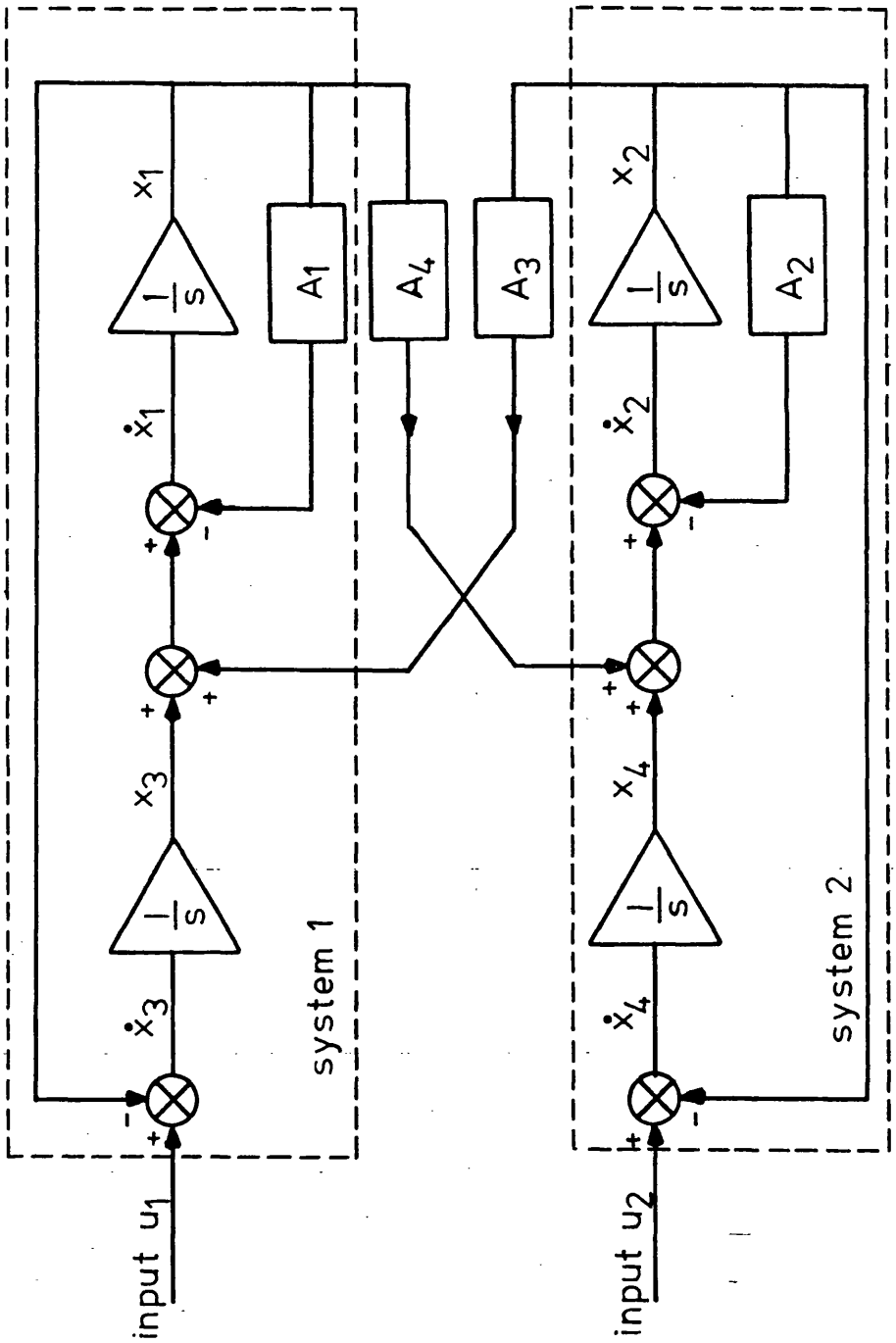

FIG. 4.9 SYSTEMS WITH UNDESIRABLE CROSS-COUPLING

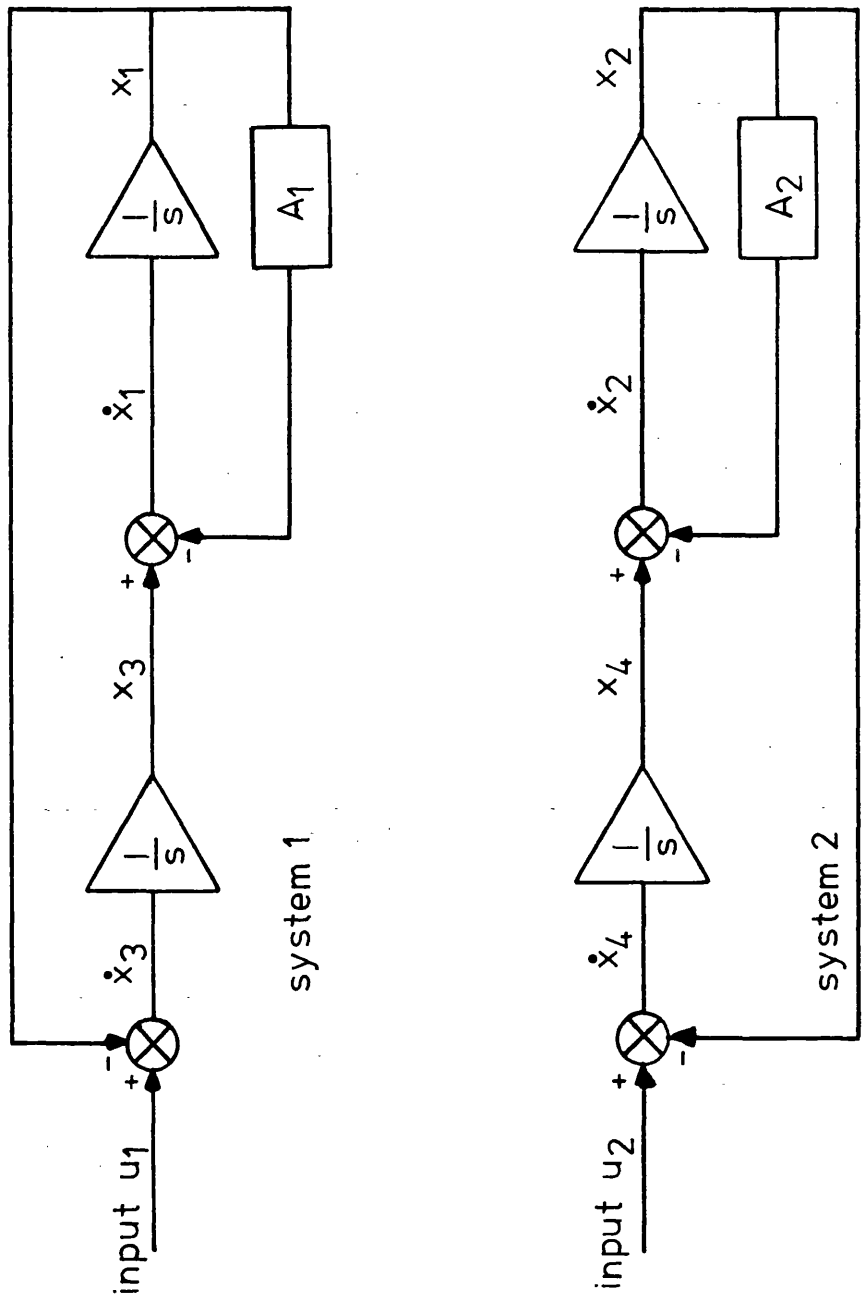

FIG. 4.10 SYSTEMS TO HAVE DEPENDENT SLIDING MODES

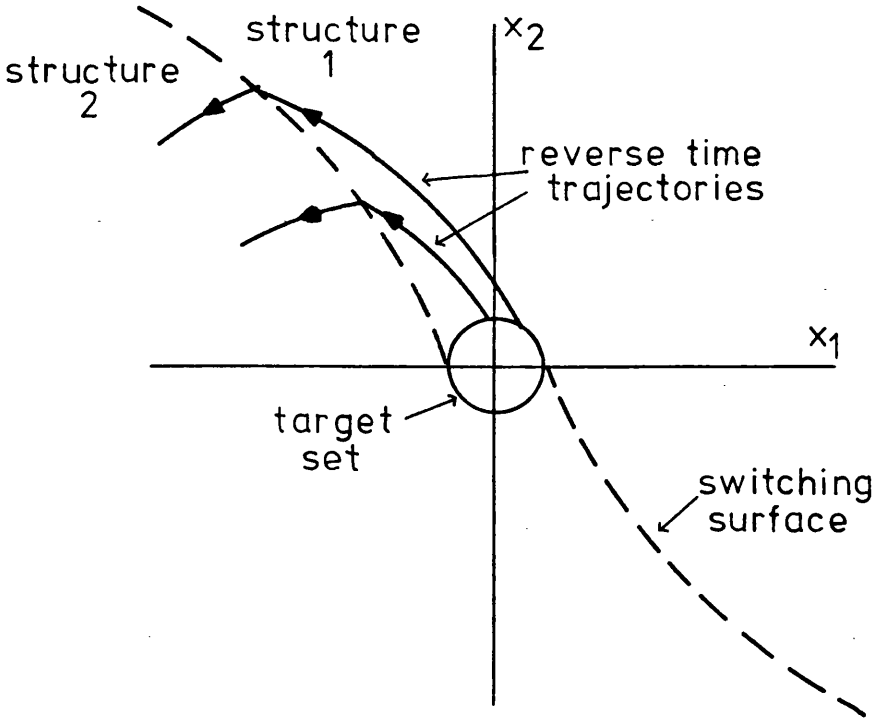

FIG. 5.1 POINT BY POINT GENERATION OF THE OPTIMAL SWITCHING SURFACE

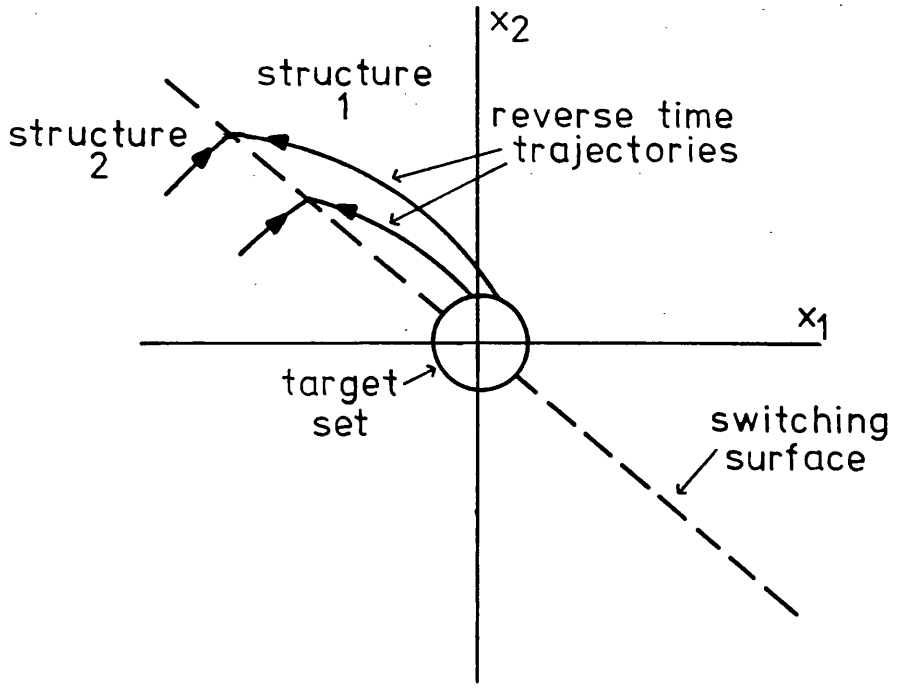

FIG. 5.2 CASE WHERE THE SWITCHING SURFACE IS SINGULAR

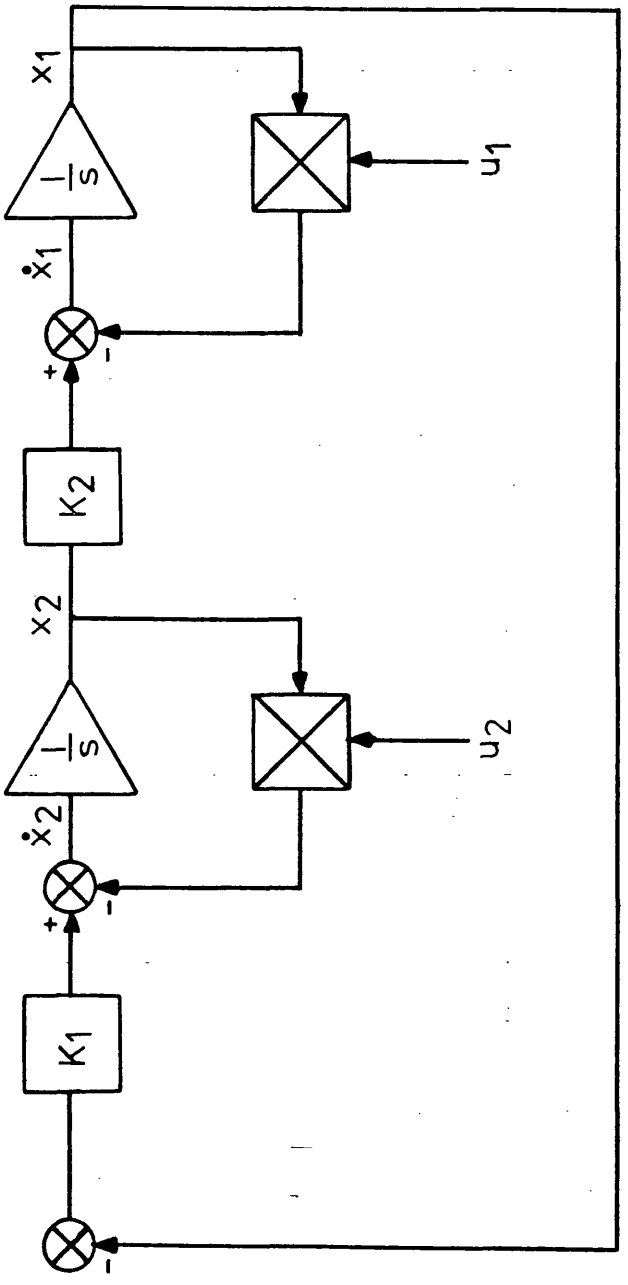

FIG. 6.1 SYSTEM FOR TIME-OPTIMAL VARIABLE STRUCTURE CONTROL

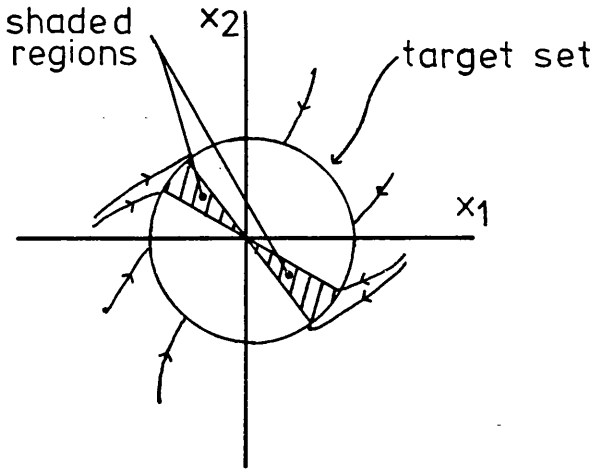

FIG. 6.2 OPTIMAL TRAJECTORIES AVOIDING SHADED REGIONS

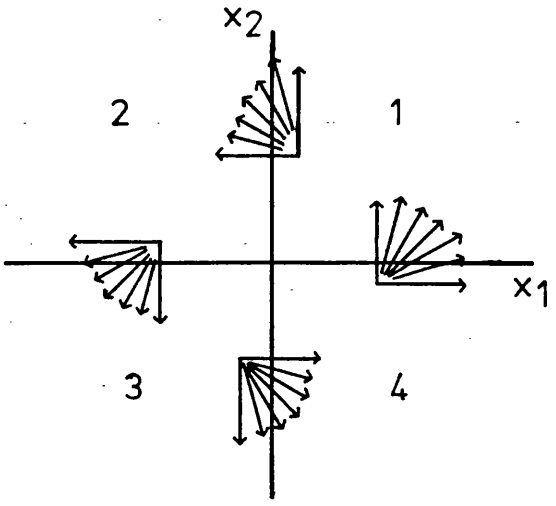

FIG. 6.3 PERMITTED CONFIGURATIONS OF AXIS CROSSING

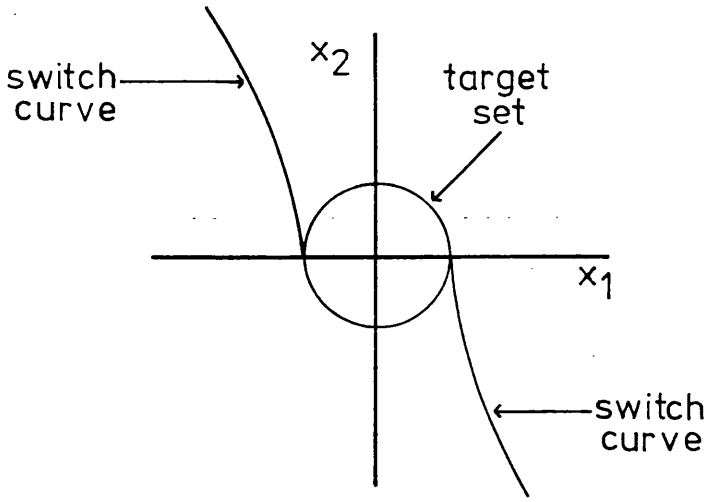

FIG. 6.4 INITIAL POSITION OF THE SWITCH CURVE WHEN u_2 IS THE CONTROL

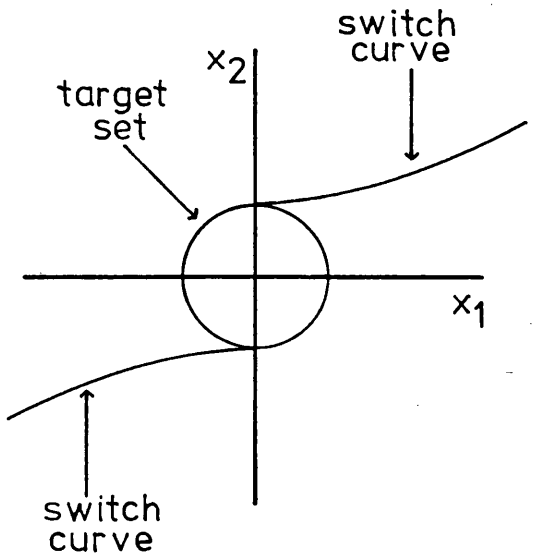

FIG. 6.5 INITIAL POSITION OF THE SWITCH CURVE WHEN u_1 IS THE CONTROL

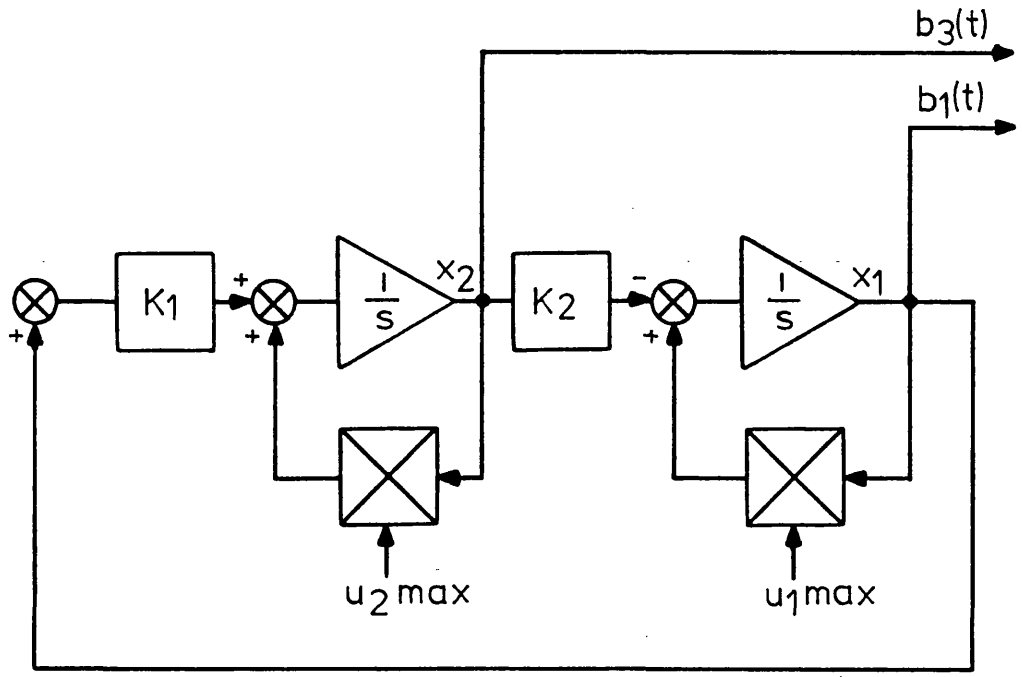

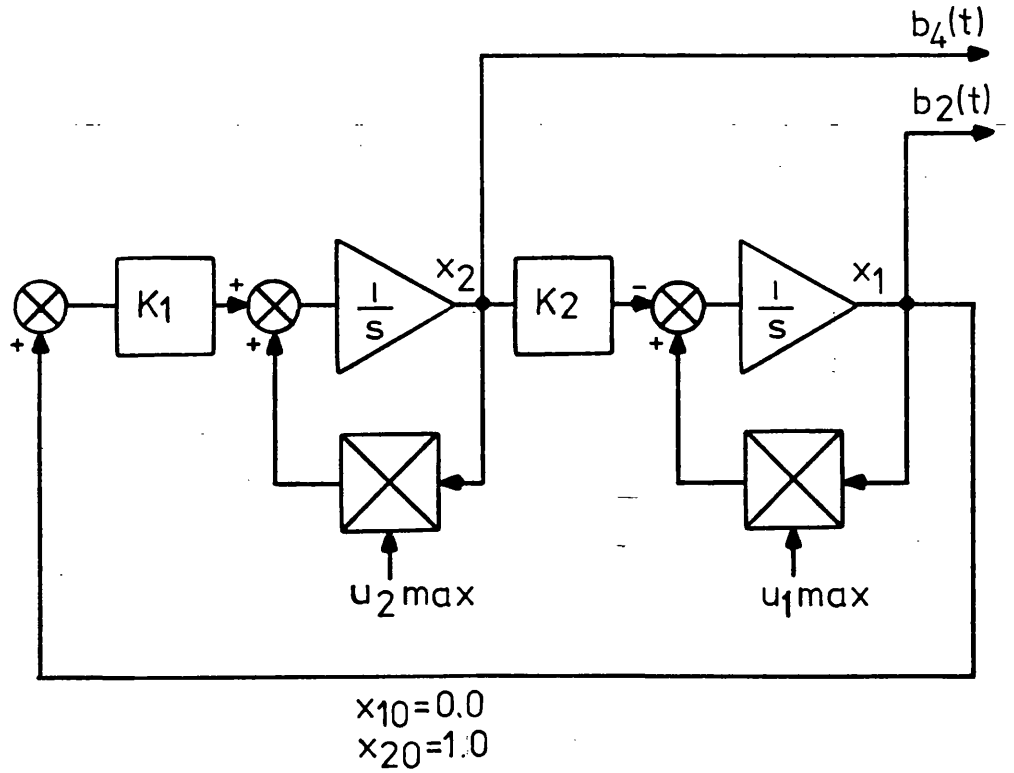

FIG. 6.6 ARRANGEMENT FOR THE GENERATION OF THE STATE TRANSITION MATRIX

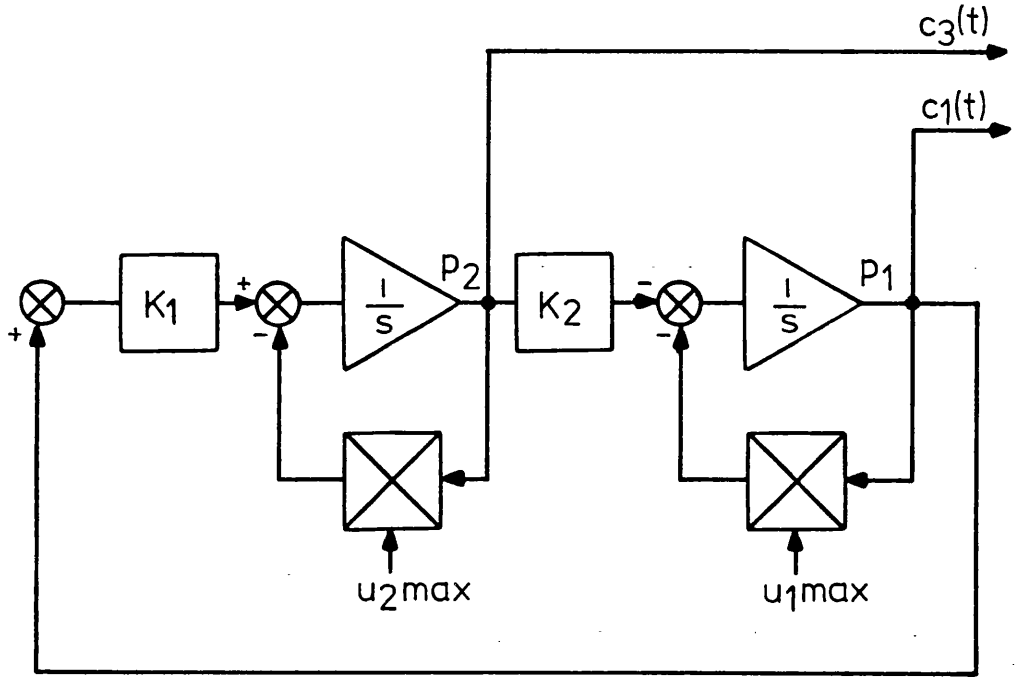

$P_{10}=1.0$
$P_{20}=0.0$

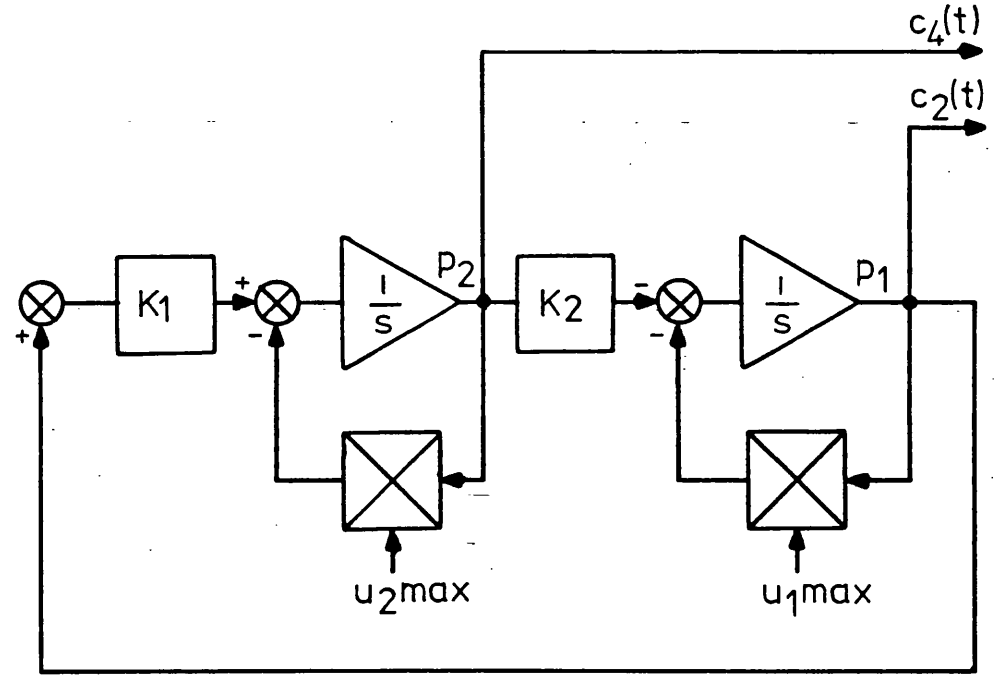

$P_{10}=0.0$
$P_{20}=1.0$

FIG. 6.7 ARRANGEMENT FOR THE GENERATION OF THE COSTATE TRANSITION MATRIX

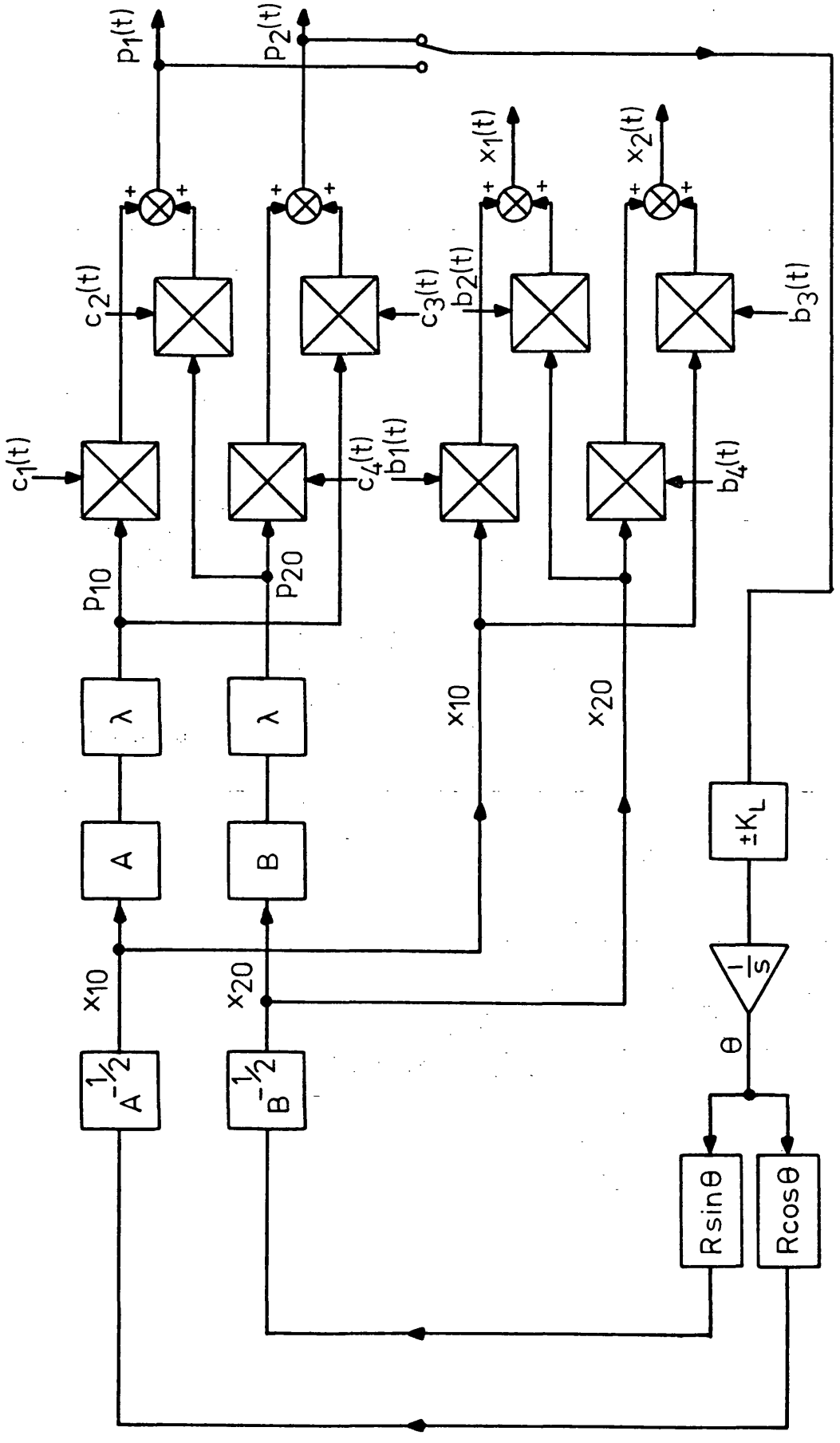

FIG. 6.8 ARRANGEMENT FOR THE DIRECT GENERATION OF TIME-OPTIMAL SWITCH CURVES

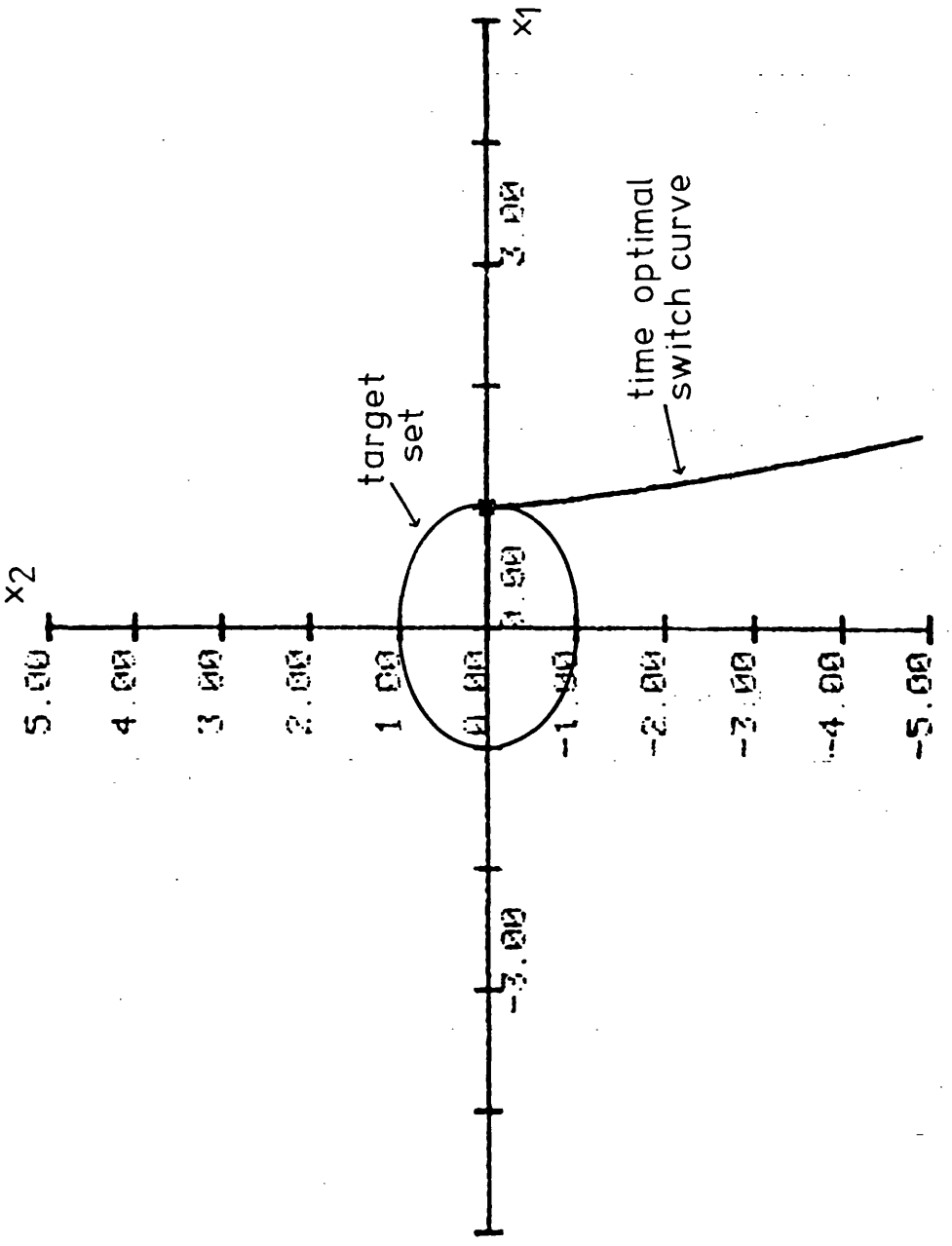

FIG. 6.9 INITIAL PORTION OF THE SWITCH CURVE FOR EXAMPLE 1

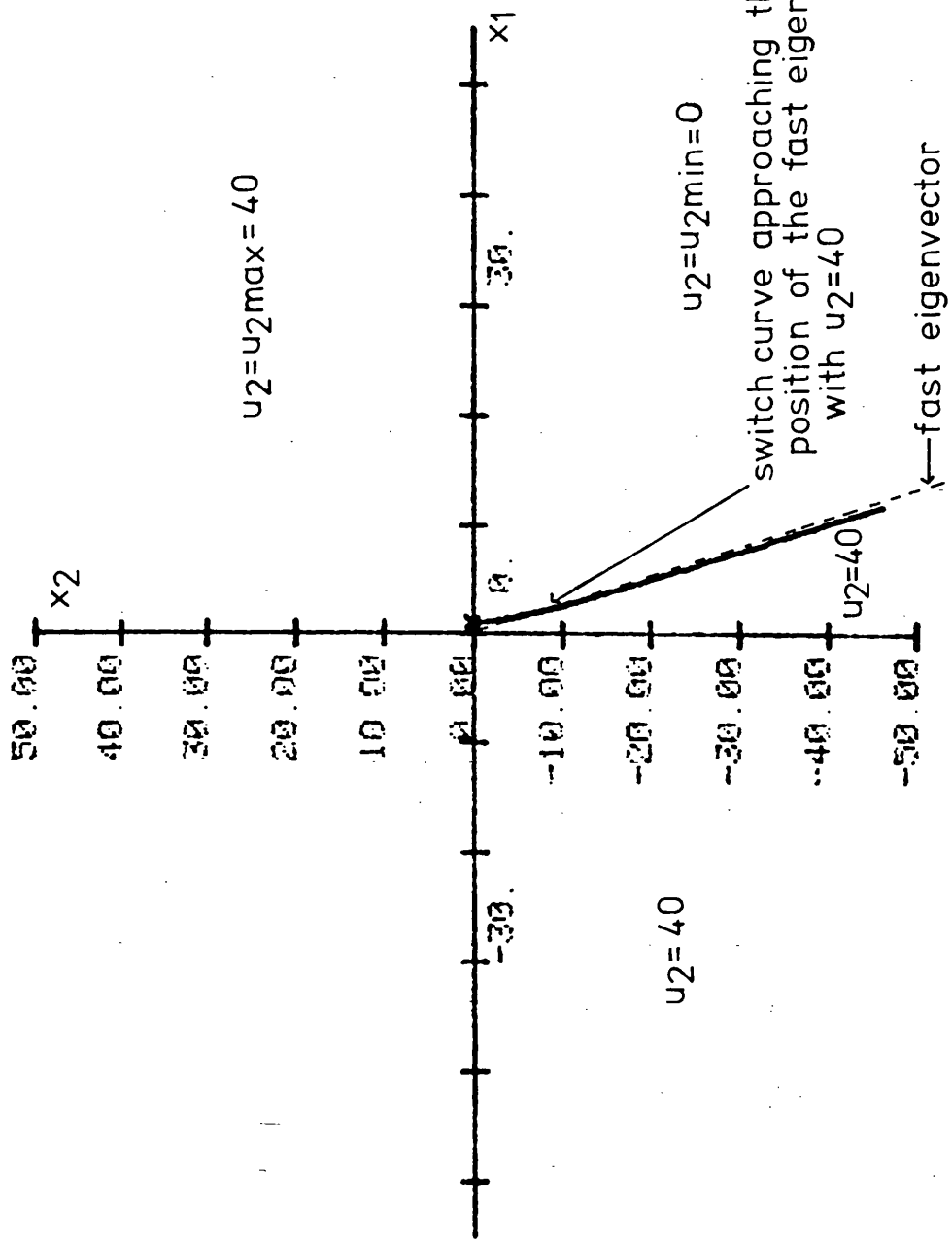

FIG. 6.10 SWITCH CURVE FOR EXAMPLE 1 AS STATE SPACE IS EXTENDED

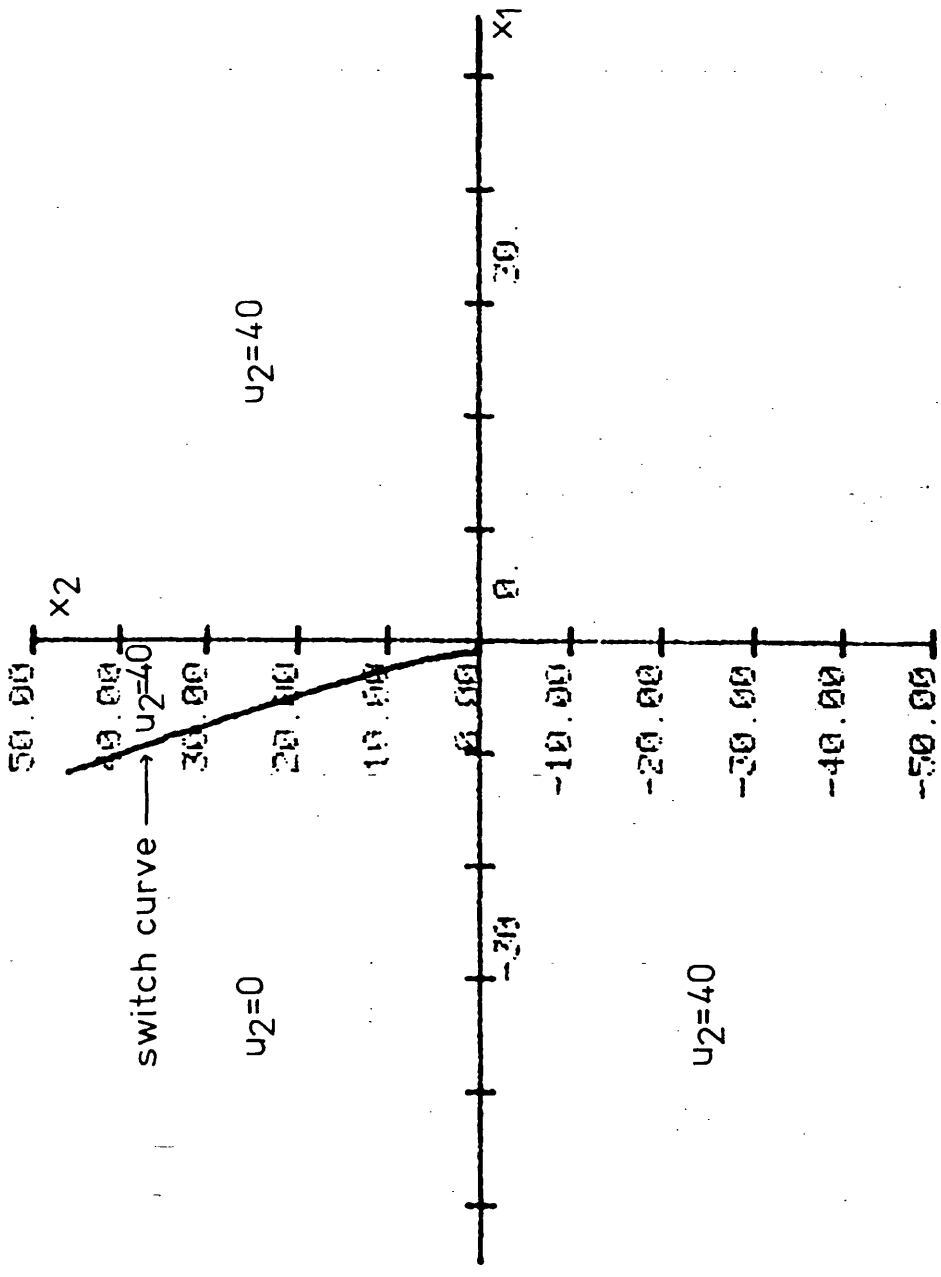

FIG. 6.11 2nd QUADRANT PORTION OF THE SWITCH CURVE FOR EXAMPLE 1

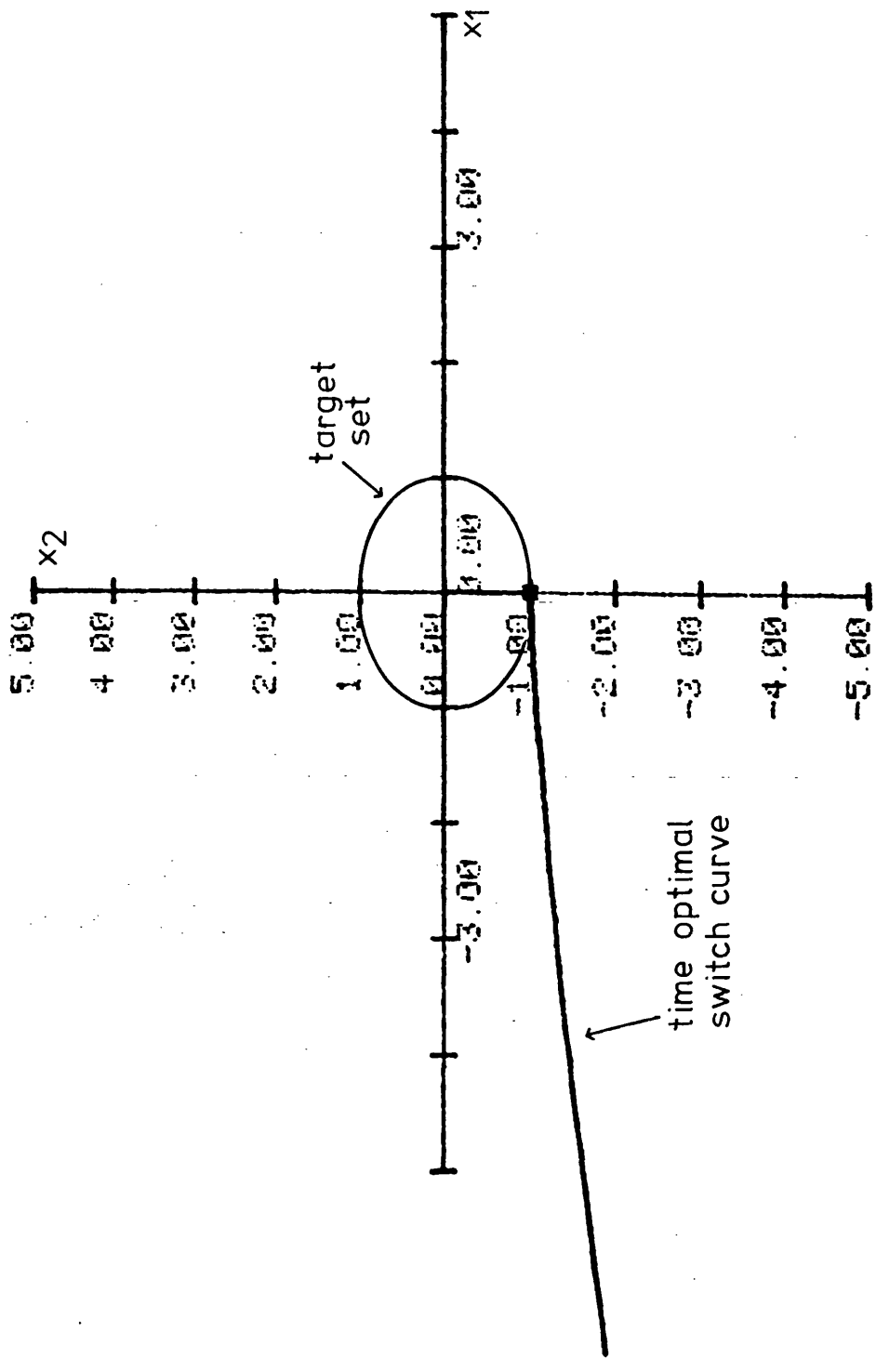

FIG. 6.12 INITIAL PORTION OF THE SWITCH CURVE FOR EXAMPLE 2

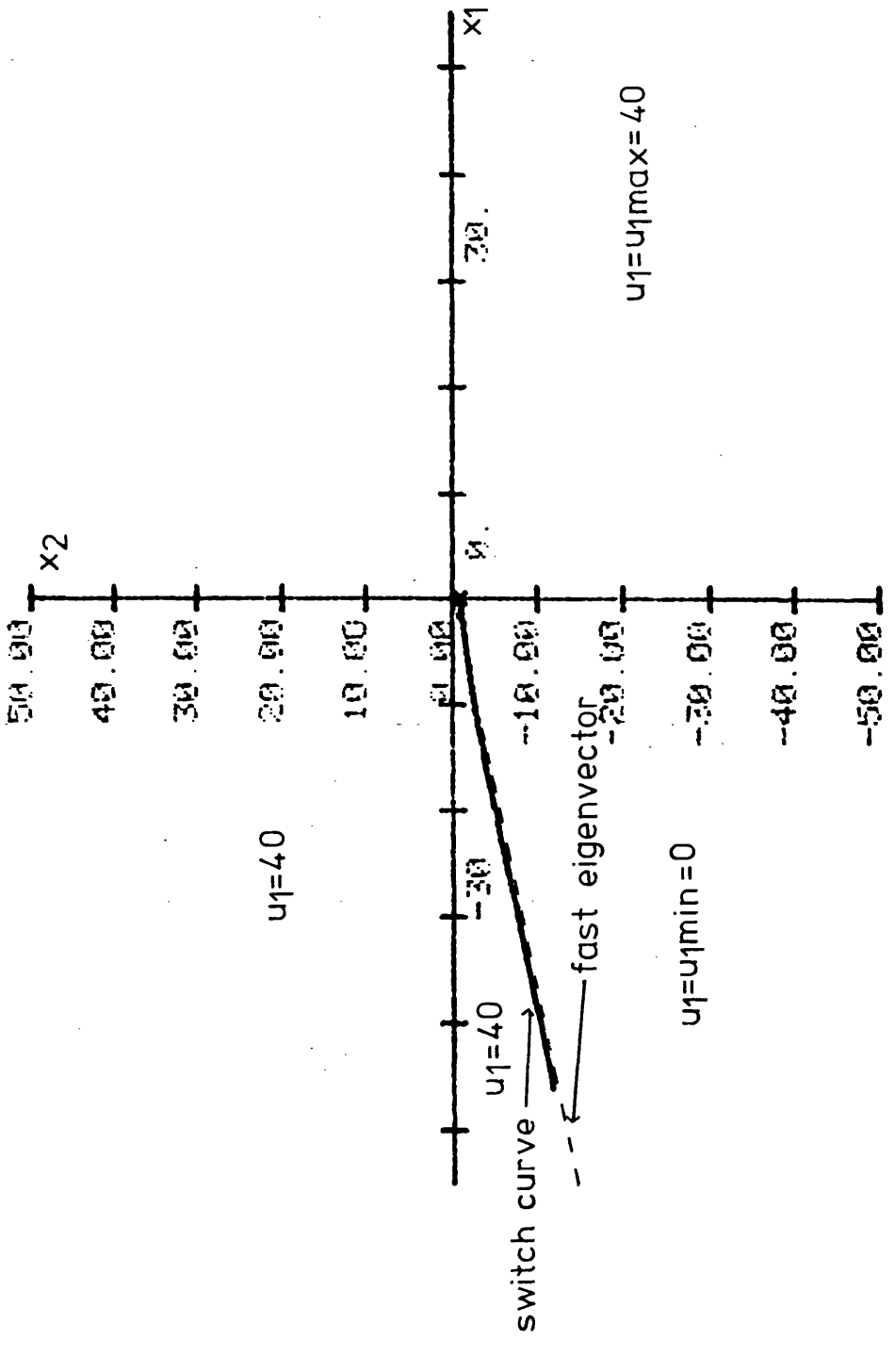

FIG. 6.13 SWITCH CURVE FOR EXAMPLE 2 AS STATE SPACE IS EXTENDED

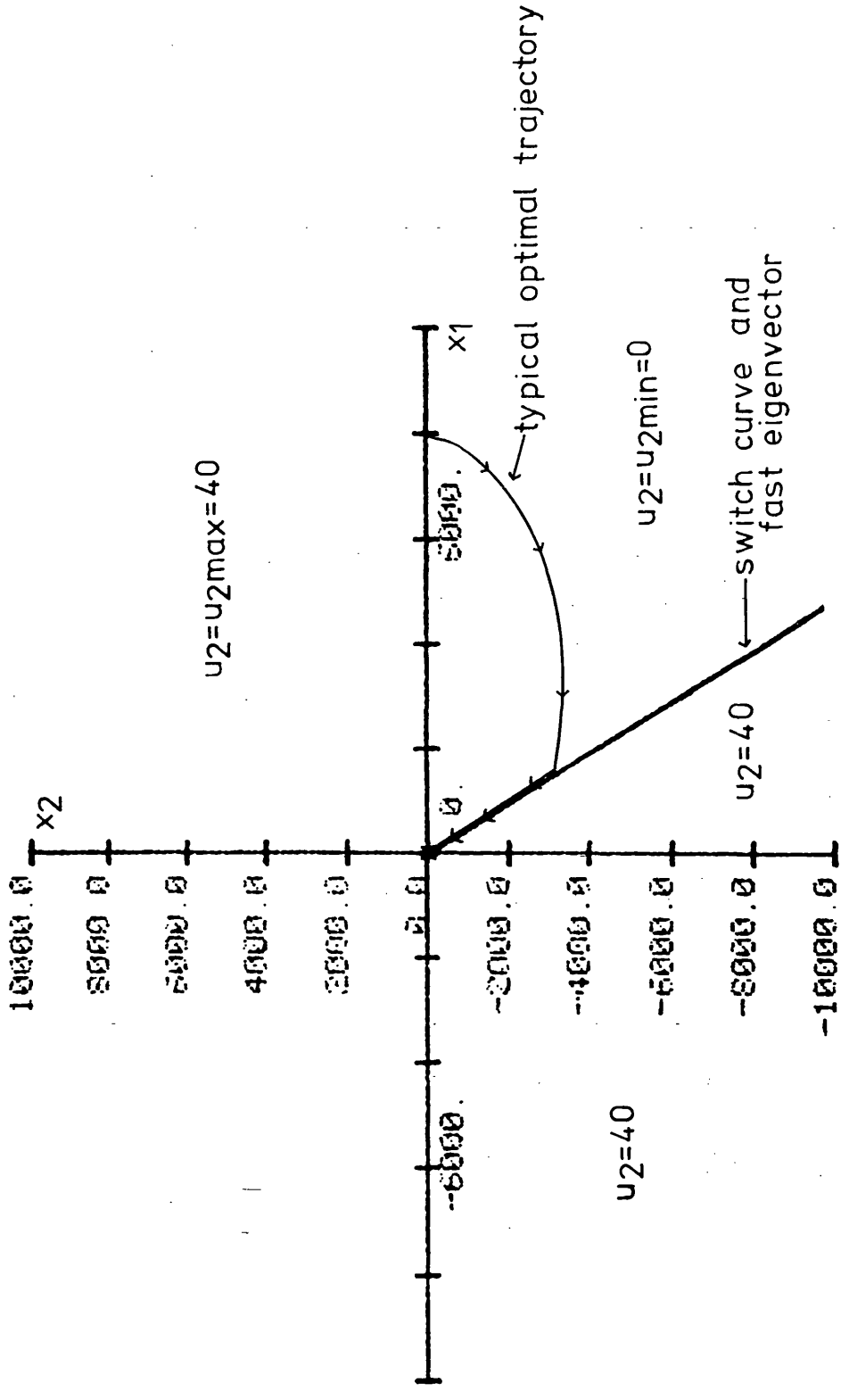

FIG. 6.14 SWITCH CURVE FOR EXAMPLE 3

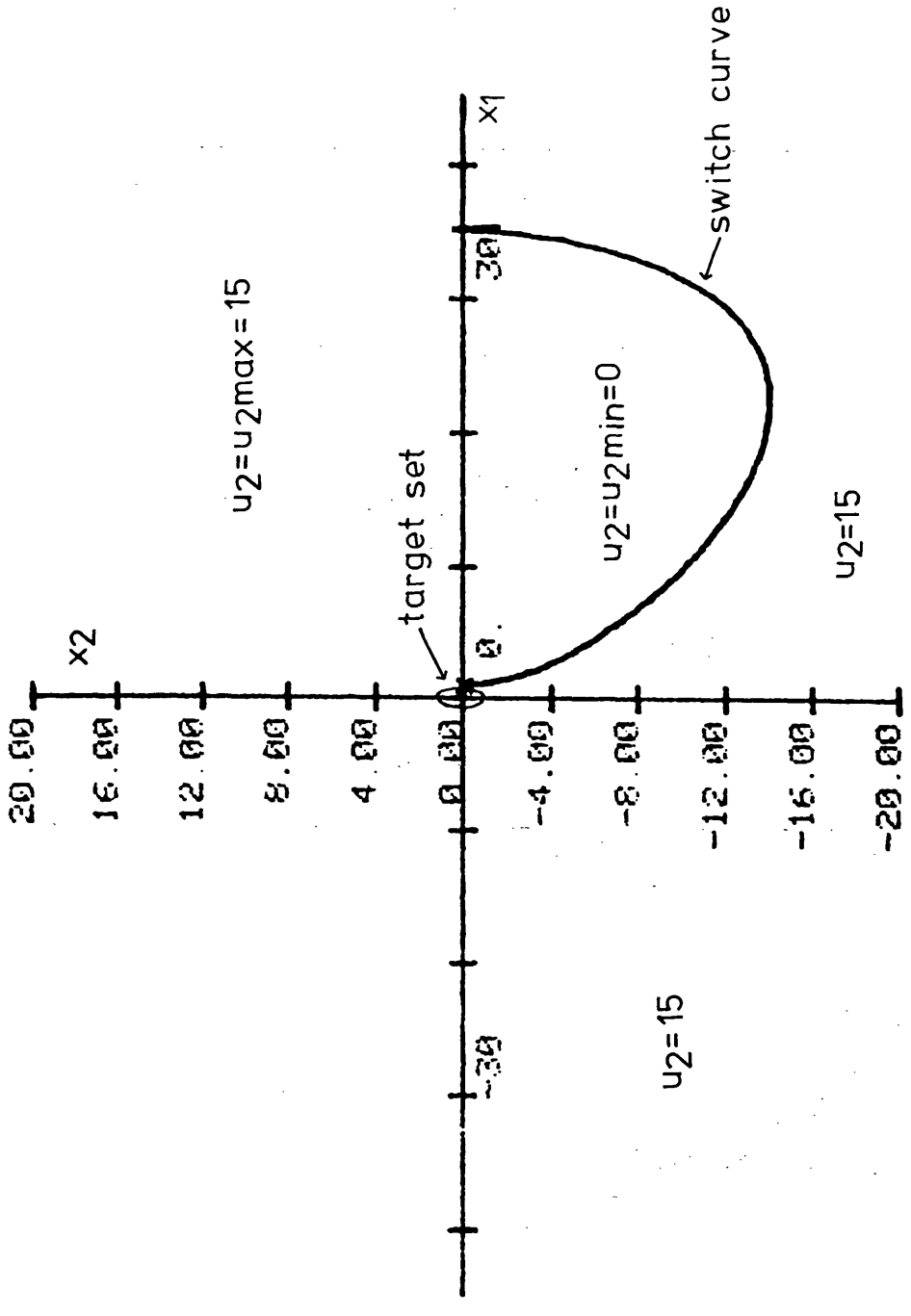

FIG. 6.15 LIMITED PORTION OF SWITCH CURVE OBTAINABLE FOR EXAMPLE 4

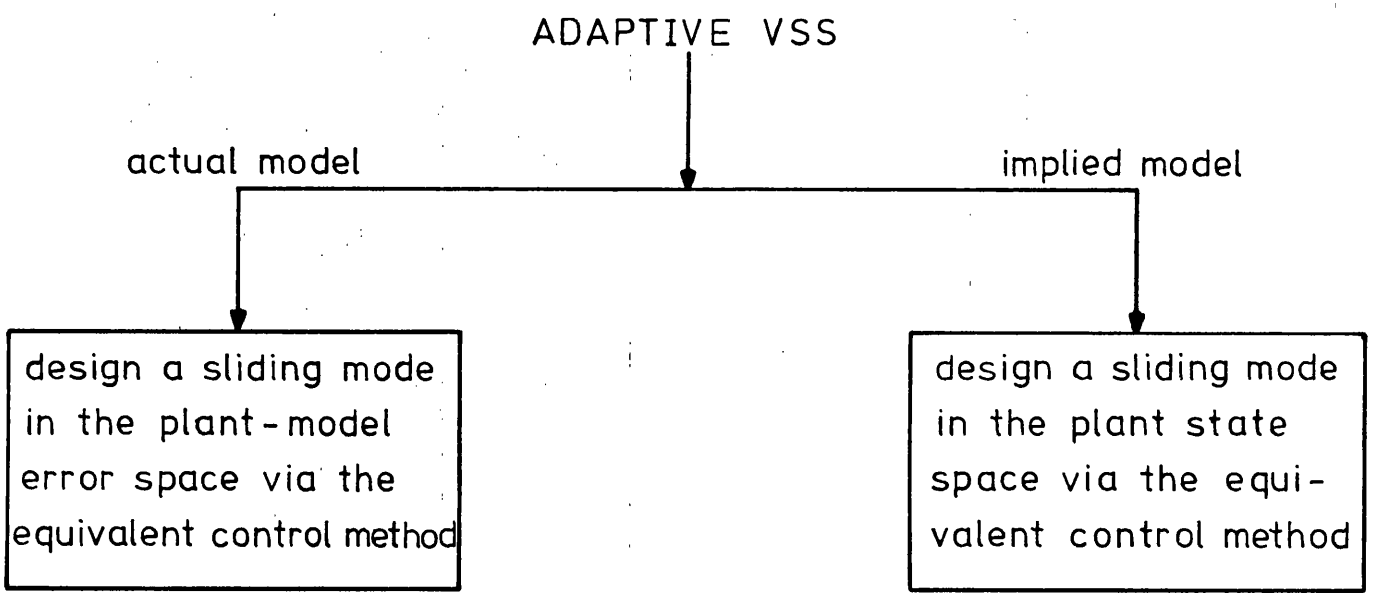

FIG. 8.1 GENERAL DESIGN OF ADAPTIVE VSS

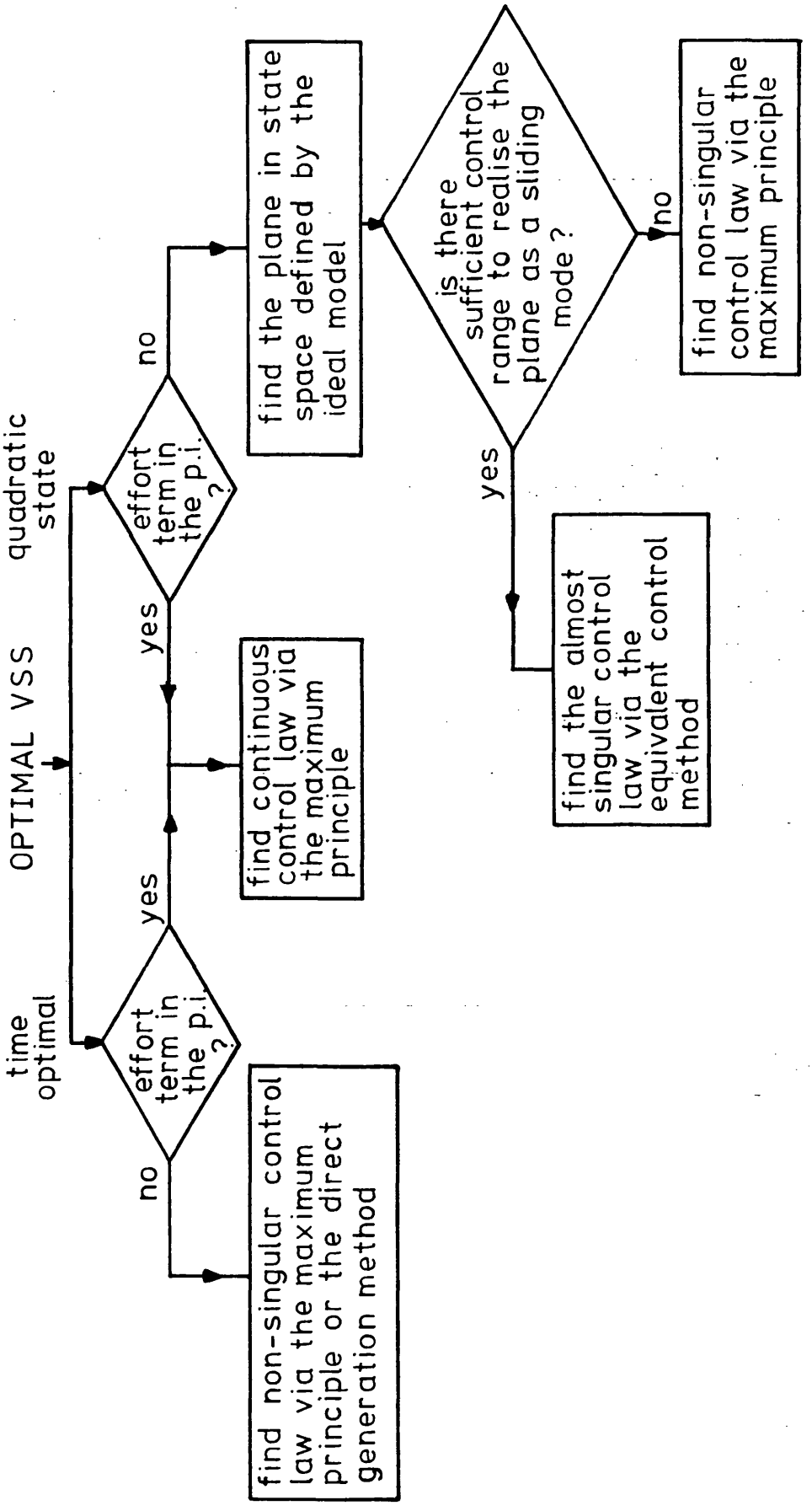

FIG. 8.2 GENERAL DESIGN OF OPTIMAL V S S

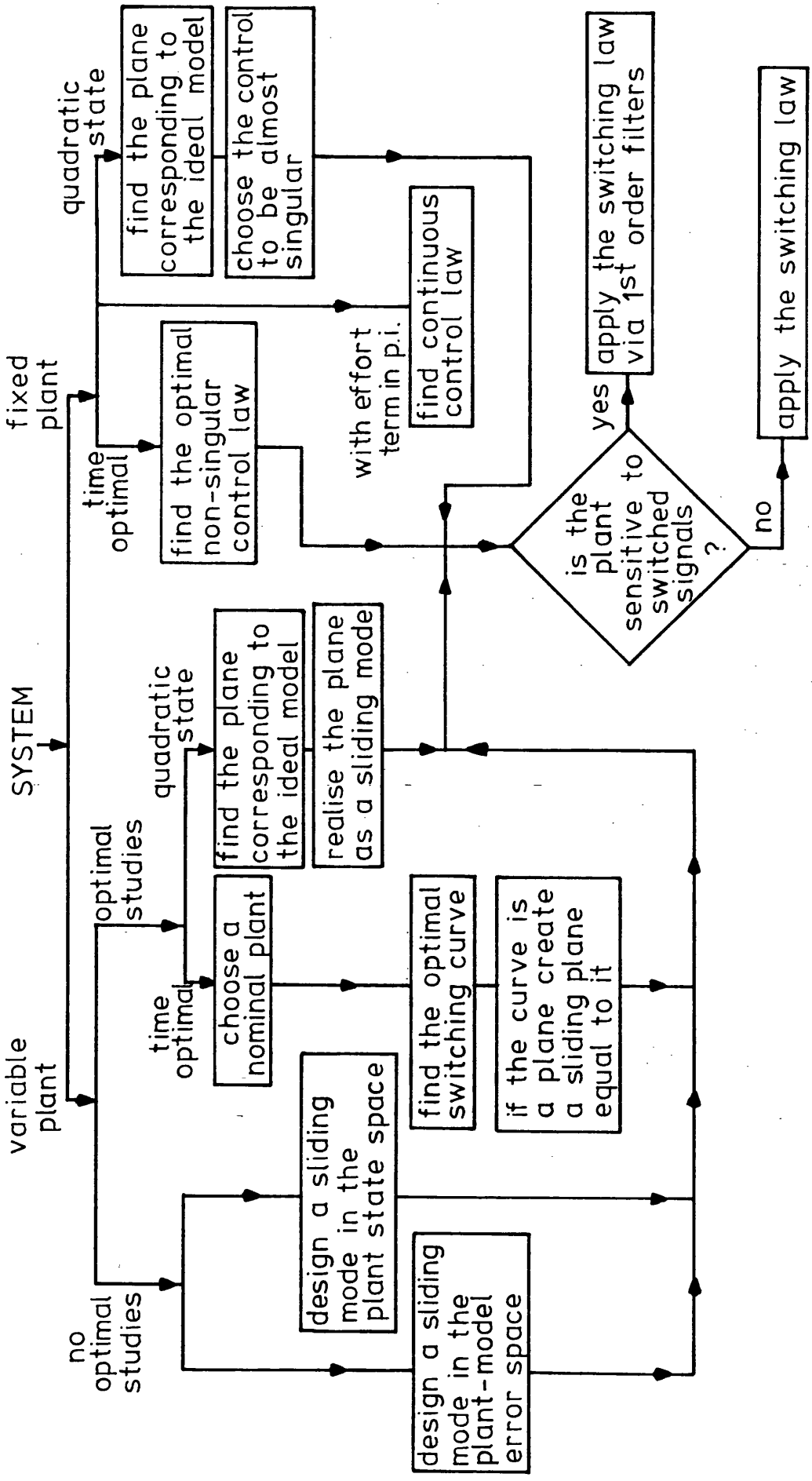

FIG. 8.3 GENERAL GUIDE TO THE DESIGN OF OPTIMAL / ADAPTIVE VSS

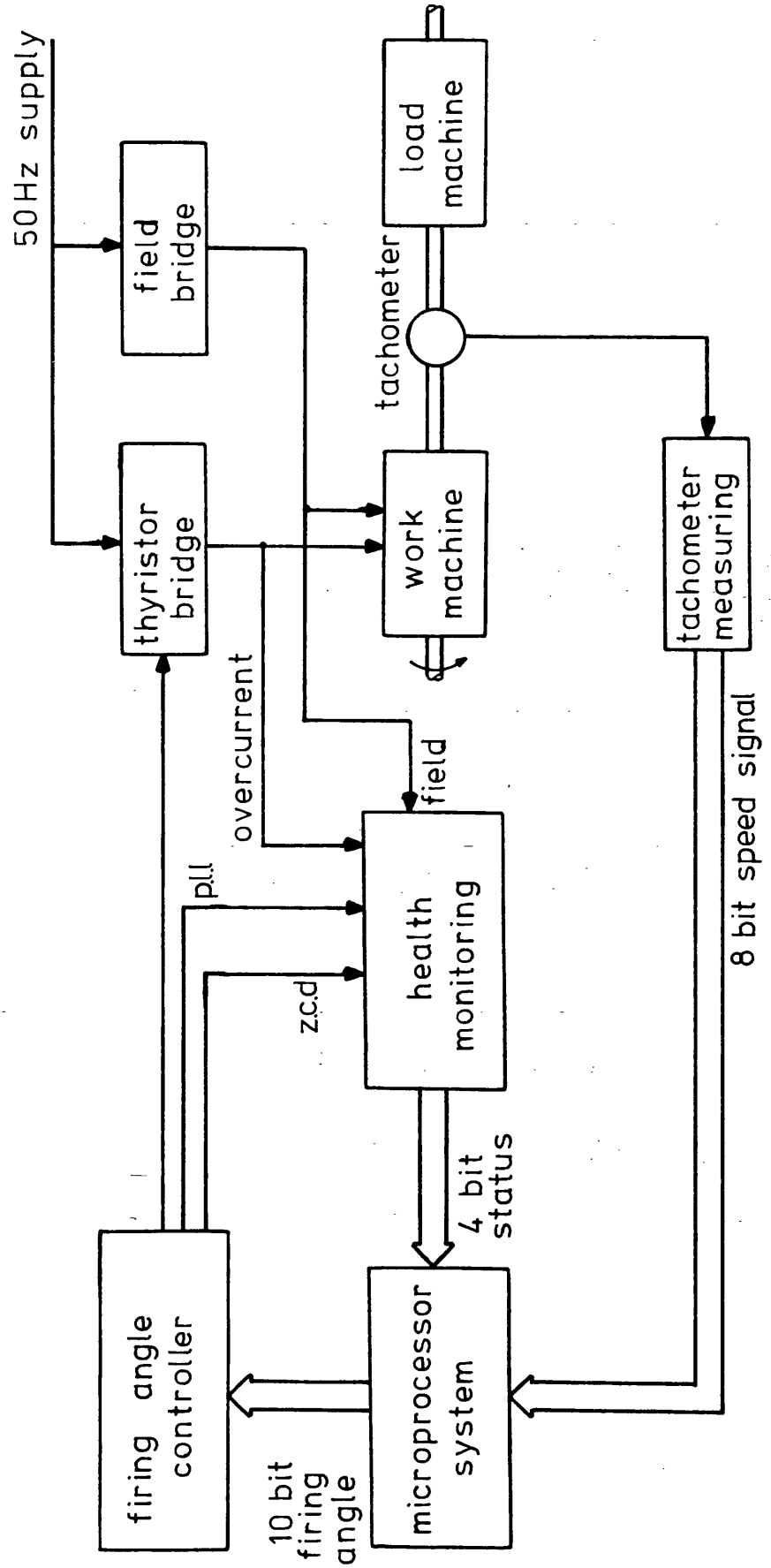

FIG. 10.1 BLOCK DIAGRAM OF THE COMPLETE SYSTEM

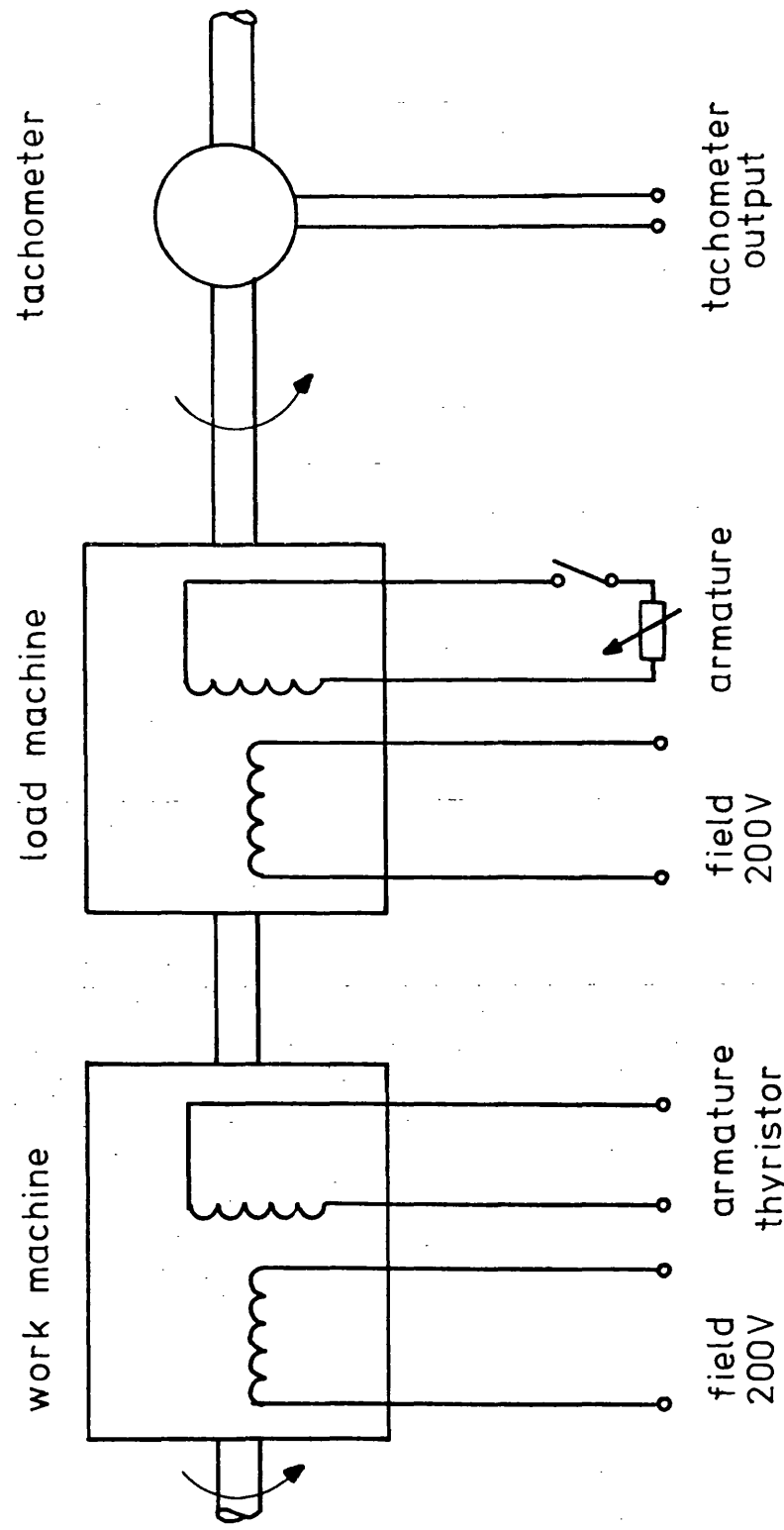

FIG. 10.2 BLOCK DIAGRAM OF THE MACHINE SET

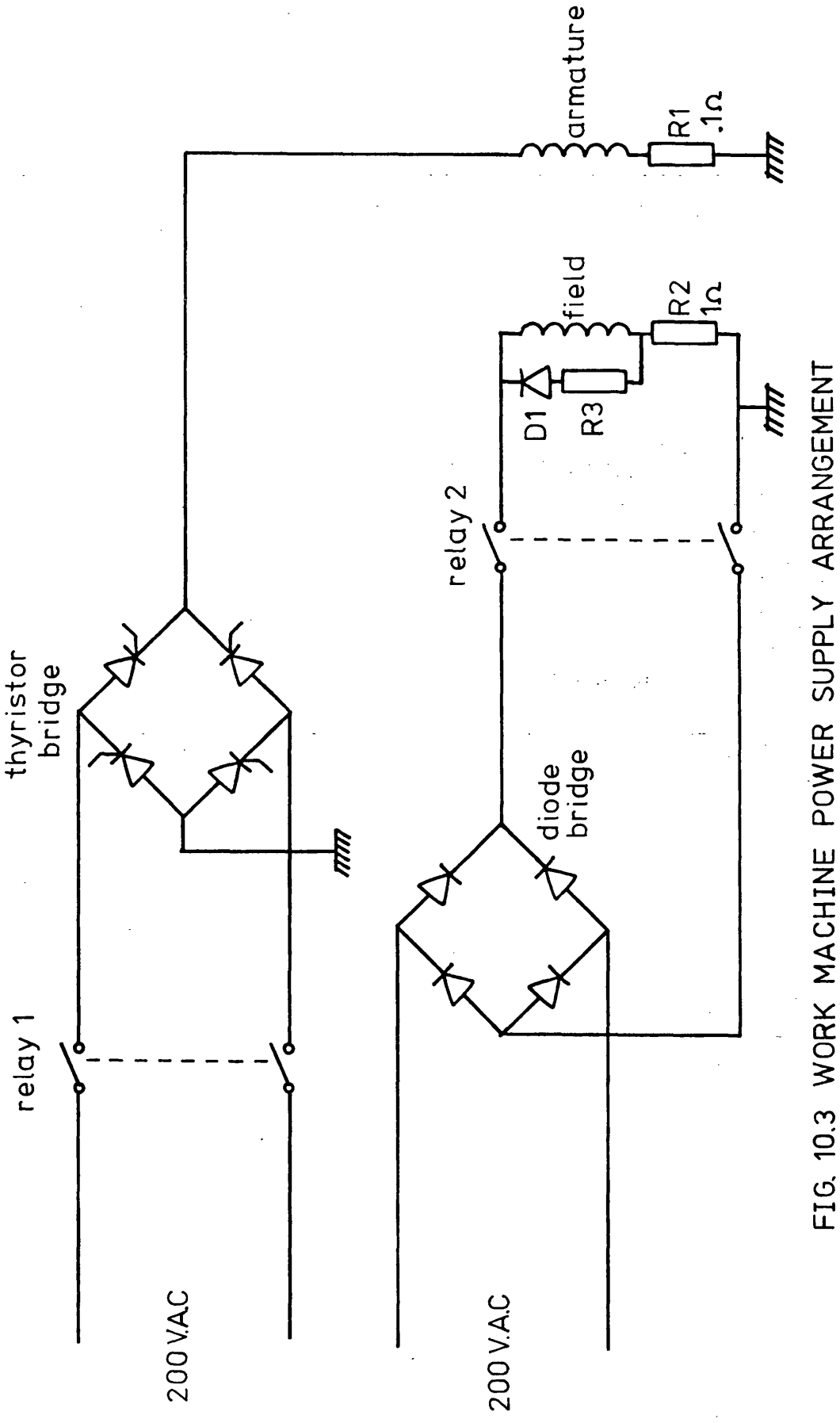

FIG. 10.3 WORK MACHINE POWER SUPPLY ARRANGEMENT

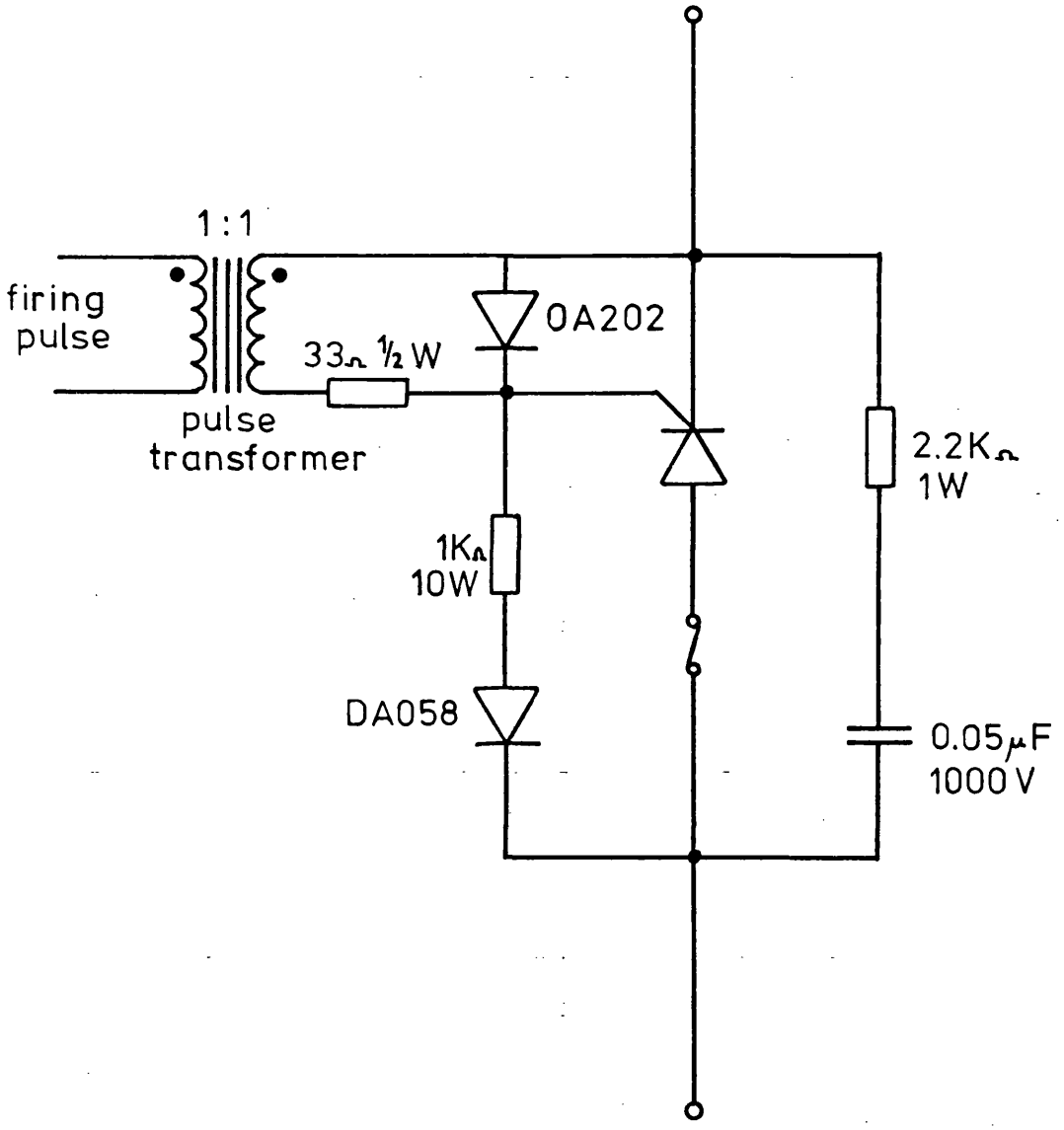

FIG. 10.4 THYRISTOR WITH ASSOCIATED PROTECTION CIRCUIT

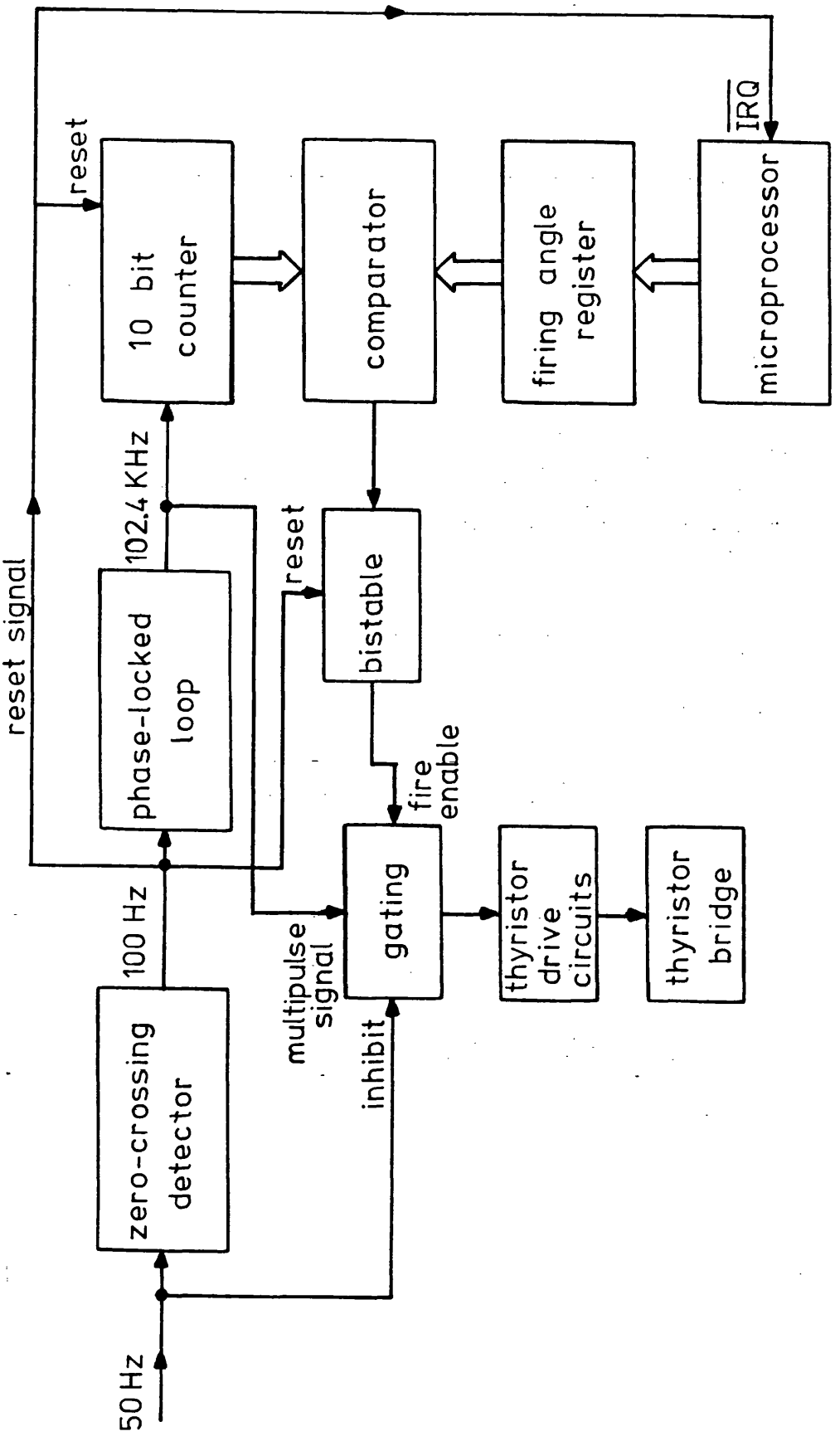

FIG. 10.5 THE THYRISTOR FIRING ANGLE CONTROLLER

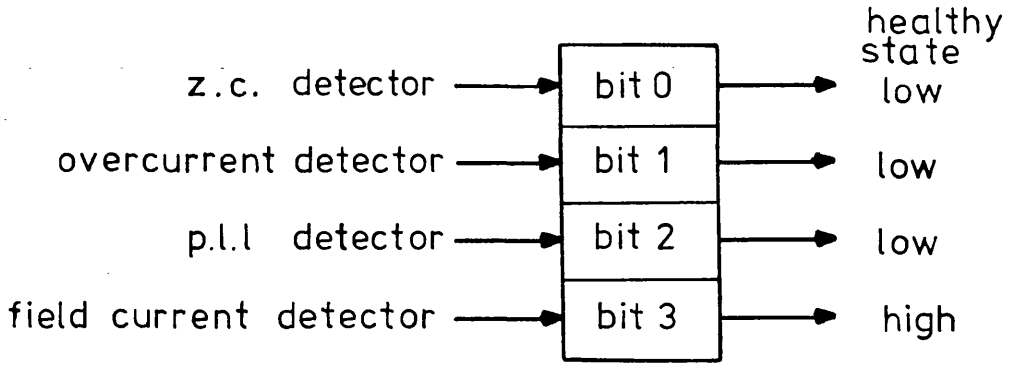

FIG. 10.6 THE STATUS REGISTER

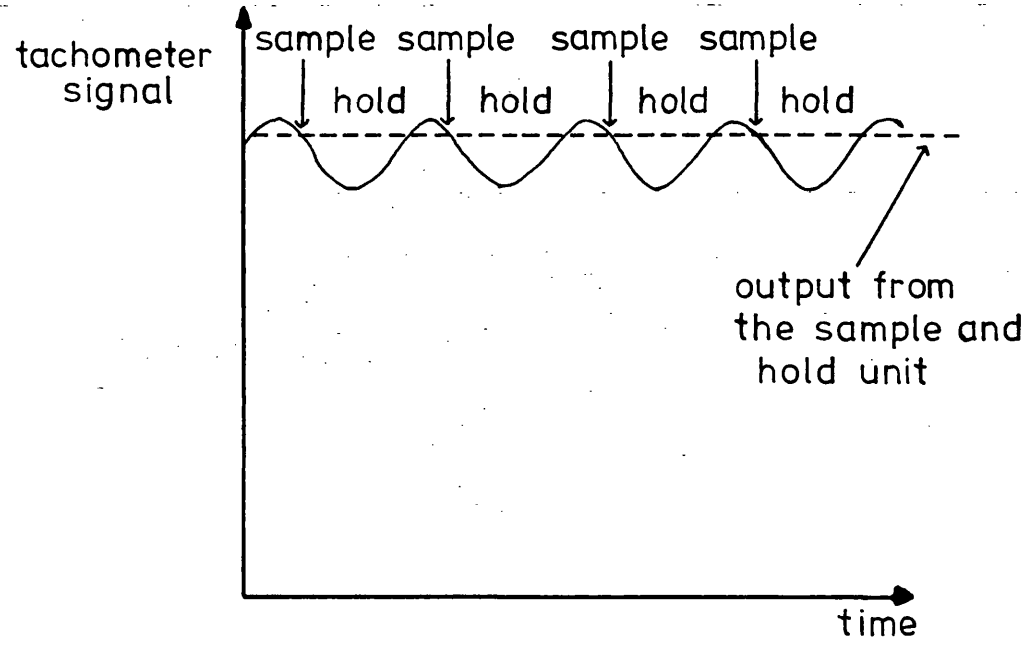

FIG. 10.7 REMOVAL OF TACHOMETER RIPPLE

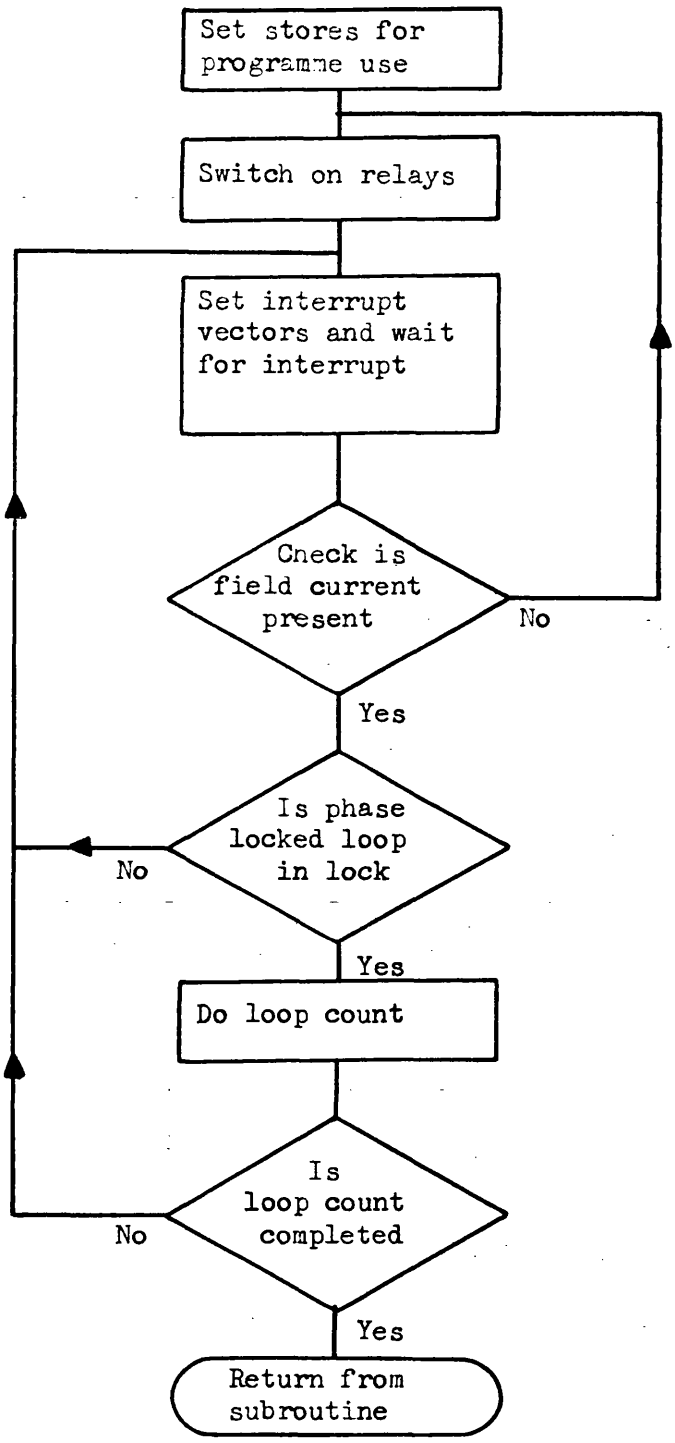

FIG. 10.8 START UP SUBROUTINE FLOW CHART

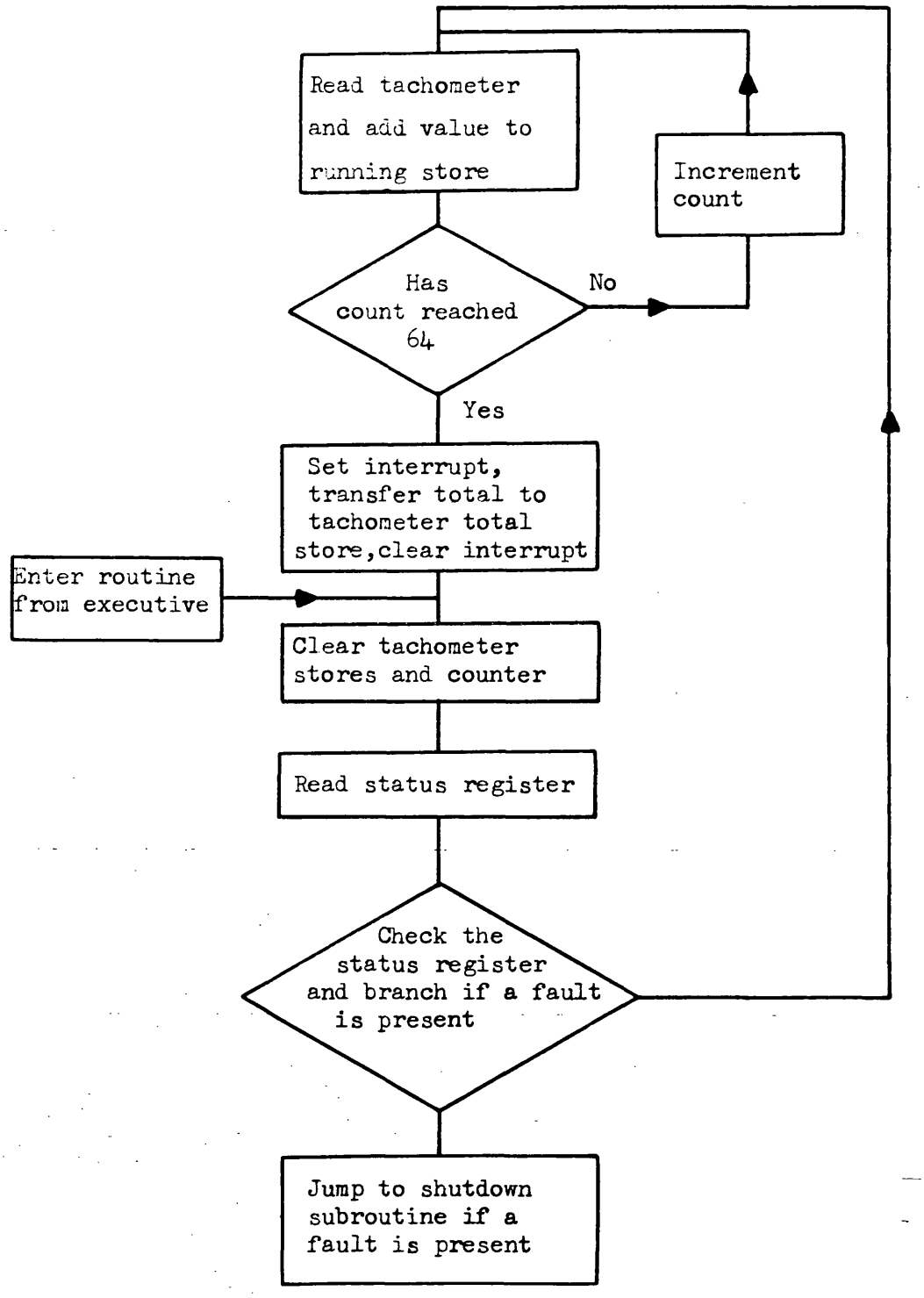

FIG. 10.9 TACHOMETER READ SUBROUTINE FLOW CHART

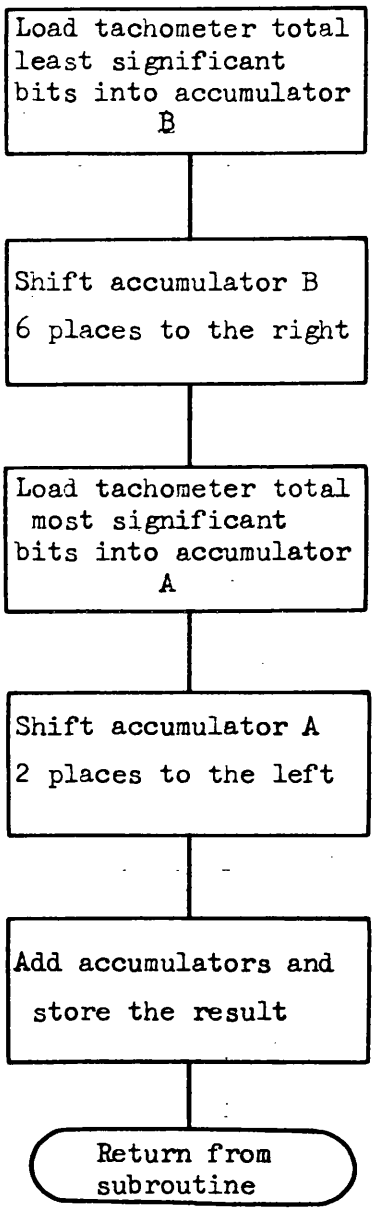

FIG. 10.10 TACHOMETER AVERAGE SUBROUTINE FLOW CHART

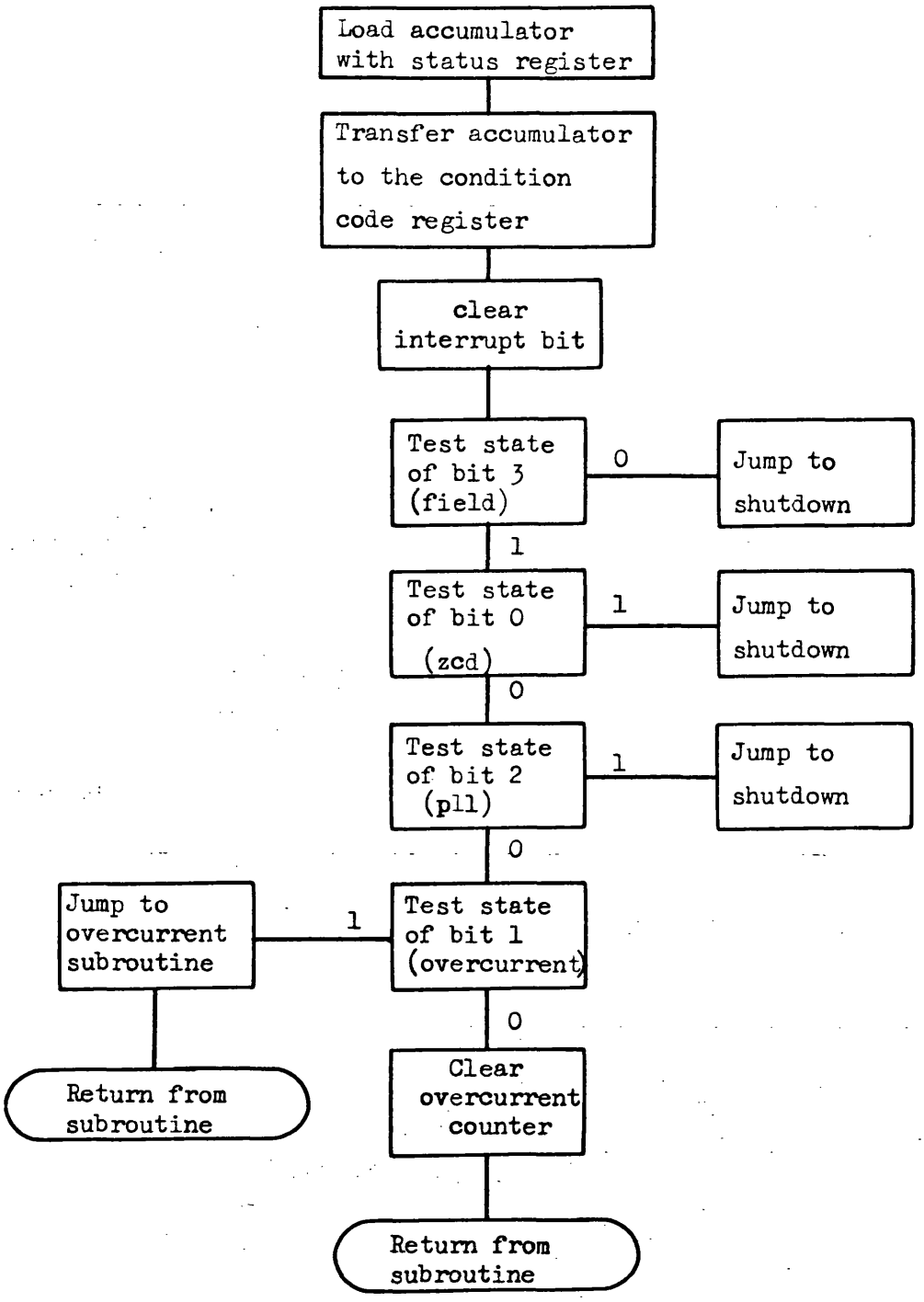

FIG. 10.11 STATUS REGISTER SUBROUTINE FLOW CHART

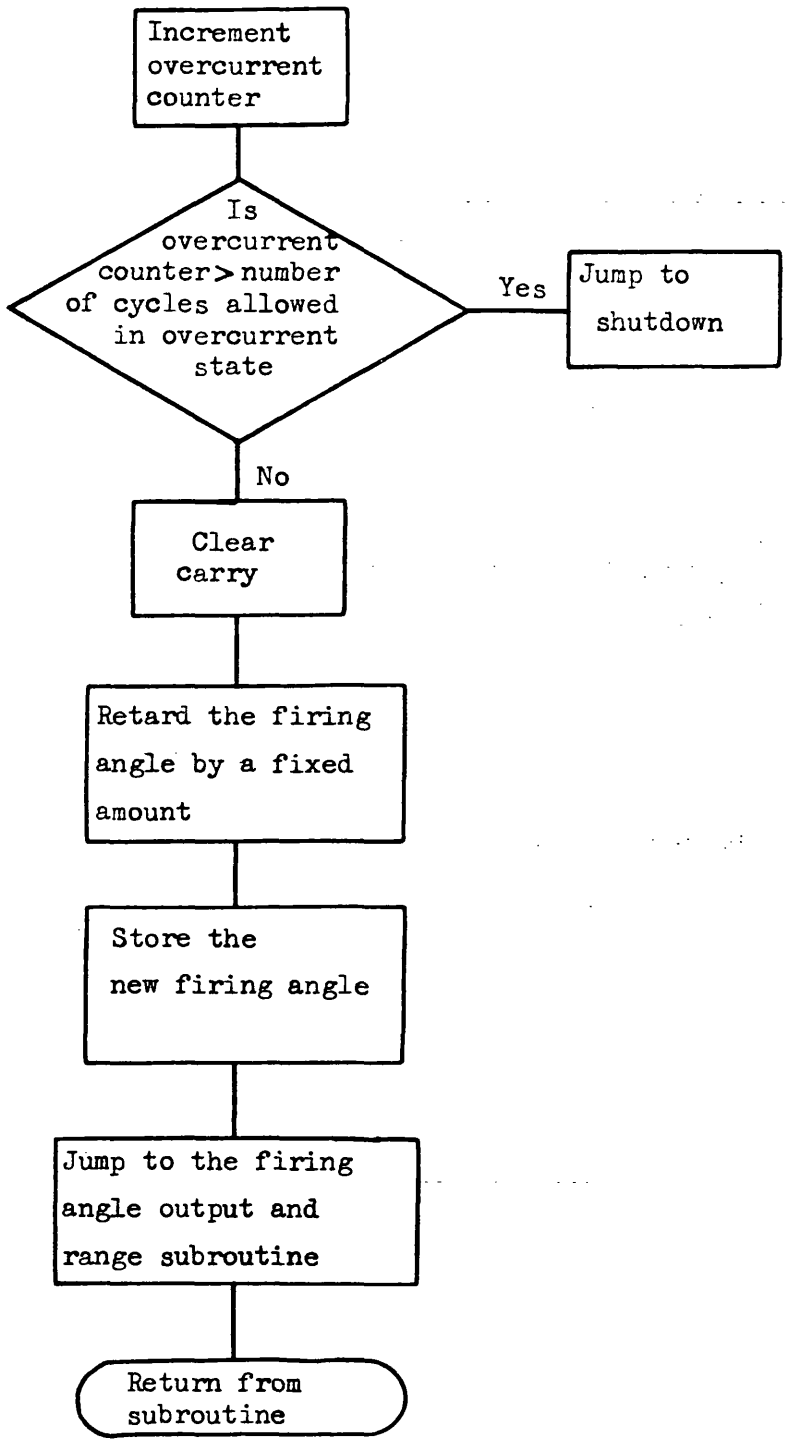

FIG. 10.12 OVERCURRENT SUBROUTINE FLOW CHART

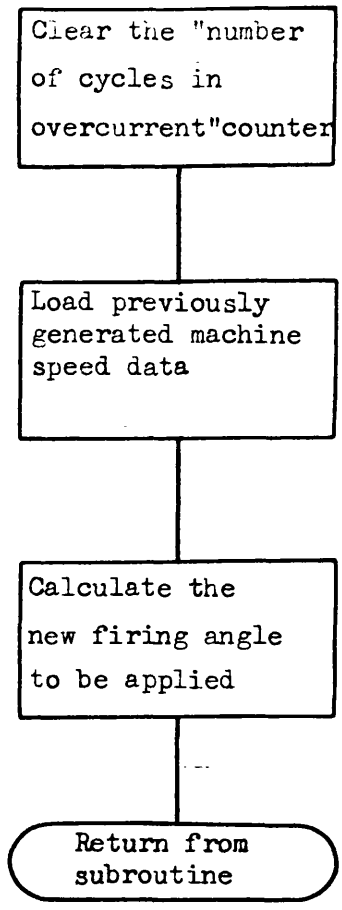

FIG. 10.13 GENERAL FORM OF THE CONTROL SUBROUTINE FLOW CHART

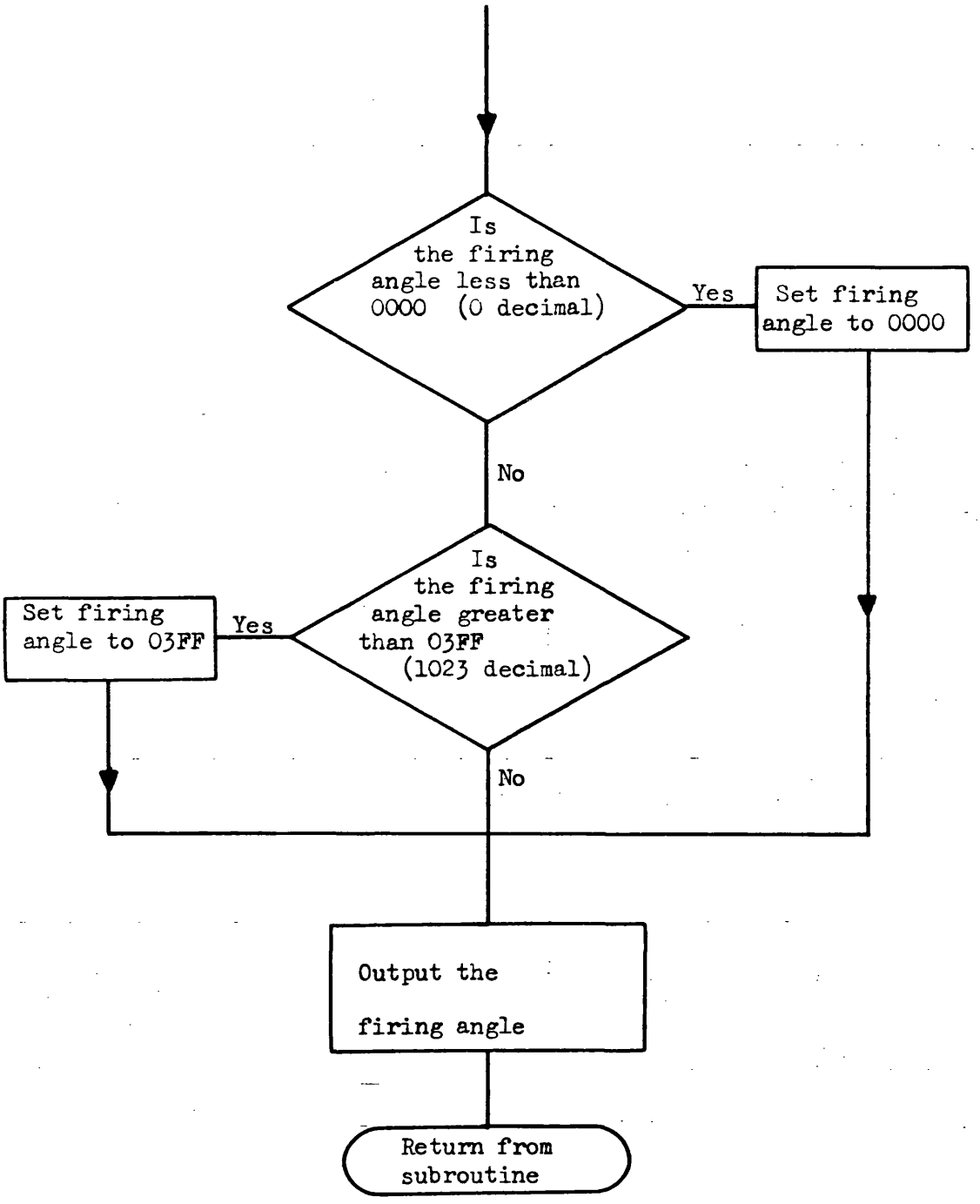

FIG. 10.14 FIRING ANGLE OUTPUT AND RANGE CHECK SUBROUTINE FLOW CHART

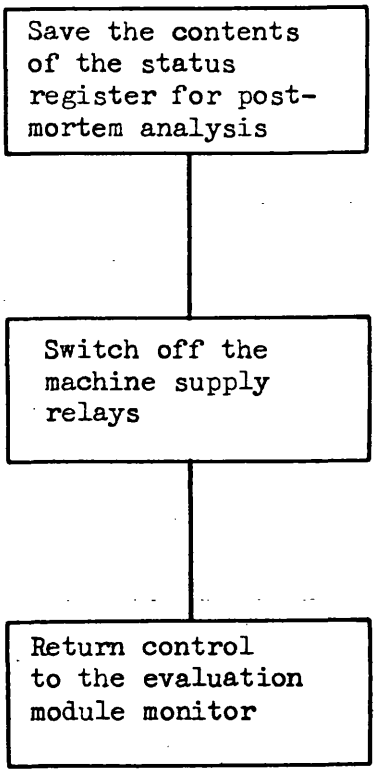

FIG. 10.15 SHUTDOWN SUBROUTINE FLOW CHART

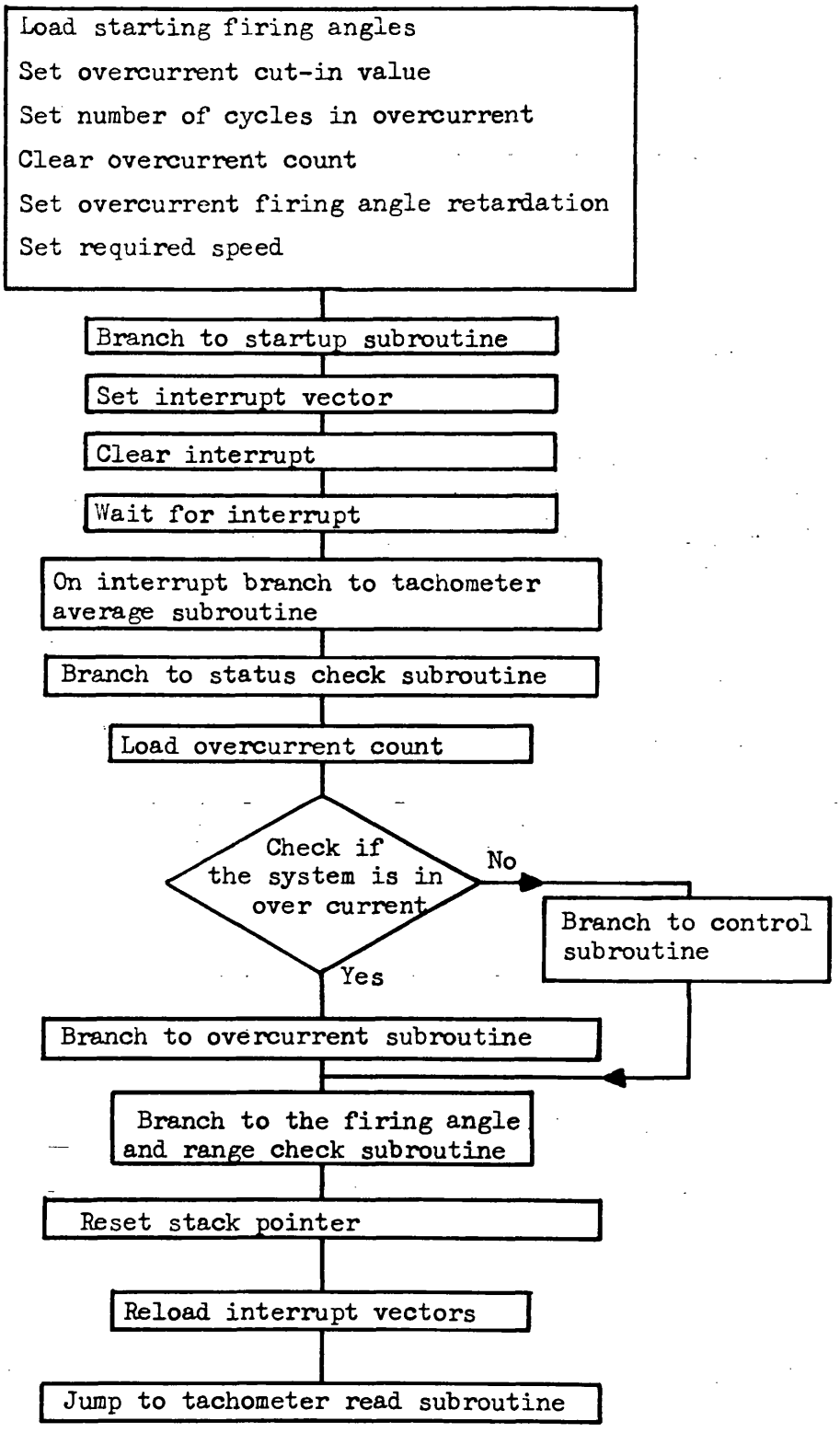

FIG. 10.16 EXECUTIVE PROGRAMME FLOW CHART

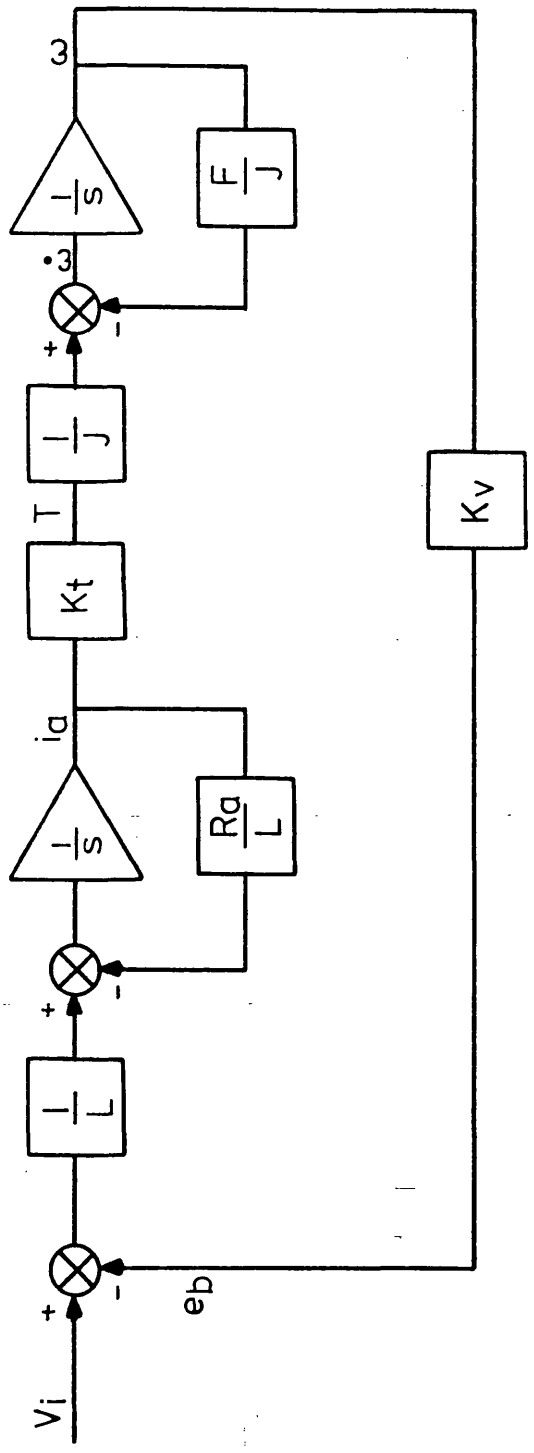

FIG. 11.1 SYSTEM REPRESENTATION OF AN ARMATURE CONTROLLED D.C. MACHINE

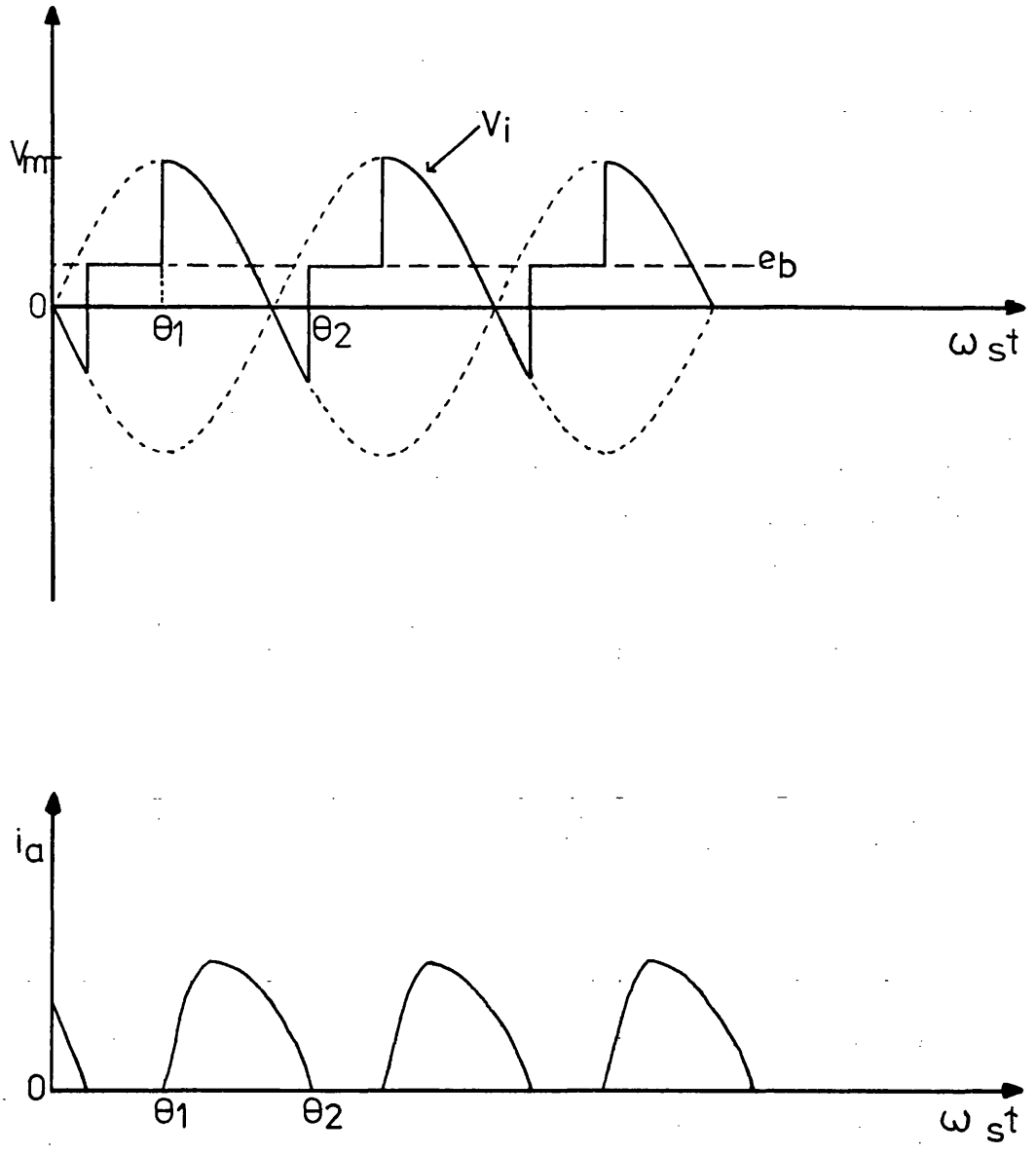

FIG. 11.2 TYPICAL ARMATURE VOLTAGE AND CURRENT WAVEFORMS

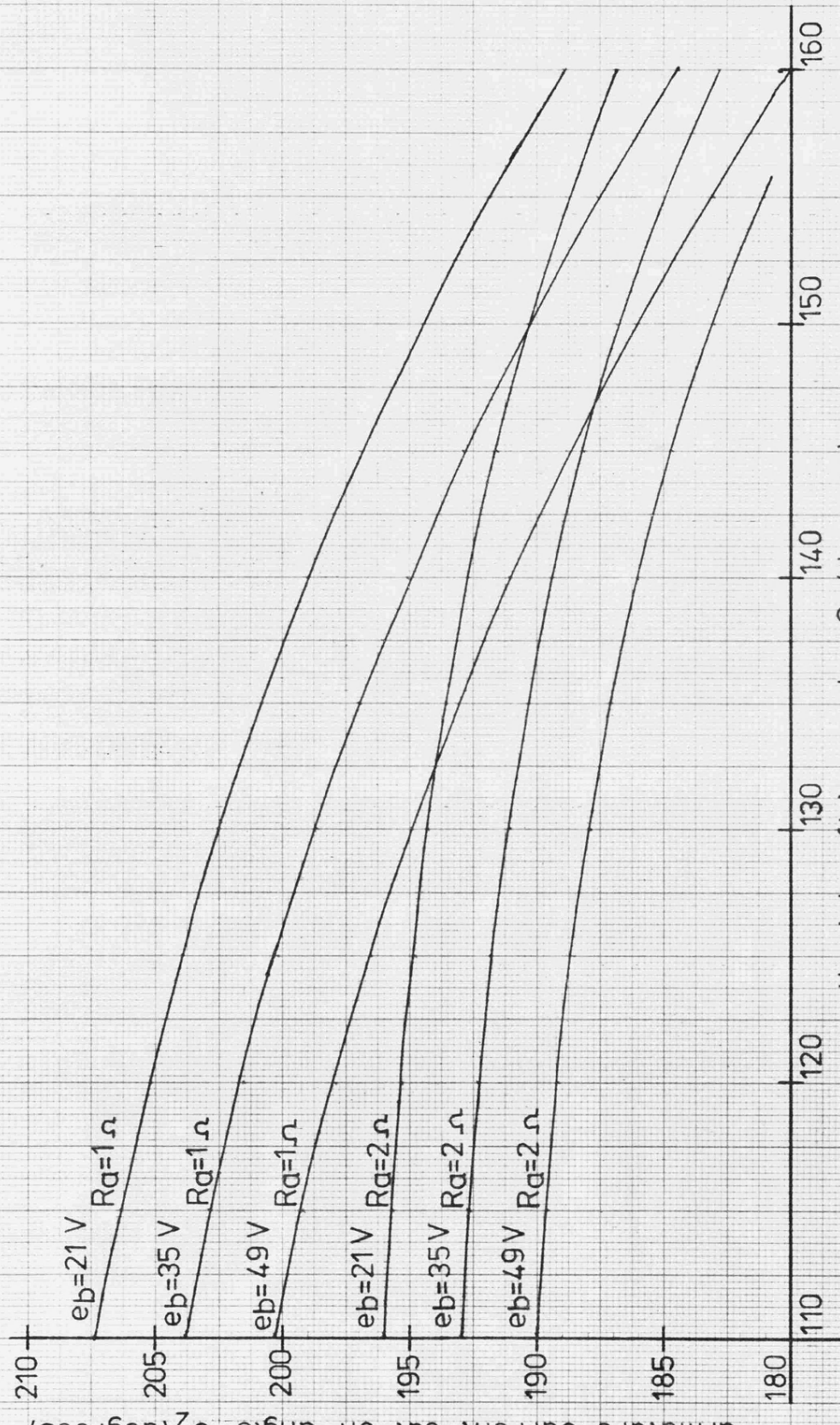

FIG. 11.3 ARMATURE CURRENT CUT-OFF ANGLE AGAINST FIRING ANGLE

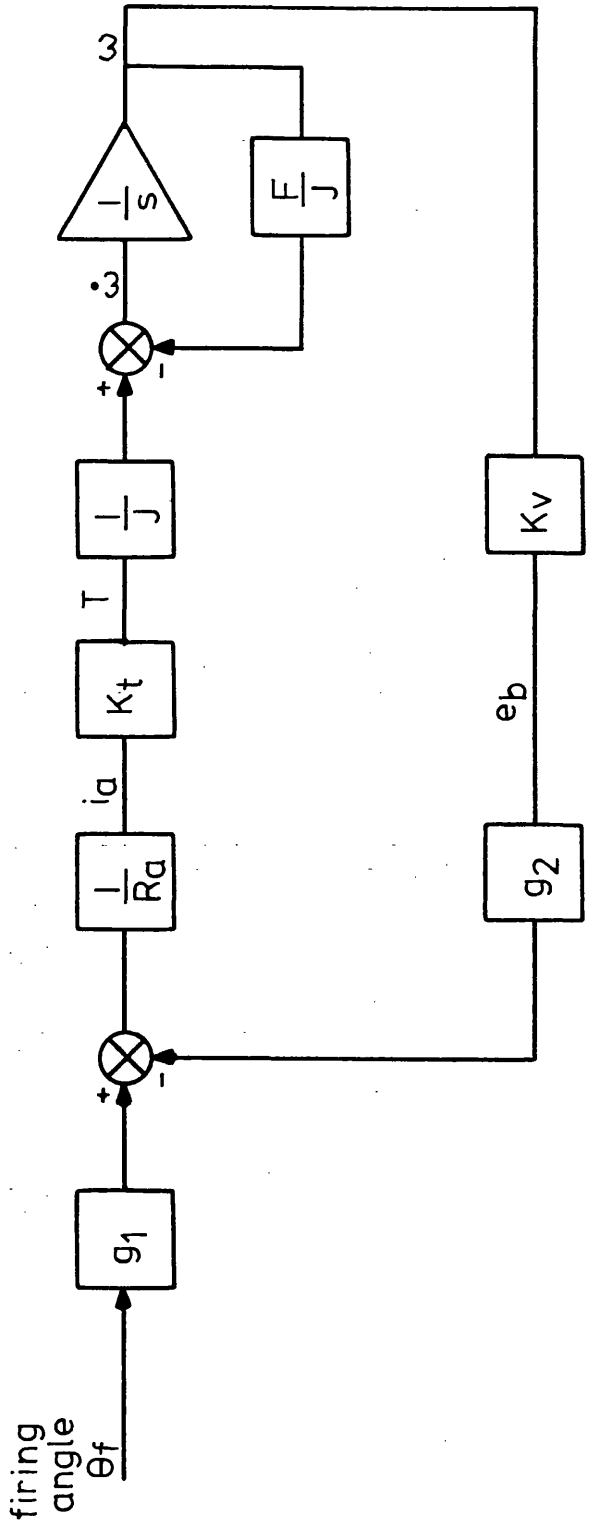

FIG. 11.4 LINEARIZED MODEL OF A D.C. MACHINE OPERATING WITH DISCONTINUOUS ARMATURE CURRENT

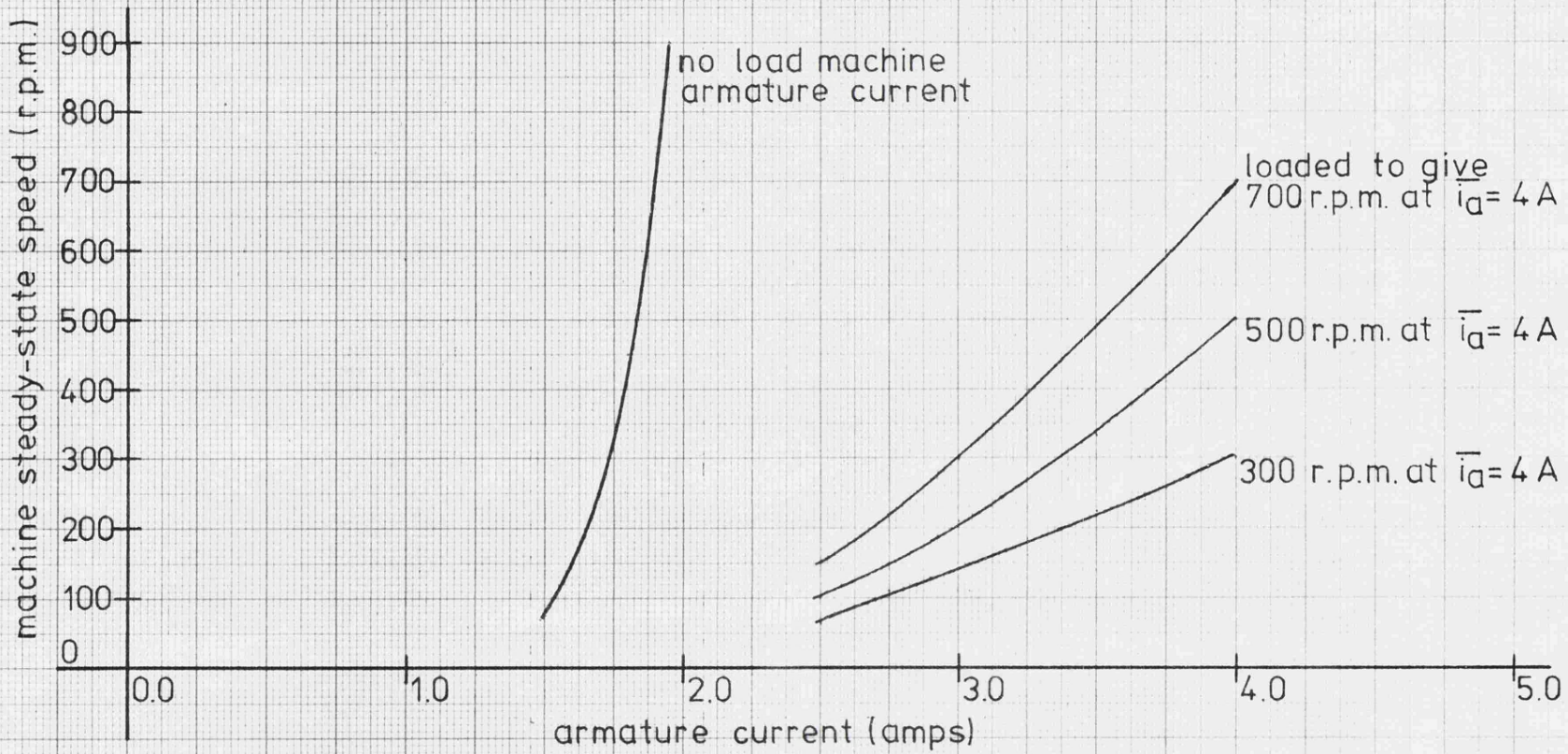

FIG. 11.5 STEADY-STATE SPEED AGAINST ARMATURE CURRENT FOR VARIOUS DEGREES OF LOADING

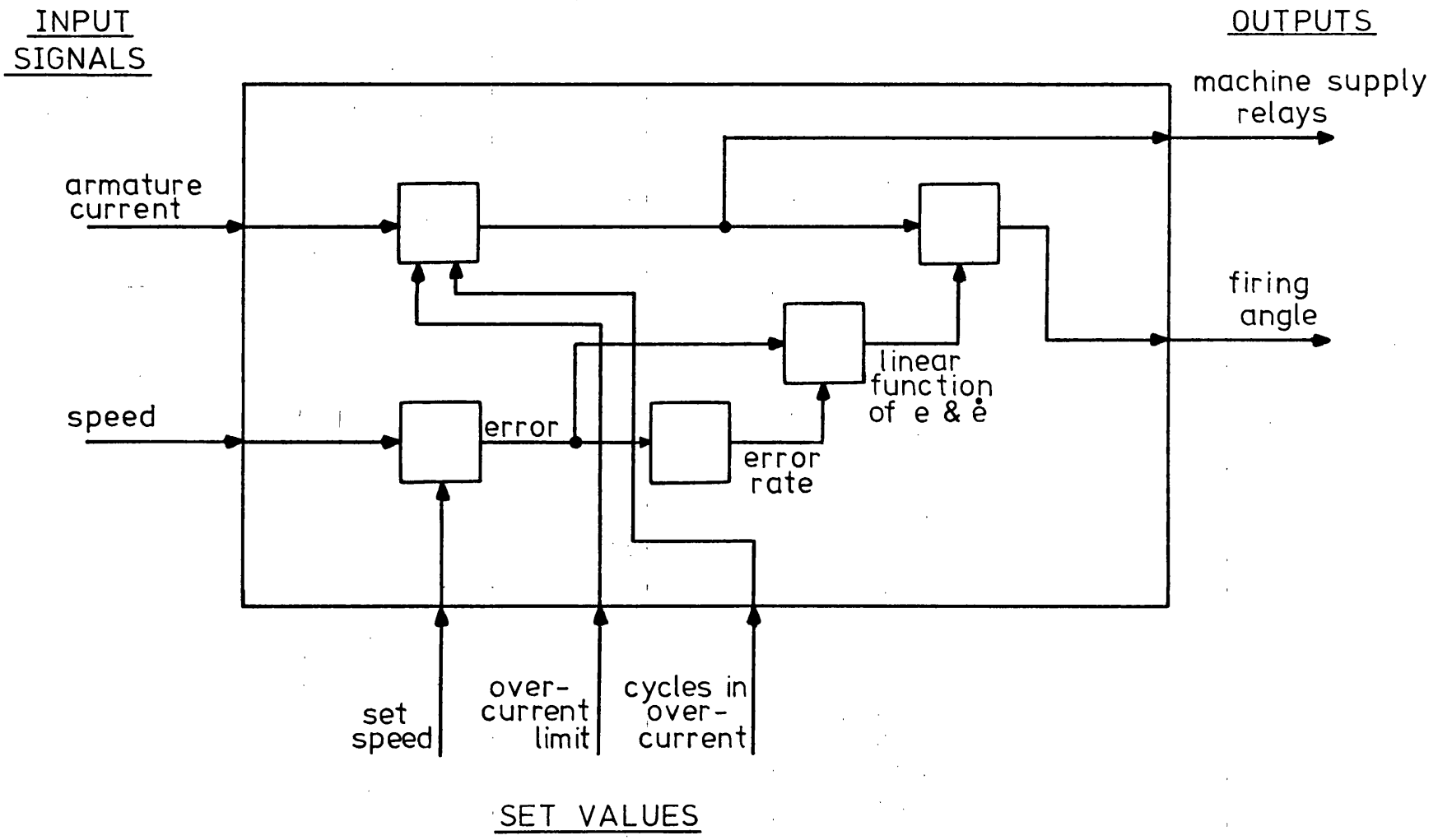

FIG. 11.6 REPRESENTATION OF THE MICROPROCESSOR AS A CONTROL ELEMENT

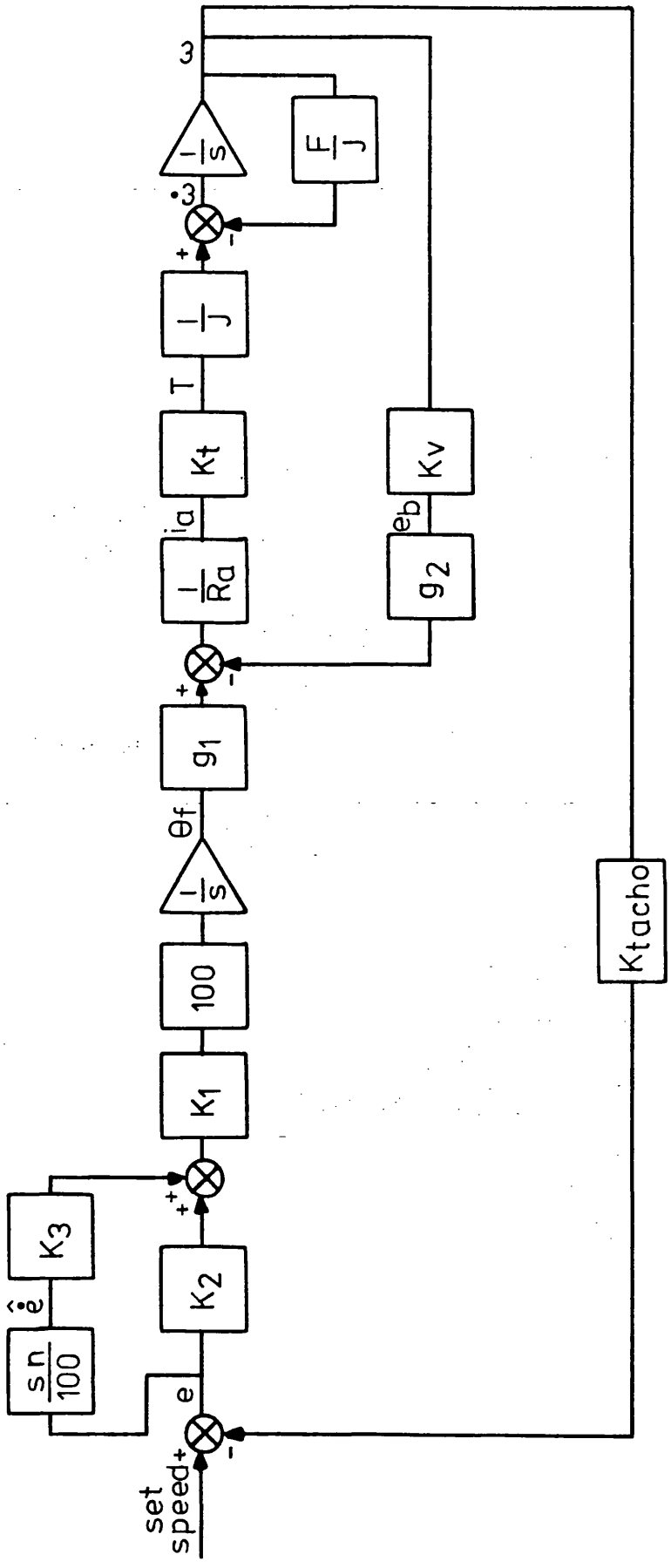

FIG. 11.7 LINEARIZED MODEL OF THE COMPLETE MICROPROCESSOR-MACHINE SYSTEM

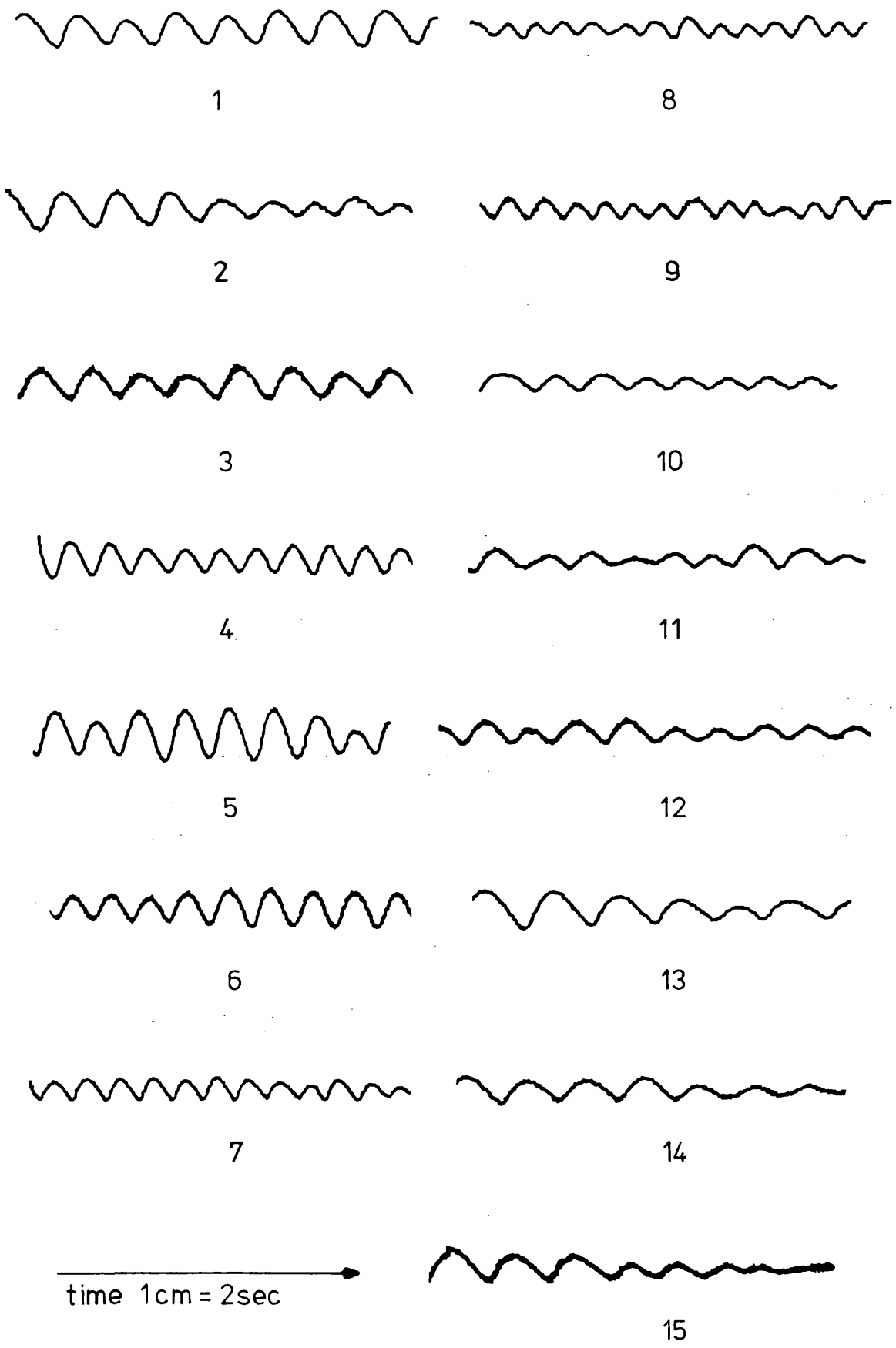

FIG.11.8 SMALL PERTURBATION RESPONSES FOR THE RANGE OF TEST CONDITIONS

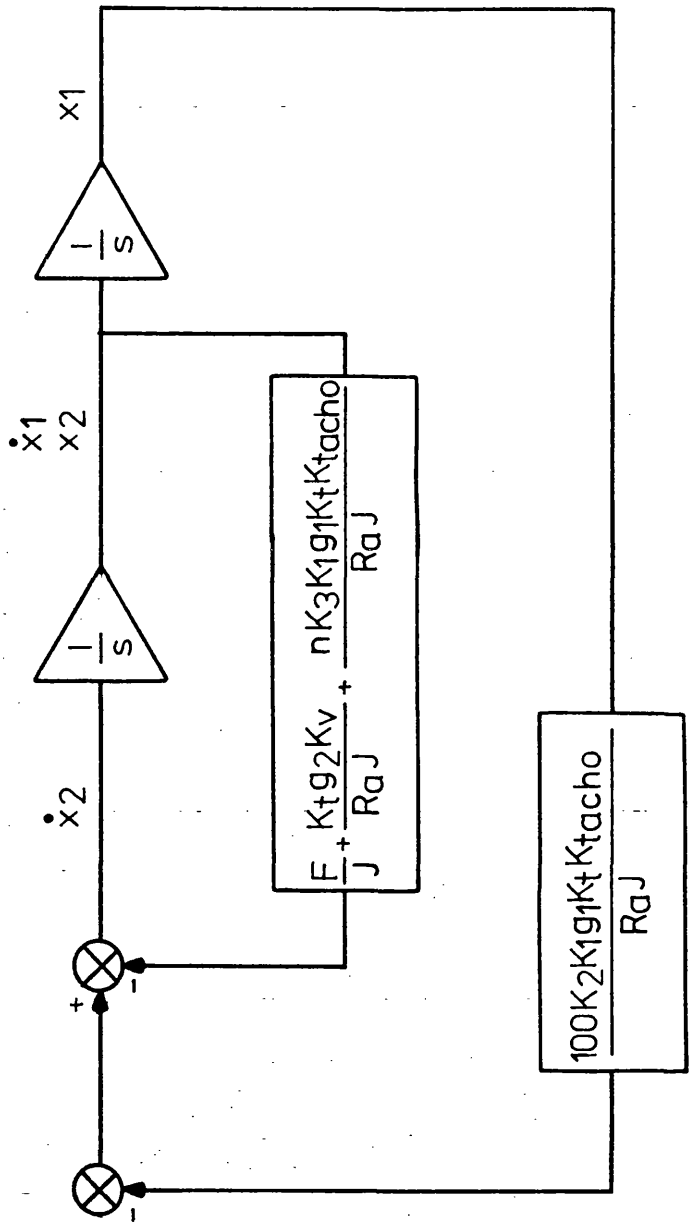

FIG. 12.1 THE PRACTICAL SYSTEM IN PHASE-CANONICAL FORM

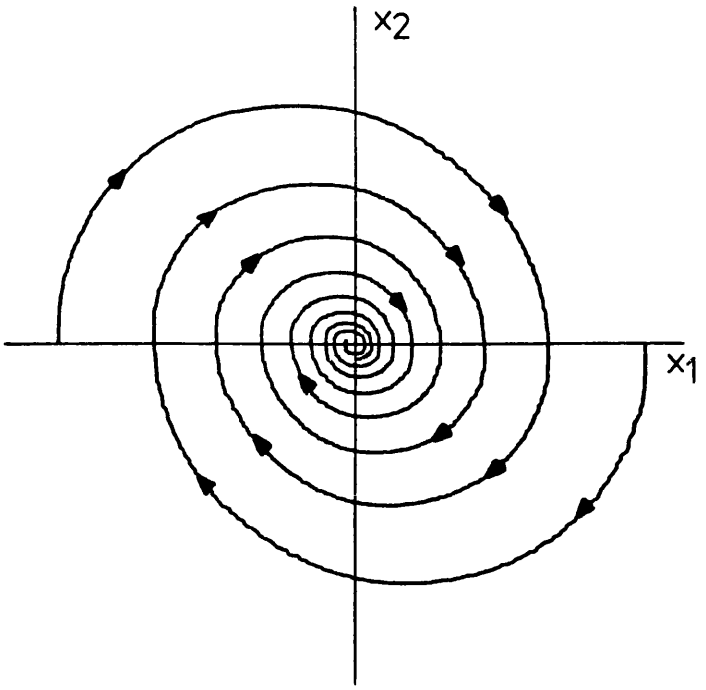

FIG.12.2 TYPICAL TRAJECTORIES FOR THE CHARACTERISTIC EQUATIONS OF TABLE 11.3

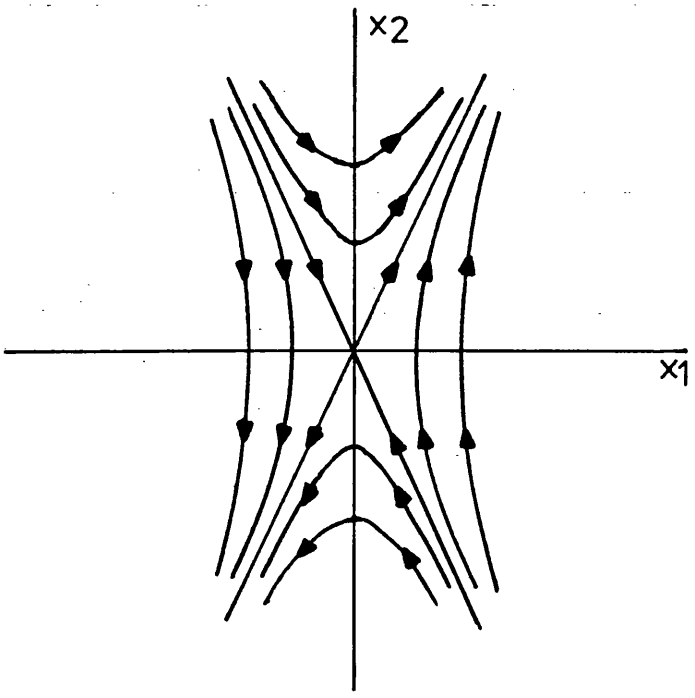

FIG.12.3 TYPICAL TRAJECTORIES FOR THE CHARACTERISTIC EQUATIONS OF TABLE 12.4

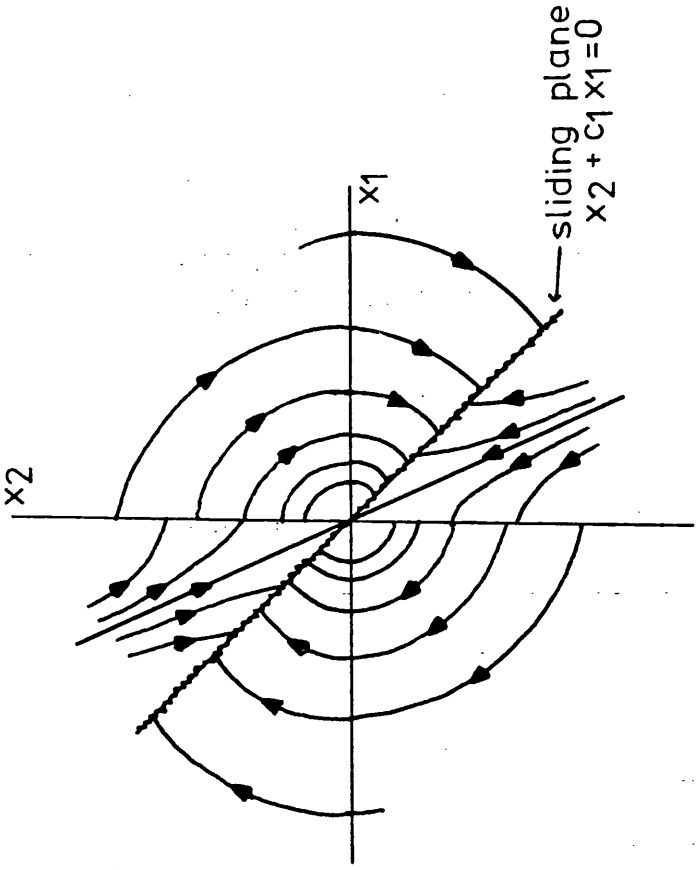

FIG. 12.4 TRAJECTORIES FOR THE FIRST VARIABLE STRUCTURE STRATEGY

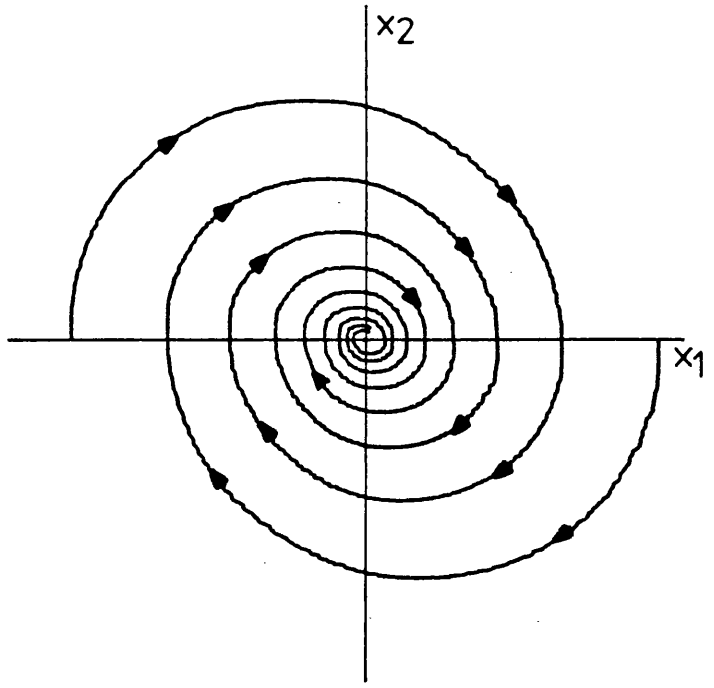

FIG. 12.5 TYPICAL TRAJECTORIES FOR THE CHARACTERISTIC EQUATIONS OF TABLE 11.3

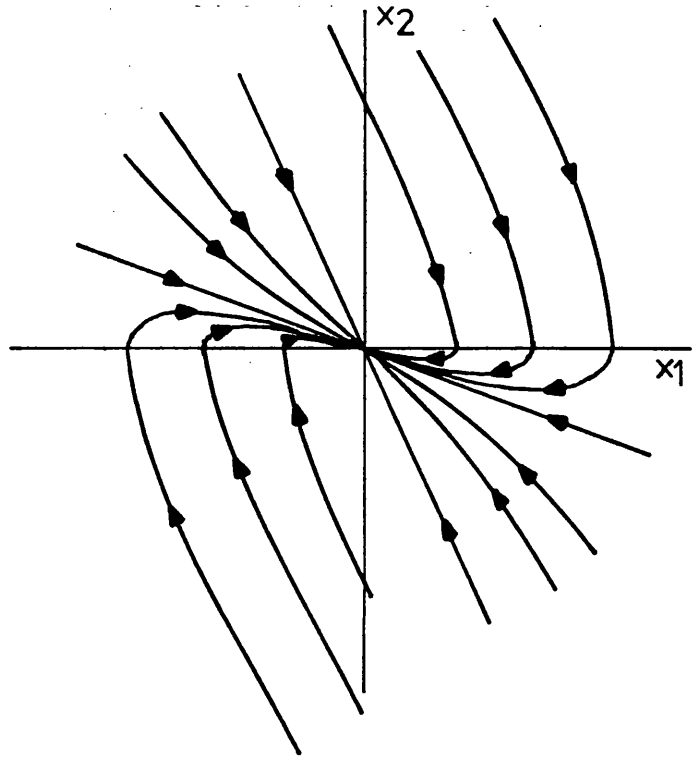

FIG. 12.6 TYPICAL TRAJECTORIES FOR THE CHARACTERISTIC EQUATIONS OF TABLE 12.6

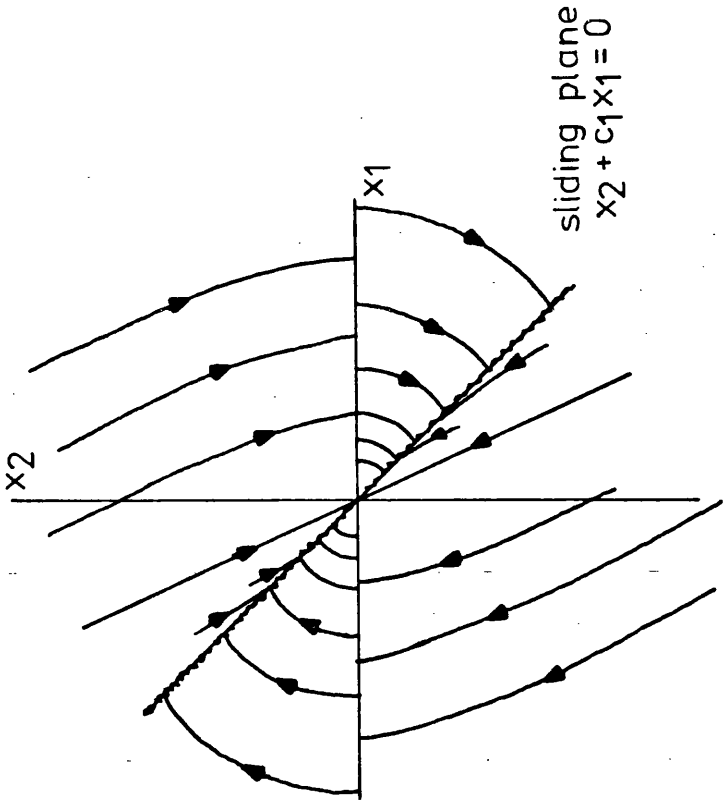

FIG. 12.7 TRAJECTORIES FOR THE SECOND VARIABLE STRUCTURE STRATEGY

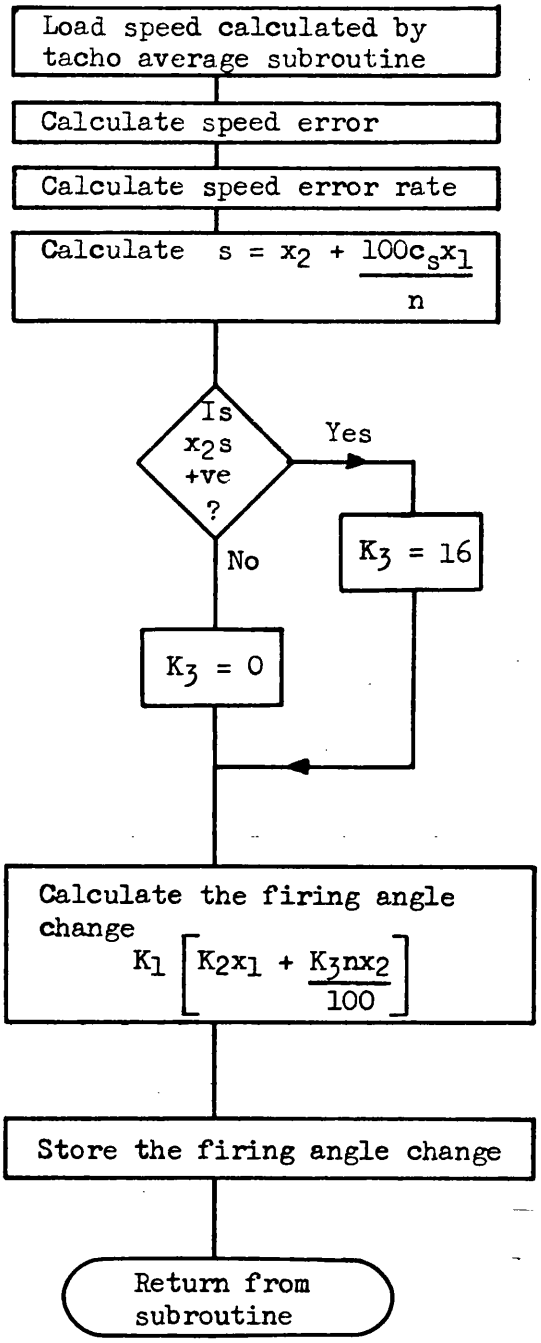

FIG. 12.8 VARIABLE STRUCTURE CONTROL SUBROUTINE FLOW CHART

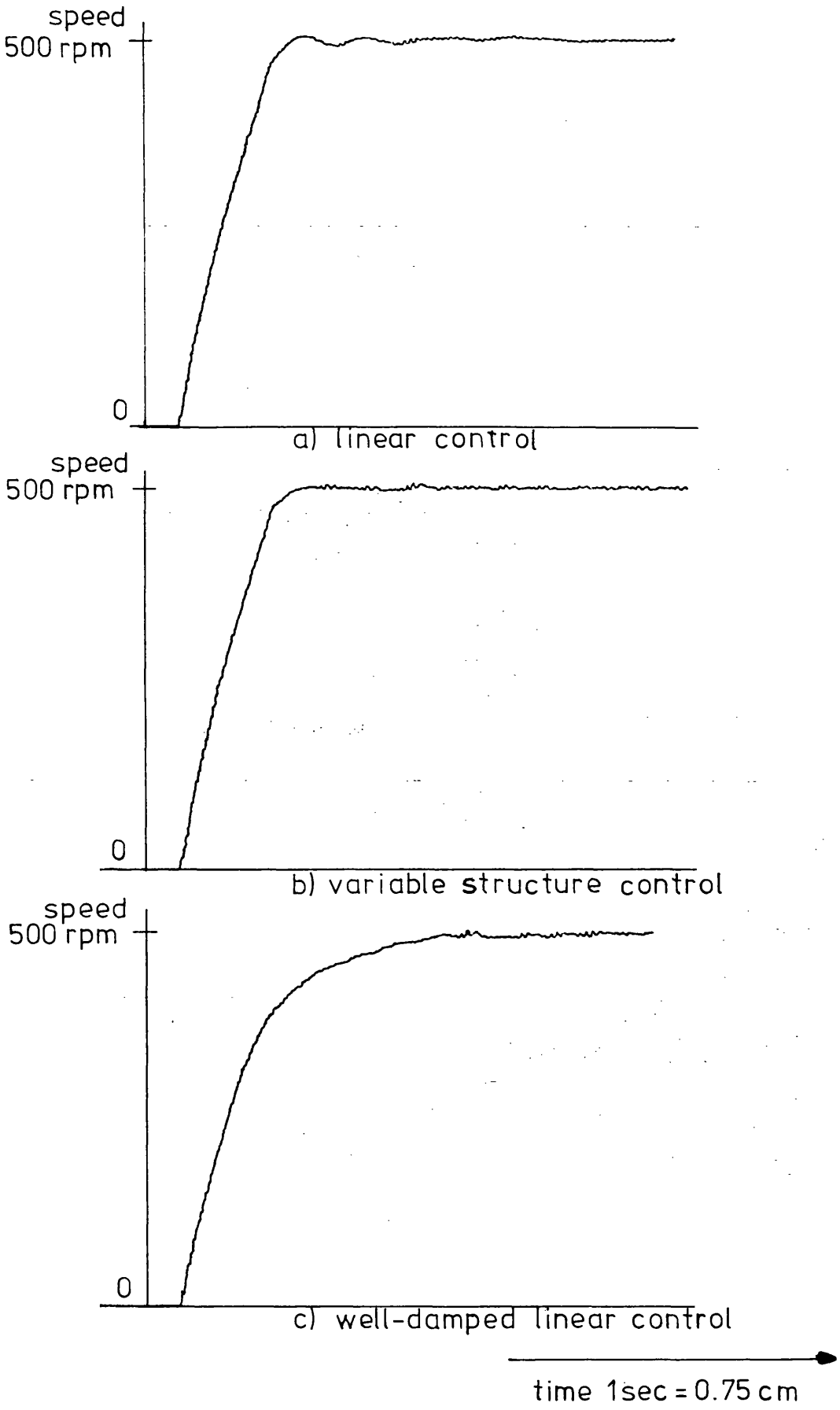

FIG. 13.1 STEP RESPONSES FOR CONDITION 2

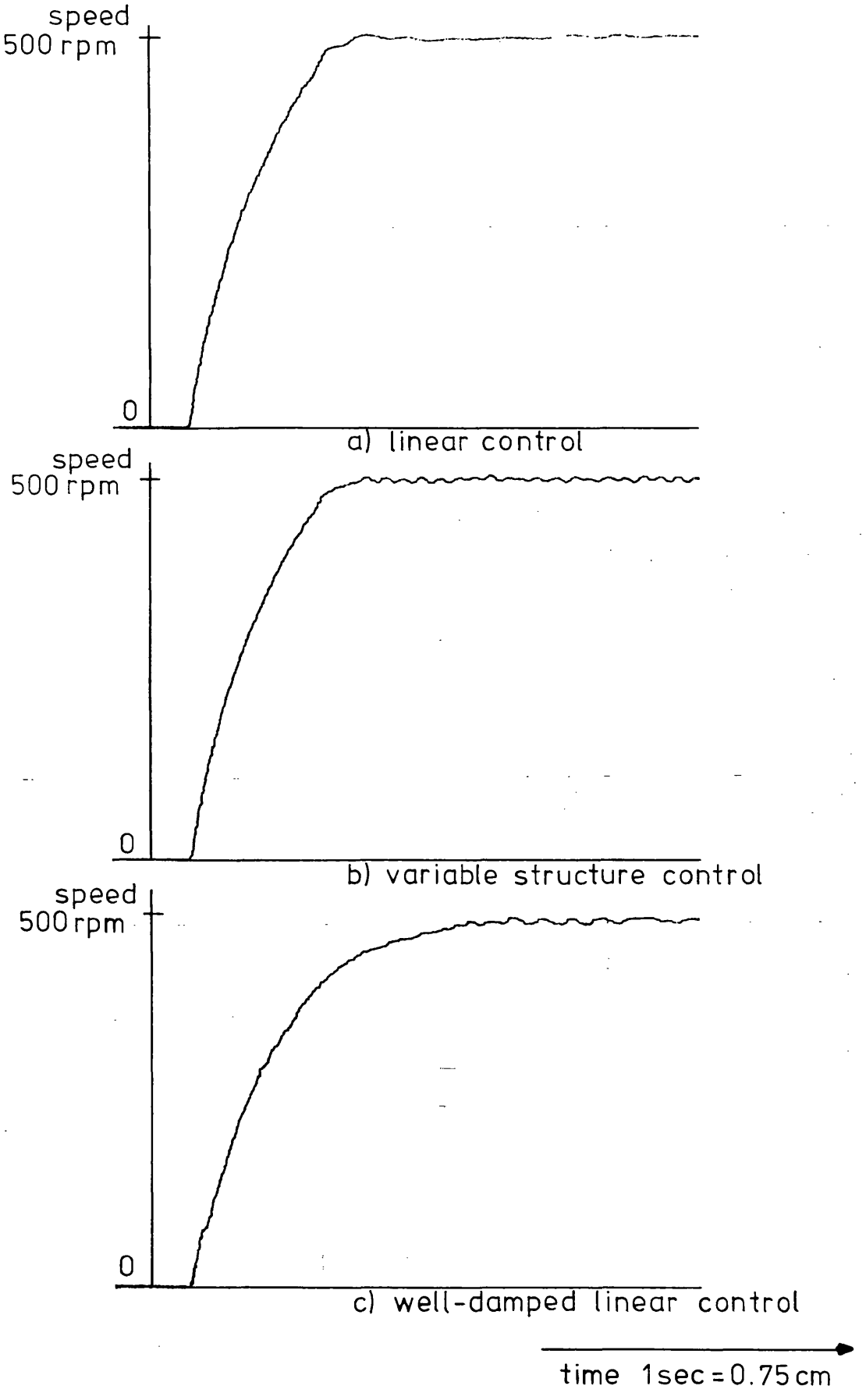

FIG.13.2 STEP RESPONSES FOR CONDITION 5

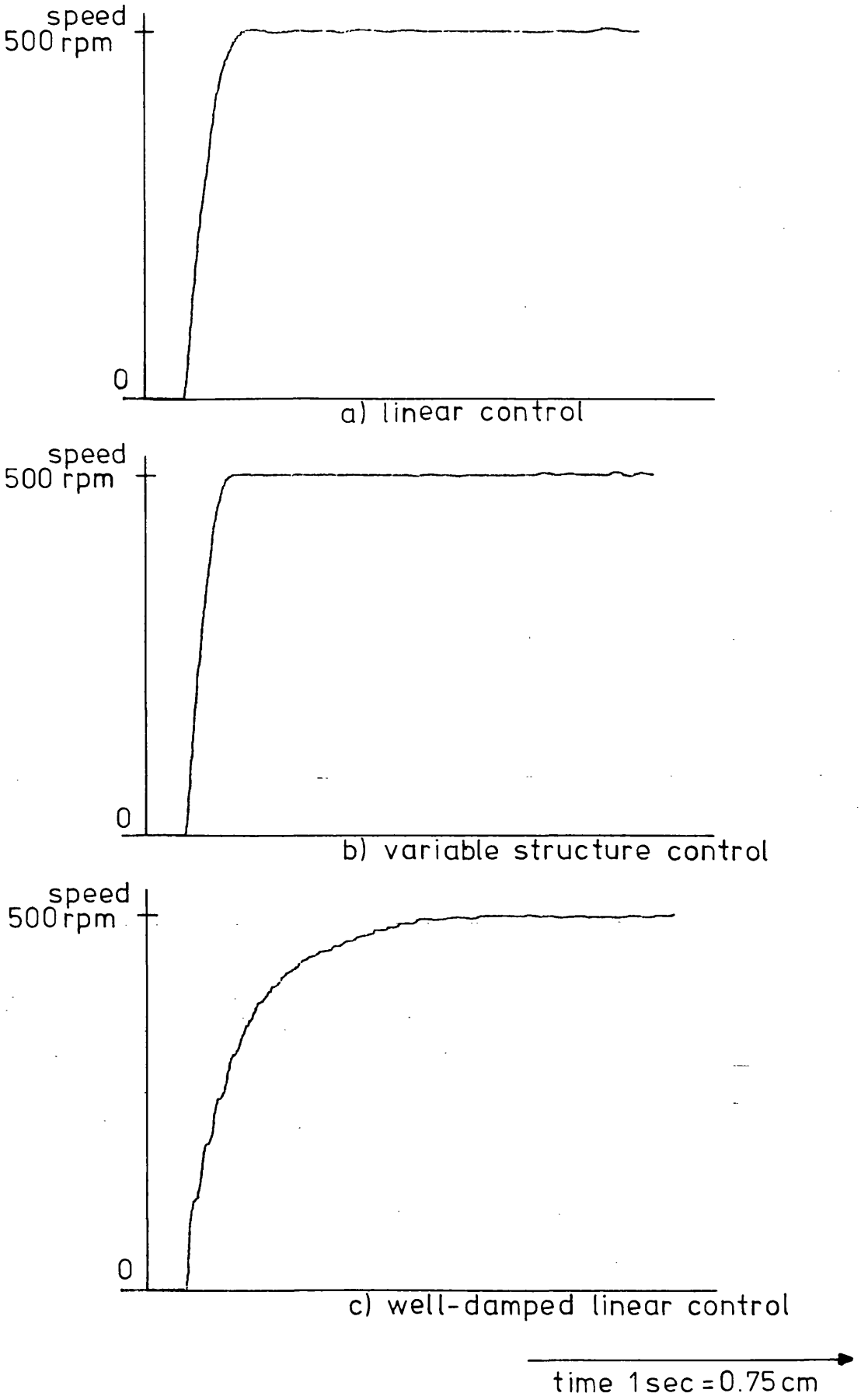

FIG. 13.3 STEP RESPONSES FOR CONDITION 8

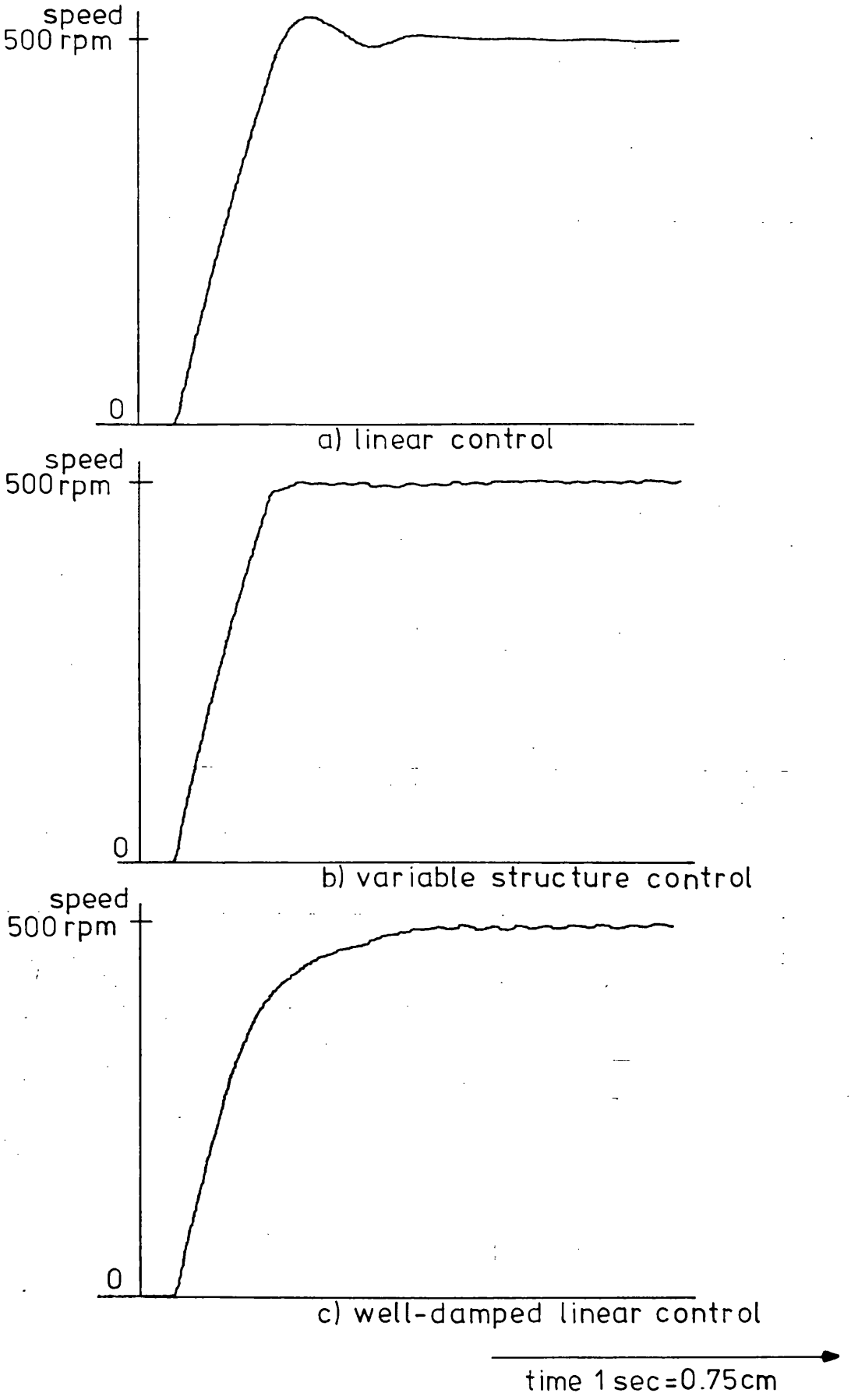

FIG. 13.4 STEP RESPONSES FOR CONDITION 11

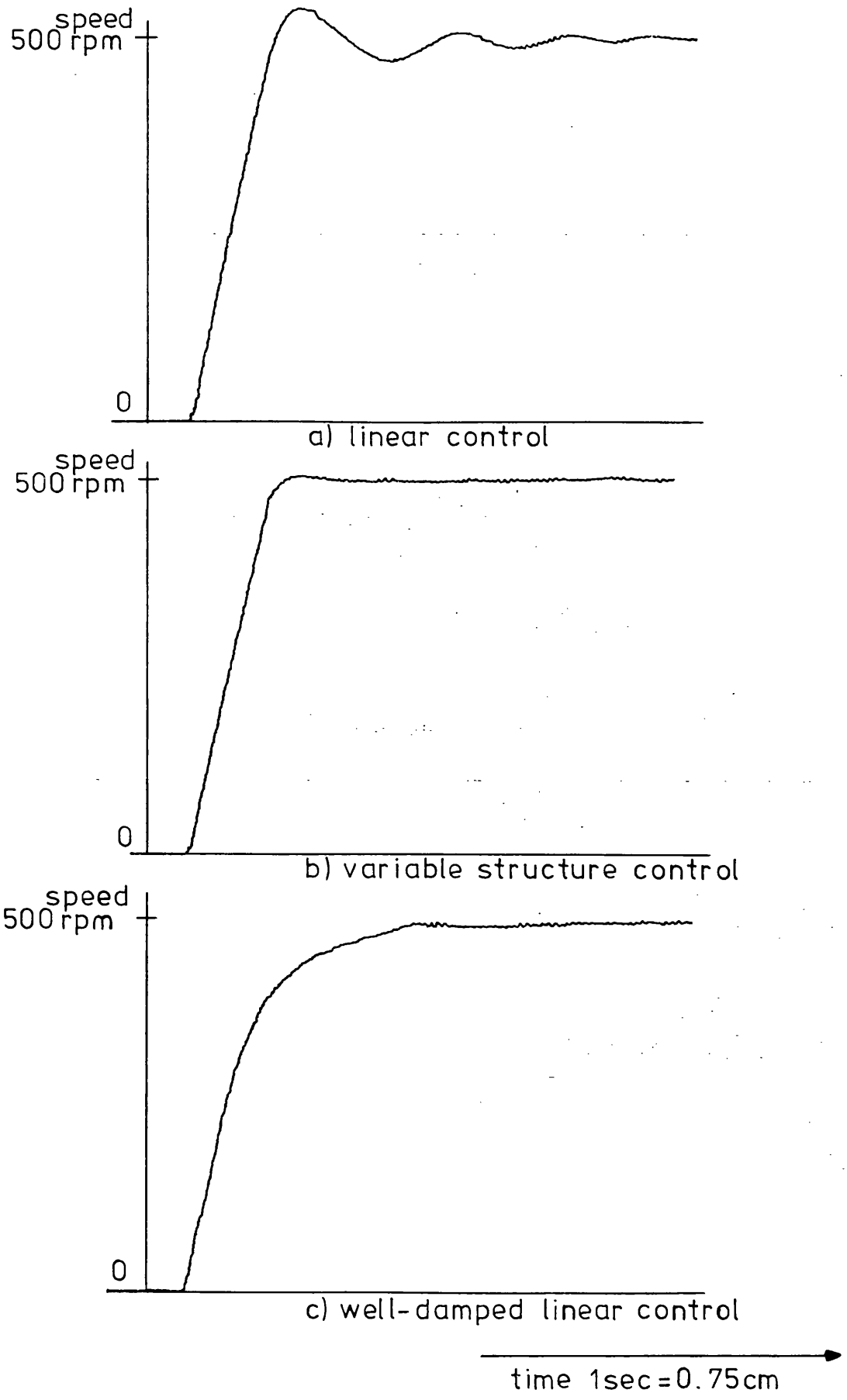

FIG. 13.5 STEP RESPONSES FOR CONDITION 14

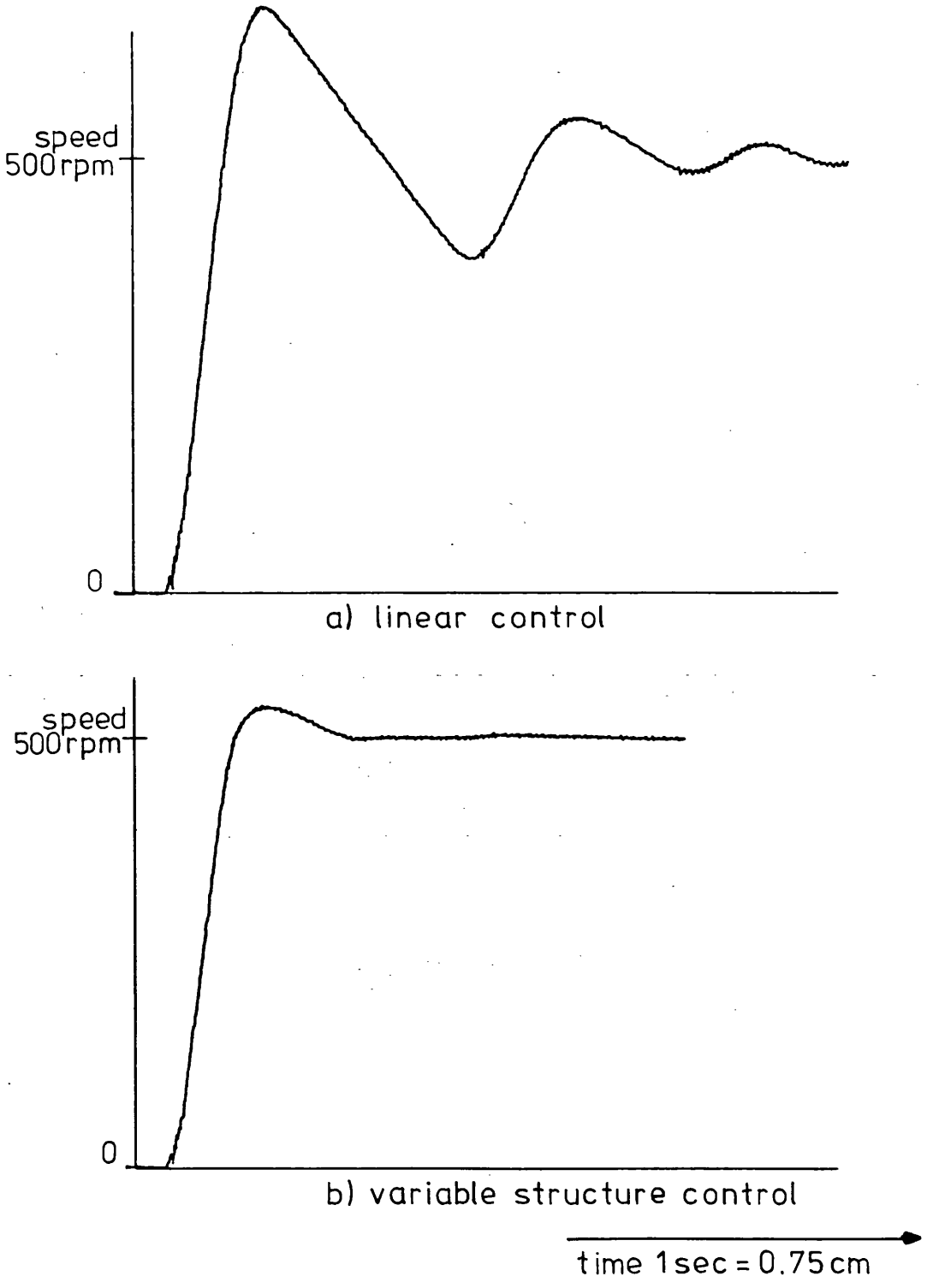

FIG. 13.6 STEP RESPONSES WITH 3Ω ADDED WORK MACHINE ARMATURE RESISTANCE

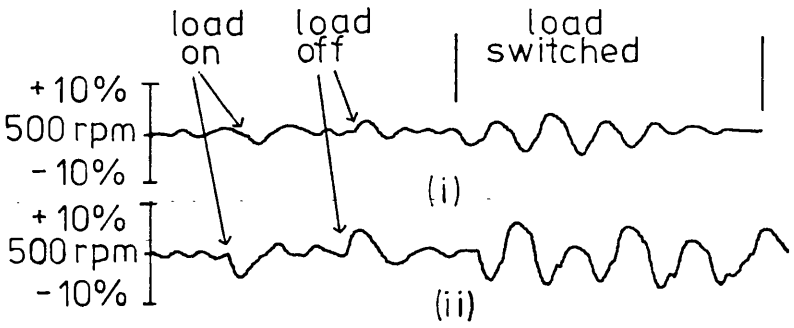

a) linear control

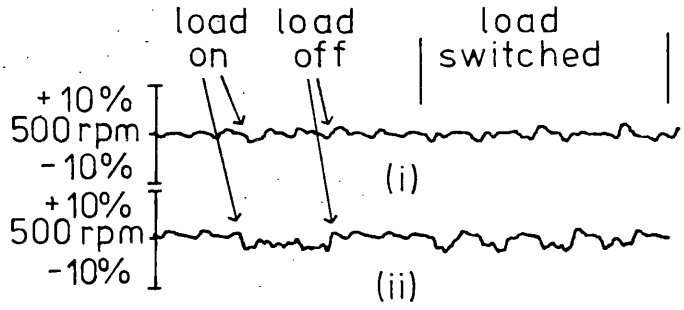

b) variable structure control

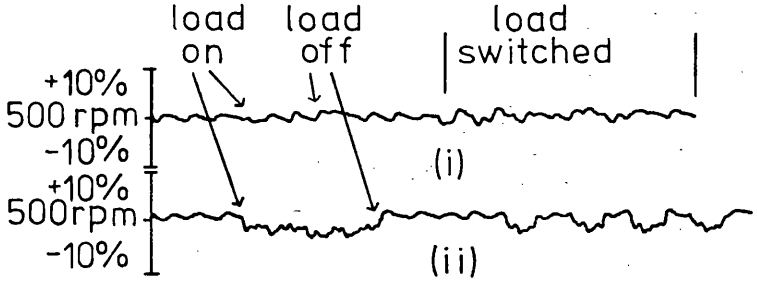

c) well-damped linear control

(i) medium load
(ii) large load

time 2 secs = 0.75cm

FIG. 13.7 SPEED RESPONSES TO MACHINE LOADING

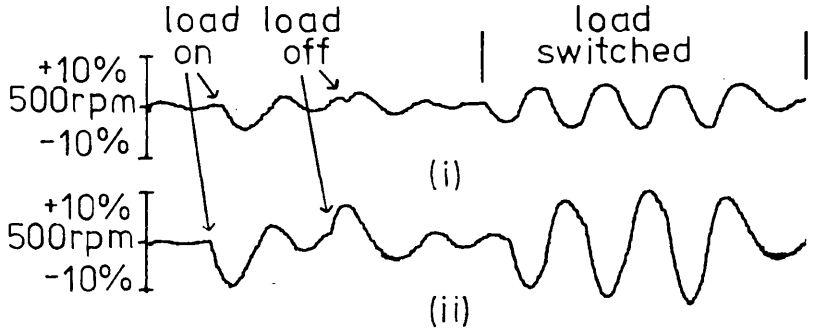

a) linear control

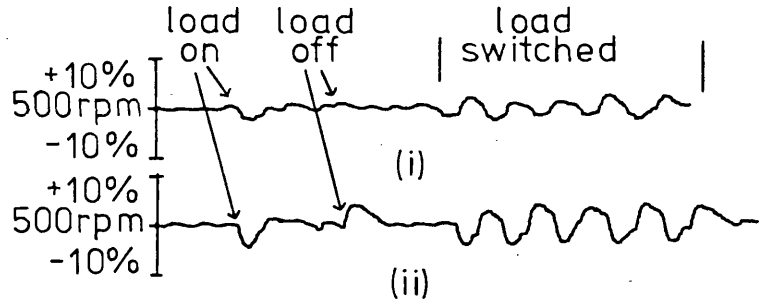

b) variable structure control

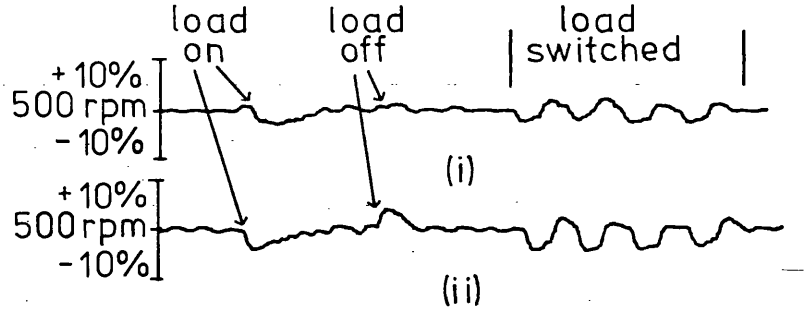

c) well-damped linear control

(i) medium load
(ii) large load

time 2secs = 0.75cm

FIG. 13.8 SPEED RESPONSES TO MACHINE LOADING WITH 1Ω ADDED WORK MACHINE ARMATURE RESISTANCE

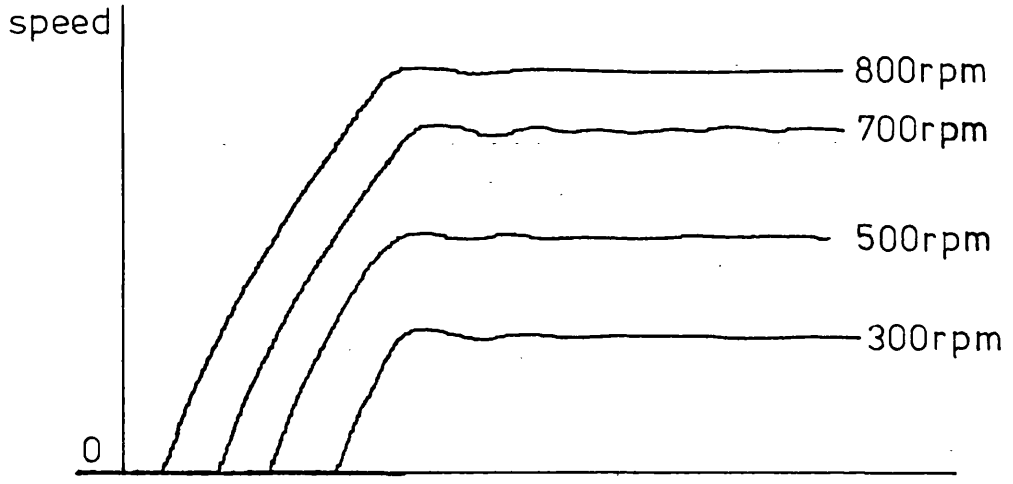

a) linear control

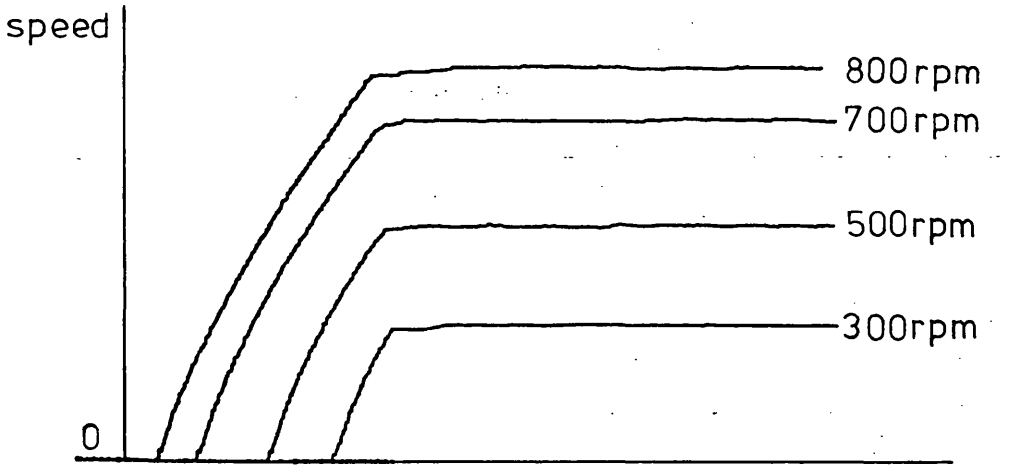

b) variable structure control

time 1sec = 0.75cm

FIG. 13.9 STEP RESPONSES FOR VARIOUS SPEED DEMANDS

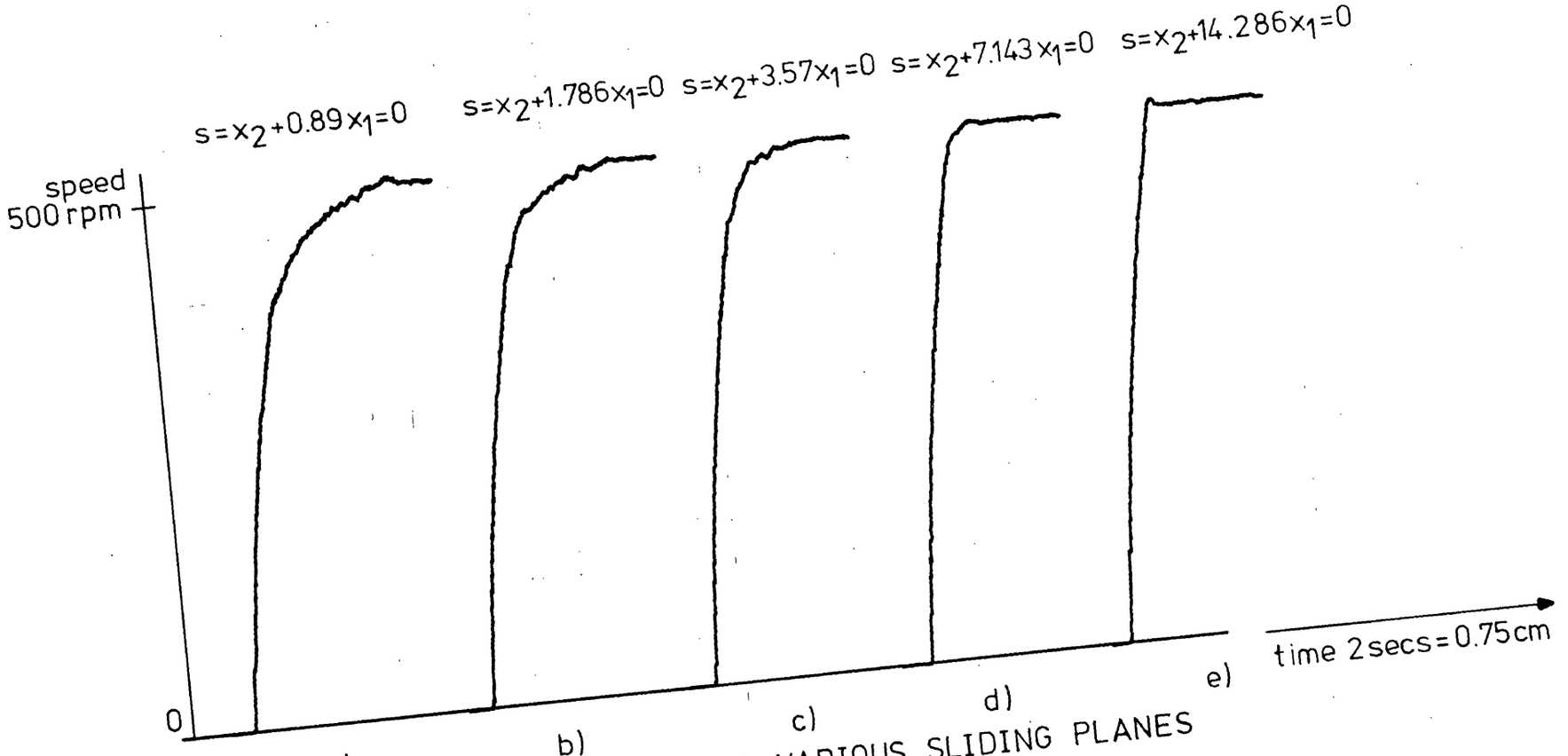

FIG. 13.10 STEP RESPONSES FOR VARIOUS SLIDING PLANES

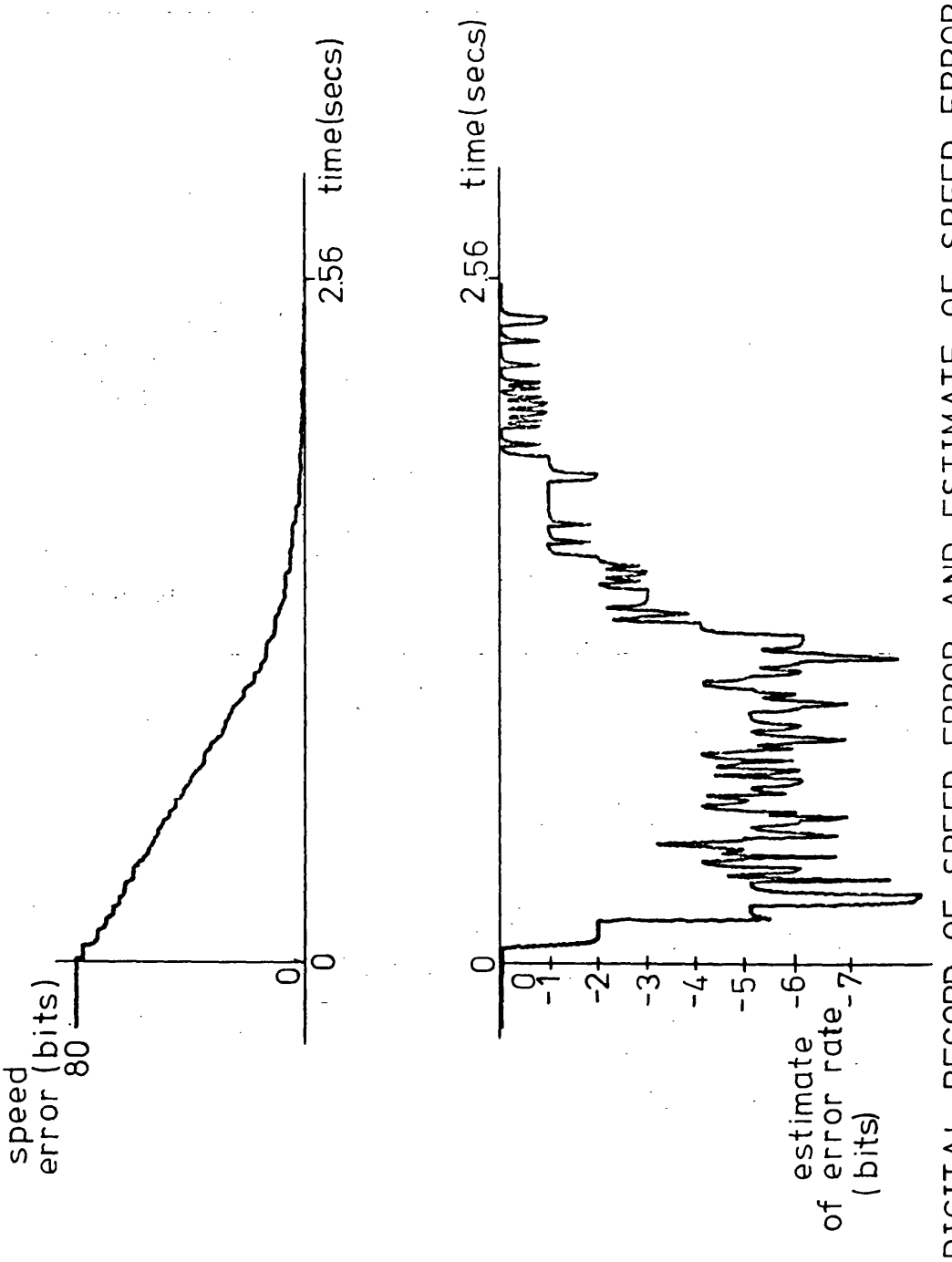

FIG.13.11 DIGITAL RECORD OF SPEED ERROR AND ESTIMATE OF SPEED ERROR RATE

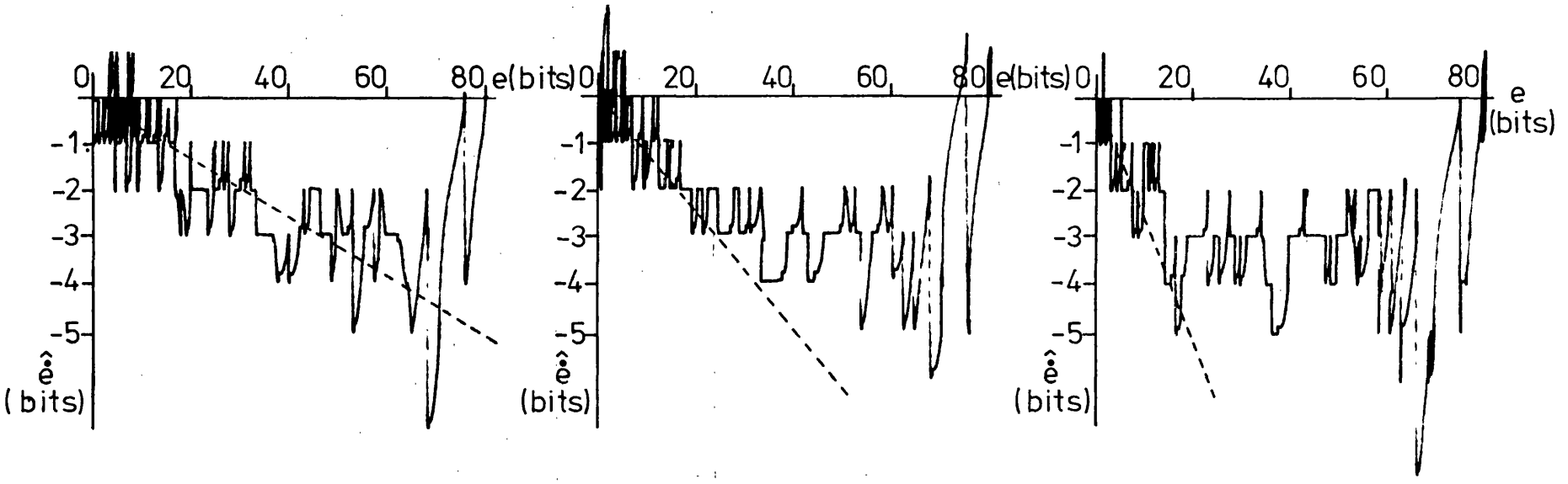

a)
$s = x_2 + 0.89 x_1 = 0$

b)
$s = x_2 + 1.786 x_1 = 0$

c)
$s = x_2 + 3.57 x_1 = 0$

--------- desired sliding mode

N.B. $x_1 = e$, $x_2 = \frac{100}{n} \hat{e}$

FIG.13.12 PHASE PLANE PLOTS FOR VARIOUS DESIRED SLIDING MODES

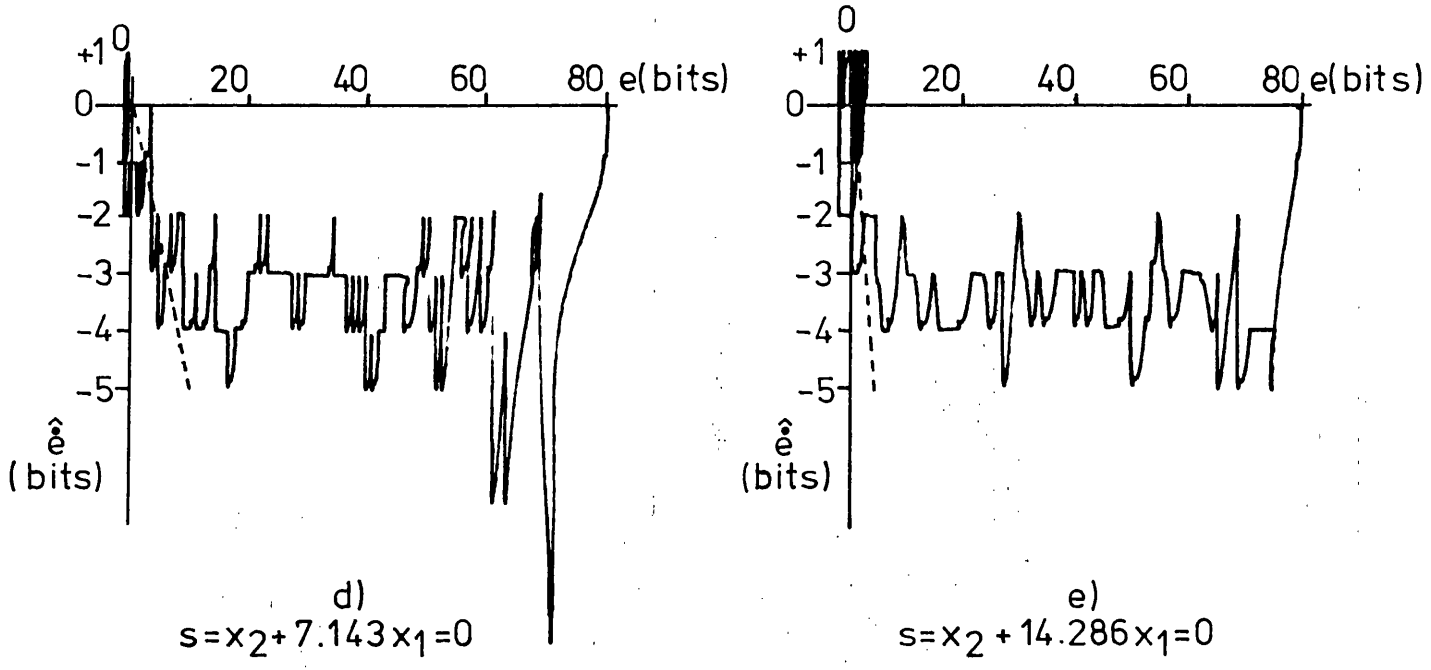

---------- desired sliding mode

N.B. $x_1 = e$, $x_2 = \frac{100}{n}\hat{e}$

FIG.13.12 PHASE PLANE PLOTS FOR VARIOUS DESIRED SLIDING MODES (cont.)

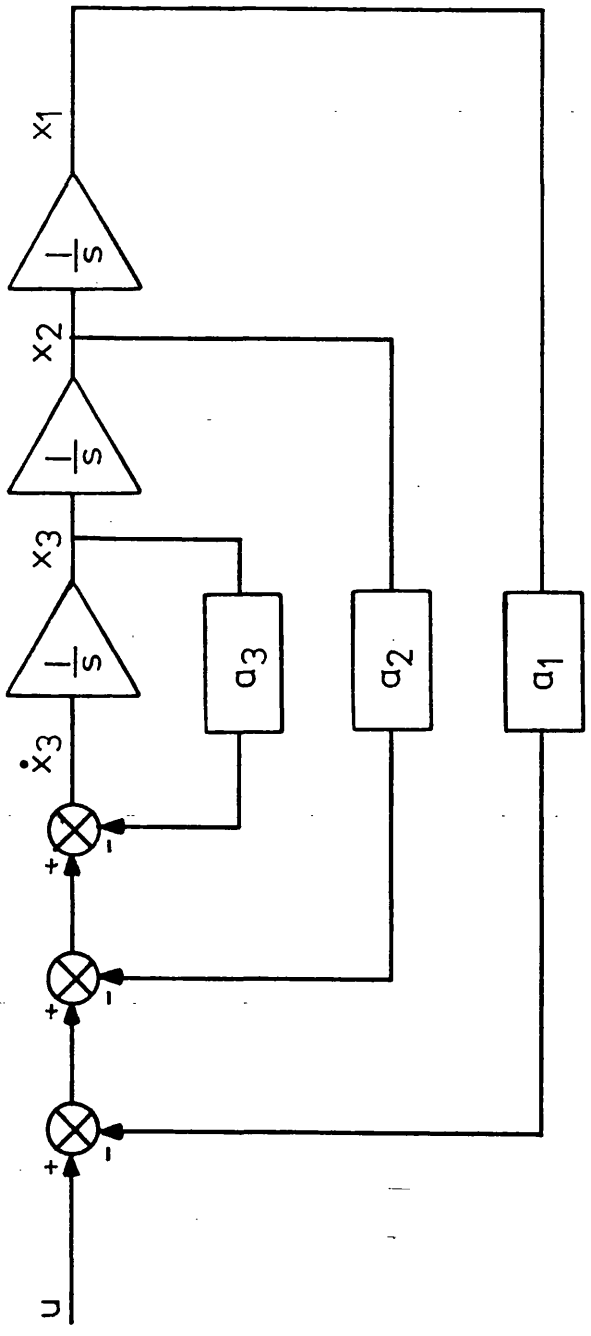

FIG. A1 THIRD ORDER SYSTEM FOR VARIABLE STRUCTURE CONTROL

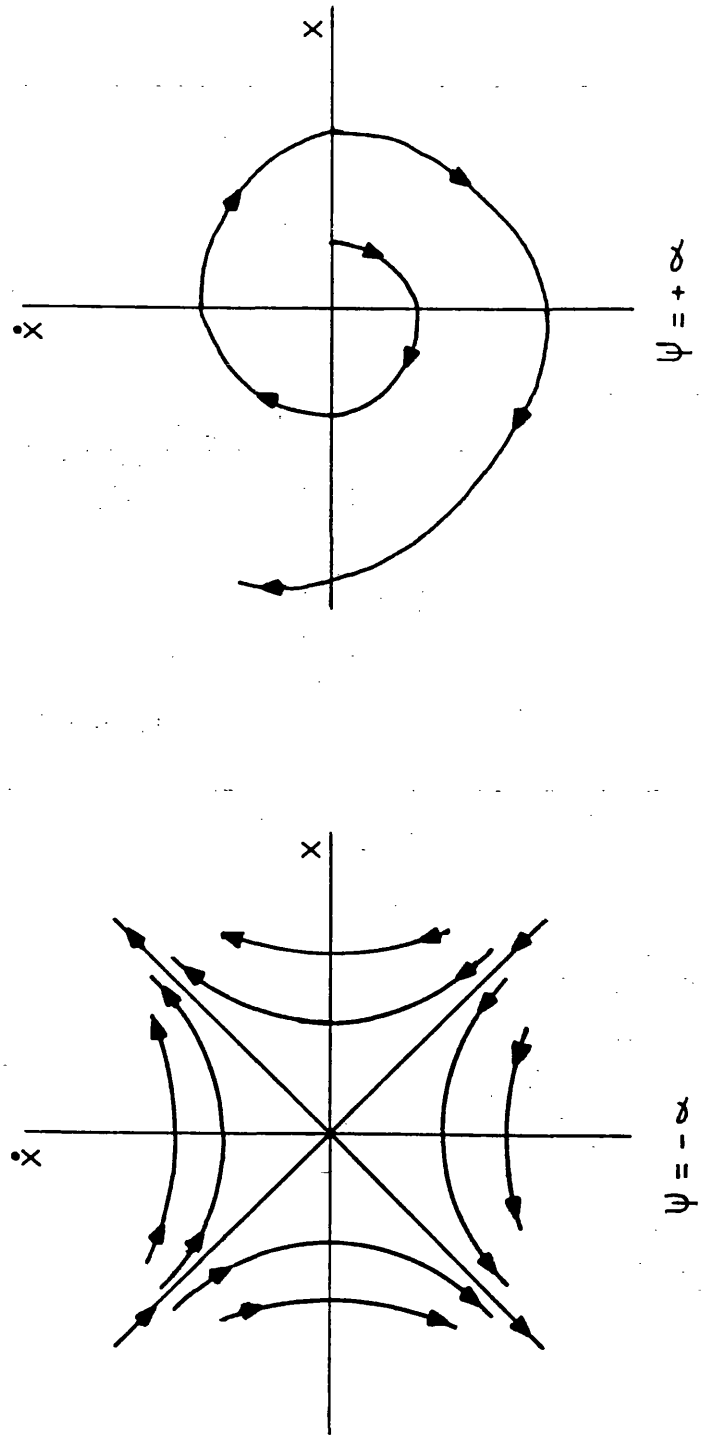

FIG. A2 STRUCTURES WITH UNSTABLE TRAJECTORIES

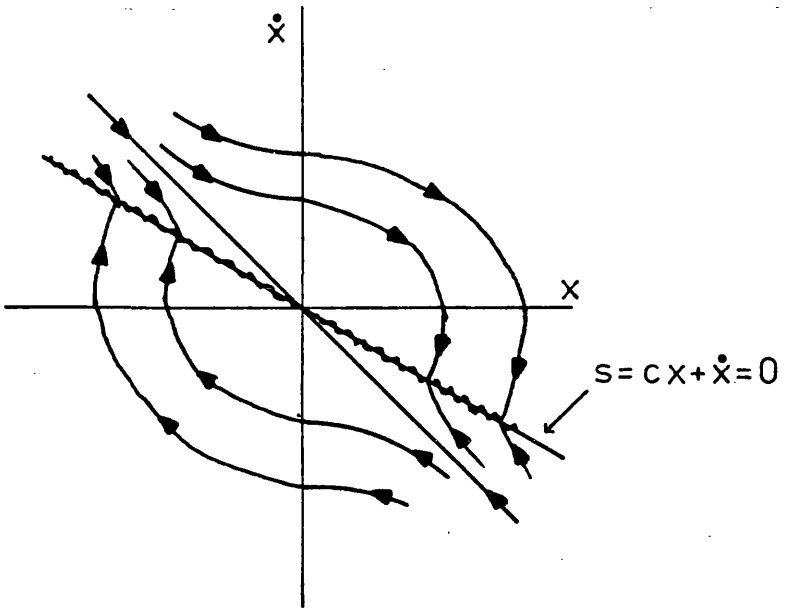

FIG. A3 STABLE SLIDING MODE WITH UNSTABLE STRUCTURES

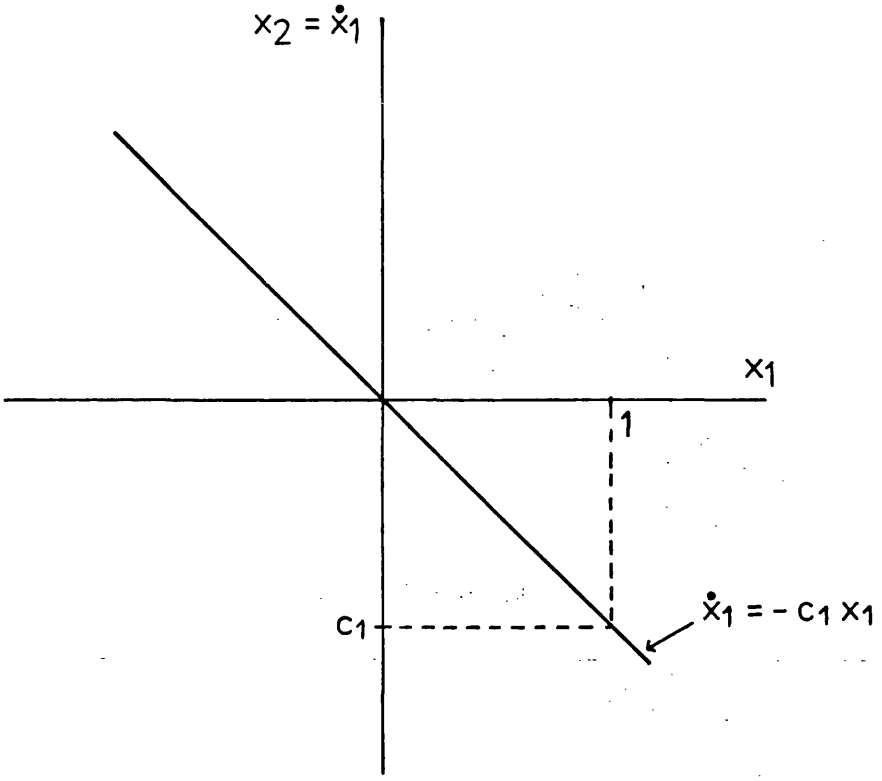

FIG. B1 FIRST ORDER RESPONSE AS A HYPERPLANE IN TWO DIMENSIONAL STATE SPACE

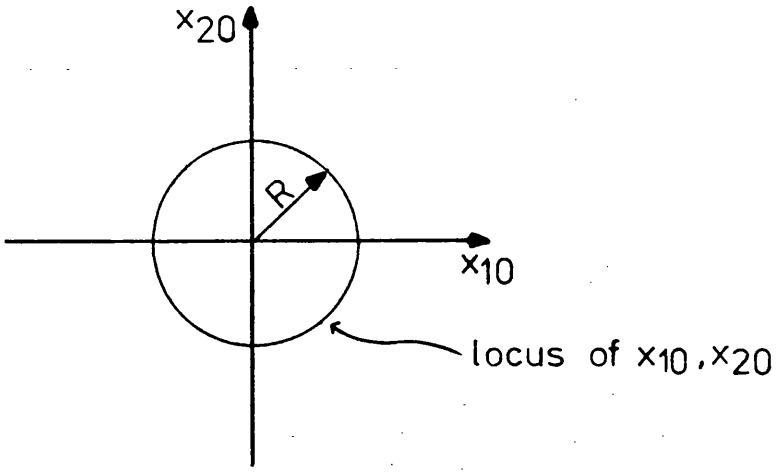

FIG. C1 SIMPLE TARGET SET FOR A SECOND ORDER SYSTEM

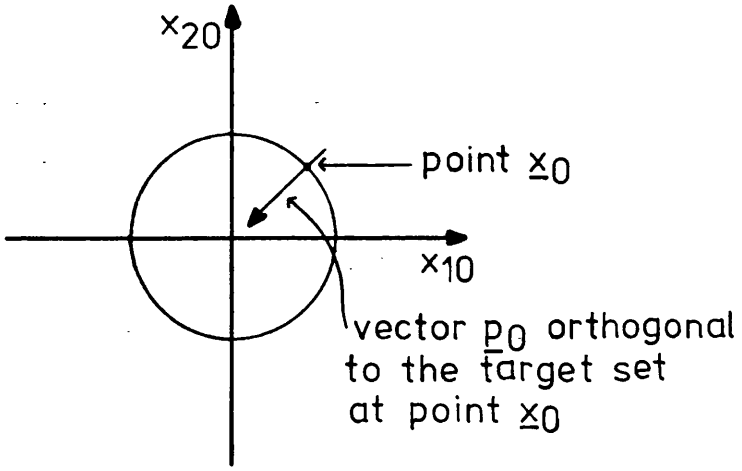

FIG. C2 ORIENTATION OF THE INITIAL COSTATE VECTOR

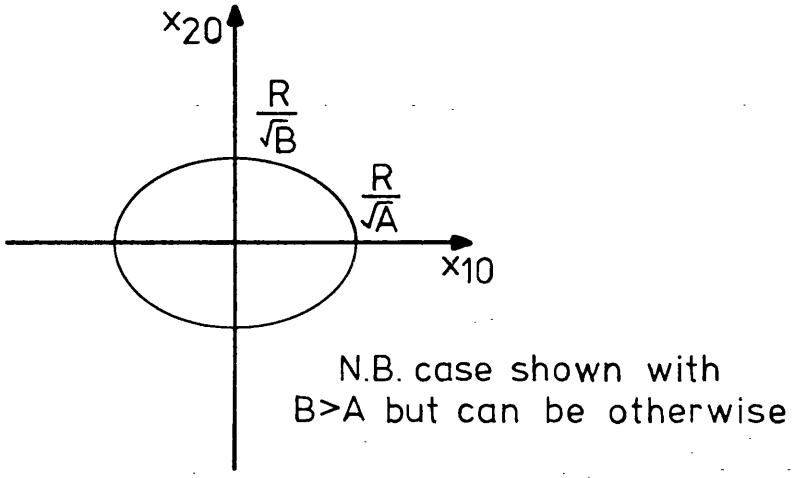

FIG. C.3 MORE GENERAL TARGET SET

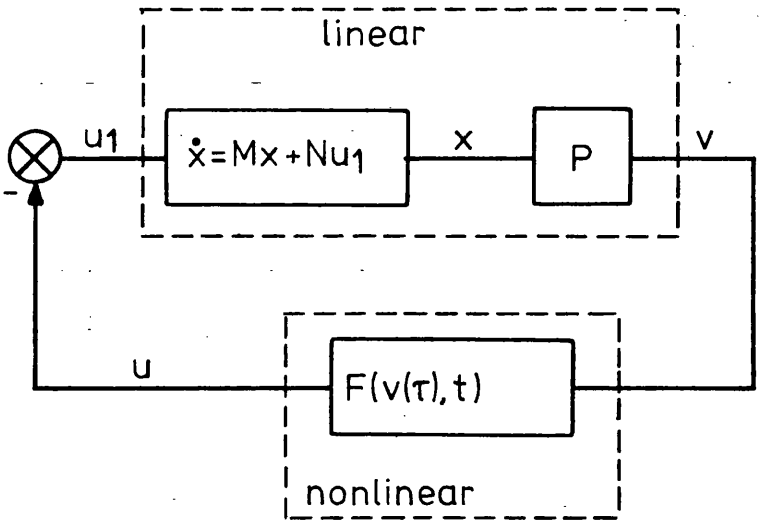

FIG. G.1 MULTIVARIABLE STANDARD SYSTEM